3L3

a New Component of the Wingless Signaling Pathway

Dissertation

zur

Erlangung der naturwissenschaftlichen Doktorwürde

(Dr. sc. nat.)

vorgelegt der

Mathematisch–naturwissenschaftlichen Fakultät

der

Universität Zürich

von

Davide Giovanni Soldini

von

Coldrerio TI

Promotionskomitee

Prof. Dr. Konrad Basler (Vorsitz und Leitung der Dissertation)

Prof. Dr. Ernst Hafen

Zürich, 2006

To my brother Nicola

To my cousin Marco

1 Summaries

1.1 Zusammenfassung

Der Wnt/Wingless-Signalweg kontrolliert grundlegende Prozesse während der Embryonalentwicklung und ist beteiligt an verschiedenen Krebserkrankungen, vor allem jener des Dickdarms. Während der letzten Jahre wurde dieser Signalübertragungsweg in grossem Detail erforscht und wir sind nun dabei, die regulatorischen Mechanismen zu verstehen, welche diesen Signalweg prägen.
Dieser signalweg besteht, in aller Kürze, aus einem extrazellulären Liganden, Wnt/Wingless, welcher nach erfolgter Bindung an seinen Rezeptor Frizzled letzlich eine transkriptionelle Reaktion auslöst. Diese Transkriptionsreaktion wird durch das zytoplasmatische Protein β-catenin/Armadillo übermittelt.

Ziel dieser Arbeit ist es, die molekularen Mechanismen der Wnt/Wingless-Signalübertragung besser zu verstehen. Sie baut auf den Arbeiten einer ehemaligen Mitarbeiterin, Corina Schütt, und einer gegenwärtigen Mitarbeiterin des Labors, Carla Bänziger, auf.
Corina führte einen Screen für neue Komponenten des Wnt/Wingless-Signalwegs durch und fand drei Komplementationsgruppen. Carla konnte zeigen, dass *CG6210* in der dritten Komplementationsgruppe, die auch 3L3 genannt wird, mutiert ist. *CG6210* kodiert für ein noch unbekanntes Protein. Interessanterweise findet man Homologe dieses Gens in allen Metazoen und dasselbe gilt auch für die anderen Komponenten des Wnt/Wingless-Signalwegs.
Genetische Analysen zeigen, dass CG6210 eine neue positive Komponente des Wingless Signalwegs ist; andere Experimente in den Imaginalscheiben führen zu der Schlussfolgerung, dass das Protein eine wichtige Funktion in den *wg*-exprimierenden Zellen ausübt. Rettungsversuche mit synthetischen Transgenen bestätigen dieses Resultat und beweisen, dass CG6210 nur in den *wg*-exprimierenden Zellen benötigt wird.
Zusätzliche Versuche richten sich nach der Rolle von CG6210 in der Bildung des Gradientes von Wingless. Diese zeigen, dass weniger Wingless in den *wg*-exprimierenden Zellen sekretiert wird, wenn diese mutant für *CG6210* sind, dass aber

kein bedeutender Effekt zu sehen ist, wenn die nicht *wg*-exprimierenden Zellen mutant sind.

Experimente mit zellbiologischen Markern zeigen, dass CG6210 in den frühen Endosomen, in den gemeinsamen Endosomen und in den späten Endosomen lokalisiert ist. Man kann ein Modell vorschlagen, in dem Wingless das gemeinsame Endosom erreicht und dort vor der Sekretion mit CG6210 assoziert. CG6210 and Wingless könnten gemeinsam rezykliert werden, indem sie zusammen in die frühen Endosomen und in die gemeinsamen Endosomen transportiert werden. Zudem könnte CG6210 Wingless von den gemeinsamen Endosomen zu den späten Endosomen begleiten und so für die Degradation von Wingless wichtig sein.

Weiterführende Experimente zielen auf die Charakterisierung der physikalischen Interaktion Zwischen CG6210 und Wingless und auf die mögliche Rolle von CG6210 in der Synthese von richtig gefaltetem Wingless Protein.

1.2 Summary

The Wnt/Wingless signaling pathway controls vital processes during embryonic development and is involved in various cancers, most prominently that of the colon. Thanks to the intense research over the last few decade, we are now beginning to understand the regulatory mechanisms that govern this pathway.
In brief, this pathway consists of an extra-cellular ligand, Wnt/Wingless, which upon binding its receptor, Frizzled, elicits a transcriptional response mediated by the cytoplasmic protein ß-catenin/Armadillo.

The goal of this thesis was to further elucidate the molecular mechanism of Wnt/Wingless signaling. It extends and complements work by a former and a current member of the laboratory, Corina Schütt and Carla Bänziger respectively. Corina performed a screen for new components of the pathway and isolated three complementation groups. Carla identified *CG6210* as the gene mutated in the third complementation group, called 3L3. *CG6210* encodes a novel protein that has homologues of this gene are found in all metazoans, similar to other members of the Wnt/Wingless signaling pathway.
Genetic analysis showed that CG6210 is a positive component of the Wingless signaling pathway. Experiments performed in imaginal discs led to the conclusion that CG6210 plays an important role in *wg*-expressing cells. Rescue assays confirmed this last result and additionally showed that the function of the gene is not required in non-*wg*-expressing cells.
Additional work was aimed at identifying the role of CG6210 in the formation of the Wingless gradient, and showed that less Wingless can be released by the *wg*-expressing cells when they are mutant for *CG6210*, whereas no significant effect is detected when non-*wg*-expressing cells are mutant.
Studies performed with cell biological markers suggested that CG6210 is located in the early endosomes, the common endosomes, and the late endosomes. We can speculate that Wingless travels from the trans-Golgi to the common endosome, then associates with CG6210 and is released to the cell membrane for secretion. Moreover, Wingless and CG6210 could also be recycled together through the early endosomes and the common endosomes. Finally, CG6210 could be important for the degradation of

Wingless by leaving together with Wingless the common endosomes to reach the late endosomes.

Further experimentation aims at characterizing the physical interaction of CG6210 with Wingless and the possible biochemical role of CG6210 in the synthesis of a properly folded Wingless protein.

2 Introduction

Some of the most profound questions in biology were first asked by ordinary people confronting events in their everyday lives. The miracle of a newborn baby raises questions about how an egg assembles itself into an animal. The tragedy of a cancer diagnosis leads to questions about how normal cells can switch to an aberrant growth (Peifer and Polakis, 2000). Although seemingly distinct, biological processes like embryogenesis and carcinogenesis both rely on cell communication via identical signaling pathways, and it is now clear that these signaling pathways have been highly conserved throughout evolution. This is why most of the studies of development can be done in a small number of "model" organisms such as the fruit fly *Drosophila melanogaster*, that are easily amenable to experimental manipulation, and many of the rules which are defined apply to human physiology as well (Wolpert, 1998).

Members of the Wingless (Wg) or Wnt gene family represent a good example of proteins, which play a pivotal role in the development of organisms and which are present from the worm *C. elegans* to humans. They were first identified in *Drosophila melanogaster* as being necessary for the formation of the wing (Sharma and Chopra, 1976), and in mice for their role in tumorigenesis (Nusse and Varmus, 1982). Wnt is an acronym composed of the name *Int-1*, that had been initially assigned to the gene over-expressed in Mouse Mammary Tumour Virus infected cells, and of the name for its fly homologue *wingless*, that describes the striking loss-of-function phenotype (Nusse et al., 1991).

2.1 Wnt/Wingless signaling in *Drosophila melanogaster*

In the organism *Drosophila melanogaster* Wg, the best-characterized member of the Wnt family, functions as a segment polarity gene in the embryo and as a morphogen in the larval development.

2.1.1 *Drosophila* embryonic segmentation and Wingless signaling

In 1980 Nüsslein and Wieschaus used the cuticle of the *Drosophila* embryo in their illustrious screen to identify patterning mutants. They recognized that the exoskeleton pattern of this insect provides a fantastic readout of the underlying genetic program, and

showed that the first steps of embryonic segmentation involve the progressive subdivision of the A/P axis into 14 parasegments by maternal, gap, pair-rule and segment polarity genes (reviewed by Ingham and Martinez Arias, 1992; St Johnston and Nüsslein-Volhard, 1992).

The key segment polarity genes are *wg*, which is expressed in the posterior region of each parasegment, and *hedgehog* (*hh*), whose product is secreted by the cells expressing *engrailed* (*en*) in the anterior region of the neighboring parasegments. The other segment polarity genes function as positive or negative regulators of either the Wg or Hh signaling pathways (reviewed by Perrimon, 1994). Early in embryogenesis, at stage 9–10, the expression of Wg and Hh is interdependent. The Wg protein maintains En expression in adjoining cells, and En-expressing cells secrete Hh, which in turn supports Wg expression in neighbouring cells (DiNardo *et al*., 1988; Martinez Arias *et al*., 1988; Hidalgo and Ingham, 1990). In this way, the parasegment boundary is maintained and stabilized (Bejsovec and Martinez Arias, 1991; Vincent and O'Farrell, 1992). At the end of stage 10, En expression becomes independent of Wg and at this point the roles of Wg and Hh in intrasegmental patterning start (Figure 1).

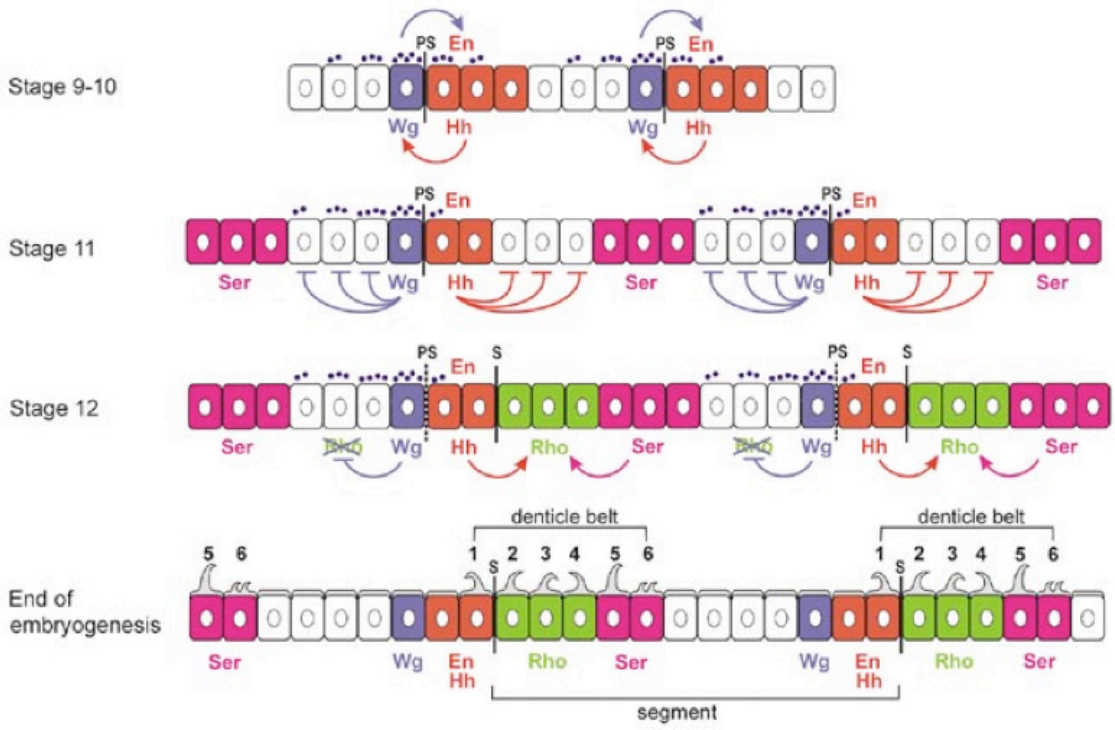

Figure 1 - Generation of an intrasegmental pattern in the *Drosophila* embryo (adapted from Sanson, 2001); S: segment boundary; PS: parasegment boundary.

In the ventral ectoderm, once Wg and En/Hh stripes are established, new stripes form; these localize ligands from two other signaling pathways: Serrate (Ser), which activates the Notch receptor, and Spitz (Spi), which activates the Epidermal Growth Factor Receptor (EGFR). The interplay of the four signaling pathways activates downstream genes in stripes as narrow as single-cell width. At the end of *Drosophila* embryogenesis, two types of cuticle are produced on the ventral side of the abdominal epidermis: some cells secrete a smooth cuticle, whereas others secrete hairs or denticles of various sizes and shapes (reviewed by Martinez Arias, 1993). About six rows of denticle-making cells build a “denticle belt”. Each abdominal belt is separated from the next by about six rows of cells secreting a smooth cuticle (Figure 2).

Two important features of the role of Wg during the embryonic development must be underlined.

First, the gene *shaven-baby (svb)* is necessary and sufficient to direct denticle formation cell-autonomously in the embryo (Payre *et al*., 1999). Thus Wg specifies smooth cuticle since it can repress the expression of *svb*, whereas the expression of *svb* seems to be activated by the EGFR signaling pathway. As a consequence, an impaired Wg signaling in the embryo will lead to a lawn of denticles of the ventral cuticle instead of the alternating pattern of naked cuticles and denticle. Since Hh and Wg signaling are interdependent during early embryogenesis, a loss of *en* or *hh* expression will finally lead to the same phenotype. On the other hand, over-expression of Wg signaling leads to a naked phenotype (Noordermeer et al., 1992).

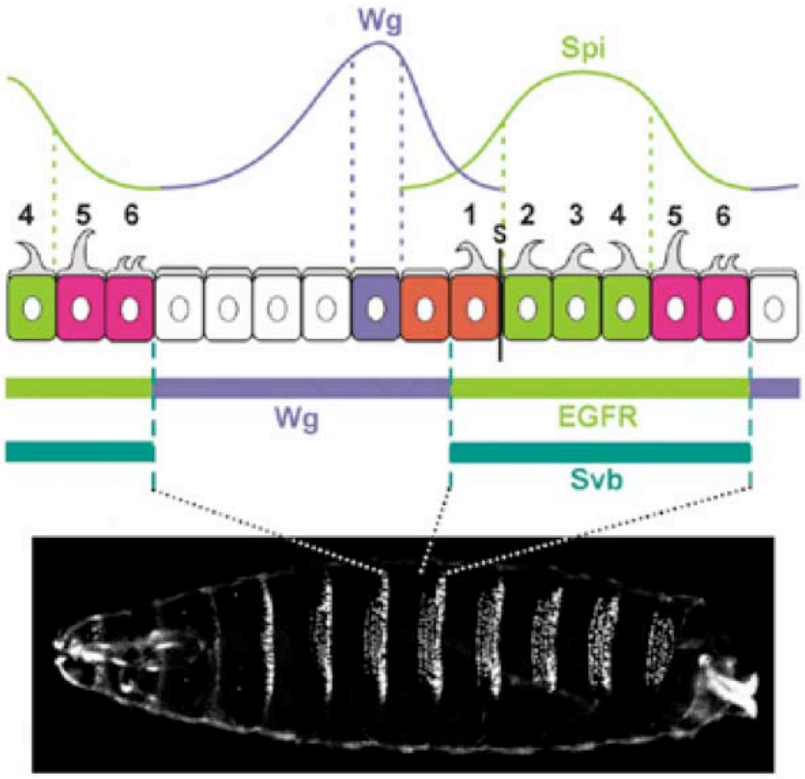

Figure 2 - Control of epidermal differentiation by the intrasegmental pattern (adapted from Sanson, 2001)

Secondly, the symmetric Wg spread in both anterior and posterior directions (Gonzales et al., 1991; van de Heuvel et al., 1989) becomes later asymmetric, indicating that the distribution of Wg ligand is regulated.

2.1.2 Imaginal discs of *Drosophila* larvae and Wingless signaling

Imaginal discs have been the best starting material to study Wg function in *Drosophila* larvae. Imaginal discs are hollow sacs of cells that make adult structures during metamorphosis. They are so named, because “imago” is the old term for an adult insect, and their shape is discoid (Figure 3). They arise as pockets in the embryonic ectoderm and grow inside the body cavity until the larva becomes a pupa; at this point they evaginate to form the body wall and appendages. In a *Drosophila melanogaster* larva there are 19 discs: nine pairs form the head and thorax, and a medial disc forms the genitalia (Lewis, 2002).

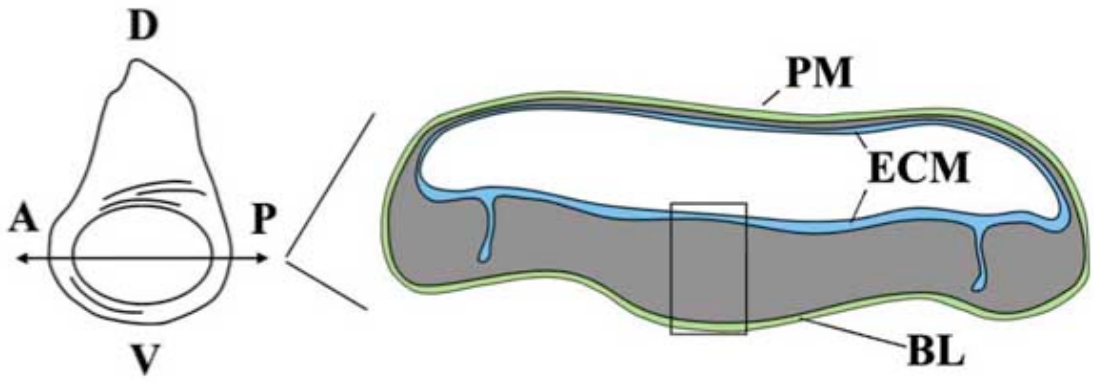

Figure 3 - General architecture of wing imaginal discs. Discs are folded epithelial structures composed of the epithelium and the overlying peripodial membrane (PM); ECM: Extracellular Matrix; BL: Basal Lamina; A: Anterior; P: Posterior; D: Dorsal; V: Ventral (Vincent and Dubois, 2002).

Wg in the wing imaginal disc has become a conventional example of a morphogen. A morphogen is defined as „any substance active in pattern formation whose spatial concentration varies and to which cells respond differently at different threshold concentrations“ (Wolpert, 1998). Wg is produced by cells along the dorso-ventral (D/V) boundary, but exerts direct and long-range effects on the adjacent tissue (Neumann and Cohen, 1997; Ng, 1996; Struhl and Basler, 1993; Zecca, 1996) (Figure 4).

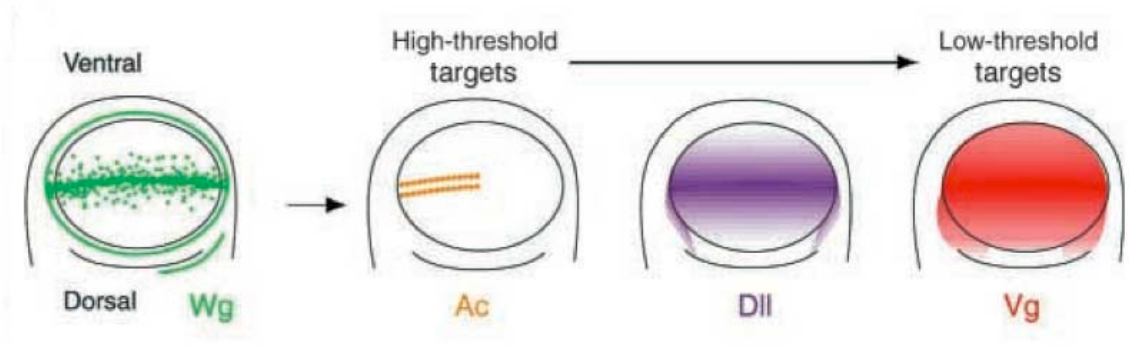

Figure 4 - Wg and its target genes; Wg is produced along the DV boundary and induces the expression of target genes, such as *Ac* (*achaete*), *Dll* (*Distalless*) and *vg* (*vestigial*) (Tabata and Takei, 2004).

In the specific case of the wing imaginal discs, *wg* needs for its expression the interplay of *apterous* (*ap*), and Notch signaling. *Ap* is a homeotic selector gene that determines the dorsal fate in the wing imaginal discs (Blair et al., 1994; Diaz-Benjumea and Cohen, 1993), and activates the Notch signaling along the D/V boundary. Notch signaling in turn activates *wg* expression (Diaz-Benjumea and Cohen, 1995; Rulifson and Blair, 1995).

2.2 The Wnt protein family

The *Wnt* genes encode a large family of secreted, cysteine-rich glycoproteins responsible for activation of the signaling pathway, which are usually 350-400 amino acids in length. These proteins share the signature WNT motif C-K-C-H-G-(LIVMT)-S-G-*X*-C and a sequence identity of at least 18%; moreover, Wnt proteins contain a signal sequence, a conserved stretch of 23-24 cysteine residues (Cadigan and Nusse, 1997), many highly charged amino acid residues, and several potential glycosylation sites. Apparently, all Wnt proteins are secreted from cells and act on cell surface receptors, either on the Wnt producing cells themselves or on adjacent cells; nevertheless, Wnt proteins do not exhibit the properties expected of soluble hydrophilic proteins, and this is most probably due to at least one lipid modification (Reichsman, et al., 1996). In vertebrates there are about 21 *Wnt* genes, while in *Drosophila* seven homologues exist. The best-characterized member of the Wnt family is *Drosophila* Wg, the vertebrate Wnt1 homologue.

For review, see (Cadigan and Nusse, 1997; Wodarz and Nusse, 1998). The *Wnt* gene homepage gives all the details and developments that are currently taking place in this field (http://www.stanford.edu/~rnusse/wntwindow.html).

2.3 The Wnt/Wingless signaling pathway

Wnt/Wg proteins can activate different intracellular cascades. Different combinations with different Frizzled receptors can also elicit different responses in the cell. These different cascades fall broadly into two categories (Figure 5): the canonical and non-canonical Wnt pathways. The non-canonical Wnt pathway is transduced through either Dishevelled or calcium, and includes the Wnt/Jnk planar cell polarity pathway and the Wnt/Ca^{2+} pathways. Although these separate Wnt pathways exist, there are cross talks and regulatory interactions between different components. Hence, Wnt signaling is considered as a signaling network rather than discrete signaling pathways (Pandur et al., 2002).

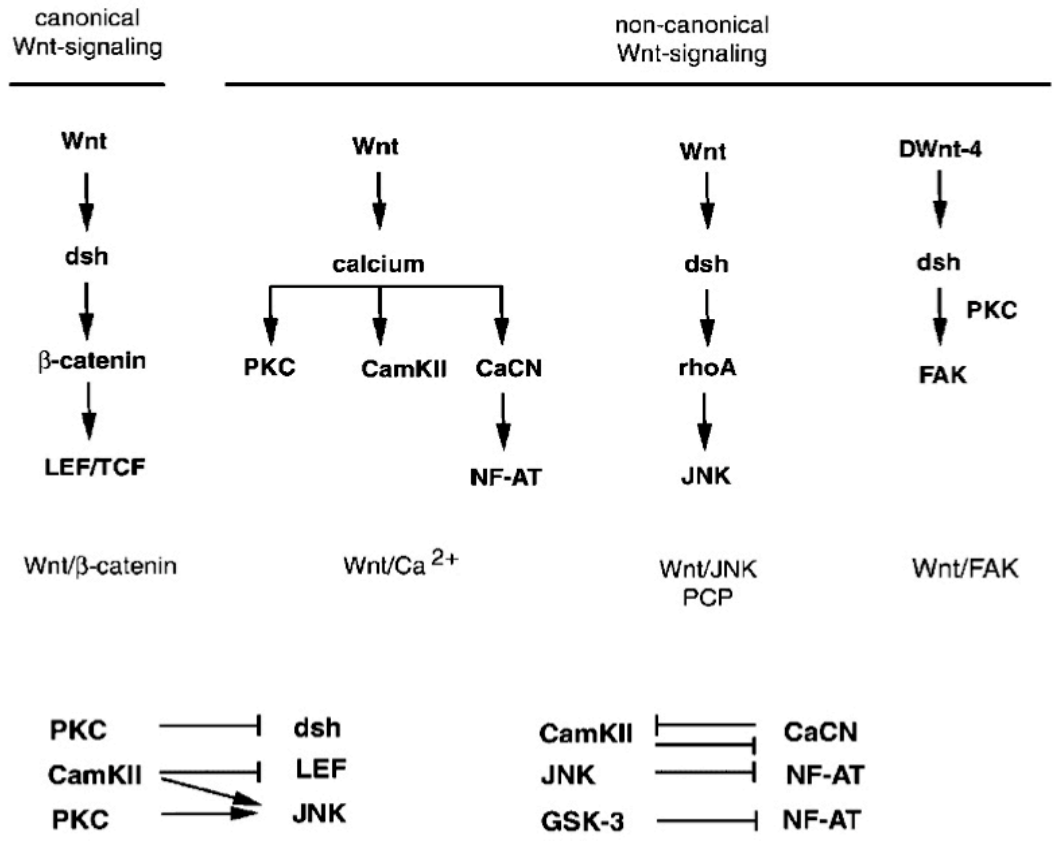

Figure 5 - Schematic representation of canonical and non-canonical Wnt signaling pathways. PKC: protein kinase C; PCP: planar cell polarity; JNK: Jun-N-terminal kinase; FAK: focal adhesion kinase (modified from Pandur et al., 2002).

The canonical Wnt signaling pathway is entirely built around regulating the state of activity of the central transducing component called Armadillo (Arm), in *Drosophila,* or β-Catenin, in vertebrates (Figure 6). In a resting cell β-Catenin is subject to constitutive degradation through the action of a cytoplasmic complex, composed by the APC protein, Axin, Glycogen Synthase Kinase-3β (GSK-3β, in *Drosophila* also named Shaggy, Sgg, or Zeste-white 3, Zw3), and Casein Kinase I□ (CKI□) (Polakis, 2001; Wodarz and Nusse, 1998). Axin is a scaffold protein and recruits Armadillo indirectly by binding APC. CKI□ and GSK-3β have been shown to sequentially phosphorylate β–Catenin on a set of N-terminal serine and threonine residues, inducing the subsequent steps of ubiquitination and proteolytic degradation through the proteasome pathway (Amit, 2002; Liu, 2002; Yanagawa, 2002).

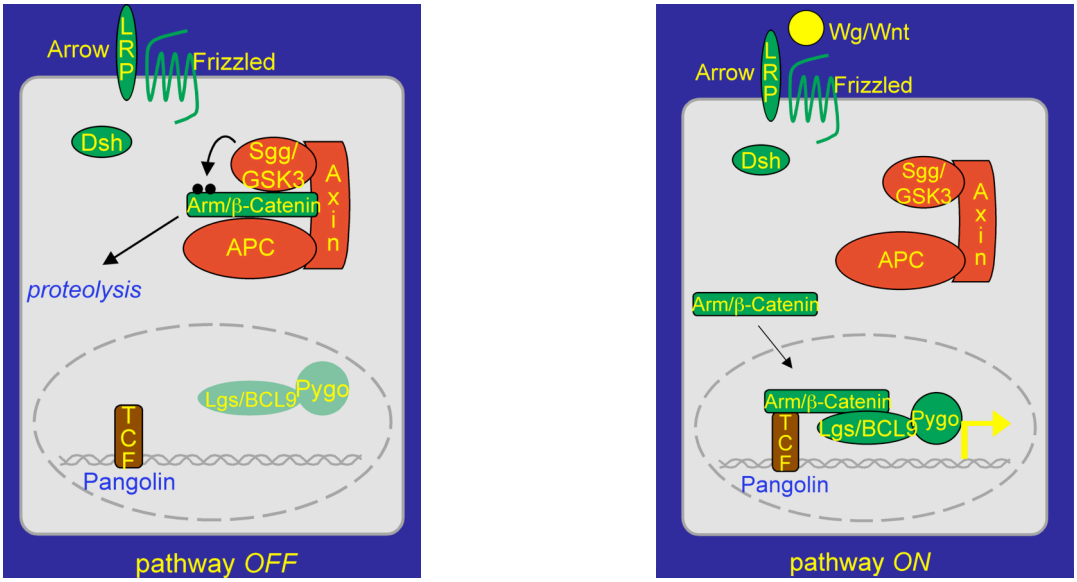

Figure 6-The canonical Wnt signaling pathway in the non activated (left) and in the activated state (right).

Upon binding of Wnt proteins to their receptors, called Frizzled and Arrow (LRPs), pathway activation is brought about by a series of cytoplasmic events that leads to stabilization and subsequent nuclear accumulation of β-Catenin (Willert and Nusse, 1998). Once in the nucleus, β-Catenin binds to the T-cell factor/Lymphoid enhancer binding factor (TCF/LEF) transcription factor proteins (Pangolin in flies) in order to activate gene expression (Behrens et al., 1996; Brunner et al., 1997). The TCF/LEF proteins contain an HMG-box DNA binding domain and have some transcriptional activator capacity. Binding of β-Catenin to TCF/LEF grants the necessary transcriptional activity to the TCF-ß-Catenin complex to activate gene expression (Cox et al., 1999; van de Wetering et al., 1997). Two nuclear proteins, BCL9/Legless and Pygopus, further aid Wnt/Wg target gene expression (Kramps et al., 2002). Besides its role in the Wnt/Wg signaling pathway, β-Catenin also binds to α-Catenin and E-Cadherin as part of the adherens junctions that physically connect cells to each other enabling the formation of solid tissues (hence the choice of the vertebrate name β-Catenin, from Latin *catena*– chain).

2.4 Wnt/Wingless processing

As previously mentioned, Wnt proteins are post-translationally modified by modifications like palmitoylation and glycosylation. A brief description of the two processes follows.

2.4.1 Palmitoylation

Many types of proteins (including cytosolic, transmembrane, and secreted proteins) are known to undergo *N*-palmitoylation or *S*-palmitoylation, i.e. the addition of palmitate via an amide or a thioester bond. This posttranslational acylation is reversible and can regulate both protein localization and function. The addition of the palmitoyl moiety increases protein hydrophobicity and promotes membrane association (Linder and Deschenes, 2003). Moreover, palmitoylation also affects intracellular trafficking in that palmitoylated proteins are frequently targeted to specific intracellular organelles as well as to detergent-resistant microdomains (DRMs) located at the plasma membrane. These DRMs, commonly referred to as lipid rafts, are rich in cholesterol and glycosphingolipids and so exist in a separate liquid-ordered phase within the plasma membrane. Raft DRMs often form signal transduction centers: the cellular machinery needed for signal transduction becomes organized as some proteins are targeted to rafts, whereas others are excluded, and cell surface receptors are sometimes localized to the same membrane microdomains where their downstream intracellular partners are also concentrated.

Secreted proteins can also be palmitoylated. Indeed, after the autoproteolytical cleavage, the N-terminal domain of Hh (HhN-p, for HhN-processed) (Lee et al., 1994) is modified by the covalent linkage of a cholesterol moiety on the C-terminus of HhN-p (Porter et al., 1996), and by the linkage of palmitate to the NH_2-terminus of HhN-p (Chamoun et al., 2001). These lipid modifications increase Hh-Np hydrophobicity, influence apical sorting of the ligand, and likely play a role in the partitioning of Hh-Np into raft DRMs (Gallet et al., 2003). Skinny Hedgehog (Ski), a putative *O*-acyltransferase, is required for the palmitoylation of *Drosophila* Hh-Np. Clonal analysis studies suggest that palmitoylation is essential for Hh signaling in the wing disc. In the absence of Skinny Hedgehog activity, HhN-p is not palmitoylated, and Hedgehog signaling activity is greatly reduced (Chamoun et al., 2001).

2.4.1.1 Palmitoylation of Wg

It was initially shown that murine Wnt-3a and *Drosophila* Wnt-8 are palmitoylated at conserved cysteine residues (Willert et al., 2003), and this discovery suggested that the lipid modifications might account for the unusual behaviour of Wnt ligands. The cysteine

necessary for the palmitoylation is the most amino-terminally conserved cysteine. Wg, the *Drosophila* Wnt-1 homologue, carries this conserved cysteine at position 93, and there is evidence that Wg is also lipid modified (Zhai, et al., 2004). The gene *porcupine* plays an important role in this process, since *porcupine,* like *skinny hedgehog*, also encodes a putative multipass transmembrane protein localized in the Endoplasmatic Reticulum (ER), which belongs to the membrane-bound O-acyltransferase superfamily (Hofmann, 2000; Kadowaki, et al. 1996). *porcupine* homologues have been identified in *Xenopus*, mouse, human, and *Caenorhabditis elegans* (Tanaka, et al., 2000; Thorpe et al., 1997; Caricasole, et al., 2002). *porcupine* is required for Wg activity, and in *porcupine* mutants Wg seems to accumulate within the expressing cells and all extracellular Wg staining appears to be absent (Hofmann, 2000; van den Heuvel, et al., 1993). The Wg secretion defect can be bypassed by driving over-expression of Wg. Studies with transgenic S2 cells (Tanaka et al., 2000; Tanaka et al., 2002) have shown that Porcupine and the N-terminal portion of Wg can be co-immunoprecipitated in the same complex, suggesting that Porcupine may interact directly with Wg. Later it has been shown that *porcupine* is necessary for lipidation of Wg, which takes place in the ER, and for its targeting to the lipid raft microdomains (Zhai, et al., 2004). It is not known whether Wnt proteins undergo multiple lipid modifications.

Regarding intracellular trafficking of Wg, the lipid group could act as a sorting signal, which prevents Wg secretion through the classical constitutive pathway: the palmitoyl moiety could target the ligand to polarized vesicles that transport Wg to unique sites at the cell surface. This pathway is similar to apical secretion in mammalian cells, where secretory proteins partition with cholesterol-sphingolipid rich microdomains within the trans-Golgi network and are then transported directly to the plasma membrane (Ikonen, 1998).

2.4.2 Glycosylation

Wg protein, which has a length of 468 AA, carries three potential sites for N-linked glycosylation at position 103, 108, and 414. Tanaka et al. showed that when *wg* is expressed in S2 cells, three forms of Wg with different molecular sizes are detected (forms I, II, and III) and that the form III is the major protein detected in early *Drosophila* embryos and imaginal discs. Since only form I is detectable in the presence of tunicamycin (an inhibitor of *N*-glycosylation), forms II and III contain one, respectively

two, *N*-linked glycan chains. In the presence of ectopic *porc*, form III is accentuated, and a larger species, form IV, is also observed. Thus, Wg is normally *N*-glycosylated at two sites, and Porc stimulates this processing, inducing also the ectopic *N*-glycosylation of Wg at a third site. Tanaka et al. further showed evidence that forms I, II, and III are located inside the ER membrane, and thus that forms I and II are probably posttranslationally *N*-glycosylated in the ER. Finally, Tanaka et al. argued that Wg is more efficiently *N*-glycosylated by a co-translational manner if disulfide bond formation is inhibited using DTT, i.e. a reversible inhibitor of disulfide bond formation (Tanaka et al., 2002).

2.5 Wingless trafficking: which route?

In epithelia of *Drosophila* embryos, Wg has been shown to pass through the endoplasmic reticulum and Golgi apparatus of *wg*-expressing cells; moreover it has been detected in intracellular vesicles and in multivesicular bodies in those cells and in adjacent non-*wg*-expressing cells (van den Heuvel et al., 1989; Gonzales et al., 1991).
In the wing discs, spots of Wg in the cells away from the source appear to reflect vesicles of internalized Wg protein (Strigini and Cohen, 2000), and in these cells Wg was also observed to co-stain with the endosome marker Hrs (Lloyd et al., 2002). In addition, using the conventional labeling protocol, most Wg appears to be concentrated above the nuclei, near the junctional complex, in *wg*-expressing cells. In contrast, extracellular Wg was mainly associated with the basolateral surface of cells, and the extracellular gradient in the wing discs seems to form on the basolateral surface of the wing disc (Strigini and Cohen, 2000).

Interesting studies performed in *Drosophila* embryos used GFP-Wg in order to visualize the localization of the morphogen (Pfeiffer et al., 2002). These studies showed that GFP, and thus Wg, is present almost only in the producing cells and that 50% of the GFP-Wg-positive vesicles are endocytic, since they co-localize with Rho-Dx (Rho-Dx is tetramethylrhodamine dextran and is readily up taken by epidermal cells, thus marking the endocytic pathway). Moreover, GFP-Wg vesicles seen in nonexpressing cells also contain Rho-Dx, thus confirming their endocytic nature. One can conclude that, although much intracellular Wg is endocytic, most endocytosis of Wg occurs in secreting cells, which have plenty of Wg available at their surface.

Pfeiffer et al. also showed for the first time that endocytic vesicles containing Wg are able to return to the cell surface, providing the first direct observation of ligand recycling in a living embryo. This result shows that planar transcytosis (see 2.7.4) is plausible, and this recycling might ensure maximal signaling (Pfeiffer et al., 2002).

In order to better understand the possible routes Wg may take in the *wg*-expressing and in the non-*wg*-expressing cells we look in more detail at the membrane trafficking pathway in polarized epithelial cells.

2.5.1 Membrane trafficking pathway in polarized epithelial cells

In all polarized cells, a central role in trafficking is played by the compartment, which carries the names of apical recycling endosome (ARE), common endosome (CE), common recycling endosome or subapical compartment (SAC) (Figure 7).

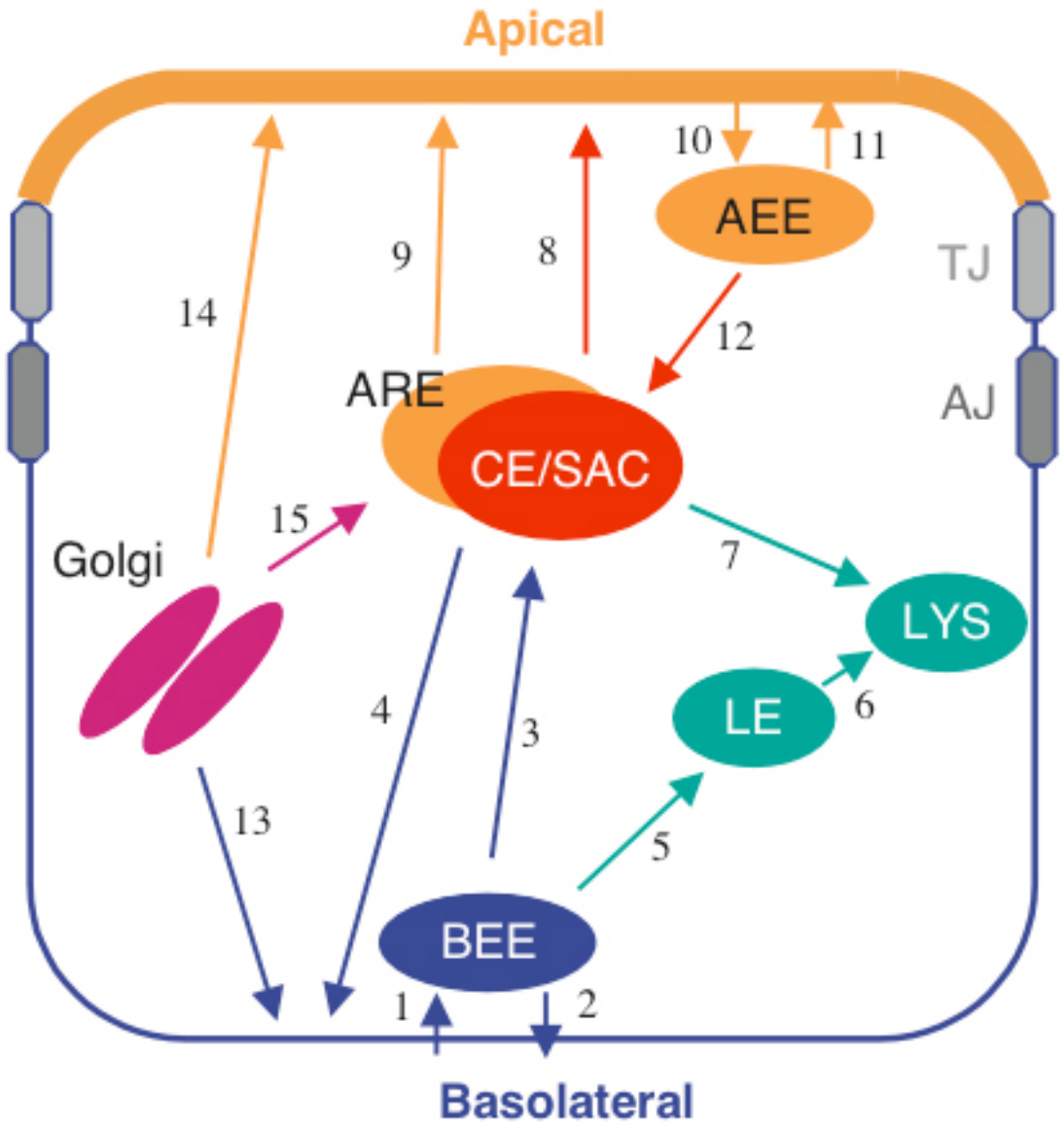

Figure 7 - Membrane trafficking pathways in polarized epithelial cells. BEEs: basolateral early endosomes; AEEs: apical early endosomes; LE: late endosome; LYS: lysosome; CE: common endosome; SAC: subapical compartment; ARE: apical recycling endosome; AJ: adherens junctions; TJ: tight junctions (adapted from Hoekstra et al., 2004).

Macromolecules, internalized either from the basolateral (1) or apical (10) surface, are delivered to basolateral early endosomes (BEEs) and apical early endosomes (AEEs), respectively. From here, molecules can recycle to the plasma membrane domain of origin (2, 11), or are directed in the degradative, late endosomal (LE)/lysosomal (LYS) pathway (5, 6). Alternatively, basolaterally (3) and apically (12) derived molecules are sorted into a recycling route and meet in a compartment, referred to as the common

endosome (CE), subapical compartment (SAC), or apical recycling endosome (ARE). From here, polarized recycling can occur to the basolateral (4) or apical (8) surface. Apical surface targeting can occur directly from the CE/SAC (8), or following a relay from the CE/SAC via the ARE (9). From the CE/SAC, proteins can also reach the lysosomes (7).

In the biosynthetic pathway, most molecules are sorted directly to the basolateral (13) or apical (14) surface. In the latter, some proteins might travel via CE/SAC, prior to their delivery to the apical surface domain (15) (Hoekstra et al., 2004).

2.5.2 Rab proteins

Rab proteins, which constitute the largest family of monomeric GTPases, and their effectors, coordinate consecutive stages of transport, such as vesicle formation, vesicle and organelle motility, and tethering of vesicles with target membranes. The ability of Rabs to cycle regularly between GTP- and GDP-bound forms imposes temporal and spatial regulation to membrane transport. Rabs mediate the first specific tethering event between a vesicle and its target membrane, and so provide a complementary layer of regulation to that subsequently provided by SNARE pairing (Zerial and McBride, 2001). Specific Rab effectors have been implicated in various membrane tethering events, including delivery of post-Golgi vesicles to the plasma membrane (for example, the exocyst complex), tethering of endosomes (EEA1) or vacuoles (the HOPS complex). It is important to notice that distinct Rab proteins become specifically expressed in the course of development of cell polarity, and some of these are closely associated with the SAC. These Rab proteins often display distinct subcompartmental localizations, which might be instrumental in the regulation of distinct transport steps, and this can be also used in order to label the different compartments (Hoekstra et al., 2004).
Finally, Rabs have been implicated in regulating vesicle motility through interaction with both microtubules and actin filaments of the cytoskeleton.

Some Rab proteins are used as markers in *Drosophila* to visualize different compartments. For example, Rab4 localizes to the CE and is involved in directing vesicular transport to the recycling endosome, possibly at the level of vesicle assembly and budding (de Wit et al., 2001); Rab11 is also involved in targeting vesicles to the recycling compartment. Rab5 is required for the fusion between endocytic vesicles and

early endosomes, whereas Rab7 mediates lysosomal targeting and localizes in the late endosomes.

2.6 Wnt/Wingless proteins are secreted molecules

The morphogens Wnt and Hh can act on other cells at distant site; this means that they need to be released from the producing cells and travel to the receiving cells. The release of Hh from cells requires an dedicated transport protein called Dispatched (Disp). Initially found in *Drosophila* (Burke et al., 1999), but functionally conserved in mammals (Caspary et al., 2002; Kawakami et al., 2002), Disp is a multiple-pass, transmembrane protein. In the absence of Disp, Hh is not secreted from cells and is unable to signal to neighbor cells. Interestingly, non-cholesterol modified HhN is not dependent on Disp; it is secreted and is fully active, suggesting that the primary function of Disp is to transport cholesterol-modified Hh (Burke et al., 1999). However, non-cholesterol modified HhN also lacks palmitate (Pepinsky et al., 1998); it therefore remains possible that Disp is specifically needed for the release of palmitoylated Hh from cells.

There is no evidence of a similar transporter for Wnt molecules, although a gene identified in *C. elegans, mom-3*, is required in Wnt-producing cells (Rocheleau et al., 1997). This gene (also called *mig-14*) still needs to be characterized molecularly.

It is unclear how the palmitate can influence Wnt and Hh transport from one cell to another. Variants of Hh that lack the palmitoylation site are secreted from cells, perhaps more efficiently than the wild-type Hh (Chamoun et al., 2001; Pepinsky et al., 1998). The same happens to Hh protein in the absence of *ski* (Chamoun et al., 2001); however, the nonpalmitoylated Hh protein is not functional. Concerning secretion, the effect of disrupting palmitoylation of the Wnt proteins is strikingly different to disrupting palmitoylation of Hh. For example, a *wg* allele (wg^{S21}), in which the palmitoylated cysteine is mutated into a tyrosine (Couso and Arias, 1994; Willert et al., 2003), leads to a protein that is not secreted. The lack of secretion of Wnt-mutant proteins is commonly seen and is usually attributed to protein misfolding. More surprising is the observation that, in the absence of *porc*, Wg is also retained within cells (van den Heuvel et al., 1993). At first glance, it might seem paradoxical that a Wnt without lipid is not secreted, in particular in comparison with Hh, as one might expect that a less hydrophobic variant

would be more easily released from cells. This difference might be explained by the overall structure of Wnt, which is rich in cysteines presumably linked by disulphide bridges. In the absence of *porc*, the conserved cysteine residue will have a free sulfhydryl group that may interfere with normal disulphide formation of other cysteines, leading to a misfolded and retained protein. Moreover it has been shown for the murine Wnt-3a that if the C77 is mutated into an A, i.e. the SH group of cysteine is missing as in the case of palmitoylated Wnt, Wnt-3a is normally secreted (Willert et al., 2003). In contrast to the palmitate of Wnt, the one on Hh is attached to a cysteine through an amide at the N terminus, which leaves the sulfhydryl group free. As a consequence, the lack of palmitate on Hh (in the *ski* mutant) does not change the overall number of free sulfhydryl groups and this could explain the different behaviour of the two proteins. In addition, none of the three cysteines in Hh are involved in disulphide formation (Hall et al., 1997).

2.7 Wnt/Wingless protein movement

It has been demonstrated that morphogens are transported over distances of tens of cell diameters and that stable gradients form, but how the distribution of a morphogen is established still remains unclear.

The range and the slope of a morphogen gradient can be affected by the rate of production from the source, the rate of transport, and the rate of degradation (Vincent and Dubois, 2002).

Focusing on the transport of morphogens, we consider two types of mechanisms:

I. Passive transport through
   diffusion (2.7.1) or
   facilitated diffusion if bound to a carrier (2.7.2).
II. Active transport through:
   long cellular extensions (2.7.3, Teleman et al. 2001) or
   transcytosis, i.e. successive rounds of internalization of the ligand by endocytosis followed by resecretion (2.7.4).

Before considering the details of the mechanism of transport, some important considerations must be noted.

First, the transport of mophogens has to be non-directional and rapid. As shown in imaginal discs, clones of cells that ectopically express either Wg or Dpp activate downstream targets symmetrically in all directions (Lecuit et al., 1996; Nellen et al., 1996). Moreover GFP-Dpp spreads symmetrically around the expressing clones (Entchev et al., 2000).
Secondly, several experiments have shown that morphogen gradients form rapidly. In one experiment it has been shown that Dpp moves at a rate of four-cell diameters/hr (Entchev et al., 2000). For Wg, a temperature-sensitive allele of *shibire* was used to investigate the temporal control of production: 1 hr after the onset of secretion the gradient is reconstituted, implying a rate of transport of about 50 μm/hr. (Strigini and Cohen, 2000). These results also rule out the possibility that gradients could be formed by inheritance of the signal through cell proliferation.

2.7.1 Diffusion

In the diffusion model of Wg transport, secreted Wg spreads through the extracellular space to the target cells independently of intracellular trafficking. Although diffusion is a very straightforward mechanism of morphogen transport, the ability of Wg to travel freely is controversial, since in cell culture, Wg is tightly associated with cell membranes and the extracellular matrix by interacting with glycosaminoglycans (Reichsman et al., 1996; Bradley and Brown, 1990). Additionally, some Wnts have been shown to be palmitoylated (Willert et al., 2003), a posttranslational modification that enhances membrane association (Resh, 1999).

2.7.1.1 The role of Shibire

Although Wg might bind to cell membranes, evidence from wing disc experiments suggest that Wg is capable of spreading even in the absence of intracellular trafficking. This was shown in experiments with wing imaginal discs of *shibire*^{ts} mutant flies (Strigini and Cohen, 2000). *shibire* encodes the *Drosophila* homologue of the GTPase Dynamin (van der Bliek and Meyerowitz, 1991; Chen, et al., 1991), and Dynamins have been implicated in the internalization of clathrin-coated endocytic vesicles and in the internalization of caveolae (Damke et al., 1994; Henley et al., 1998; Oh et al., 1998).
In wing imaginal discs, it was first shown that clones of *shibire*^{ts1} mutant cells (larvae were then shifted to 32°C for 3 hours to inactivate Shibire) lack punctate Wg, indicating

that dynamin activity is required for Wg internalization. Moreover, extracellular Wg on the surface of these *shibire* mutant clones was present at higher concentration than on nearby wild-type cells, and it can be detected in wild-type cells on either sides of mutant clones (Strigini and Cohen, 2000) (Figure 8).

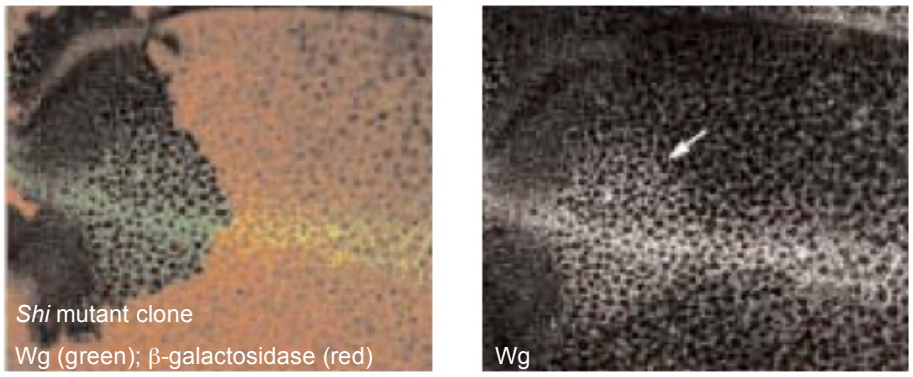

Figure 8 – Left side: Wg expression visualized by extracellular labeling (green) in a disc carrying a large *shibire* mutant clone; cells mutant for *shibire* are marked by the absence of β-galactosidase (red). Wg expression is shown separately on the right side (modified from Strigini and Cohen, 2000).

Wg on the *shibire* mutant clones probably reflects Wg secreted by nearby wild-type tissue that has moved across the clone and the local accumulation reflects impaired endocytosis. Dynamin-mediated endocytosis appears thus to play a significant role in removing secreted Wg from the extracellular space and therefore it may help to maintain a steep gradient. Taken together, these data strongly suggest that Wg is capable of spreading through a patch of *shibire* mutant cells, and it can therefore travel in the absence of Dynamin-mediated endocytosis in the wing disc. In contrast to these results, previous studies have proposed that in the embryo *shibire* dependent endocytosis has an important role in Wg transport (Bejsovec and Wieschaus, 1995; Moline et al., 1999), and so different mechanisms may be used between the embryonic ectoderm and the imaginal discs.

Additionally, *shibire* seems to be important in the secretion of Wg. This hypothesis is derived from studies made with discs of *shibire*^{ts1} larvae, which shows little or no extracellular Wg (extracellular Wg turn-over may be rapid when the entire disc is *shibire* mutant, see 2.9), and an intense band of intracellular Wg accumulation is observed at the D/V boundary (Figure 9 and Figure 10).

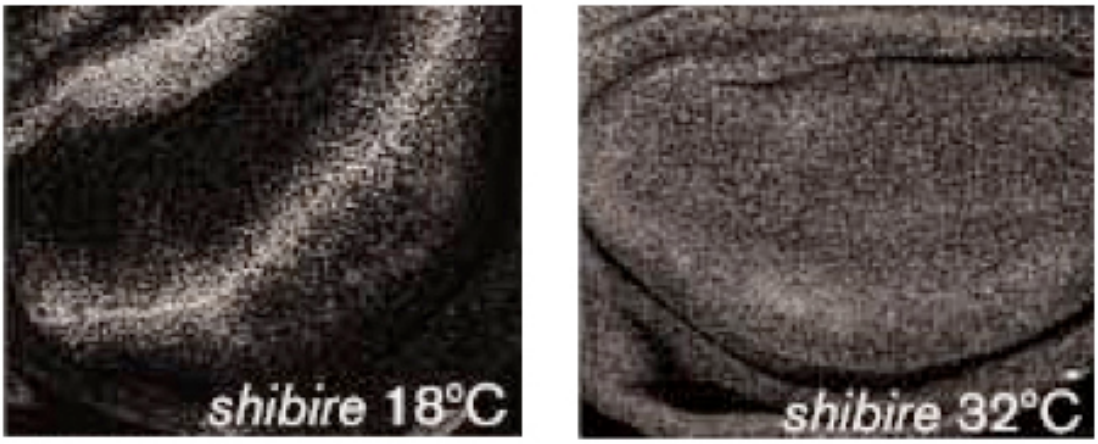

Figure 9 - Extracellular Wg expression in *shibire*^{ts} mutant discs at 18 (at this temperature Shibire is active) or 32 degrees (Shibire is then inactivated) (modified from Strigini and Cohen, 2000).

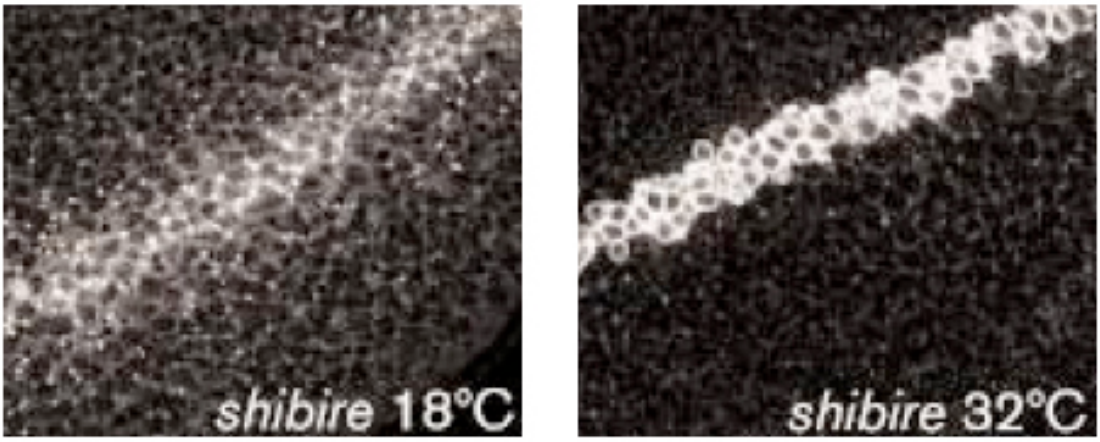

Figure 10 - Wg expression in *shibire*^{ts} mutant discs at 18 or 32 degrees (modified from Strigini and Cohen, 2000).

The role in secretion may make more sense if one considers that *shibire* encodes the only *Drosophila* dynamin identified to date (van der Bliek, 1999), and that Shibire protein may thus have a role in the formation of transport vesicles at the trans-Golgi network. In fact, it has been shown that Dynamin-2, one of the Shibire vertebrate homologues, localizes at the trans-Golgi network and that it is necessary for the vesicles formation from the trans-Golgi network (Jones, 1998). Hence, the traffic of vesicles from the trans-Golgi to the plasma membrane might be blocked in *shibire* mutant cells. Alternatively, blocking Shibire-dependent endocytosis might impair membrane traffic, and indirectly reduce Wg secretion. Moreover it has also been shown that Dynamin plays a crucial role

in the membrane fusion (Peters et al., 2004), and this function could be necessary in the process of Wg secretion. In the *Drosophila* embryo, however, *shibire* function is not required for Wg secretion. In fact, in *shibire*^{ts} mutant embryos shifted to the restrictive temperature just before the beginning of Wg expression, downstream targets of Wg signaling are still induced (Bejsovec and Wieschaus, 1995). This difference further suggests that there might be differences in the mechanism of Wg secretion in the embryo ectederm and the imaginal discs.

2.7.1.2 Heparan sulfate proteoglycans

Studies in *Drosophila* and vertebrates have demonstrated the crucial roles of heparan sulfate proteoglycans (HSPGs) in Wnt/Wg, Hedgehog (Hh), transforming growth factor-ß (TGFß) and fibroblast growth factor (FGF) signaling pathways during development (Lin, 2004).

HSPGs are cell-surface and extracellular matrix (ECM) macromolecules that are composed of a core protein to which heparan sulfate (HS) glycosaminoglycan (GAG) chains are linked (Bernfield et al., 1999; Esko and Selleck, 2002). HSPGs are classified into several families based on their core protein structure (Figure 11). Glypicans and Syndecans are two major cell surface HSPGs, and are linked to the plasma membrane by a glycosylphosphatidylinositol (GPI) linkage or a transmembrane domain, respectively. Perlecans are secreted HSPGs that are mainly distributed in the ECM. Although Glypicans and Perlecans exclusively bear HS GAG chains, Syndecans are decorated with both HS and chondroitin sulfate (CS). Glypicans, which are linked to the plasma membrane by a glycosyl phosphatidylinositol (GPI) linker, represent the main cell surface HSPGs. All three families of HSPGs are evolutionarily conserved from vertebrates to *Drosophila* and *C. elegans* (Esko and Selleck, 2002; Nybakken and Perrimon, 2002). The *Drosophila* genome encodes four HSPG homologues:

- one Syndecan (Sdc) (Johnson et al., 2004; Spring et al., 1994; Steigemann et al., 2004),
- two Glypicans [Division abnormally delayed (Dally) and Dally-like protein (Dlp)] (Baeg et al., 2001; Khare and Baumgartner, 2000; Nakato et al., 1995),
- one Perlecan [Terribly reduced optic lobes (Trol)] (Datta, 1995; Voigt et al., 2002).

To date, most HSPG studies have demonstrated the importance of their HS chains. HS chains are polysaccharides synthesized in the Golgi apparatus and contain repeating disaccharide units of uronic acid linked to glucosamine (Esko and Selleck, 2002).

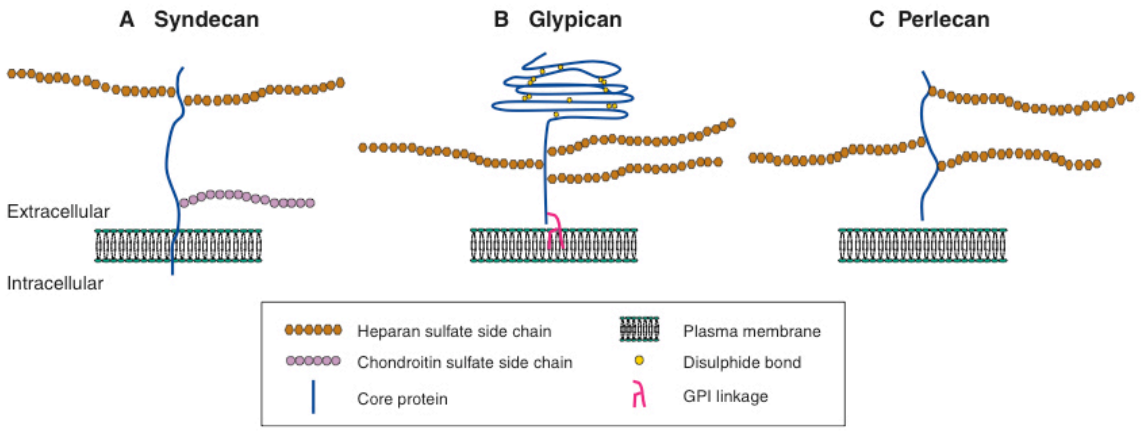

Figure 11 - The three main classes of cell-surface heparan sulfate proteoglycans (HSPGs). (A) Syndecan core proteins are transmembrane proteins. (B) The glypican core proteins are disulphide-stabilized globular core proteins that are linked to the plasma membrane by a glycosylphosphatidylinositol (GPI) linkage. (C) Perlecans are secreted HSPGs that carry HS chains (from Lin, 2004).

HS chain biosynthesis is initiated at the GAG attachment site(s) of the core protein, which contains two to four Ser-Gly sequences. Various glycosyltransferases and modification enzymes are involved in the polymerization and modification processes of HSPG biosynthesis. These enzymes are conserved in *Drosophila* and vertebrates (Esko and Selleck, 2002; Lin and Perrimon, 2003; Nybakken and Perrimon, 2002) (Figure 12).

Mutant (gene)	Protein (mammalian homolog)	Function
sugarless (*sgl*)	UDP-glucose dehydrogenase	GAG biosynthesis; effects on Wg, FGF, Dpp signaling
sulfateless (*sfl*)	N-deacetylase/N-sulfotransferase	HS modification (mainly in sulfation); effects on Wg, Hh, and FGF signaling
tout-velu (*ttv*)	EXT1	HS co-polymerase; effects on Hh signaling and movement, Wg distribution, Dpp signaling and distribution
sister of ttv (*sotv*)	EXT2	HS co-polymerase; effects on Hh signaling and movement, Wg distribution, Dpp signaling and distribution
brother of ttv (*botv*)	EXTL3	HS polymerase; effects on Hh signaling and movement, Wg signaling and distribution, Dpp signaling and distribution
fringe connection (*frc*)	UDP-sugar transporter	Transfer of UDP-glucuronic acid, UDP-N-acetylglucosamine and possibly UDP-xylose from the cytoplasm into the lumen of the ER/Golgi; effects on Wg, Hh, FGF, and fringe-dependent Notch signaling
slalom	Adenosine 3′-phosphate 5′-phosphosulfate transporter	Transporter for adenosine 3′-phosphate 5′-phosphosulfate from the cytosol into the Golgi lumen; effects on Wg, Hh, FGF and DV patterning mediated by Pipe

Figure 12 - Drosophila heparan sulfate (HS) biosynthesis mutants (modified from Lin, 2004).

The role of HSPGs in Wg signaling was first revealed by the identification of sugarless (*sgl*) (Binari et al., 1997; Hacker et al., 1997; Haerry et al., 1997) and sulfateless (*sfl*) (Lin and Perrimon, 1999) as segment polarity genes in *Drosophila*. The *Drosophila* EXT proteins, Tout-velu (Ttv), Sister of ttv (Sotv) and Brother of ttv (Botv) are all required for normal Hh, Wg and Dpp functions during wing development (Bornemann et al., 2004; Han et al., 2004a; Takei et al., 2004). Consistent with their reported roles in HS GAG biosynthesis, mutations in any of these genes lead to striking reductions in HS levels (Bornemann et al., 2004; Han et al., 2004a; Takei et al., 2004; Toyoda et al., 2000a; Toyoda et al., 2000b), since these proteins do not function redundantly in HS GAG biosynthesis (Han et al., 2004a).

It has been shown that mutations in any of the EXT genes in the *Drosophila* wing lead to a reduction of Hh, Dpp and Wg, both in the morphogen-expressing region and in the receiving region. Moreover, morphogens accumulate at the front of the mutant clones for EXT genes (Takei et al., 2004).

2.7.1.2.1 HSPGs and Dpp

Elegant experiments performed with Dpp showed that extracellular Dpp fails to move across mutant clones for *sfl*, which are expected to impair the function of all HSPGs (Lin and Perrimon, 1999; Lin and Perrimon, 2000), or double mutant clones for *dally* and *dlp*. Additionally, extracellular Dpp levels were reduced in wild-type cells behind clones of *dally-dlp* mutant cells or cells mutant for *sfl* (Belenkaya et al., 2004). These data suggest that HSPGs create an environment that supports the efficient movement of the morphogen molecules as a scaffold: secreted Dpp molecules in the A-P border could be immediately captured by HSPGs on the cell surface located in either the A or P compartments, and the differential concentration of Dpp on the cell surface of producing cells and receiving cells drives the displacement of Dpp from one GAG chain to another toward more distant receiving cells (Figure 13). Alternatively, Dpp molecules bound by HSPGs could also move along the cell surface through a GPI linkage that is inserted in the outlet leaflet of the plasma membrane and is enriched in raft domains (Simons and Ikonen, 1997).

2.7.1.2.2 HSPGs and Wingless

Evidence for the involvement of HSPGs in Wg distribution comes from studies of *wingful* (*wf*), also called *notum*. *wf* encodes a secreted protein that belongs to the $\tilde{\alpha}/\beta$-hydrolase superfamily with similarity to pectin acetylesterases. In both embryos and wing discs, *wf* expression mirrors *wg* expression. Mutations in *wf* lead to enhanced Wg levels and increased Wg signaling, while over-expression of *wf* blocks Wg signaling activity (Gerlitz and Basler, 2002; Giraldez et al., 2002). In *Drosophila* S2 cells, co-expression of Dally and Dlp with Wf reduces the amount of Dally and alters the electrophoretic mobility of Dlp, respectively. Taken together, these data suggest that Notum may regulate Wg signaling by modulating the activity of the HSPGs Dlp or/and Dally (Giraldez et al., 2002; Han et al., 2005).

Another important line of evidence is that, as in the case of Dpp, extracellular Wg fails to move across mutant clones for *sfl* or double mutant clones for *dally* and *dly*. Moreover, extracellular Wg levels were reduced in wild-type cells behind clones of *dally-dly* mutant cells or cells mutant for *sfl* (Han et al., 2005). This suggests a common mechanism in the movement of Wg and Dpp.

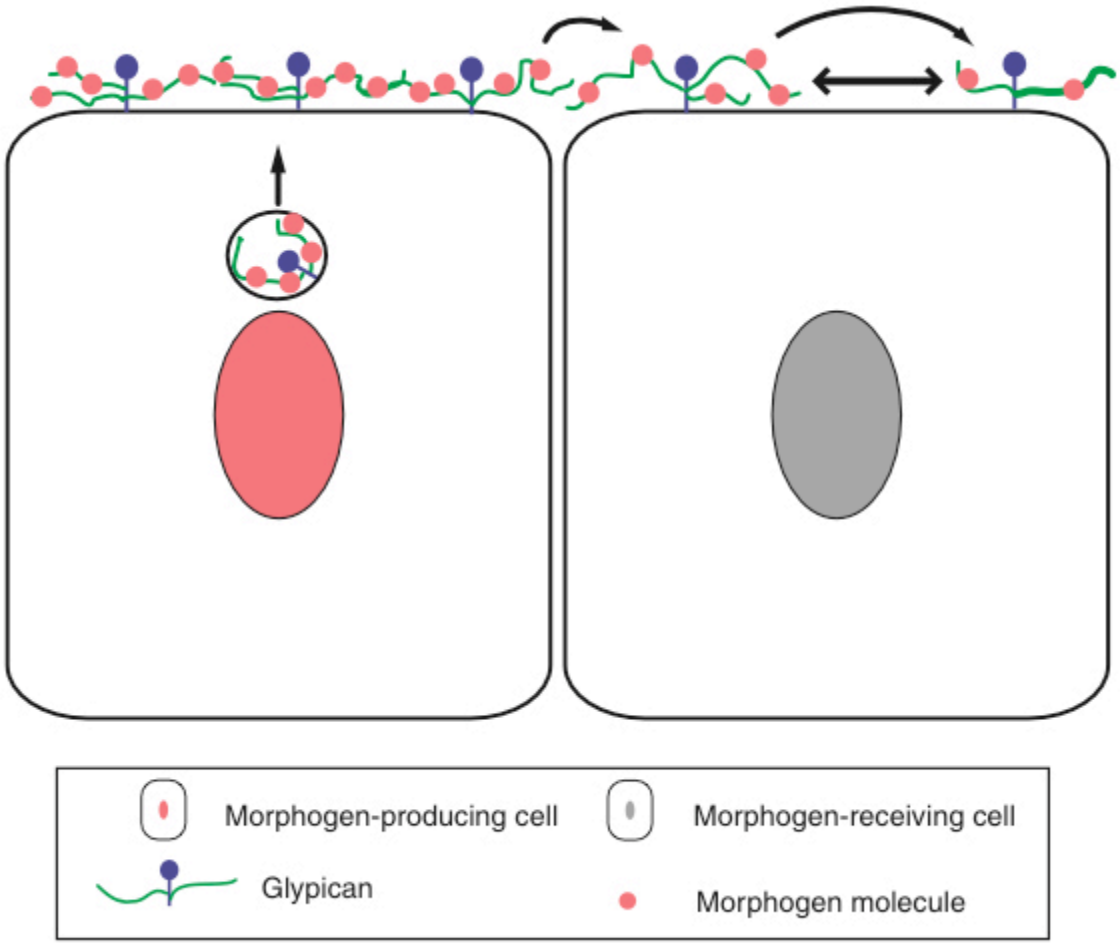

Figure 13 - HSPG-mediated morphogen movement along the cell surface by a restricted diffusion mechanism (modified from Lin, 2004).

Another function of HSPGs is associated with the necessity, within the context of epithelia, of planar transport of morphogens, since three-dimensional diffusion would imply that much of the ligand would be lost without ever getting a chance of reaching its receptors. This function could be accomplished together with the lipid modification of the morphogens Wg and Hh.

2.7.2 Facilitated diffusion with argosomes

Recently, a new model has been proposed in light of the observation that Wg and Hh could be transported by small vesicular structures called argosomes (Greco et al., 2001). Argosomes appear to be lipoproteins produced in the fat body, which are composed of a central core of lipids surrounded by an outer layer of polar phospholipids, cholesterol

and specialized proteins called apolipoproteins. Using their lipid adducts as anchors, Wnt and Hh proteins could in principle easily reside in the outer phospholipid layer of lipoprotein particles (Panakova et al., 2005). Since lipoproteins are already known to interact with HSPGs, which are also important in lipid metabolism, the influence of HSP on the morphogen distribution could also be explained by this theory.

Although the “argosome theory” is appealing, several questions need to be answered: how efficiently are peripheral tissues, such as the lumens of *Drosophila* imaginal discs, bathed by lipoproteins? Are lipoproteins the sole carriers for Hh and Wg? Do individual lipoprotein particles carry both morphogens at the same time? Finally, does the same mechanism operate in *Drosophila* and vertebrate embryos?

2.7.3 Cellular Projections

This model is based on the observation that some cells of the *Drosophila* wing imaginal disc have thin cellular extensions, which make contact with other cells of the disc (Gibson and Schubinger. 2000; Ramirez-Weber and Kornberg, 1999). Cellular extensions from the expressing cells could be hypothesized to directly release the morphogen onto target cells. Alternatively, expressing cells could release the morphogen to cellular extensions from the target cells. Two types of cellular projections have been identified in the wing disc.

Cytonemes are actin-based cellular extensions from the outlying cells of the wing pouch towards the anterior–posterior (AP) boundary (Figure 14).

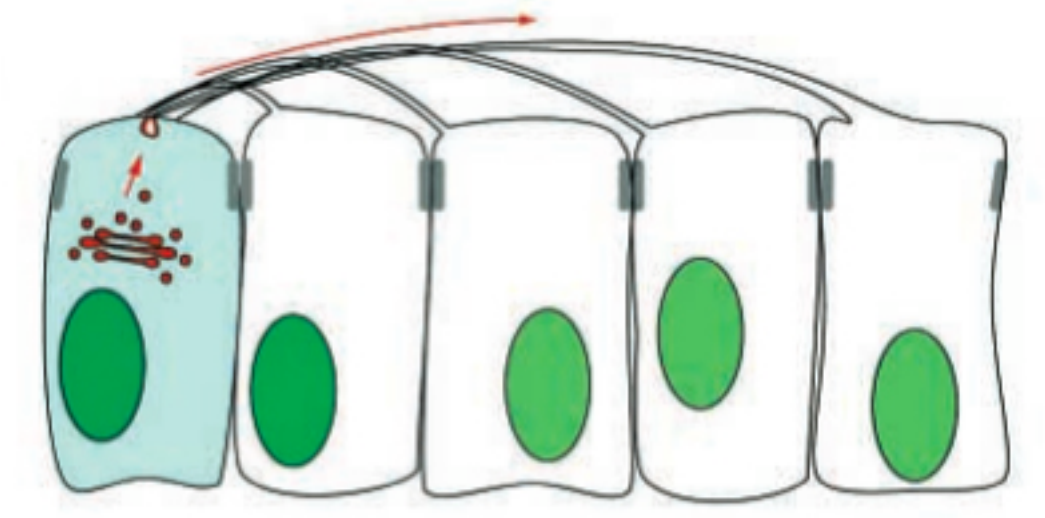

Figure 14 - A model for cytonemes; cells at the periphery of the imaginal disc extend long processes (cytonemes) towards the AP border (modified from Tabata and Takey, 2004).

Although cytonemes could theoretically mediate protein transport, this has not been demonstrated experimentally and their functional significance remains unclear. Assuming that cytonemes do transport proteins, their orientation along the AP axis suggests that they are more probable to be involved in the spread of Decapentaplegic than in Wg transport. Moreover, this intrinsic orientation of cytonemes is in contrast with the observation that ligand movement appears to be nondirectional in imaginal discs (Teleman et al., 2001).

The second type of cellular projections extends from the peripodial membrane of the imaginal disc to the columnar cells of the disc that give rise to adult structures (Gibson and Schubinger. 2000; Cho et al., 2000). In the eye-antennal disc, peripodial cells express Wg, Decapentaplegic and Hedgehog (Cho et al., 2000). Misexpression of proteins in the peripodial membrane can affect the growth and patterning of the eye (Gibson and Schubinger. 2000; Cho et al., 2000). Additionally, ablation of the wing disc peripodial membrane causes dramatic changes in wing morphology. However, detailed analysis of Wg expression and signaling in the peripodial cells of the wing has not been performed.

Therefore, although two types of cellular projections have been identified in the *Drosophila* wing disc, it is unclear if they play any role in Wg transport.

2.7.4 Planar transcytosis

Although Wg is capable of spreading by a Dynamin-independent mechanism in the wing disc, studies on the *Drosophila* embryo have provided conflicting evidence with respect to the transcytosis model of Wg transport. In the transcytosis model, the morphogen is passed from cell to cell through successive rounds of internalization, recycling to the cell surface and release into the extracellular space for uptake by the neighboring cell (Figure 15). Visualization of the trafficking of Wg–GFP protein has revealed that in live embryos, Wg can be internalized and recycled to the cell surface (Pfeiffer et al., 2002; see 2.5).

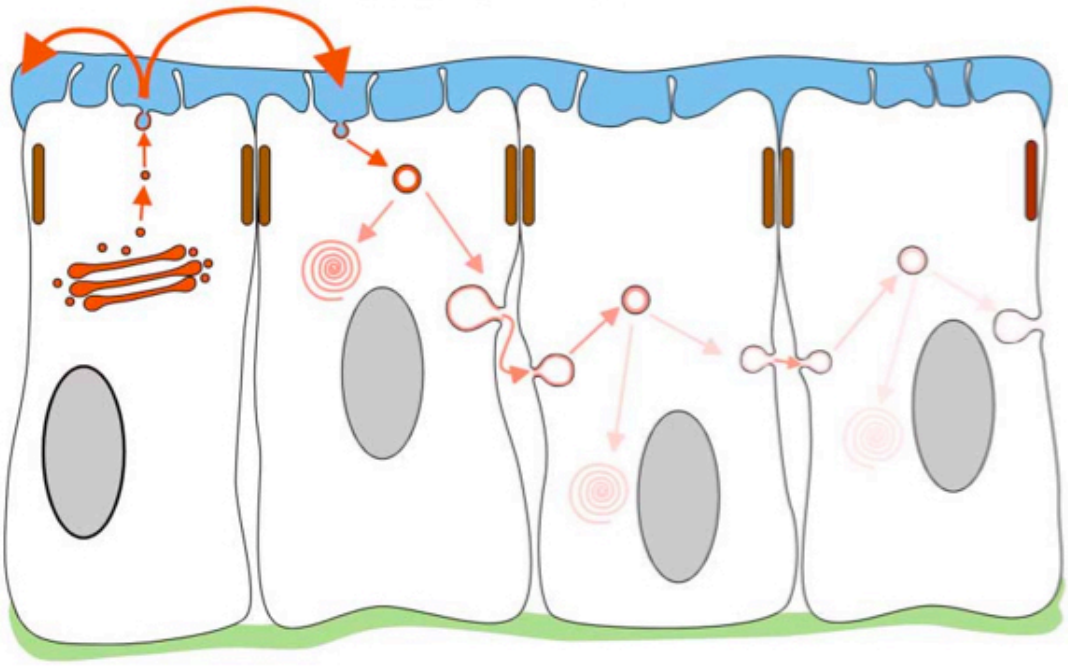

Figure 15 - Model of planar transcytosi: ligand is transported along the plane of the epithelium by repeated cycles of endocytosis and recycling to the cell surface (modified from Vincent and Dubois, 2002).

The possible role of transcytosis in Wg transport is confirmed by the impairment of protein internalization through *shibire,* which results in the restriction of Wg to the Wg-expressing cells in embryos (Bejsovec and Wieschaus, 1995; Moline et al., 1999). This finding suggests that, at least in embryos, transcytosis might play an important role in Wg transport. In contrast to these results, Dubois et al. showed that in embryos mutant for *clathrin* (which is required for endocytosis) the spread of Wg appears to be broadened (Dubois et al., 2001). Therefore, the apparent reduction in the spread of Wg

in *shibire* mutant embryos could be due to reduced secretion.

The strongest evidence about the role of endocytosis in morphogen transport came from analysis of Dpp gradient formation in the *Drosophila* wing disc, since *shibire* mutant clones were shown to “cast a shadow” in the Dpp gradient (the transgene Dpp-GFP was used) (Entchev et al., 2000). This theory was later rejected, when it was demonstrated that a blockage of endocytosis by the mutant *shibire* does not block Dpp movement, but rather inhibits Dpp signaling, and leads to an accumulation of the Dpp receptor Tkv. As for Wg, shibire mutant clones showed an extracellular accumulation of Dpp (visualized by the transgene GFP-Dpp), suggesting that Dynamin mediated endocytosis is normally required for downregulating extracellular Dpp levels. The last and most important observation is that in the extracellular Dpp expression no shadow was detected behind Dynamin-defective cells (Belenkaya et al., 2004).

The increase of the receptor expression and the possible formation of a shadow behind the *shibire* mutant clones in a dynamic situation (see last part of discussion in Belenkaya et al., 2004) were also predicted by a mathematical model. Moreover, the same mathematical model made a rapid gradient formation incompatible with planar transcytosis, because it would require many trafficking processes to occur at unusually high rates (Lander et al., 2002).

2.8 Wingless internalization

Experiments made with *shibire*^{ts} and *clathrin* mutant embryos showed that Wg is capable of signaling from the cell surface, i.e. in absence of internalization (Bejsovec and Wieschaus, 1995; Dubois et al., 2001). Nonetheless, these findings do not exclude the possibility that Wg might also signal from an internal compartment as has been demonstrated for several other signaling pathways (Seugnet et al., 1997). To date, there is only limited evidence for the intracellular transduction of Wg signaling. In the *Drosophila* embryo, when internalization is impaired in Wg-receiving cells, the expression domain of *engrailed* is narrowed, and this could reflect reduced Wg signal transduction (Moline et al., 1999). Furthermore, when Wg accumulates in an intracellular compartment because of the inhibition of lysosomal trafficking, enhanced Wg signaling is observed (Dubois et al., 2001).

Concerning Dpp, it has been observed that mutant clones for *shibire* (*shi*^{ts}) show a reduced p-MAD level when shifted to restrictive temperature, meaning that Dpp signaling is reduced (Belenkaya et al., 2005). This suggests that internalization of the activated Dpp receptor complex might be essential for Dpp signaling.

Within the context of the diffusion model, mathematical models predict that only a limited amount of receptor would be tolerated before diffusion becomes unable to contribute significantly to transport, and that the tolerated amount of receptor would be so low that signal transduction would be compromised unless signaling can continue after internalization. Thus, endocytosis would be an essential component of a diffusion-based model, since it would allow robust signaling under conditions of low extracellular receptor level (Lander et al., 2002).

2.9 Wingless degradation

As morphogen gradients form rapidly (Entchev et al., 2000; Strigini and Cohen, 2000), Wg and Hh are expected to turn over rapidly. Indeed, surface-labeled Wg or GFP-Dpp (with biotin) is rapidly brought to undetectable levels within a 3 hrs chase period (Teleman and Cohen, 2000). Degradation could occur either as a result of proteolytic action in the extracellular space or by internalization and targeting to lysosomes, and both processes probably occur.

For example, when whole *shibire*^{ts} discs are placed at restrictive temperature, Wg supply is cut off and such discs lose the whole extracellular Wg immunoreactivity and the intracellular Wg immunoreactivity in the non-*wg*-expressing cells within 3 hrs of the shift (Strigini and Cohen, 2000). Thus, when its production is impaired, the ligand is cleared from the epithelium even in the absence of endocytosis and this suggests that degradation in the extracellular space occurs.

Even though extracellular proteases probably contribute to signal degradation, current evidence suggests that endocytic trafficking is the key regulatory process. In fact, extracellular Wg and Dpp accumulate at the surface of *shibire* mutant cells (Strigini and Cohen, 2000; Belenkaya et al., 2004). Ultrastructural analysis has detected Wg in endocytic vesicles and multivesicular bodies (Gonzalez et al., 1991; van den Heuvel et al., 1989), and since multivesicular bodies fuse with lysosomes, Wg might be digested

by degradative enzymes within the lysosomes. According to this, compromised lysosomal degradation of Wg either genetically (by reducing the activity of *deep orange*) or chemically (with chloroquine, an inhibitor of lysosomal function) leads to an increased range of Wg and excess signaling in the embryonic epidermis (Dubois et al., 2001). Conversely, in imaginal discs, expression of a dominant active Rab7 (a small GTPase required for sorting into late endosomes) reduces the range of Dpp (Entchev et al., 2000). Further experiments showed that internalized fluorescent Dextran (from an externally applied solution) co-localizes, at least partially, with intracellular Dpp or Wg (Entchev et al., 2000; Pfeiffer et al., 2002), and that Wg is indeed internalized by a Dynamin-dependent process (Strigini and Cohen, 2000). Likewise, no internalized Dpp can be detected in *shi*^{ts} cell clones kept at the restrictive temperature for 6 hrs (Entchev et al., 2000). As expected, a secreted form of GFP, a protein that is unlikely to be internalized by receptor-mediated endocytosis, fills the extracellular space without forming a gradient in embryos (Pfeiffer et al., 2002) and in imaginal discs (Entchev et al., 2000). One can conclude that, independently of the mode of transport, the slope of a morphogen gradient is modulated by its rate of lysosomal degradation.

3 Results

3.1 A screen for recessive components of the Wingless signaling pathway

Since one of the main interests of our group is the understanding of the Wg/Wnt-signaling pathway, several screens were performed in order to find new components.

In general, one can distinguish two types of screens: “loss-of-function” and “gain-of-function” screens.

Gain-of-function screens rely on the ectopic over-expression of randomly tagged genes. This has the advantage that genes, which are missed in a loss-of-function screen (due to lethality, redundancy, or small size of the gene), can be found.

In a loss-of-function screen, genomes are mutagenized using chemicals, ionizing radiations, or transposable elements in order to eliminate or reduce the function of genes. A “loss-of-function” screen has already performed by our group with the aim to find dominant suppressors of the Wg/Wnt-pathway; in these experiments, EMS was used to mutagenize flies, which carry the transgene *sev-wg* (Brunner et al., 1997). The *sevenless* enhancer leads to the ectopic expression of *wg* in the eyes, and these flies show a so-called “rough-eye phenotype”, resulting from a reduction in the number of photoreceptor cells and a loss of interommatidial bristles. This phenotype could be used as read-out for the screen, since mutations in a positive component of the Wg signaling would block the pathway and lead to a rescue of the eye roughness (Figure 16).

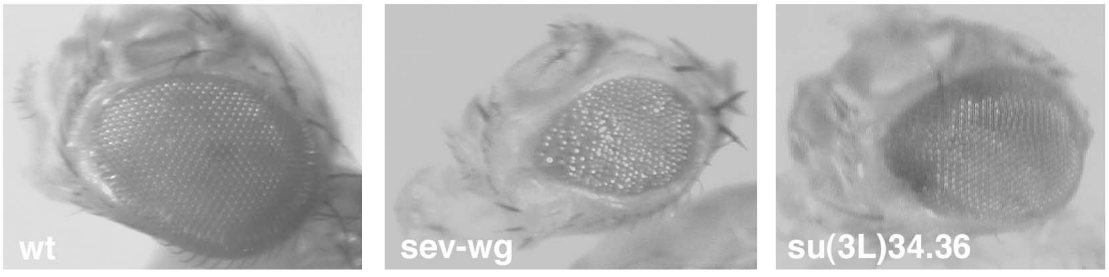

Figure 16 – Eye phenotypes. To the left: eye of a wild-type fly. In the center: eye of a fly carrying the *sev-wg* construct, which causes the “rough-eye phenotype”. To the right: eye of a suppressor found in the screen, which shows a rescue of the “rough-eye phenotype”.

However, in this system one still allows the presence of one wild type copy of the mutated gene and so the synthesis of the encoded protein will still take place. That is the reason why only “dominant suppressors” can be found in such a screen.

This screen for dominant suppressors led to the discovery of important components of the Wg pathway such as *pangolin*, *legless*, and *pygopus*, and seems now to be saturated. For this reason another approach was started: an EMS mutagenesis screen for so-called recessive components of the Wnt/Wg signaling pathway. The idea behind a screen for recessive suppressors is to have a homozygous mutant tissue where *wg* is being over-expressed. This can be obtained by the induction of mitotic recombination in the eye of *Drosophila*, when a yeast specific recombinase (Flp*)* is driven by the *sevenless* enhancer. Flp recognizes specific FRT sites, which are located on the chromosome arm of interest, and this makes it possible to generate homozygous clones for the putative mutation in the Drosophila eyes simply by using a recessive cell lethal mutation on the same chromosome arm of the FRT (Figure 17).

In addition to being more sensitive, such a screen can lead to the discovery of good targets for cancer therapy, since normal cells would probably survive with a low amount of the targeted protein.

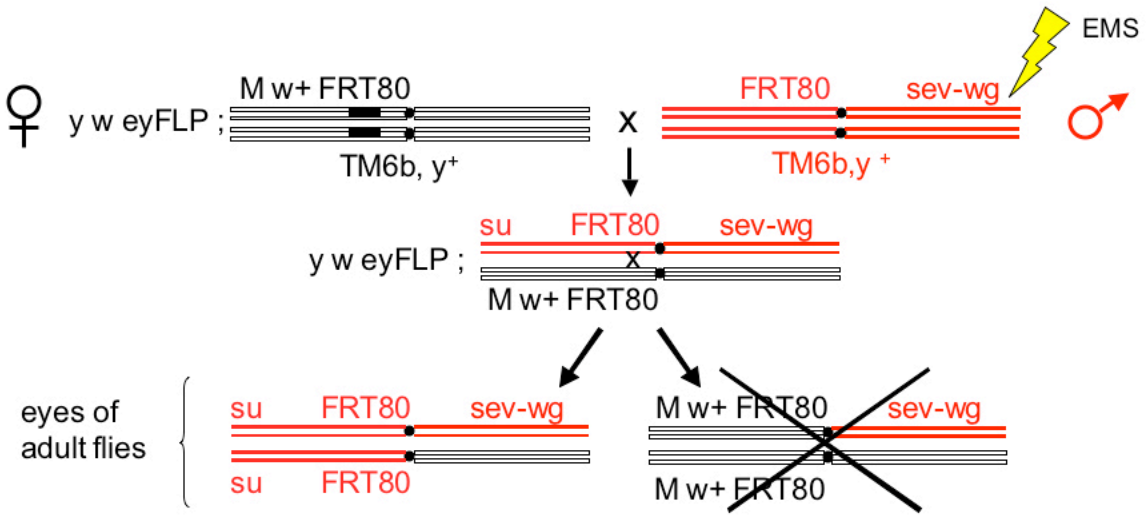

Figure 17 - Scheme of the crossings used for the screen for recessive suppressors. M: recessive cell lethal mutation.

Corina Schütt performed the screen and analyzed around 38'000 flies. Apart from the many single hits, 3 complementation groups on the 3rd chromosome arm were found and called 3L1, 3L2, and 3L3.

3.2 The third complementation group of recessive suppressors of the Wingless signaling pathway

The third complementation group was called 3L3, and it is formed by the following two independent alleles:

- *su20.53,* which is a strong suppressor of the rough-eye phenotype
- *su20.54,* which is also a strong suppressor of the rough-eye phenotype, and even has a slightly dominant effect.

Through complementation analysis with different deficiencies, Carla Bänziger could narrow down the critical region to 240 kb, i.e. to around 50 genes. SNP mapping and sequencing were then crucial for the determination of the gene responsible for the observed phenotype. The gene affected in the complementation group 3L3 turned out to be *CG6210*.

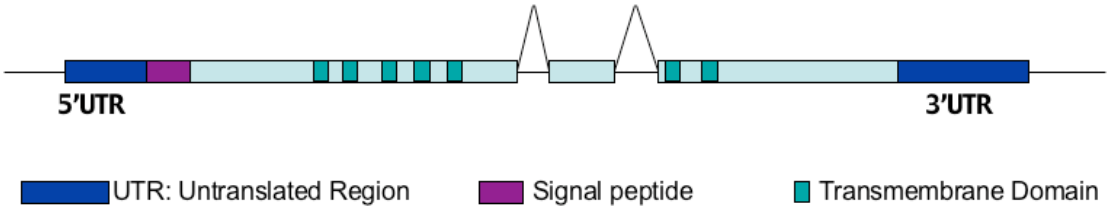

Figure 18 - Structure of the gene *CG6210*.

The gene *CG6210* maps to the cytologic position 69A9 and encodes a yet uncharacterized protein. Database searches revealed that its transcript may be differentially spliced and this leads to the formation of a shorter (CG6210-PA, of 594 aa) and a longer form (CG6210-PB, of 562 aa) (Figure 18). Sequencing of the two alleles of the 3L3 complementation group revealed a mutation in the coding region of both of them.

- *su20.53* presents a 47 bp deletion, which is responsible for a frameshift in the signal

sequence and leads to a premature stop 13 aa after the signal sequence.

- *su20.54* presents a C to T transition, responsible for the aa change Pro->Ser in the first transmembrane domain.

Both alleles were found to be homozygous lethal, and since they form a complementation group, lethality was also found when they were crossed to each other. In order to confirm that the mutation found in the coding sequence of *CG6210* was responsible for the lethality phenotype, we performed a rescue experiment. We crossed flies heterozygous mutant for *3L3* (*su20.54*) with flies, which were also heterozygous mutant for *3L3* (*su20.53*) and in addition carried the transgene *tubα1-3L3*. This transgene drives the expression of *3L3* in all cells under the control of the *tubulinα1* promoter. Since *tubα1-3L3* was able to rescue the lethality, we conclude that the mutations in the coding sequence of the *3L3* gene are responsible for the observed phenotype.

Performing a BLAST search gave a very interesting result: homologues of the gene *CG6210* were found in all the investigated metazoans. In particular: *Caenorhabditis elegans, Caenorhabditis briggsae, Drosophila melanogaster*, *Anopheles gambiae, Danio rerio, Xenopus laevis* (2 isoforms predicted), *Oikopleura dioica, Rattus norvegicus, Gallus gallus, Mus musculus* (5 isoforms predicted), *Homo sapiens* (5 isoforms predicted).

It is worth noticing that Wnt/Wg signaling is present in all the metazoans listed above and this could be a hint that *CG6210* evolved along with the pathway.

Through the comparison of the homologues found through the BLAST search and the program SMART, a putative signal sequence and 7 putative transmembrane domains were defined. Moreover, a conserved domain with unknown function called DUF1171 was found (DUF simply stands for “Domain of Unknow Function”).

3.3 Embryonic segmentation phenotype

As described above, the exoskeleton pattern of *Drosophila* offers a useful readout of the genetic program, which drives the embryonic segmentation. Since *wg* is one of the key segment polarity genes, a change in the Wg signaling pathway leads to a disruption of

the physiological segmentation, which is normally present on the ventral side of the epidermis. In fact, a reduction of Wg signaling leads to a fusion of the denticle belts and to the so-called “lawn-of-denticle phenotype”, whereas an increase in Wg signaling gives a “naked phenotype”, since denticle formation is impaired.

In order to study the role of *CG6210* in the patterning of the exoskeleton, germline clones were performed. This genetic tool is necessary to get rid of the maternal component of the gene of interest, which is often present at the early stages of development.

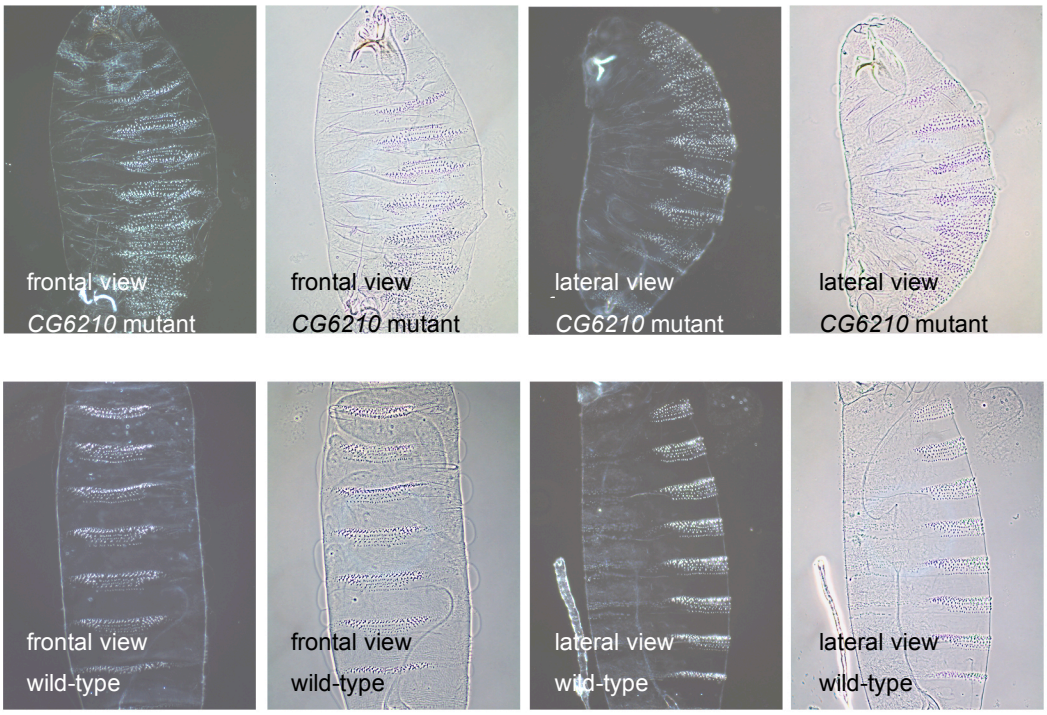

Figure 19 – Cuticle phenotype of wild-type embryos (lower row of pictures) and of germline clone embryos mutant for *CG6210* (upper row). The left pictures show the frontal view, whereas the right pictures show the lateral view of the embryonic exoskeleton. Each cuticle is shown in bright and dark field.

When we looked at the exoskeleton of wild-type embryos we saw a nice alternation of segments, which show a smooth cuticle, and of segments, which carry denticles. In contrast, germline clones for *CG6210* resulted in a “lawn-of-denticle phenotype” (Figure 19). This observation suggested that there was a reduction in the Wg signaling pathway when *3L3* was absent. It is important to notice that at early stages of embryogenesis (stage 9-10) Wg and Hh expression are interdepent and so the primary cause for the

phenotype could be a reduction in either the Wg or the Hh signaling pathway. To distinguish between the two possibilities, we performed further experiments, which are described below.

3.4 Pharate adult phenotypes

The combination of the allele *su20.53* with the allele *su20.54* led to lethality at the stage of pharate adults; as a consequence, 20 pharate adults raised at 25 degrees and 20 pharate adults raised at 29 degrees were analyzed. Apart from the unexpected weaker antenna phenotype at 29 degrees, no significant differences caused by the temperature were detected in the phenotype, and this suggests that *su20.53* and *su20.54* are probably not temperature sensitive alleles. The analysis of the phenotypes was not performed with pharate adults raised at 18 degrees.

Apart from the lethality, very interesting phenotypes of the appendages antennae, legs, and wings were observed (Figure 20), and this is remarkable, since these are all dependent on Wg signaling for their proper development.

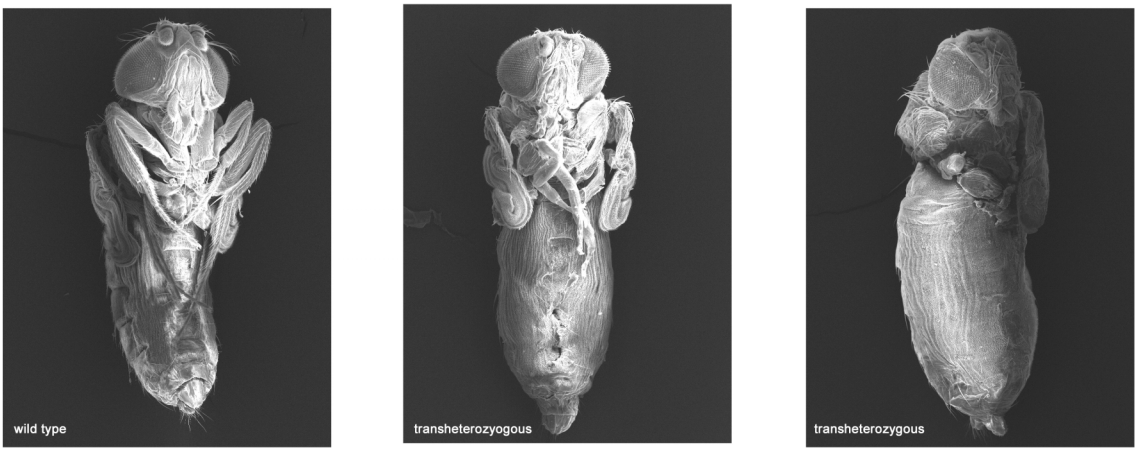

Figure 20 – Left picture: wild-type pharate adults. Center and right: transheterozygous mutant pharate adults showing abnormal antennae, legs (center and right) and wing-to-notum transformation (right picture).

Normally, each antenna is composed of 5 segments and the arista, but in the mutant situation aristae are usually missing. In more severe cases other segments are abnormally developed (Figure 21). Surprisingly, at 29 degrees the phenotype was less strong.

Figure 21 - Transheterozygous pharate adults with dysmorphic legs (left) and dysmorphic antennae (right).

The wing phenotype was probably the most striking one, since in 5-10% of the cases wing-to-notum transformation was observed.

Finally, each pharate adult showed rudimental development of all leg pairs. The first leg pair was most frequently affected and showed in 20% (at 25 degrees) and in 30% (at 29 degrees) of the cases loss of tibia and/or of the 5 tarsi and bifurcations (Figure 21).

3.5 Effect of the *CG6210* mutation on leg development

In order to better understand the phenotypes arising in the development of the appendages, a brief introduction is necessary.

In the early 1970s, Garcia-Bellido and colleagues showed that the developing appendages of *Drosophila* are subdivided into anterior-posterior and dorsal-ventral compartment (Garcìa–Bellido et al., 1973). Compartments were first recognized by virtue of the boundaries of cell lineage restriction that separate them, and each compartment in most imaginal discs is now known to establish separate groups of “signaler” and “receiver” cells (Lawrence et al., 1996; Zecca et al., 1995). The cells of the posterior (P) compartment emit the Hh signal to which the cells of the anterior (A) compartment can respond (Domìnguez et al., 1996). In the thoracic discs (as leg and wing discs) A versus P identities are implemented by two different transcription factors: En, a transcription factor of the homeodomain class (Desplan et al., 1985), and Ci, a transcription factor of

the zinc finger class (Alexandre et al., 1996). In P cells, En activates *hh* transcription so that P cells secrete Hh. Simultaneously, En represses *ci* transcription and P cells become refractory to their own signal (Ci is needed for Hh transduction).

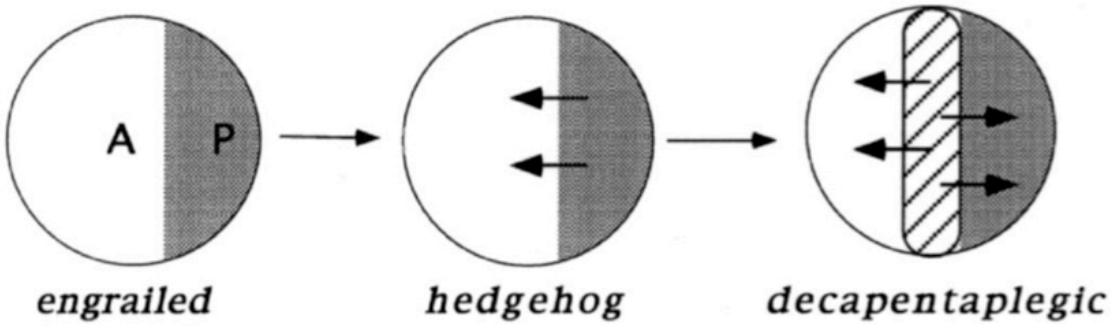

Figure 22 – Formation of compartments in the thoracic imaginal discs (modified from Brook et al., 1996).

In the leg discs Hh was shown to turn on *wg* in the ventral half of the border, and to turn on *dpp* in both the dorsal and ventral halves (Basler et al., 1994); in addition, *wg* partially represses *dpp* ventrally and *dpp* represses *wg* dorsally. While ventral *dpp* transcription is relatively meager, Wg and Dpp cooperate to direct *Dll* expression in the center of the disc, thereby initiating P/D (proximo-distal) axis formation.

In the leg imaginal disc, the sectors of expression of the morphogens Dpp and Wg coincide roughly with the prospective dorsal (D) and ventral (V) midlines. D and V states in the anterior compartment are maintained by the Dpp and Wg signals themselves (Brook and Cohen, 1996): cells within the range of Dpp signal adopt D competence in the anterior compartment, while those within range of Wg adopt V competence in the anterior compartment.

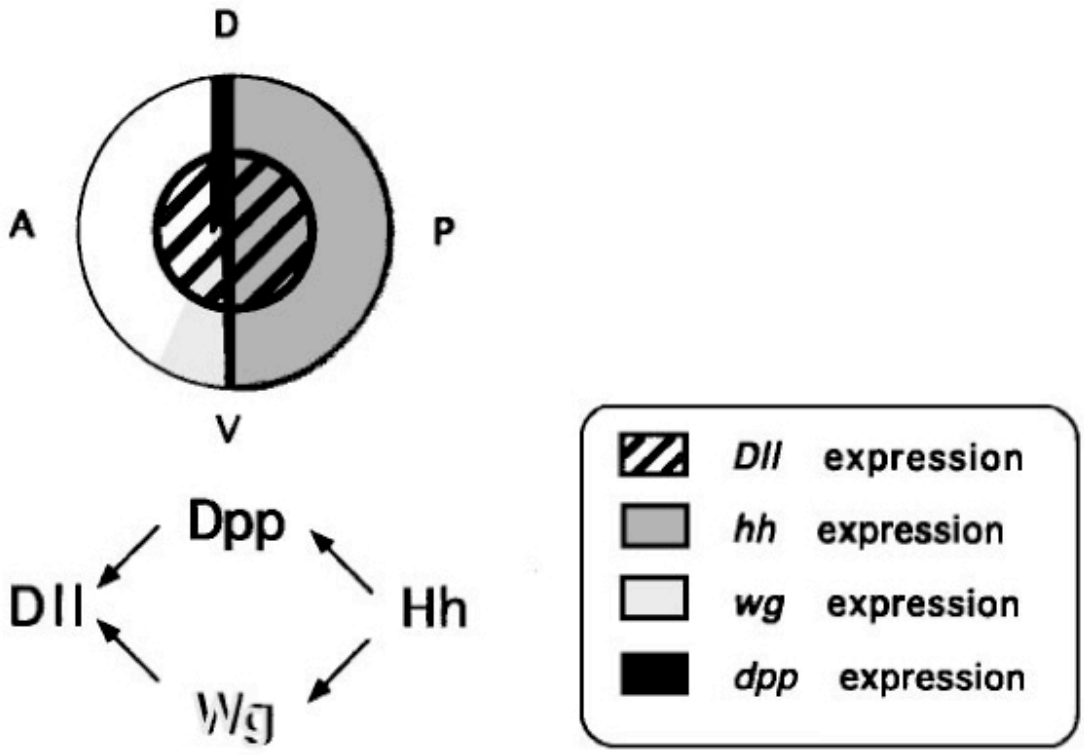

Figure 23 - Pattern of expression of *hh*, *wg*, *dpp* and *Dll* in a wild-type leg imaginal disc (modified from Brook et al., 1996).

Reduction of *dpp* or *wg* function results in loss of the dorsal or ventral structures of the legs, respectively. Missing structures are replaced by a mirror-image copy of the remaining parts (Held et al., 1996).

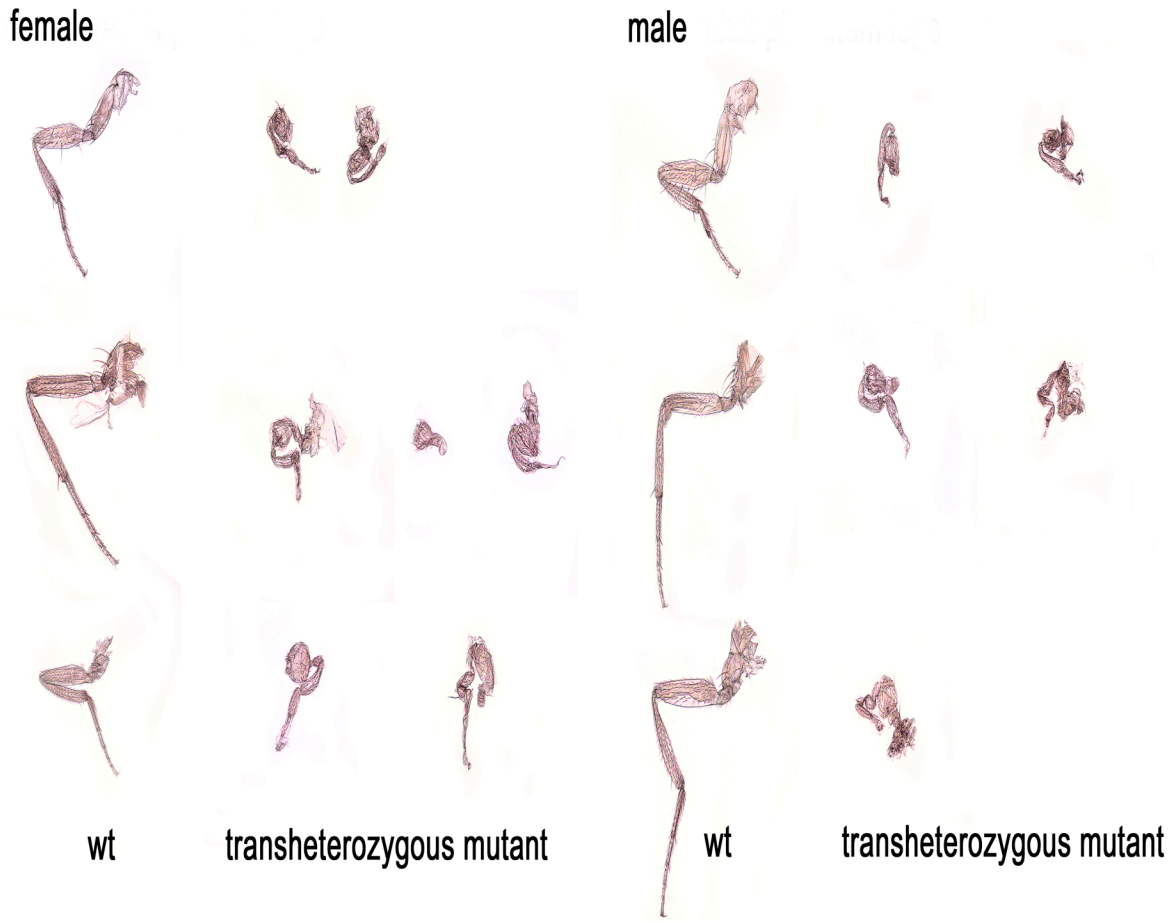

Figure 24 - Legs of wild-type and transheterozygous female (left) and male pharate adults (right); the upper row shows the first pair of legs; the middle row shows the second pair of legs; the lower row shows the third pair of legs.

We carefully looked at the legs of transheterozygous mutants (*su20.53* crossed with *su20.54*) pharate adults. We could never observe an increase of the ventral structure. In fact, we found a reduction of the ventral structures (i.e. loss of the ventral naked part of the femur), and an increase of the dorsal structure (i.e. duplication of pre-apical bristle of the tibia, which is a dorsal structure). This suggests that *3L3* loss of function leads to a reduction of the Wg signaling pathway, and that *3L3* is a positive component of the pathway.

As previously stated, by manipulating *dpp* or *wg* expression directly or by interfering indirectly with components of their pathway, it was shown that there is a mutual antagonism between Wg and Dpp (Brook and Cohen, 1996; Jiang et al., 1996). In order

to understand the role of *3L3* in this regulatory mechanism, leg discs of mutant third-instar larvae were analyzed.

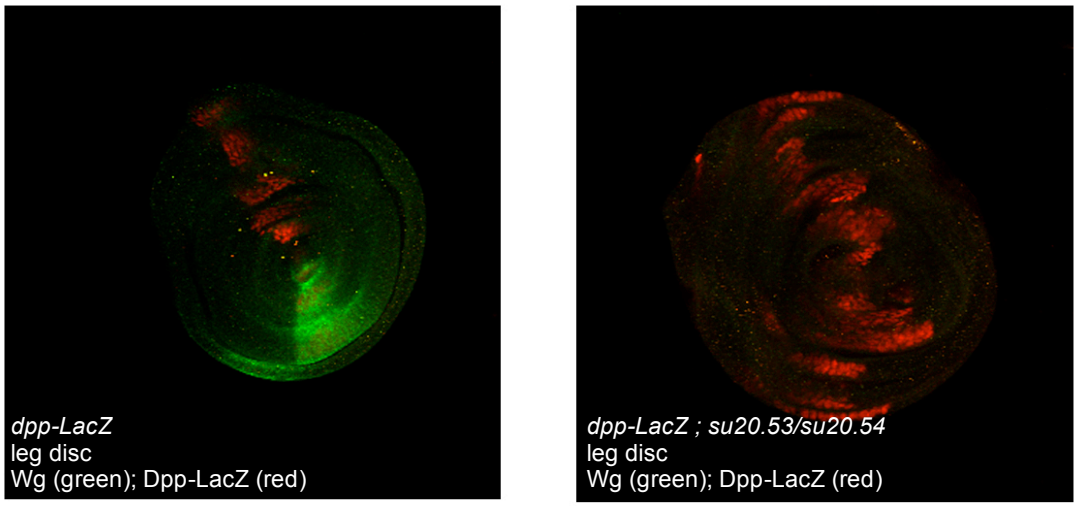

Figure 25 – Leg discs showing the pattern expression of *dpp-LacZ* in red and of Wg in green; the left picture shows a wild-type disc, whereas the right picture shows a transheterozygous mutant disc (*su20.53* crossed with *su20.54*).

In homozygous mutant leg discs, Wg protein was almost absent. In contrast, the expression of *dpp* (shown by the *dpp-lacZ*) was expanded and almost replaced the one of *wg*.

This suggests that Wg is not able to suppress *dpp* expression, which increases and strongly downregulates *wg* expression. In this mutant situation, Wg appears to reach the receiving cells in insufficient amounts (i.e. through reduced secretion or inhibited transport), to be less active or the signal transduction is impaired.

3.6 Adult wing phenotype

The normal wing margin has at its anterior edge a triple row of mechanosensory (MS, straight) and chemosensory (CS, curved) bristles. The medial row has stout bristles, and the dorsal row has CS bristles, while the ventral row has a 4:1 ratio of slender MS to evenly spaced CS bristles. More posterior a double row and a single row are present. The triple and double rows have innervated bristles, but the posterior row only has nonsensory hairs. Such a fine patterning of the tissue of the wing disc is achieved during

the third larval instar and the pupal development through Wg, and reduction of the Wg signaling pathway was shown to induce loss of all kind of bristles (Couso et al., 1994). In addition, large clones of *wg* null alleles produce notches when they reach the wing margin (Baker, 1988).

In order to test the role of *3L3* in the wing margin development, we induced the formation of Minute$^{+/+}$ clones mutant for *3L3* in a Minute$^{+/-}$ background and studied the phenotype of adult wings.

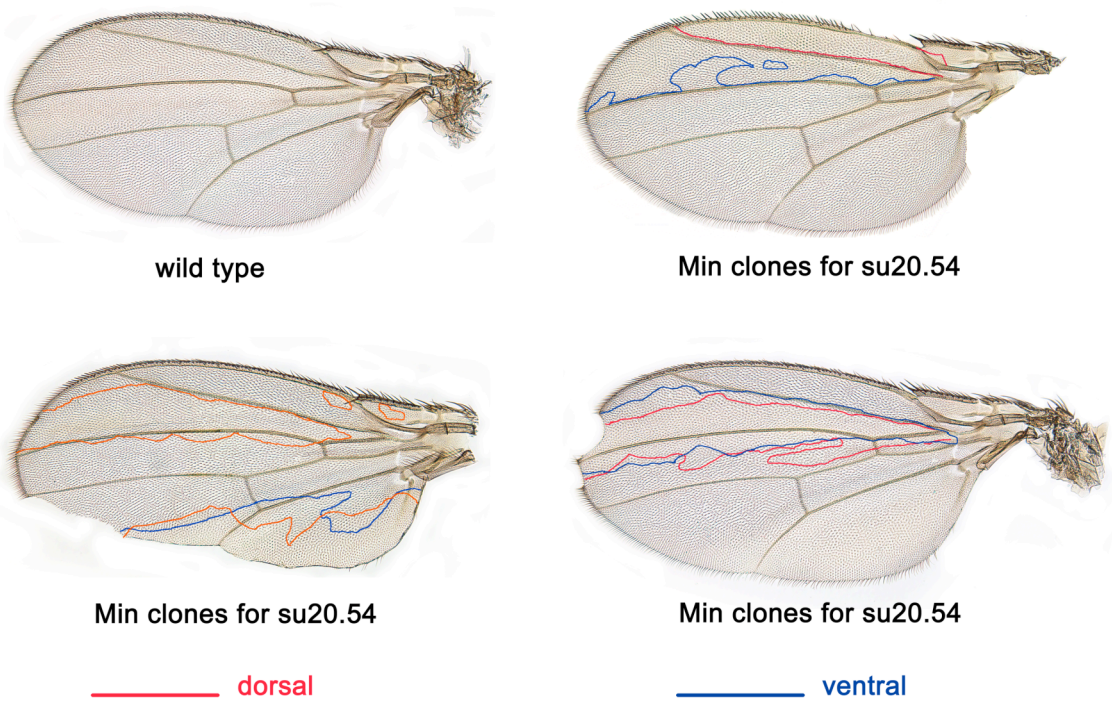

Figure 26 – Adult wings of wild-type flies and adult wings carrying homozygous mutant clones for *su20.54*. Red and blue lines mark the borders of the clones on the dorsal and the ventral wing surfaces, respectively.

To detect the presence and the extent of the clones, we utilized the recessive wing cell marker *multiple wing hair* (*mwh*). This marker was recombined on the left arm of the third chromosome, which carried the *su20.54* mutation and the FRT80 sequences.

We could observe all the known phenotypes typical for reduction in Wg signaling, such as wing notches and loss of all kind of bristles (Figure 26).

Thank to the *mwh* marker, we could exactly determine the borders of the clones, and we observed that the phenotypes arose only if the wing margin and the nearby tissue on both sides were mutant for *3L3*.

3.7 Wing imaginal discs: the behaviour of Wingless and Wingless target genes behaviour in cells mutant for *CG6210*

The anterior and posterior compartments of the *Drosophila* wing, which derive from two populations of cells during embryogenesis, are further subdivided into dorsal and ventral subcompartments during larval life (Bryant, 1997; Garcia-Bellido et al., 1973). Once allocated, cells of the dorsal and ventral compartments interact across the compartment boundary to induce the expression of *wg* in a narrow stripe of cells that straddles the boundary (Diaz-Benjumea et al., 1995; Kim et al., 1995). This stripe marks the future margin of the wing and is associated with overlying stripes of expression of the genes *Distalless* (*Dll*) and *vestigial* (*vg*), which encode putative transcription factors required for normal wing development (Cohen et al., 1989; Williams et al., 1991). These two genes are so-called “long-range” target genes, since their expression extends many cell diameters on either side of the *wg*-expressing cells (Williams et al., 1991; Carroll et al., 1994). The boundaries of expression of *Dll* and *vg*, as visualized by the expression of Dll and Vg protein, are not sharp; instead, expression grades out over a few cell diameters at the edges of each stripe.

wg-expressing cells along the dorsoventral (D/V) compartment boundary are also associated with the segregation on either side of rows of cells expressing the marker for sensory organ precursors cells *neuralized* (*neu*) (Boulianne et al., 1991; Phillips et al., 1993), and the Zn finger transcription factor *senseless* (*sens*) (Nolo et al., 2000; Srivastava, et al., 2003). These two genes are instead so-called “short-range” target genes, due to the narrow expression pattern close to the D/V boundary.

3.7.1 Requirement for CG6210 function for the expression of the long-range target gene *Dll*

Since the expression of Wg target genes is dependent on the activation of the Wg signaling pathway, they are good tools to analyze the effect of *3L3* loss of function on

the signal transduction. The expression of *Distalles* as a long-range target gene was thus studied in different situations in wing imaginal discs.

We first looked at the expression of the Dll protein in wild-type versus *3L3* homozygous mutant wing discs of third instar larvae. For the homozygous mutant situation we used the allele *su20.53*. We found that Dll is still expressed in the mutant situation, but at a lower level compared to the wild-type situation. This result suggests that *3L3* is a positive component of the Wg signaling pathway, but that its absence does not completely block the signaling cascade.

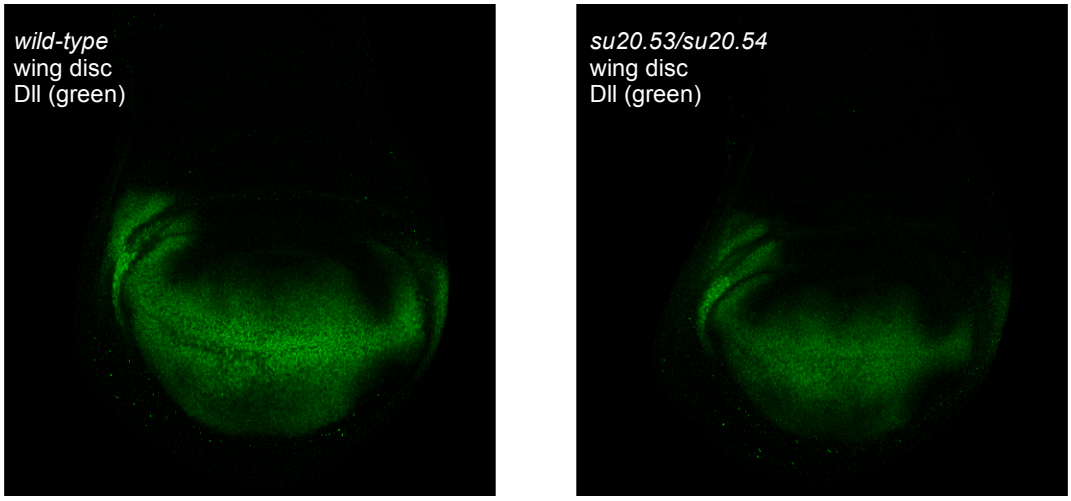

Figure 27 – Wing imaginal discs showing Dll staining: a broader and stronger staining is shown in the wild-type disc (on the left) compared to the one in the transheterozygous mutant disc (on the right). The settings at the confocal microscope were kept identical in both situations.

In order to confirm a role of *CG6210* in the activation of the target gene *Dll* and to better characterize its function, we induced the formation of *3L3* homozygous mutant clones (with *su20.54*) marked by the absence of GFP. As a control we induced *pygo*^{130} clones, which are homozygous mutant for a well-known positive component of the Wg pathway. In the case of *3L3* mutant clones no suppression of Dll protein expression was detectable, whereas *pygo*^{130} clones showed a clear down-regulation of the Dll staining.

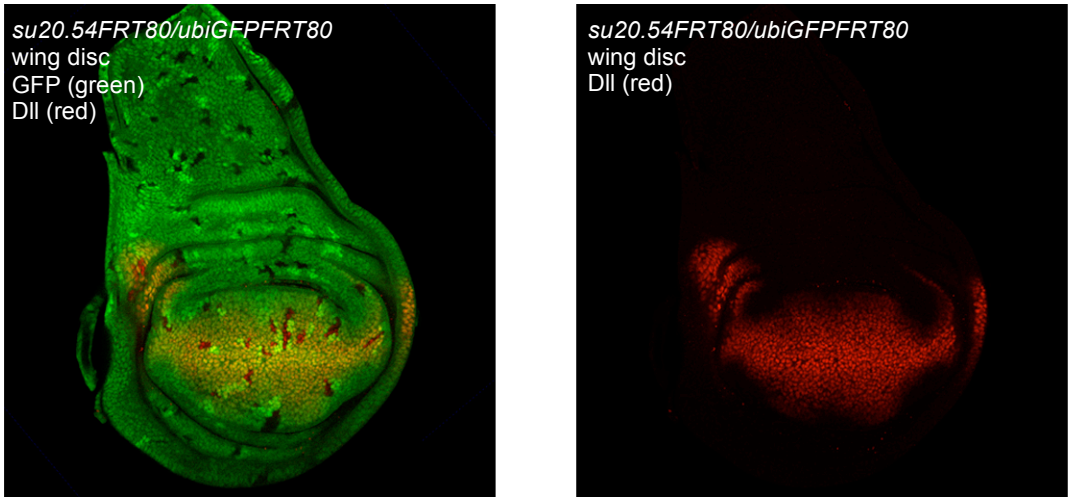

Figure 28 – Wing disc with mutant clones homozygous for *su20.54*. On the left: mutant clones marked by the absence of GFP (green) show no reduction of the staining of the Wg target gene Dll (red). On the right: Dll staining alone.

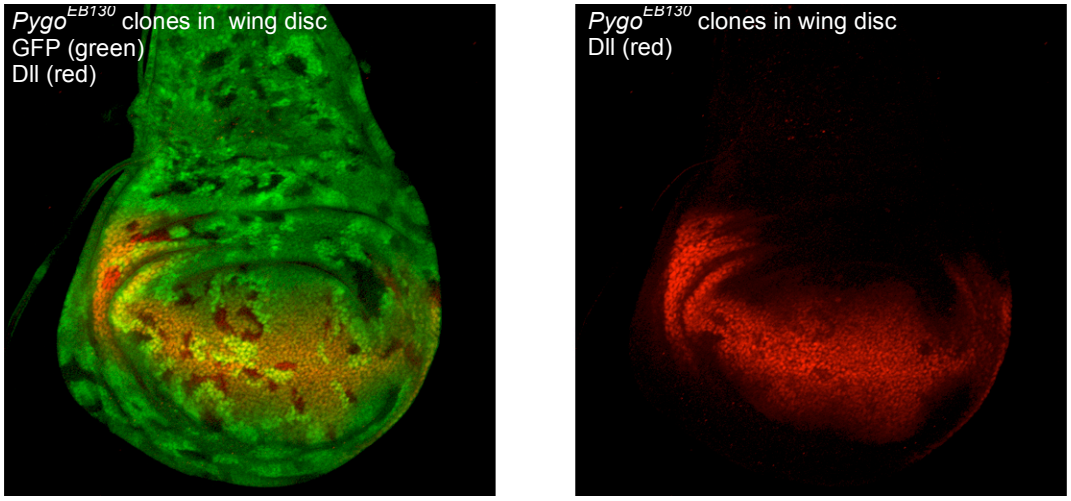

Figure 29 – Wing disc with mutant clones homozygous for *pygo*^{130}. On the left: mutant clones marked by the absence of GFP (green) show a reduction of the staining of the Wg target gene Dll (red). On the right: Dll staining alone.

The reason why no suppression of Wg target gene *Dll* is detected could be due to the small size of the mutant clones. In fact, *CG6210* could be necessary in the *wg*-expressing cells and not in the *wg*-receiving cells. In this case, the possible down-regulation of the signal would be non cell-autonomous, i.e. would not be confined to the mutant cells.

To investigate this possibility, we generated bigger clones, i.e. Minute$^{+/+}$ clones mutant for *3L3* in a Minute$^{+/-}$ background and looked at the expression of the *Dll-lacZ* in wing discs. The allele *su20.53* was used.

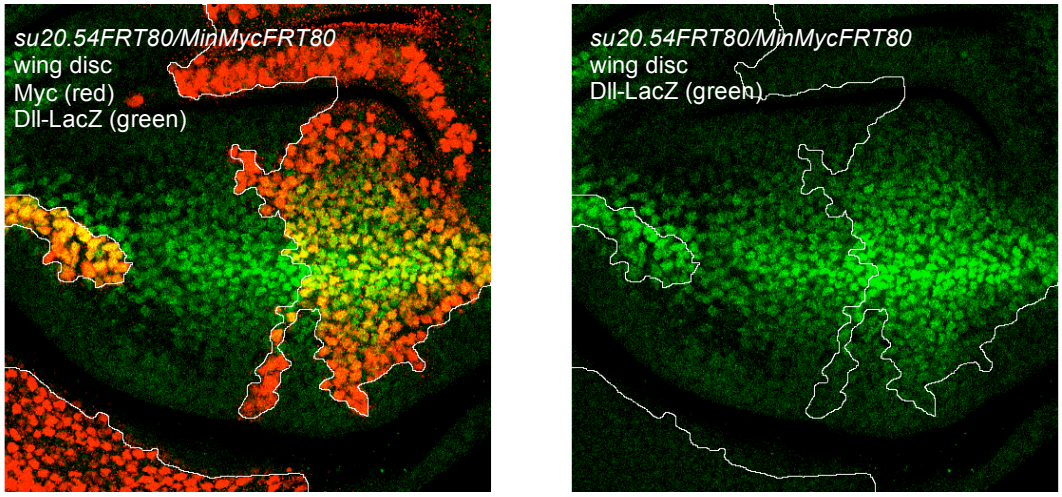

Figure 30 – Wing disc with Minute$^{+/+}$ clones homozygous for *su20.54*. On the left: mutant clones marked by the absence of the red staining (Myc tag) show a reduction of the staining for the *Dll-LacZ* (green). On the right: *Dll-LacZ* staining alone.

Under these conditions we could see a reduction of *Dll-lacZ* expression when the clones were very big and were involving also the Wg producing cells.

3.7.2 Requirement for CG6210 function for the expression of the short-range target gene *senseless*

As a next step, we wanted to study the effect of the loss of function of *CG6210* on the expression of the Wg short-range target gene *senseless* (*sens*).

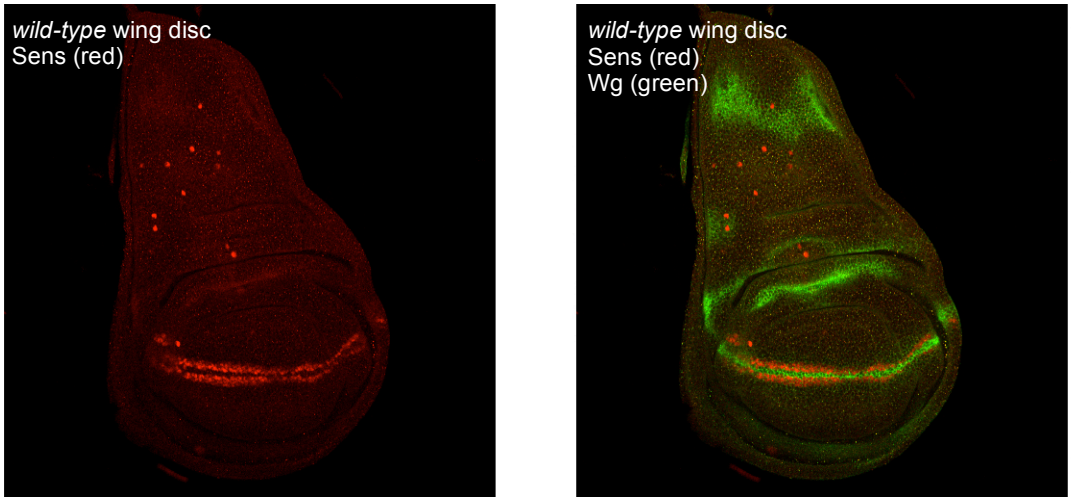

Figure 31 – Wing imaginal discs showing the expression of Sens (in red) with and without the expression pattern of Wg (in green).

The expression of *sens* in the wing disc is very dynamic: its expression is detectable at the third-instar stage in the entire wing margin, and later its expression decreases in the precursors of the bristles of the posterior wing margin that are not innervated (Nolo et al., 2000). For this reason the stage at which the larvae were dissected was very important and kept constant at 120-168 hrs AEL.

We first analyzed the *sens* expression in wing discs of wild-type versus *3L3* homozygous mutant third instar larvae. We could see a clear reduction of *sens* expression in the mutant situation, supporting our hypothesis that *3L3* plays a role as a positive component of the Wg signaling pathway.

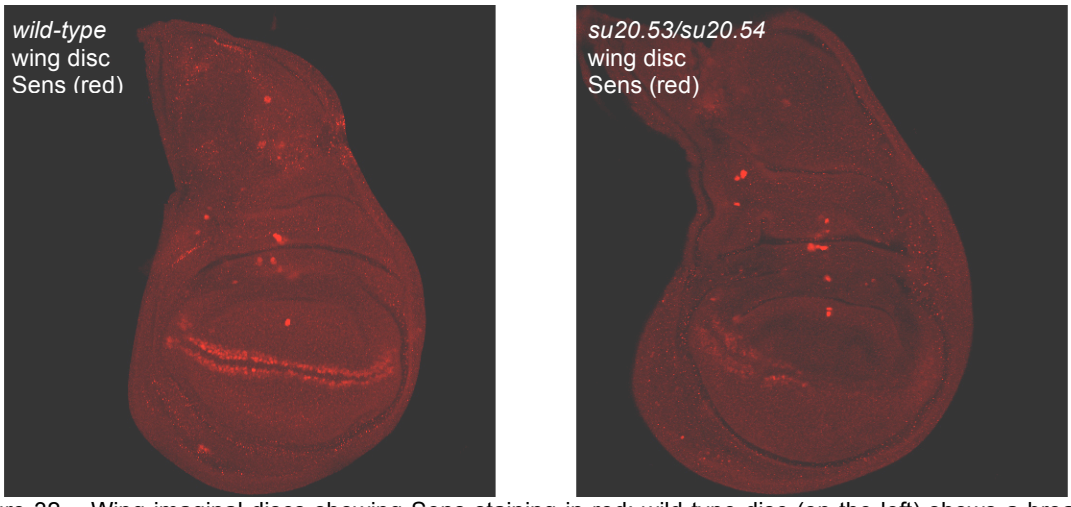

Figure 32 – Wing imaginal discs showing Sens staining in red: wild-type disc (on the left) shows a broader and stronger staining than transheterozygous mutant disc (on the right).

As for the long-range target gene *Dll,* we generated Minute$^{+/+}$ clones mutant for *3L3,* using the allele *su20.53*, in a Minute$^{+/-}$ background. We looked at the expression of *senseless* by anti-Sens antibody staining.

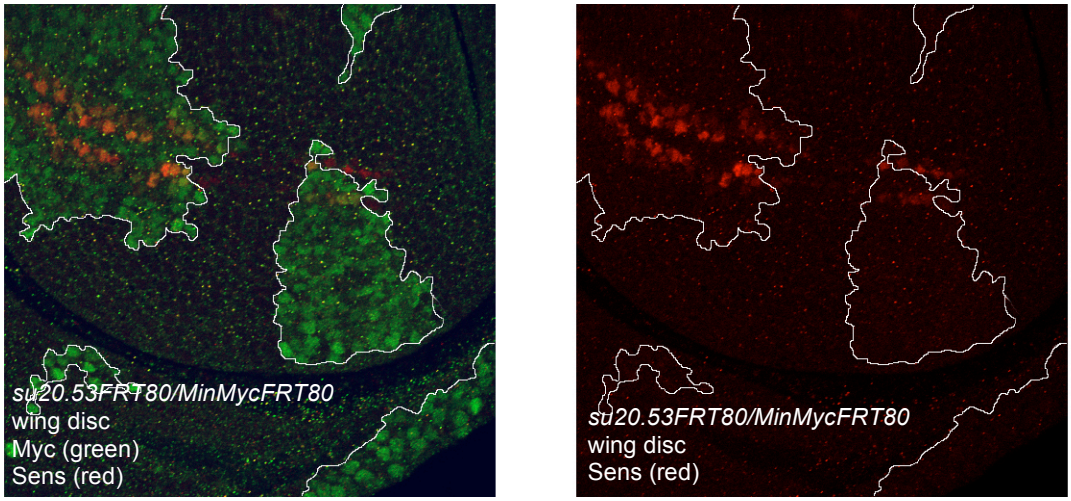

Figure 33 - Wing disc with Minute$^{+/+}$ clones homozygous for *su20.53*. On the left: mutant clones marked by the absence of the green staining (Myc tag) show a reduction of the staining for Sens (red). On the right: Sens staining alone.

We analyzed many wing discs carrying different clones and, in most cases, a reduction of the staining for the target gene *sens* was observed. We also looked at small clones and found that the size of the clone was not important. The only requirement to detect a reduction of Sens was that the Wg producing cells next to the *sens*-expressing cells were mutant for *3L3*.

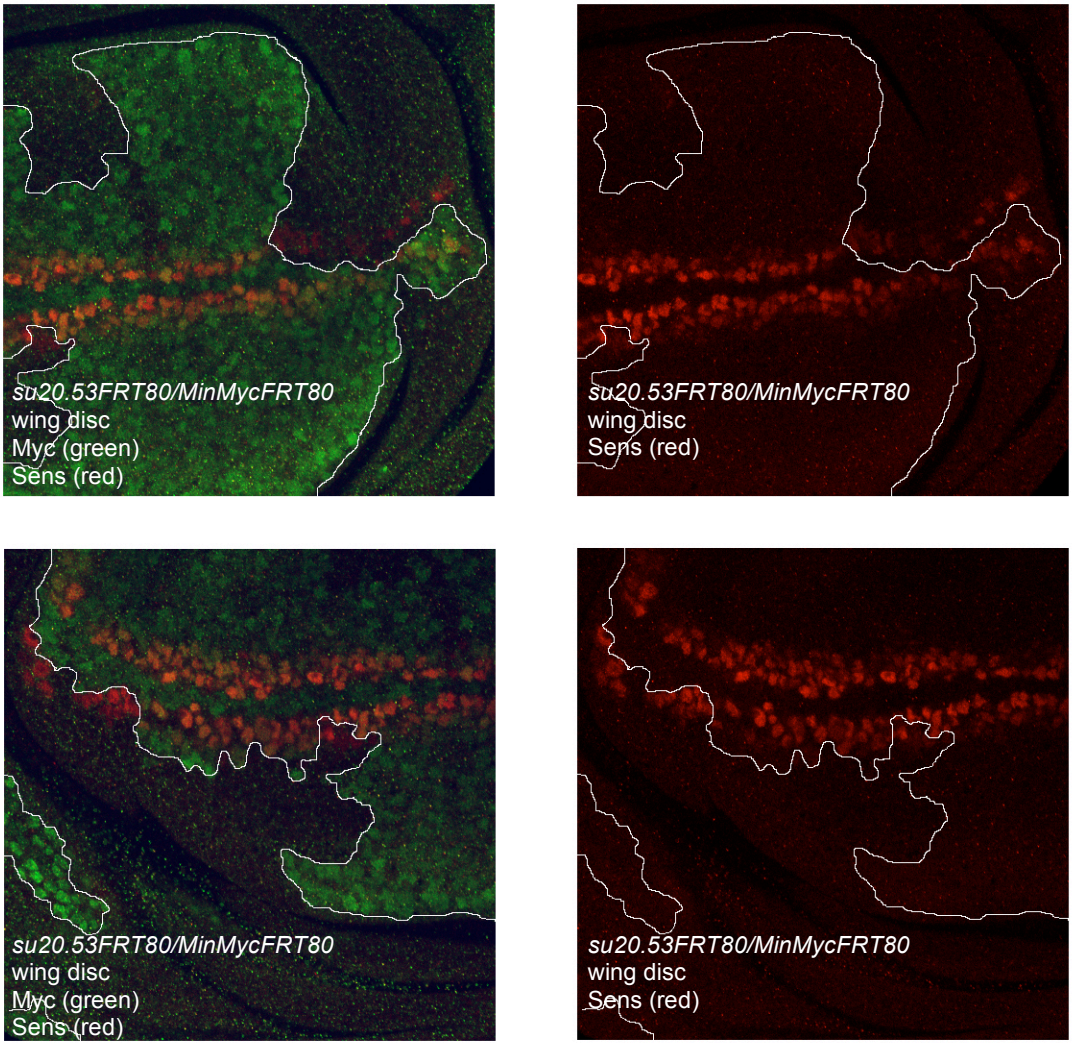

Figure 34 - Wing disc with Minute$^{+/+}$ clones homozygous for *su20.53*. On the left side of the panel: mutant clones marked by the absence of the green staining (Myc tag) and staining for Sens (red). On the right side of the panel: Sens staining alone.

If the Wg receiving cells, but not the *wg*-expressing cells, were mutant for *3L3* no suppression of Sens was observed. This suggested that Wg signaling still takes place in mutant Wg receiving cells.

In contrast, if the *wg*-expressing cells are mutant for *CG6210*, a weaker staining for Sens was observed in nearby cells. Interestingly, the reduced expression of the target gene was observed in both mutant and wild-type *sens* expressing cells.

We then tried to confirm the above described result in mutant the wing discs expressing *CG6210* from a transgene. For this purpose, we expressed *3L3-HA* under the control of the *en-Gal4* driver, which actives *3L3* expression in the posterior compartment of the disc. This set up is analogous to a *3L3* mutant clone, which covers the whole anterior compartment.

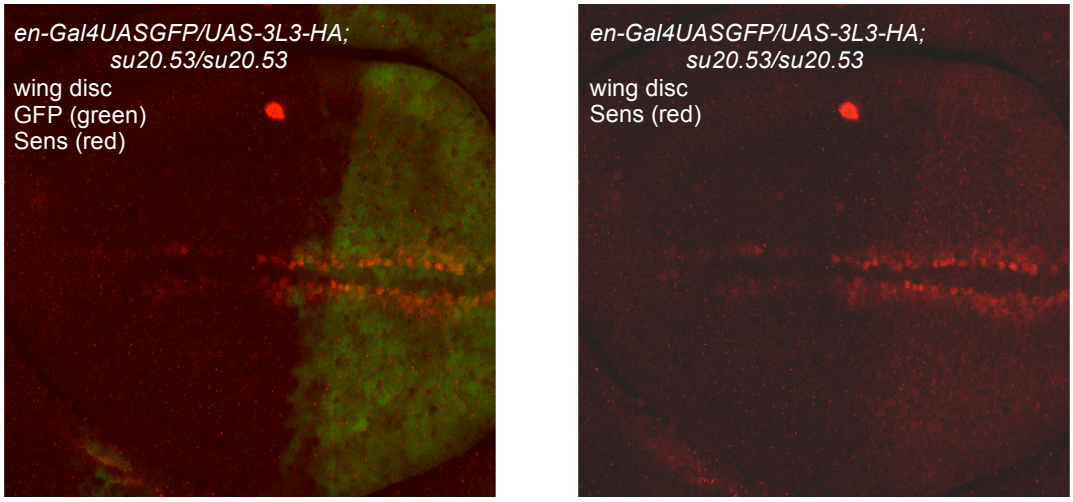

Figure 35 – Homozygous mutant wing discs expressing *CG6210* in the posterior compartment. Sens staining is shown in red (left and right picture), whereas the posterior compartment is marked by GFP (green, left picture).

As expected, we observed a reduction of the Sens protein expression in the mutant tissue of the anterior compartment, whereas the posterior compartment expressing *CG6210* showed a wild-type expression of the target gene.

The fact that big clones are needed to get a reduction of *Dll-lacZ* expression, but not for the suppression of *sens* expression, can be explained by the different amount of Wg necessary to induce the two target genes. In fact, target genes of morphogens are elicited at different threshold concentrations (Zecca et al. 1996), and the expression of *sens,* as a short-range target gene, is dependent on a high concentration of Wg, and thus more sensitive to a reduction of the signaling pathway. *Dll* is instead a long-range target gene and its expression is dependent on a lower stimulation of the Wg pathway; as a consequence, it is less sensitive to a reduction of the signaling pathway.

From these results obtained through the staining of wild-type versus *3L3* homozygous mutant tissue in wing discs of third-instar larvae, we can deduce that the absence of 3L3 probably leads to a reduction of Wg production, but not to a complete loss.

3.7.3 CG6210 and the ligand Wingless

In early third-instar wing discs (48 hrs before pupariation), *wg* is expressed at low levels throughout the perspective wing blade. Beginning at mid-third-instar (24 hrs before pupariation), this pattern refines, and *wg* becomes expressed at high levels along the perspective wing margin in a stripe, which is 3-6 cells wide just to either side of the dorso-ventral boundary (Rulifson et al., 1996).

In order to better understand the role of *3L3* in Wg production and release, we studied the behaviour of Wg itself.

The first experiment we performed was simply the observation of Wg in wing discs of wild-type versus *3L3* homozygous mutant third-instar larvae.

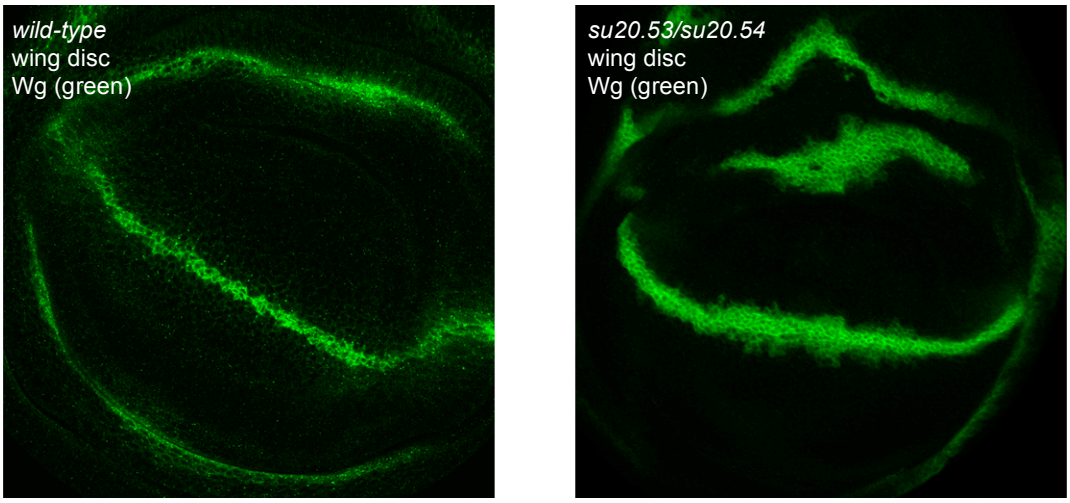

Figure 36 - Wg expression pattern in wild-type (left) and in transheterozygous mutant wing discs (right).

We could observe a clear difference in the expression of Wg in mutant versus wild-type wing discs: Wg staining is stronger and broader in the mutant condition. Moreover, in mutant wing discs Wg staining does not show the gradual decrease in intensity and in the number of spots typical of Wg gradient, which has its source at the D/V boundary.

In order to better characterize this difference, we generated Minute$^{+/+}$ clones mutant for *3L3* in a Minute$^{+/-}$ background. For this experiment the allele *su20.53* was used.

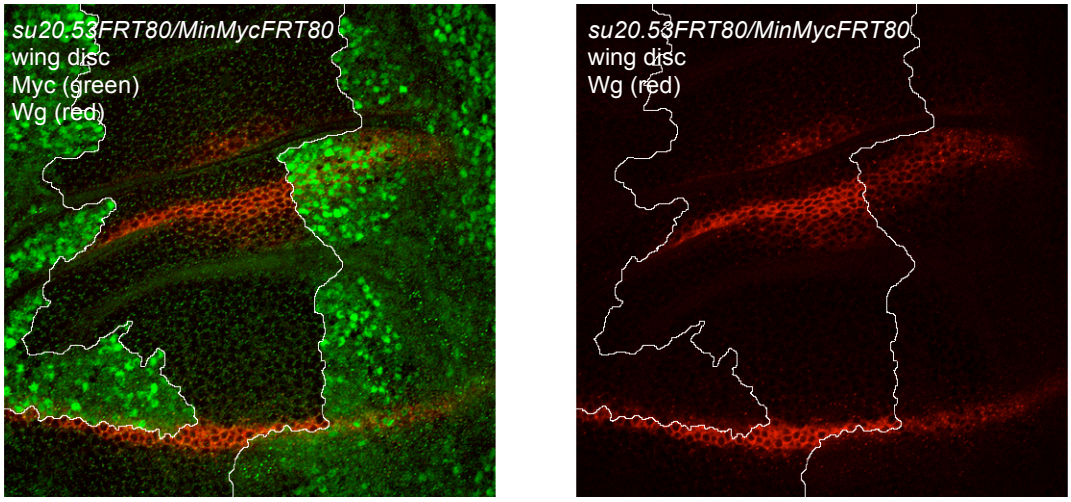

Figure 37 - Wing disc with a Minute$^{+/+}$ clone homozygous for *su20.53*. On the left: a mutant clone, marked by the absence of the green staining (Myc tag), shows an increased staining for Wg (red). On the right: Wg staining alone.

In all cells, which are mutant for *3L3* and are supposed to secrete Wg, we found a strong accumulation of the Wg protein. This effect did not seem to be dependent on the size of the clone, and for this reason, we performed the same experiment without the growth advantage of the Minute system.

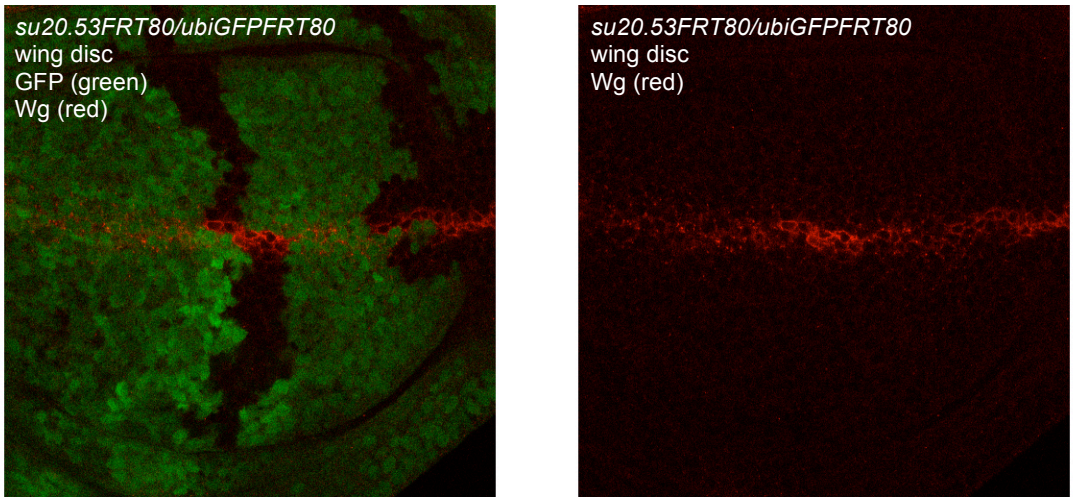

Figure 38 - Wing disc with clones homozygous for *su20.53*. On the left: mutant clones, marked by the absence of the GFP, show an increased staining for Wg (red). On the right: Wg staining alone.

In this case, mutant clones were marked by absence of GFP and Wg showed the same behaviour as in Minute$^{+/+}$ clones.

It is important to stress the fact that Wg accumulation was confined inside the *wg*-expressing cells, which are mutant for *3L3*, and that nearby wild-type *wg*-expressing cells behave, regarding Wg, exactly the same as cells in a wild-type disc.

3.7.4 CG6210 and transcriptional level of *wingless*

Since Wg is known to repress its own expression in adjacent cells at the D/V boundary (Rulifson et al., 1996), the effect we observed could be due to a disruption of this negative feedback, and a consequent up-regulation of the transcription. In order to test this idea, i.e. that the accumulation of Wg in 3L3 mutant tissue was due to an increased transcription, we looked at *wg-LacZ* expression in mutant versus wild-type tissue.

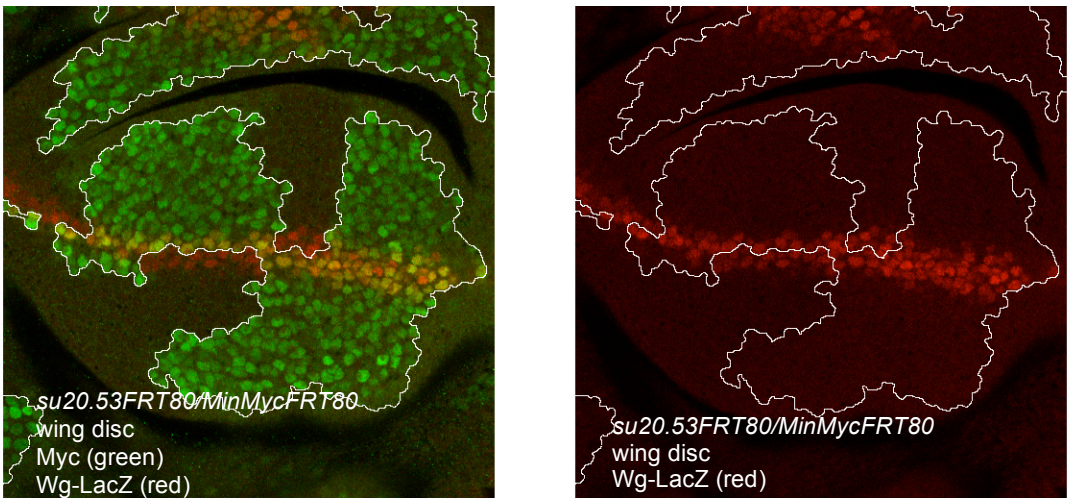

Figure 39 - Wing disc with Minute$^{+/+}$ clones homozygous for *su20.53*. On the left: a mutant clone, marked by the absence of the green staining (Myc tag), shows an unchanged staining for *wg-LacZ* (red). On the right: *wg-LacZ* staining alone.

In mutant clones for 3L3 we never saw any increase in the expression of the *wg-LacZ*, leading us to conclude that the accumulation of Wg protein takes place at the post-transcriptional level.

The observation that Wg protein does not accumulate as a consequence of an increased transcription is confirmed by experiments made with transgenic larvae carrying the *sev-wg* construct. These larvae express *wg* in the eye imaginal discs, since two copies of the *sevenless* enhancer drive *wg* expression. This way of driving *wg* expression is independent of Wg pathway activity (Brunner et al., 1997).

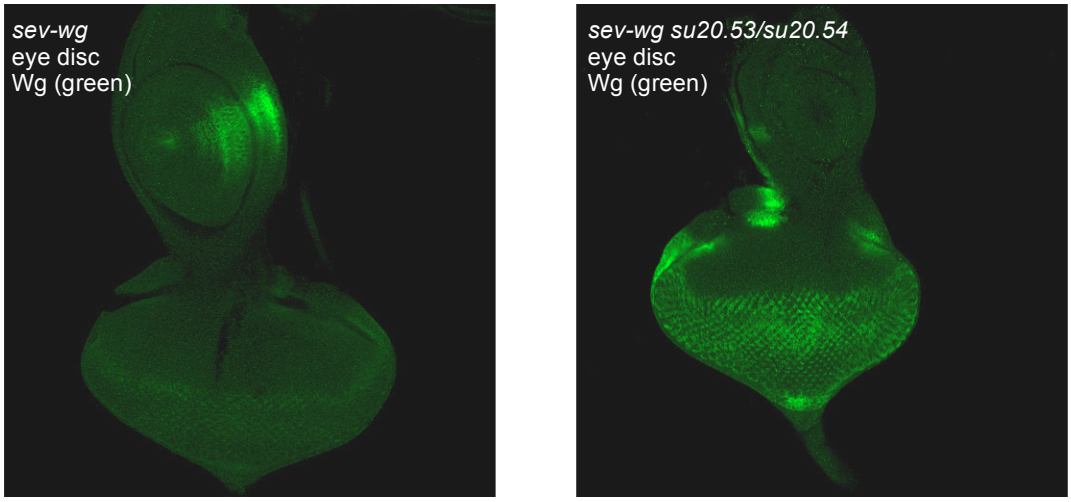

Figure 40 – Wg staining in wild-type (left) and transheterozygous mutant (right) eye discs carrying the *sev-wg* transgene.

We first looked at Wg staining in heterozygous (with the allele *su20.53*) versus transheterozygous (alleles *su20.53* over allele *su20.54*) eye discs, and observed a clear increased staining in the mutant situation. In order to confirm this result, we then generated mutant clones for *3L3* (using the allele *su20.53*) marked by the absence of the marker GFP.

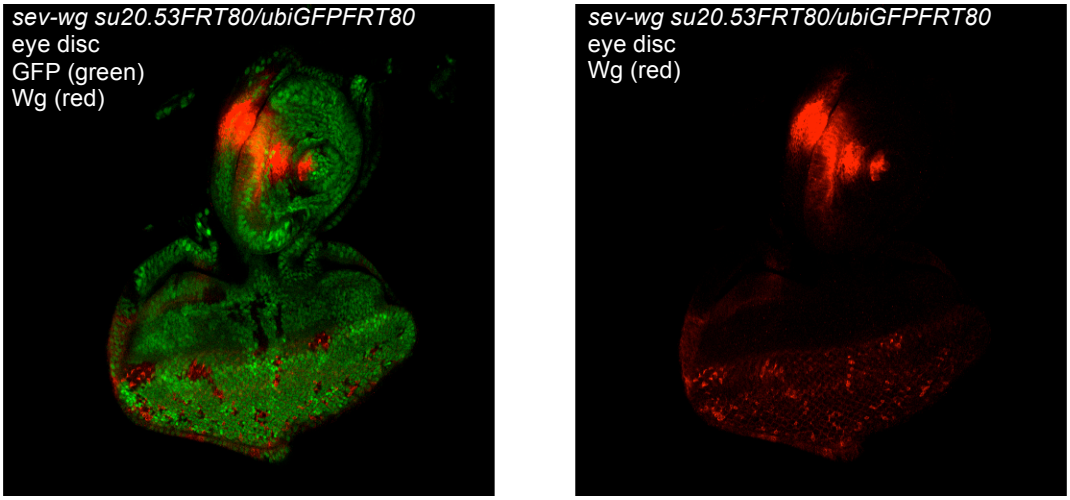

Figure 41 – Eye discs of larvae carrying the *sev-wg* construct show clones homozygous mutant for *3L3*. On the left: clones marked by the absence of GFP staining (green) show an increased staining for Wg (red). On the right: Wg staining alone.

We could detect in the eye discs a clear accumulation of Wg inside the clones mutant for *3L3*, and thus confirm that *3L3* regulates Wg post-transcriptionally.

Another experiment was made to confirm that the observed Wg accumulation in *3L3* mutant tissue takes place at a post-transcriptional level. We used in this case eye and wing discs of larvae carrying the *sev-wg* transgene. Due to the fact that the *sev-wg* construct also carries a *heat-shock* (*hsp70*) promoter, we could drive *wg* expression ubiquitously simply by a heat-shock. We generated Minute$^{+/+}$ clones mutant for *3L3* (using the allele *su20.53*) in a Minute$^{+/-}$ background, and induced the synthesis of Wg before dissection.

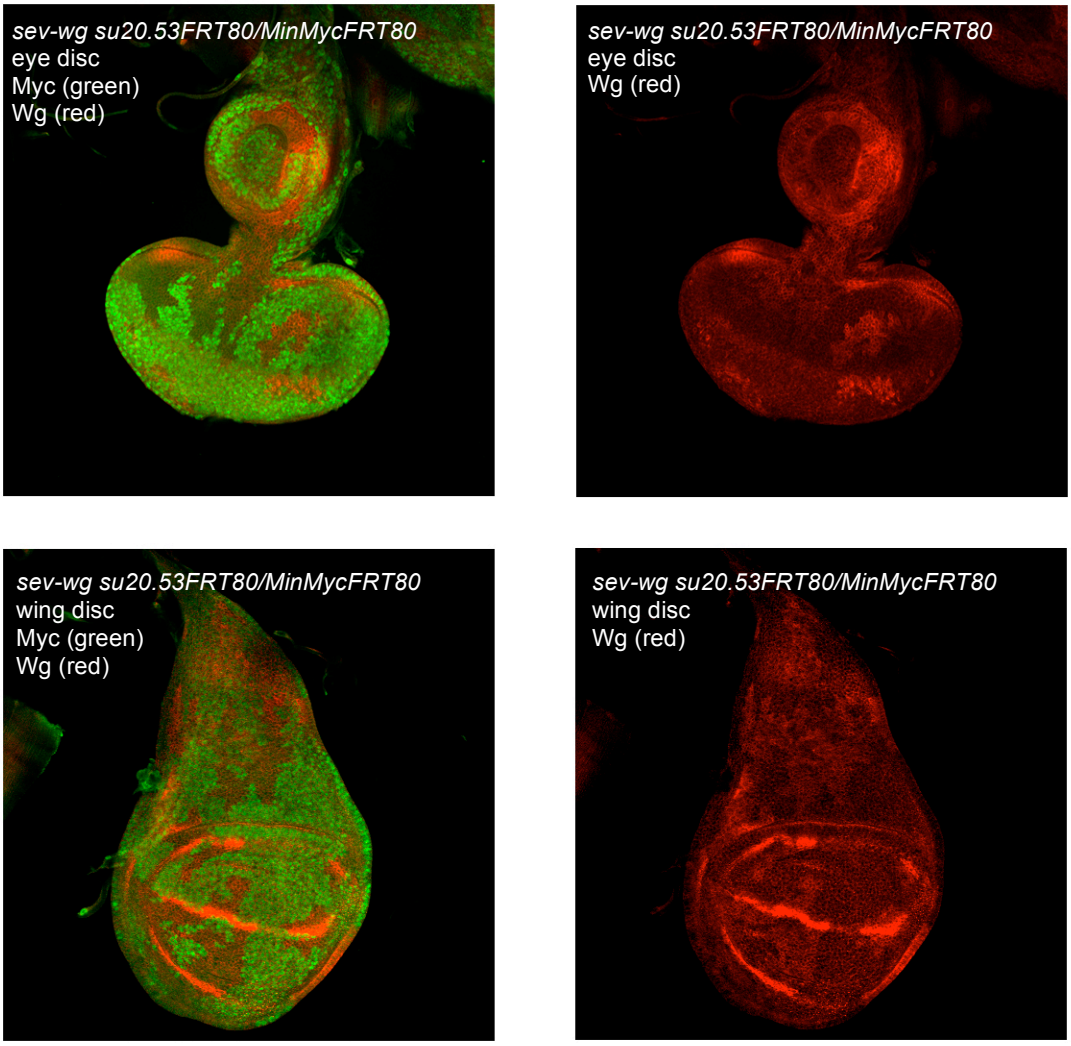

Figure 42 – Eye discs (upper part) and wing discs (lower part) of larvae carrying the *sev-wg* construct are exposed to heat-shock before dissection. On the left: Minute$^{+/+}$ clones homozygous for *su20.53* are marked

by the absence of the green staining and show an increased staining for Wg (red). On the right side: Wg staining alone.

We examined wing and eye imaginal discs and observed again in both cases an accumulation of Wg in homozygous mutant cells.

From all the experiments performed so far we have the impression that *3L3* loss of function leads to an accumulation of Wg only in the *wg*-expressing cells. In order to confirm this hypothesis, we performed double staining of *wg-LacZ* and Wg in wing discs of wild-type versus *3L3* homozygous mutant larvae. Interestingly, we observed in the mutant situation that Wg was detected only in cells which also expressed Wg-LacZ (data not shown).
This result supports our hypothesis.

3.7.5 The Wingless signaling pathway and the specificity of CG6210

An important issue is to know whether the effects observed on Wg and on the Wg signaling pathway are specific.

We first checked whether in *3L3* mutant tissue there was an accumulation of Hedgehog (Hh). The choice of Hh was due to the fact that Hh is also a ligand for a signaling cascade and that Hh, like Wg, undergoes a hydrophobic modification. Indeed, after autoproteolytical cleavage, the N-terminal domain of Hh (HhN-p, for HhN-processed) (Lee et al., 1994) is modified by the covalent linkage of a cholesterol moiety on the C-terminus of HhN-p (Porter et al., 1996) and by the linkage of palmitate to the NH_2-terminus of HhN-p (Chamoun et al., 2001). In wild-type wing discs, *hh* is expressed in the whole posterior compartment and is known to induce the expression of target genes, such as *patched* (*ptc*) and *decapentaplegic* (*dpp*).

We first generated Minute$^{+/+}$ clones mutant for *3L3* (using the allele *su20.53*) in a Minute$^{+/-}$ background and stained for Hh in wing discs.

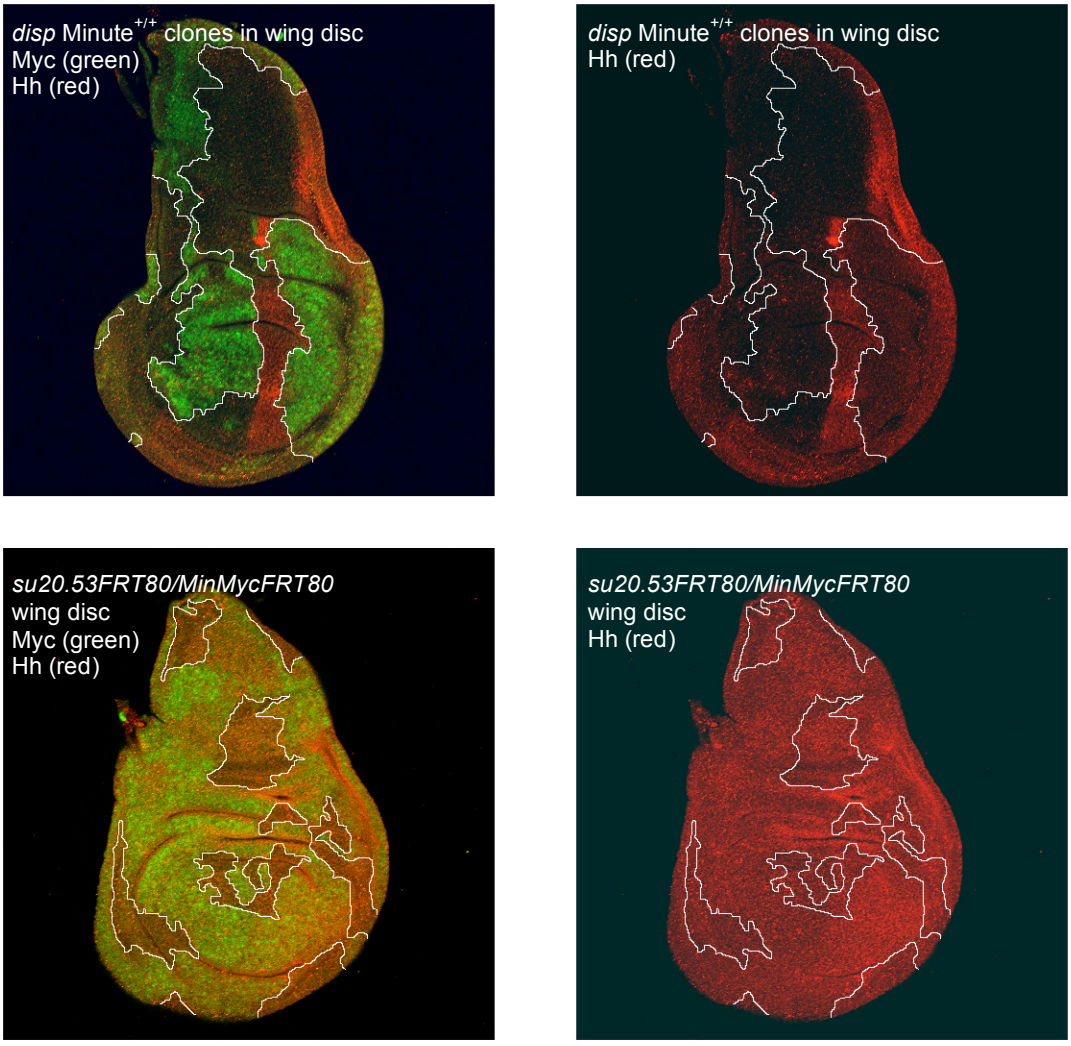

Figure 43 – Wing discs stained for Hedgehog (in red). Upper part: Minute$^{+/+}$ clones mutant for *dispatched* (*disp*) are marked by the absence of the green labeling and show an accumulation of Hh; lower part: Minute$^{+/+}$ clones mutant for *CG6210* do not show any accumulation of Hh.

In homozygous mutant tissue for *CG6210* we could never observe a change in the expression of Hh: this rules out a possible role of *3L3* in the release of Hh.

As a control, we induced in wing discs Minute$^{+/+}$ clones mutant for *dispatched* (*disp*) in a Minute$^{+/-}$ background; *disp* is a segment polarity gene known to be necessary for the release of Hh by the *hh*-expressing cells, and in its absence Hh protein was shown to

accumulate (Burke et al., 1999). As expected, we detected a notable increase in the level of the staining for Hh in *disp* mutant tissue.

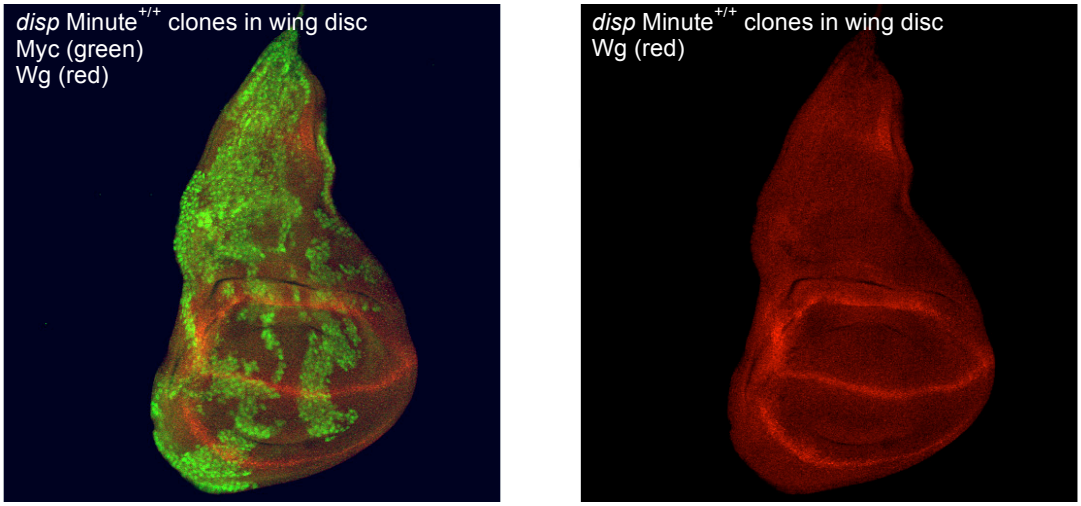

Figure 44 – Wing disc stained for Wg (in red) shows Minute$^{+/+}$ clones mutant for *disp*, which are marked by the absence of the green labeling and show no accumulation of Wg.

We then wanted to know whether *disp* is able to influence the release of Wg and so we performed the same experiment, but stained wing discs for Wg. In contrast to the effect seen on Hh, mutant tissue for *disp* had no effect on the expression of Wg.

As a next step in the analysis of the specificity, we studied the effect of *3L3* mutant tissue on the *hh* target genes *ptc* and *dpp*. The main purpose of these experiments was to exclude any role of *3L3* in the Hh pathway in the transduction of the signal, as well as in the synthesis of a functional Hh protein. In fact, if Hh is not properly processed (e.g. if Hh is not palmitoylated) no change in the protein expression is seen, and an effect of the erroneous modification is detectable only at the level of the target genes (Chamoun, et al. 2001).

We induced in wing discs Minute$^{+/+}$ clones mutant for *3L3* in a Minute$^{+/-}$ background, and looked for the expression of *ptc-LacZ* and *dpp-LacZ*.

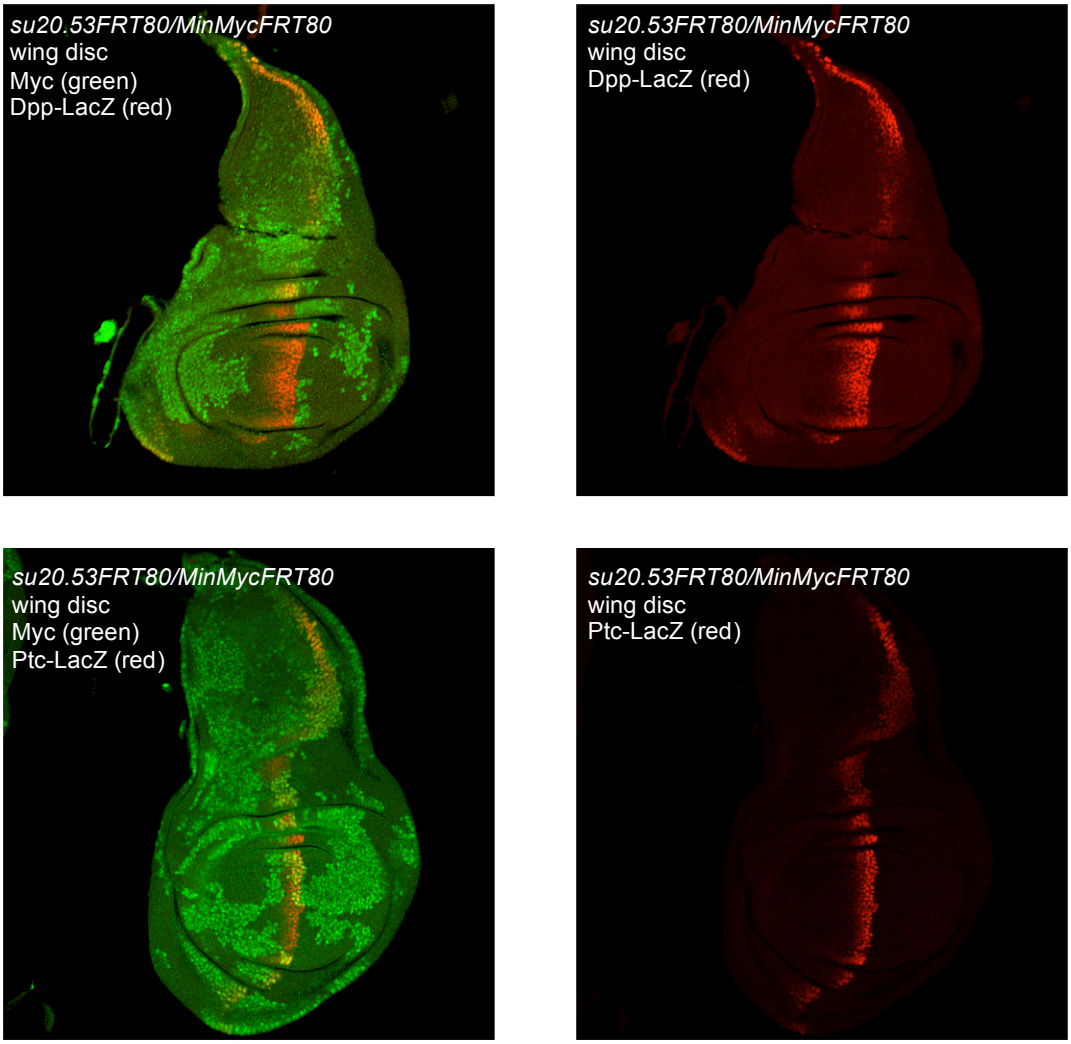

Figure 45 – Left upper part: Minute$^{+/+}$ clones mutant for *CG6210*, which are marked by the absence of the green labeling, do not show any change in the staining for *dpp-LacZ* (red). Left lower part: Minute$^{+/+}$ clones mutant for *CG6210* do not show any change in the staining for *ptc-LacZ* (red). Right half: *lac-Z* staining alone.

In both cases no effect was noticed in the mutant tissue, even if the mutant clone was very big and occupying almost the whole posterior compartment. The size and the location of the mutant tissue is important, since a small number of wild-type Hh producing cells is enough to induce the expression of the *ptc-LacZ* and *dpp-LacZ* (Chamoun, et al. 2001).

To further exclude a role of *3L3* in the release of N-glycosylated proteins, which are

tethered to the membrane, we investigated the expression of CD2 in transgenic flies carrying the construct *actin5c-CD2*. CD2 is a transmembrane protein present in mammalians (in our case we used the rat form), which is normally expressed in thymocytes and mature T-lymphocytes. CD2 carries three N-linked glycosylations.

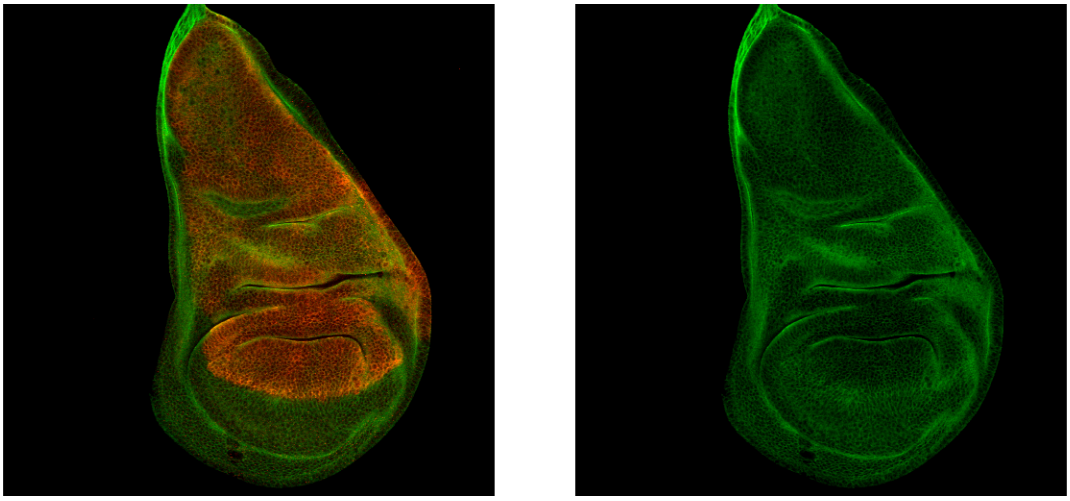

Figure 46 – Wing imaginal disc, which ubiquitously expresses CD2 and is mutant for *3L3* in the ventral compartment. CD2 staining (green) is not influenced by the presence or absence of CG6210 (in red).

We investigated wing discs of larvae, which are *3L3* homozygous mutant and express 3L3 protein only in the dorsal compartment by means of the transgene combination *ap-Gal4* and *UAS-3L3*. In addition, these larvae carry the *actin5c-CD2* transgene, so that each cell is positive for CD2. Performing a CD2 staining, we could not perceive any difference in the level of CD2 protein expression between the dorsal (wild-type for *3L3*) and ventral (mutant for *3L3*) compartment.

These results support the hypothesis that *3L3* is a specific component of the Wg signaling pathway and that it does not interfere with synthesis and release of other proteins than Wg.

3.8 Rescue experiments of the lethality phenotype

As previously discussed, *3L3* homozygous mutant animals die at the pupal stage, and show leg, antennae and wing phenotypes. In order to determine in which cells 3L3 protein is necessary for survival and normal development, we carried out the following rescue experiments.

As already discussed, the ubiquitous expression of *3L3* by the transgene *tubα1-3L3* can rescue all the phenotypes. We then tested whether the expression of *3L3* in all cells by the Gal4 system through the combination of *actin5c-Gal4* and *UAS-3L3* was also able to lead to a complete rescue. So we crossed flies heterozygous mutant for *3L3* (*su20.54*) and transgenic for the construct *UAS-3L3* with flies, which were also heterozygous mutant for *3L3* (*su20.53*) and carried the transgene *actin5c-Gal4.*
The cross gave a complete rescue of all the observed phenotypes, when both *actin5c-Gal4* and *UAS-3L3* were present.
We can draw the following conclusions from these results. First, the transgene *UAS-3L3* is functional and, when expressed in all cells, can lead to a complete rescue. Second, the transgene *UAS-3L3* alone does not lead to a rescue, which means that it is not leaky. This is important for the following rescue experiments. Third, no Wg gain-of-function phenotypes developed and this means that Wg signaling pathway does not show any dosage dependence on the amount of 3L3.

Since the *UAS-3L3* transgene could rescue the observed phenotype when expressed ubiquitously, we crossed it with other *Gal4* drivers in order to get additional information about which cells need to express *3L3*. Given that the accumulation of the Wg protein occurs in *wg*-expressing cells, we were very much interested to use *wg-Gal4* drivers for the rescue experiment. We combined *UAS-3L3* with the following *Gal4* drivers: *ap-Gal4*, *en-Gal4*, *ND382* and *S180* (both of which are *wg-Gal4*), and *MD618* (which might also be a *wg-Gal4*).
ap-Gal4 and *en-Gal4* drivers did not rescue the lethality phenotype, whereas *ND382*, *S180* and *MD618* drivers were able to rescue most phenotypes. The rescue made with these last three *Gal4* drivers were however not complete: for the combination with *ND382,* 50% of the transheterozyogous flies showed a wing-to-notum transformation; for *S180,* the wing-to-notum transformation was present even at a higher frequency; for *MD618,* 50% of the transheterozyogous flies showed antenna and leg phenotypes.
We can conclude that *3L3* has to be expressed in the *wg*-expressing cells and that this expression is, at least in some cases, enough for the proper development of the fly. The fact that no complete rescue was achieved in all cases can be explained by the inefficiency of the *Gal4* drivers. Alternatively, *3L3* may also play a minor role in other cells, as in part of the population of the non-*wg*-expressing cells, and this requirement may then be responsible for the partial rescue.

Observation:
There was a strong genetic interaction between the *3L3* alleles and the *wg-Gal4* drivers. We observed that fly stocks carrying a *wg-Gal4* driver and the mutation in *CG6210* (*su20.53*) are less viable and this is probably due to the fact that the *wg-Gal4* are hypomorphic or null alleles of *wg*. In fact, *wg-Gal4* are also recessive lethal. The most striking phenotype appears when *S180* is combined with the allele *su20.54*: most of the flies show wing-to-notum transformation.

3.9 CG6210 and the Wingless gradient

Previous experiments performed in the *Drosophila* embryonic epidermis showed that Wg passes through the endoplasmic reticulum and Golgi apparatus of *wg*-expressing cells. Moreover, Wg can be detected in intracellular vesicles and in multivesicular bodies in those *wg*-expressing cells and in adjacent non-*wg*-expressing cells (van den Heuvel et al., 1989; Gonzales et al., 1991).
In the wing discs, dots of Wg in the cells away from the source appear to reflect vesicles of internalized Wg protein (Strigini and Cohen, 2000), and these Wg dots form a gradient starting at the D/V boundary.

When we looked at Wg staining performed in wing discs of wild-type *Drosophila* larvae, Wg appeared to be present at the cell membrane of the *wg*-expressing cells and in the form of dots in *wg*- and non-*wg*-expressing cells. This observation agrees with the data from the literature outlined above.
Interestingly, when we analysed the behaviour of Wg in wing discs homozygous mutant for *CG6210*, we found that, in addition to the Wg accumulation in the *wg*-expressing cells, the Wg dots noted above are absent from *wg*-expressing and non-*wg*-expressing cells.

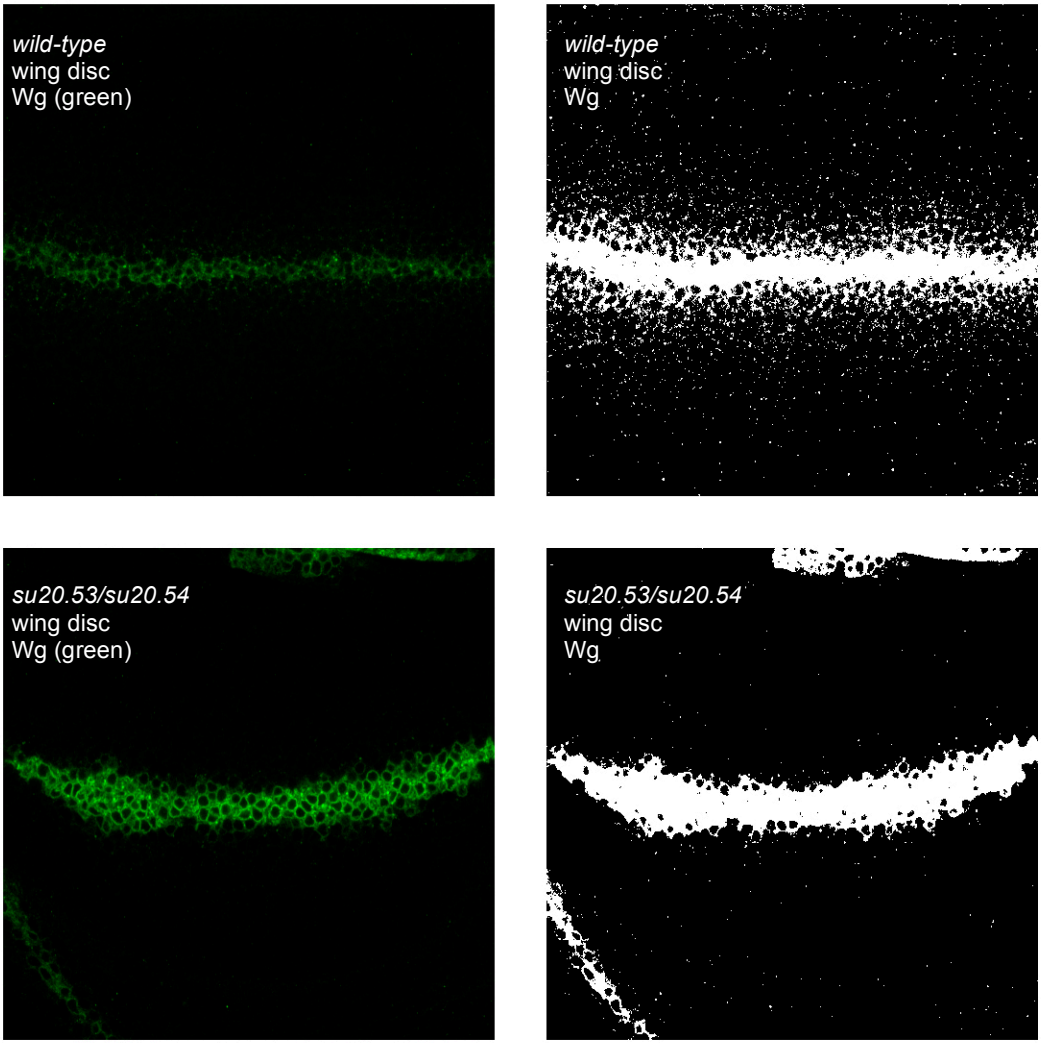

Figure 47 – Upper figures show Wg staining at the D/V boundary of a wild-type wing disc: Wg gradient and dots of Wg are visible. Lower figures: in a *3L3* mutant wing disc Wg accumulates in the *wg*-expressing cells and no gradient and no dots of Wg are visible.

In order to get some more information about which cells are responsible for the observed phenotype, we performed the same staining in wing discs of homozygous mutant larvae, which expressed *3L3* under the control of some *Gal4* drivers.

First, wing discs carrying the combination of *ap-Gal4* with *UAS-3L3-HA* were stained for 3L3 and Wg. These showed invariably an accumulation of Wg at the level of the mutant *wg*-expressing cells. In contrast to the rescued cells in the dorsal compartment, which behave normally, mutant non-*wg*-expressing cells in the ventral compartment show only

very few dots close to the *wg*-expressing cells.

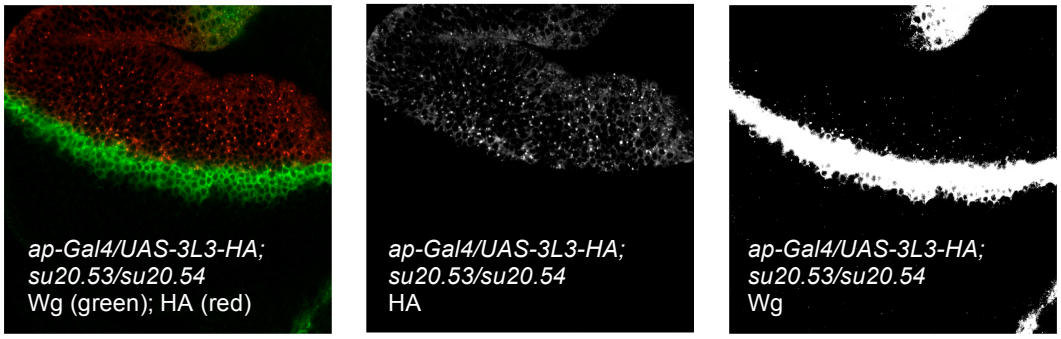

Figure 48 – A *3L3* mutant wing disc rescued dorsally by the combination *ap-Gal4/UAS-3L3-HA*. A gradient of Wg with dots of Wg (shown in green) is present only where *3L3* (in red) is expressed. Middle picture shows 3L3 staining alone, whereas the right picture shows Wg staining alone.

Subsequently, wing discs carrying the combination of *ND382* (a *wg-Gal4* driver) with *UAS-3L3-HA* were examined after performing the staining against 3L3 (i.e. against HA) and Wg.

In this case, a certain Wg gradient and the presence of Wg dots are visible in the rescued situation. This means that for the formation of a Wg gradient the expression of *3L3* in the *wg*-expressing cells is sufficient.

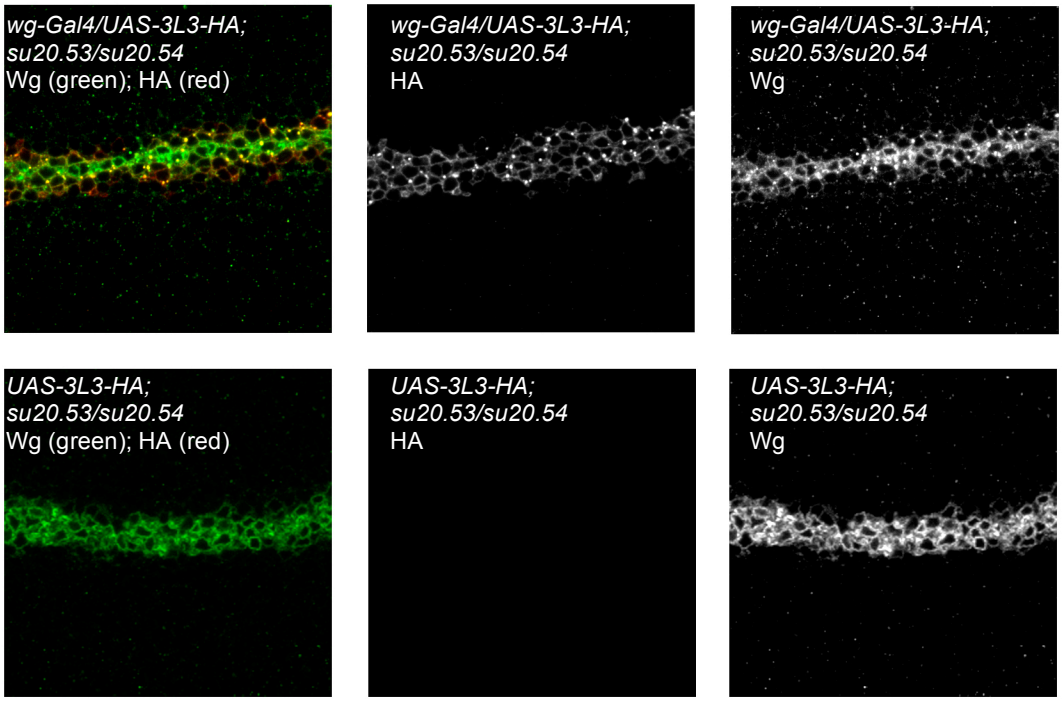

Figure 49 – Upper figures show the D/V boundary of a *3L3* mutant wing disc, where the *wg*-expressing cells were rescued by the combination of *ND382/UAS-3L3-HA*. Lower pictures show Wg staining of a wing disc mutant for *3L3*. The presence of 3L3 in the *wg*-expressing cells seems to be enough to restore a certain gradient of Wg. Wg is shown in green and 3L3 in red. Middle column displays 3L3 staining alone, whereas the right column displays Wg staining alone.

Finally, Minute$^{+/+}$ clones mutant for *CG6210* were induced in wing discs, which were stained for 3L3 and Wg. Interestingly, inside the mutant clones dots of Wg can still be observed, meaning that 3L3 is not necessary for their formation in the non-*wg*-expressing cells. This result agrees with the previous experiment performed with the combination *ND382/UAS-3L3-HA*, since also in that case Wg dots formed in mutant tissue for *CG6210*.

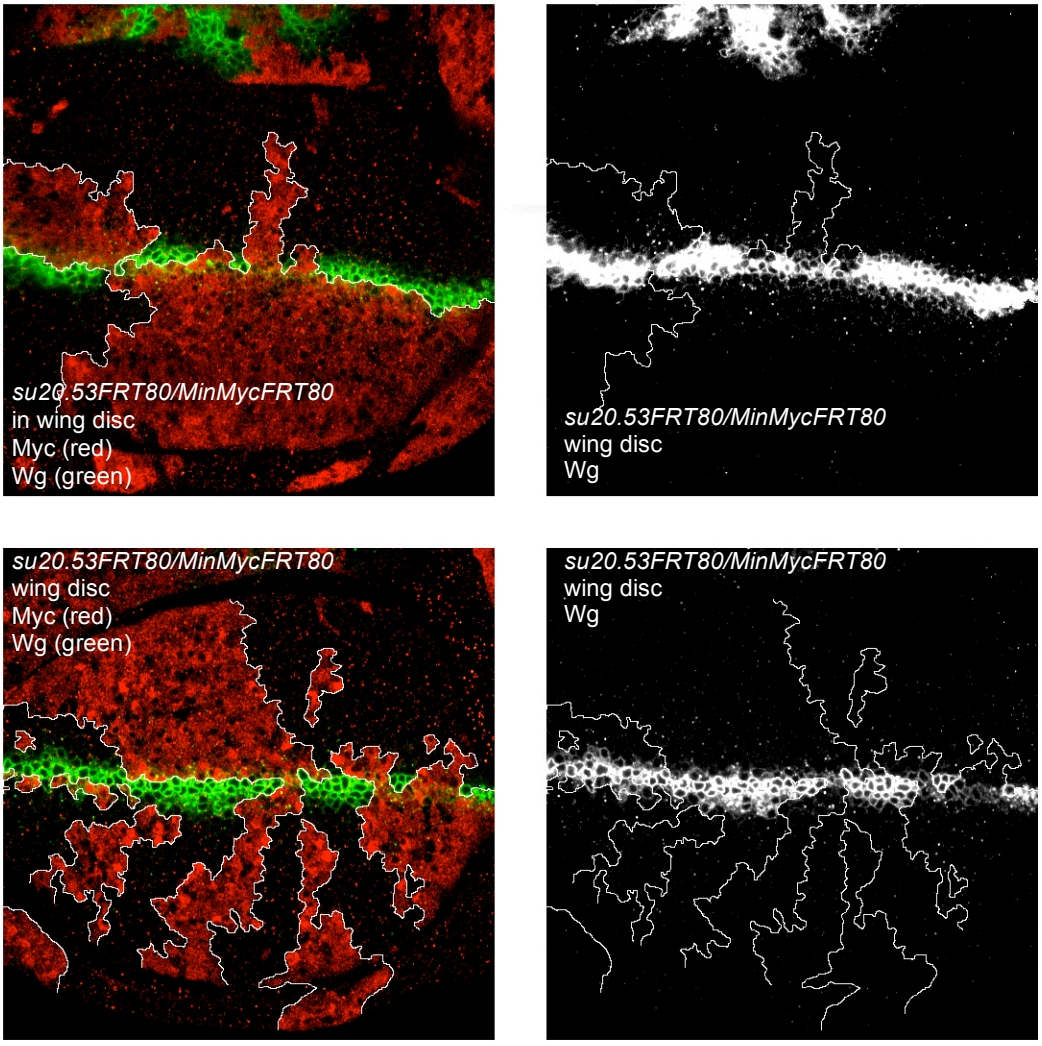

Figure 50 – Two wing discs showing Minute$^{+/+}$ clones mutant for *CG6210*, which are marked by the absence of the red labeling, and Wg, which is marked green. On the right: boundary of the clones and Wg are shown.

3.10 CG6210 and extracellular Wingless

Strigini and Cohen (Strigini and Cohen, 2000) established a new protocol for the labeling of extracellular proteins in imaginal discs, in which the primary antibody is incubated on ice. The low temperature is supposed to block endocytosis and to avoid any antibody molecules to be up-taken into the cells (see 6. Methods and Materials).

Control experiments showed that Legless (Lgs), an abundant intracellular protein, is readily visualized using the conventional protocol, but was not detected using the

extracellular staining protocol. The same result was obtained using anti-Tubulin antibodies (data not shown).

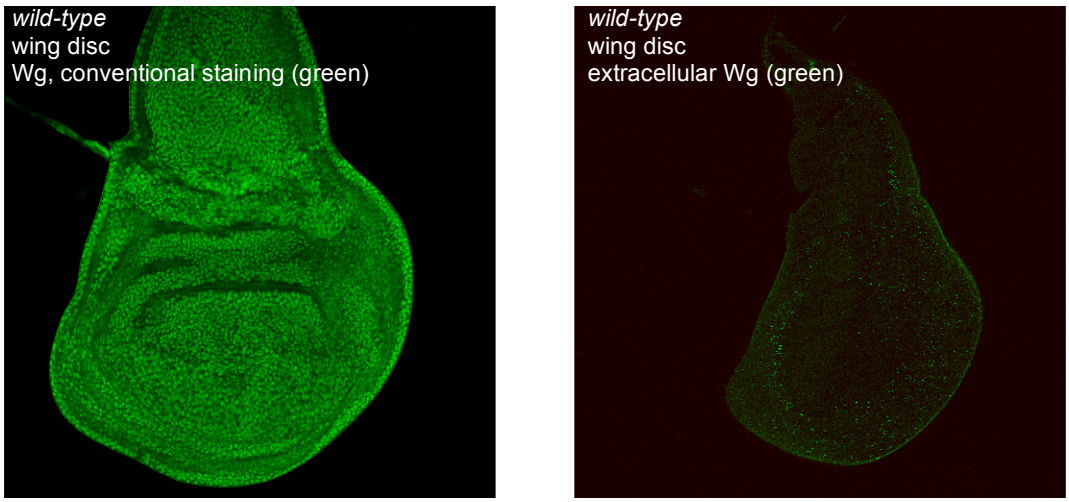

Figure 51 – Wing discs labeled with anti-lgs antibodies using the conventional (left) and extracellular (right) protocol.

We then made use of this protocol to monitor the behaviour of the extracellular Wg protein in wild-type versus *3L3* mutant tissue. First, we induced in wing discs Minute$^{+/+}$ clones mutant for *3L3* in a Minute$^{+/-}$ background. We labeled the imaginal discs with α-Wg antibody and then fixed before the labeling of the clones with α-Myc antibody.

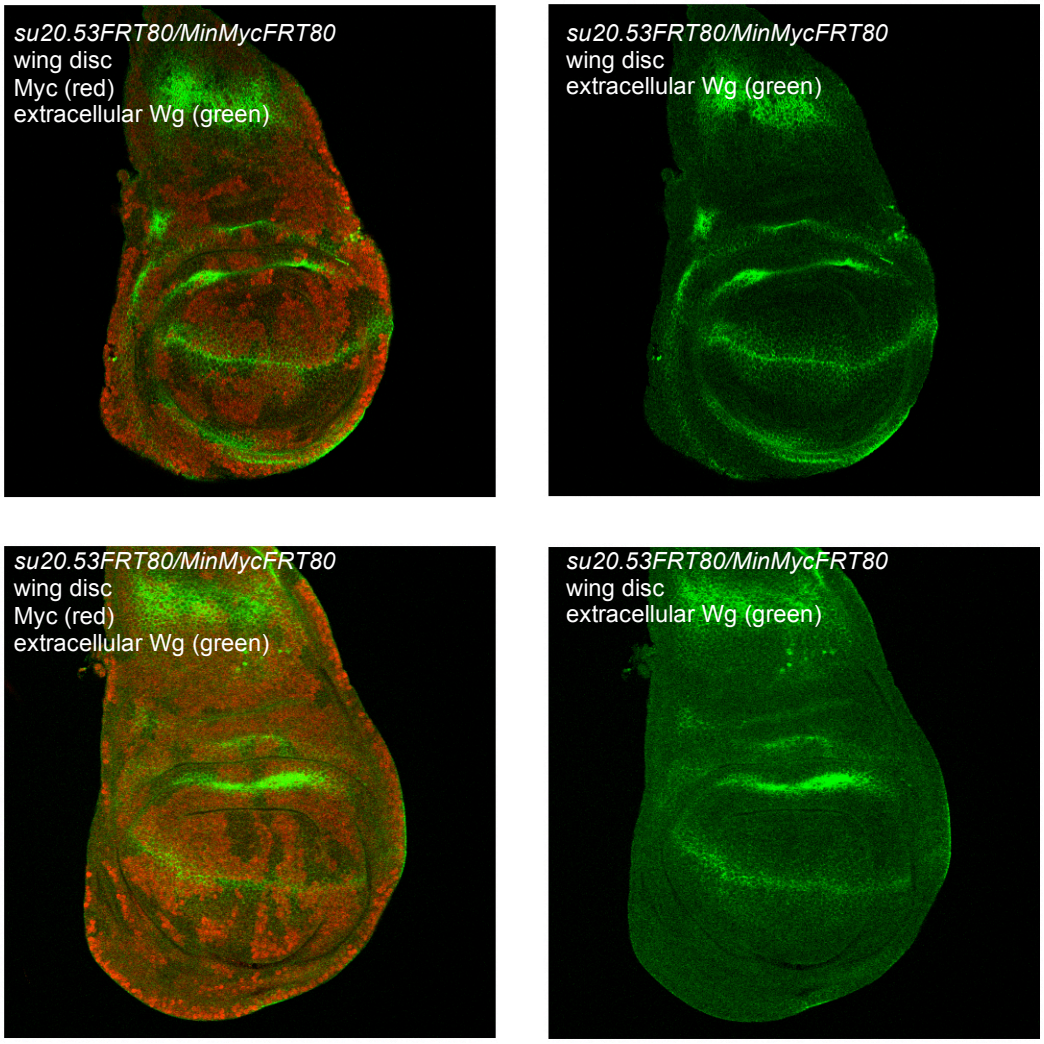

Figure 52 - Two wing discs showing Minute$^{+/+}$ clones mutant for *CG6210*, which are marked by the absence of the red labeling, and extracellular Wg, which is marked green.

We noted that in the *3L3* mutant tissue there was a slight increase in the extracellular Wg protein staining. In some cases this increase was very weak and barely detectable, and this contrasts with the striking increase viewed with the normal protocol. We further observed that the extracellular accumulation is not only present on the Wg producing cells, but also on the surrounding mutant cells. This test tells us that Wg protein accumulates mainly, but not exclusively in the intracellular space.

Subsequently, we performed some experiments using the Gal4 system. We first rescued the posterior compartment of *3L3* mutant wing discs by means of the combination of the

en-Gal4 driver with the *UAS-3L3* transgene. This allowed us to observe the behaviour of the posterior rescued part of the wing disc in comparison with the still mutant anterior part. In this case it is possible to notice that the recued (posterior) *wg*-expressing cells do not behave very differently from the mutant (anterior) *wg*-expressing cells. The main difference is seen in the nearby non-*wg*-expressing cells. Here the gradient of extracellular Wg is clearly broader in the posterior half of the wing disc. This difference might be due to the different amount of Wg, which leaves rescued versus mutant *wg*-expressing cells or to an influence of the surrounding cells.

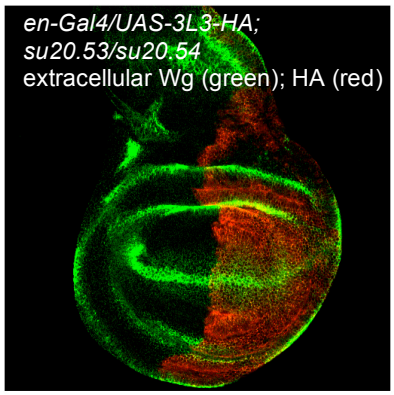
en-Gal4/UAS-3L3-HA;
su20.53/su20.54
extracellular Wg (green); HA (red)

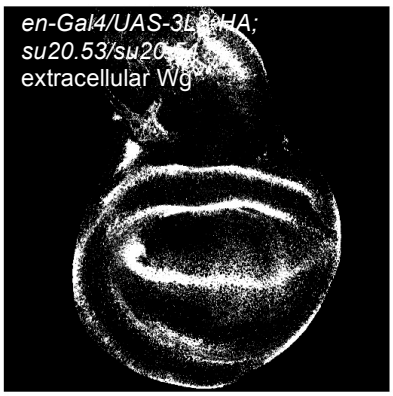
en-Gal4/UAS-3L3-HA;
su20.53/su20.54
extracellular Wg

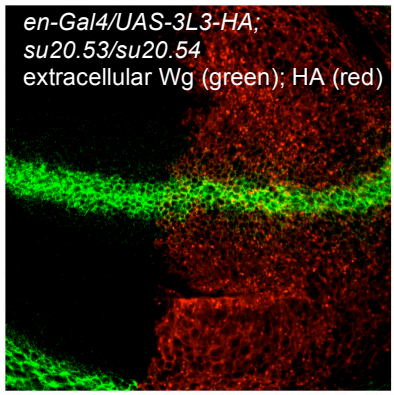
en-Gal4/UAS-3L3-HA;
su20.53/su20.54
extracellular Wg (green); HA (red)

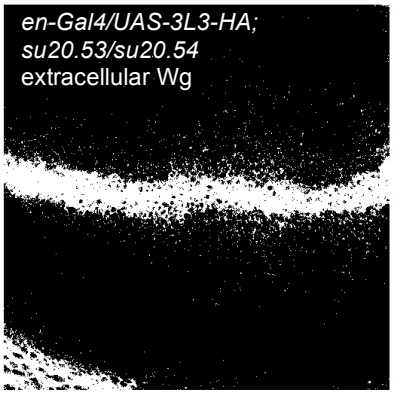
en-Gal4/UAS-3L3-HA;
su20.53/su20.54
extracellular Wg

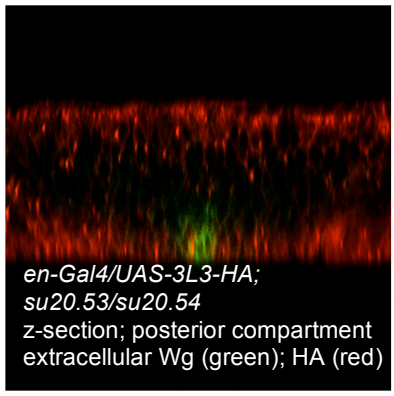
en-Gal4/UAS-3L3-HA;
su20.53/su20.54
z-section; posterior compartment
extracellular Wg (green); HA (red)


en-Gal4/UAS-3L3-HA;
su20.53/su20.54
z-section; posterior compartment
extracellular Wg

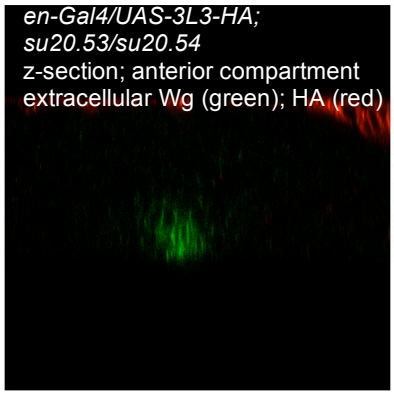
en-Gal4/UAS-3L3-HA;
su20.53/su20.54
z-section; anterior compartment
extracellular Wg (green); HA (red)

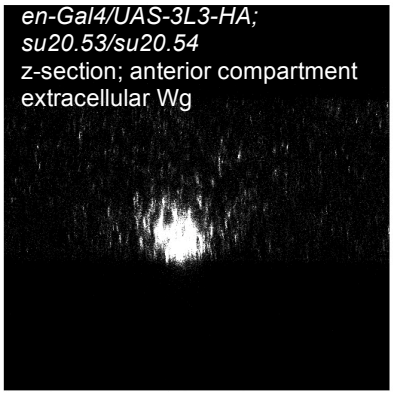
en-Gal4/UAS-3L3-HA;
su20.53/su20.54
z-section; anterior compartment
extracellular Wg

Figure 53 – Extracellular Wg is shown in green, whereas 3L3 is shown in red. The right column shows extracellular Wg alone. Two upper rows of pictures: wing disc of *3L3* mutant larvae rescued posteriorly by the combination of *en-Gal4* with *UAS-3L3* at different magnifications. Third row of pictures: z-section of the posterior (rescued) part. Last row: z-section of the anterior (mutant) part.

The vertical section through *3L3* expressing tissue also shows a broader gradient of extracellular Wg than the equivalent section through mutant tissue.

A very similar result was obtained when the dorsal part of *3L3* mutant wing discs was rescued by means of the combination of *ap-Gal4* and *UAS-3L3*. In fact, rescued (dorsal) *wg*-expressing cells do not behave very differently from the nearby mutant (ventral) *wg*-expressing cells. The main difference is again seen between mutant versus rescued non-*wg*-expressing cells: the gradient of extracellular Wg is clearly broader in the wild-type dorsal half of the wing disc. The same was confirmed by the vertical section through the wing disc.

Finally, the extracellular staining was performed on a *3L3* mutant wing disc, where only the *wg*-expressing cells were rescued by the combination of *ND382* (a *wg-Gal4* driver) with *UAS-3L3*. Compared to mutant wing discs, in this situation the extracellular Wg staining showed again a broader gradient.

From this we can conclude that the presence or absence of 3L3 in the *wg*-expressing cells influences the extracellular gradient of Wg. However, the possibility that non-*wg*-expressing cells do interfere with the distribution of extracellular Wg cannot be ruled out.

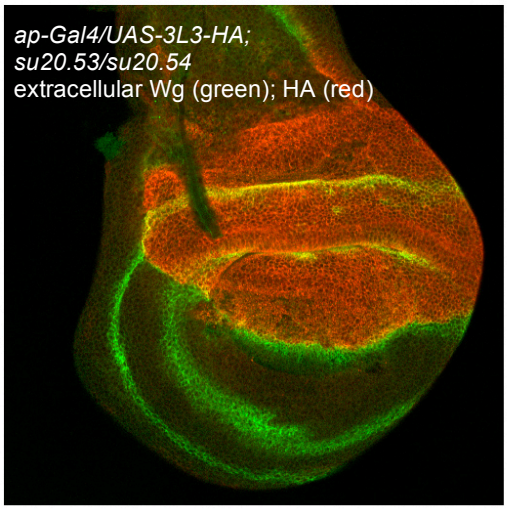
ap-Gal4/UAS-3L3-HA;
su20.53/su20.54
extracellular Wg (green); HA (red)

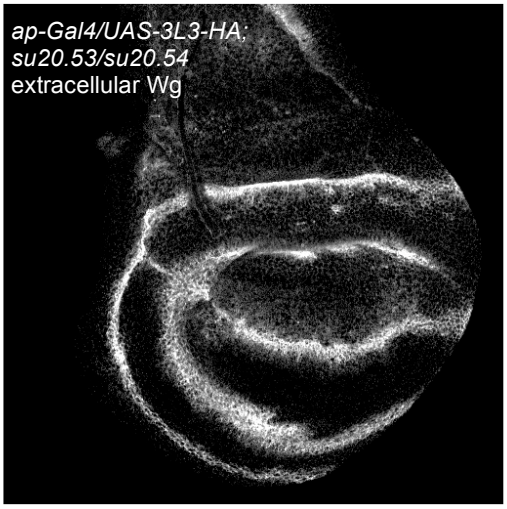
ap-Gal4/UAS-3L3-HA;
su20.53/su20.54
extracellular Wg

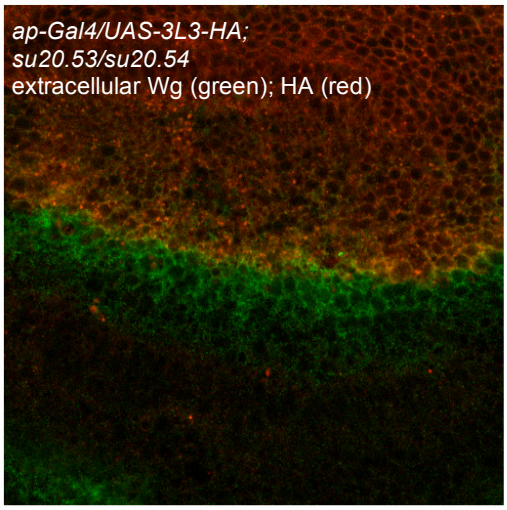
ap-Gal4/UAS-3L3-HA;
su20.53/su20.54
extracellular Wg (green); HA (red)

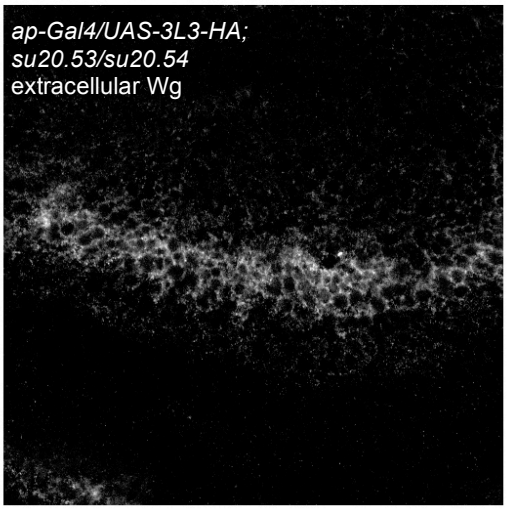
ap-Gal4/UAS-3L3-HA;
su20.53/su20.54
extracellular Wg

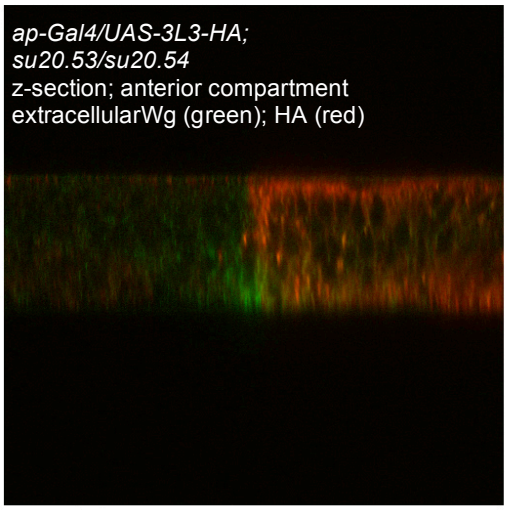
ap-Gal4/UAS-3L3-HA;
su20.53/su20.54
z-section; anterior compartment
extracellularWg (green); HA (red)

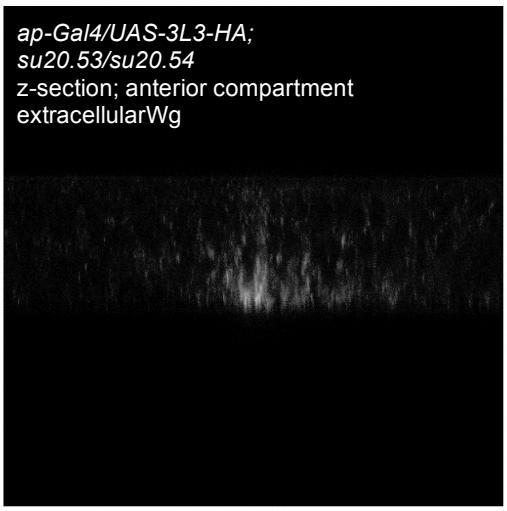
ap-Gal4/UAS-3L3-HA;
su20.53/su20.54
z-section; anterior compartment
extracellularWg

Figure 54 - Extracellular Wg is shown in green, whereas 3L3 is shown in red. The right column shows extracellular Wg alone. Two upper rows of pictures: wing disc of *3L3* mutant larvae rescued dorsally by the combination *ap-Gal4/UAS-3L3* at different magnification. Last row of pictures: z-section showing the ventral mutant part on the left part of each picture, and the dorsal wild-type part on the right part of the picture.

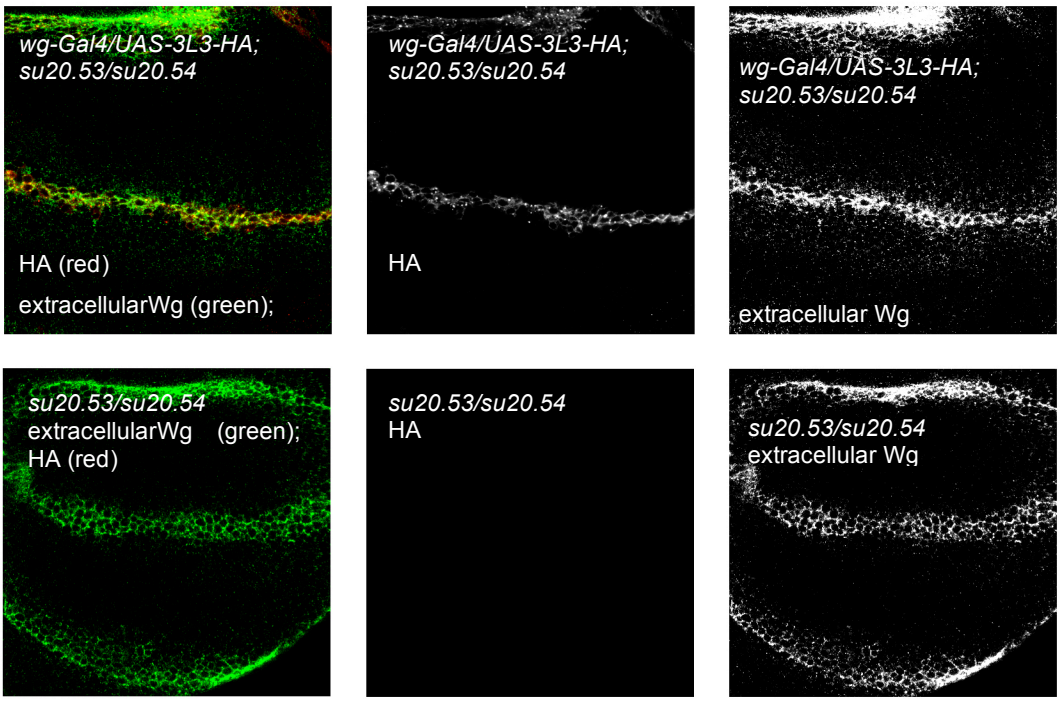

Figure 55 - The upper row shows a wing disc of *3L3* mutant larvae rescued by the combination *ND382/UAS-3L3*, whereas the lower row shows a completely mutant wing disc for *3L3.* In the left column extracellular Wg is shown in green, and 3L3 in red. The middle column shows 3L3 staining, and the right column extracellular Wg alone.

3.11 CG6210, Wingless and the receptor Dfz2

Wg relays its signal through two functionally redundant receptors, Frizzled (Fz) and Fz2, both of which belong to the family of seven-pass transmembrane proteins (Nusse, 2003; Wodarz and Nusse, 1998). Arrow (Arr), a member of the LDL receptor-related protein (LRP) family of proteins, is also required for Wg signaling and has been postulated to act as a co-receptor for Wg (He et al., 2004; Tolwinski et al., 2003; Wehrli et al., 2000). Cadigan et al. have proposed that Fz2 played essential roles in shaping the Wg morphogen gradient in the wing disc (Cadigan et al., 1998). This conclusion is mainly based on the following observations. First, over-expression of Fz2 in the wing disc stabilizes Wg and expands the range of Wg-target gene expression. Second, Fz2

expression in the wing disc is inhibited by Wg signaling and appears to occur in an inverse gradient to that of Wg. This inverse gradient of Dfz2 is thought to facilitate the spread of Wg into more distant areas, but this function of Dfz2 in the modification of the Wg gradient is not essential. In fact, it has been demonstrated that Dfz2 and Dfz are functionally redundant for Wg signaling in both embryos and in the wing disc (Bhanot et al., 1999; Chen and Struhl, 1999). Recently, Han et al. (Han et al., 2004) showed that Dfz-Dfz2 double mutant cells in the wing disc lead to an increase in the extracellular level of Wg probably due to an increase of Dlp caused by a down-regulation of Wg signaling. Interestingly, internalized Wg was also observed in these cells by a co-staining with the endosome marker Hrs (Lloyd et al., 2002), suggesting that Dfz and Dfz2 are not essential for Wg internalization.

In order to rule out any influence of Dfz2 in the Wg expression observed in tissue mutant for *3L3* we performed the following experiment. In the wing discs, we induced the formation of clones, which are mutant for *3L3*, and looked at the expression of Dfz2 by means of anti-Dfz2 antibodies.

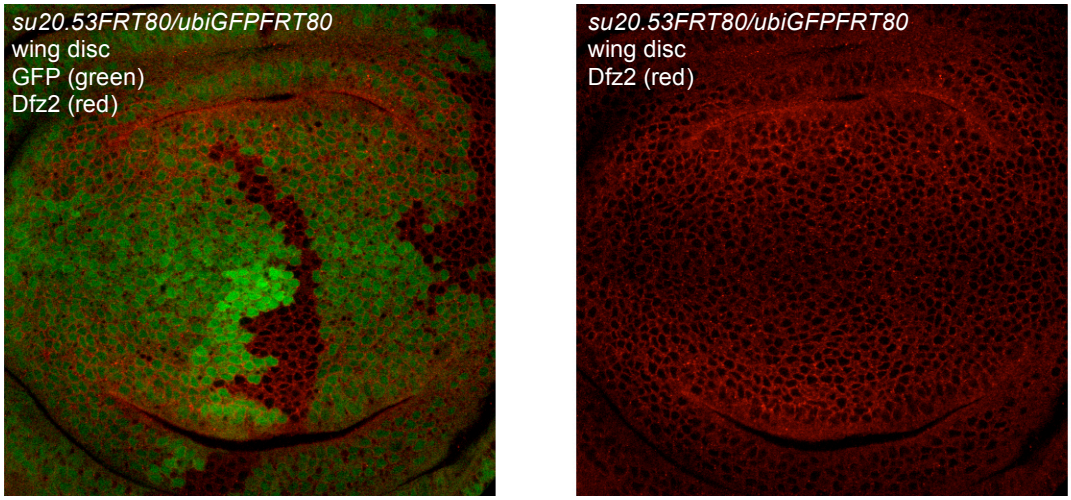

Figure 56 – Dfz2 staining (red) is unchanged in homozygous mutant clones for *CG6210* marked by the absence of the green staining.

As expected, we observed the presence of Dfz2 protein in the whole wing imaginal disc, and a reduced staining in the region of the D/V boundary (Cadigan et al., 1998). This is due to the known negative effect of Wg signaling on Dfz2 expression. In *3L3* mutant tissue we could not see any change at the protein level of Dfz2 or its pattern of expression.

Hence, we can conclude that the observations made on Wg expression are independent of any mechanism, which indirectly works through Dfz2.

3.12 The localization of CG6210

Thus far we have examined the distribution and function of Wg in mutant versus wild-type *wg*- and non-*wg*-expressing cells of wing imaginal discs.
In the following experiments we have examined the localization of CG6210 and the possible co-localization of CG6210 and Wg. This was achieved by the use of several intracellular markers to define different subcellular locations.

First of all, we looked at the wing discs of larvae, which expressed *3L3* under control of the *tubulinα1* promoter (*tubα1-3L3-HA*), and stained them for Wg and HA (thus showing 3L3).

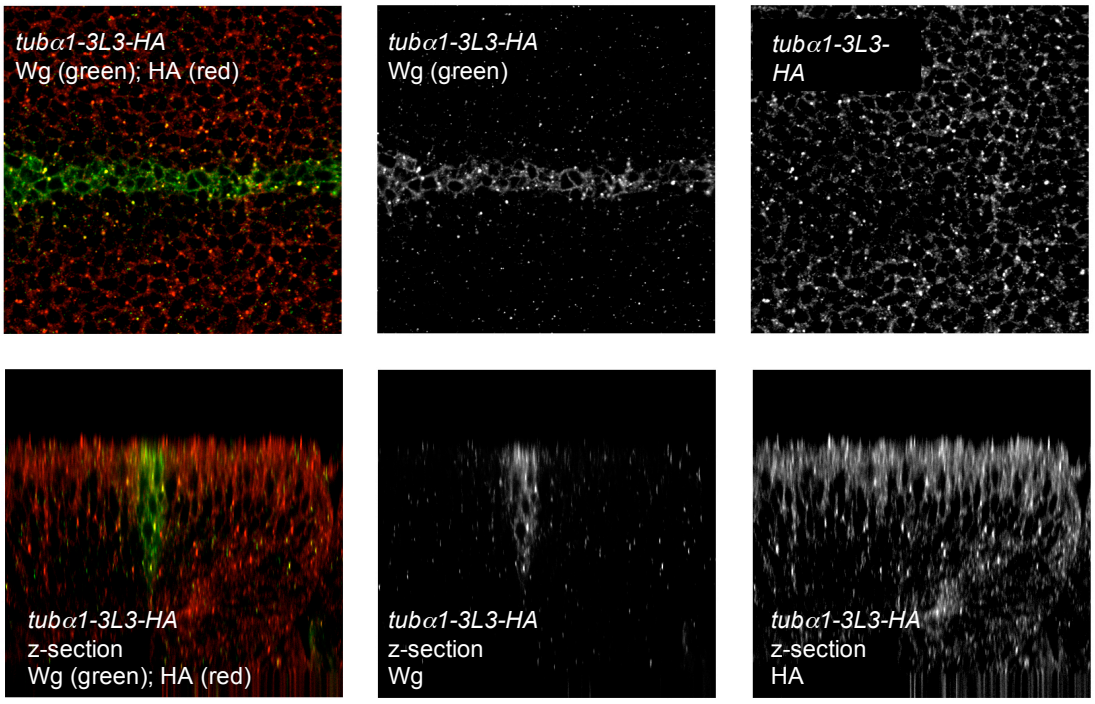

Figure 57 – Imaginal wing disc of a *tubα1-3L3-HA* transgenic larva stained for Wg (in green) and HA (red). Upper row: horizontal section shows a good co-localization of most Wg dots with the ones of 3L3. Lower row: vertical section of the same imaginal wing disc. The pictures in the middle column show Wg and the ones in the right column show 3L3 alone.

We could observe that almost all dots of Wg co-localized with the ones of 3L3. This result suggests that the two proteins could interact physically and that 3L3 might function in the synthesis, secretion, transport, recycling, or degradation of Wg. It is important to notice that these dots of 3L3 are present in all cells of the wing disc (because of the *tubulinα1* promoter) and that there are much more dots of 3L3 than dots of Wg in the non-*wg*-expressing cells.

We next made use of antibodies, which are specific for the Golgi vesicular system, and performed a co-staining for 3L3. In this case no co-localization at all was observed in the wing imaginal discs or in the salivary glands. This suggests that 3L3 does not carry out its (main) function in the Golgi, but in other compartments or at the cell membrane.

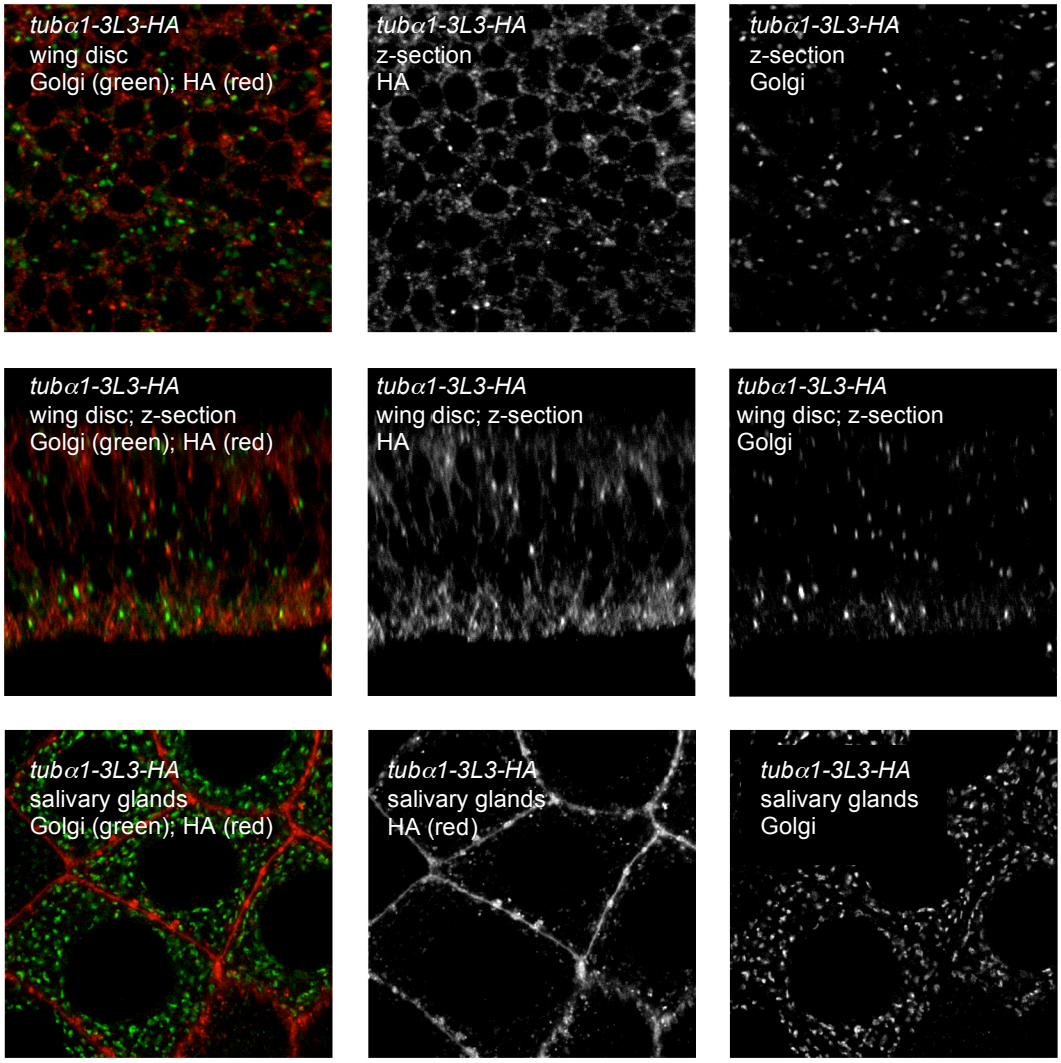

Figure 58 – Two upper rows: horizontal and z-section of imaginal wing discs of a larva, which carries the construct *tubα1-3L3-HA*. Lowest row shows a salivary gland of the same larva. Golgi is stained in green and 3L3 (anti-HA antibody) in red. The pictures in the middle column show 3L3 and the ones in the right column show Golgi alone.

Rab4 localizes to the common endosomes (CEs) and is involved in directing vesicular transport to the recycling endosome, possibly at the level of vesicle assembly and budding (de Wit et al., 2001). In order to visualize it, we made use of the *UAS-rab4RFP* transgene, which was driven by the *ap-Gal4* driver. Moreover, these larvae were carrying the *tubα1-3L3-HA*. In this situation, we observed that some 3L3 positive dots co-localised with Rab4 dots, and that most Rab4 dots give also a signal for 3L3.

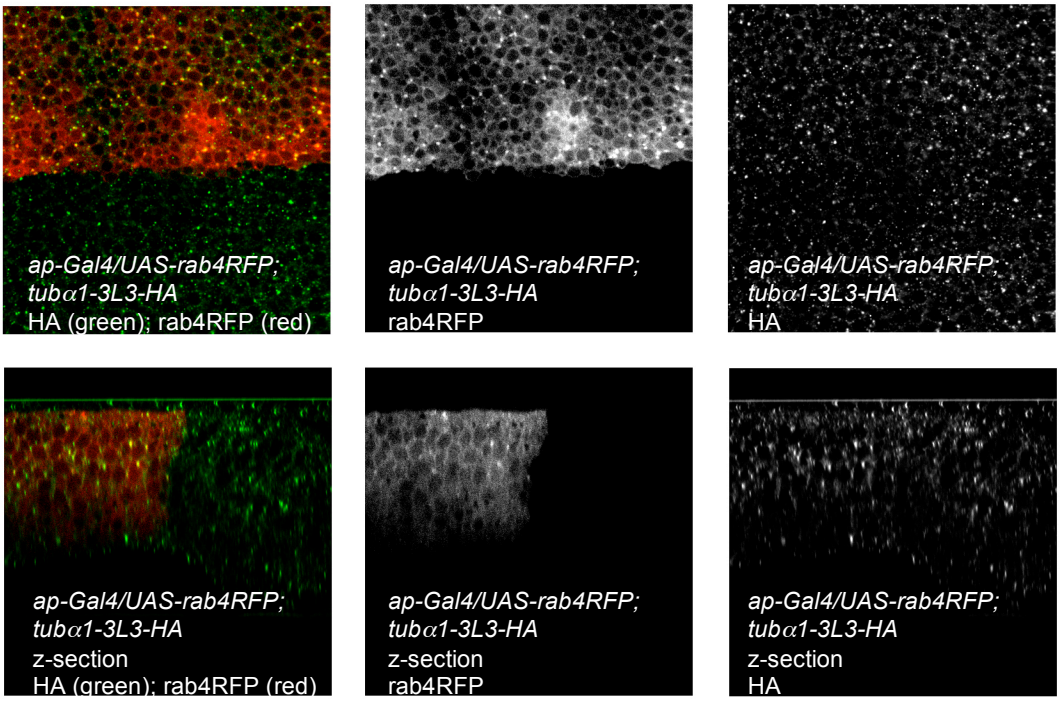

Figure 59- Horizontal section (upper row) and vertical section (lower row) of an imaginal wing disc of a larva, which carries the transgenes *tubα1-3L3-HA, ap-Gal4* and *UAS-rab4RFP*. Rab4 is shown in red, whereas 3L3 in green. The pictures in the middle column show Rab4RFP and the ones in the right column show 3L3 alone.

Rab5GFP was also used as a marker for the fusion between endocytic vesicles and early endosomes. The combination of *UAS-Rab5GFP* with *ap-Gal4* allowed us to visualize the expression of Rab5 in the dorsal compartment; moreover, the transgene *tubα1-3L3-HA* was also present. We first looked at 3L3 and Rab5 staining and noticed that few dots positive for 3L3 were also positive for Rab5, and that most Rab5 positive dots were also positive for 3L3.

Taken together these results suggest that 3L3 is well present inside the early endosomes and the common endosomes.

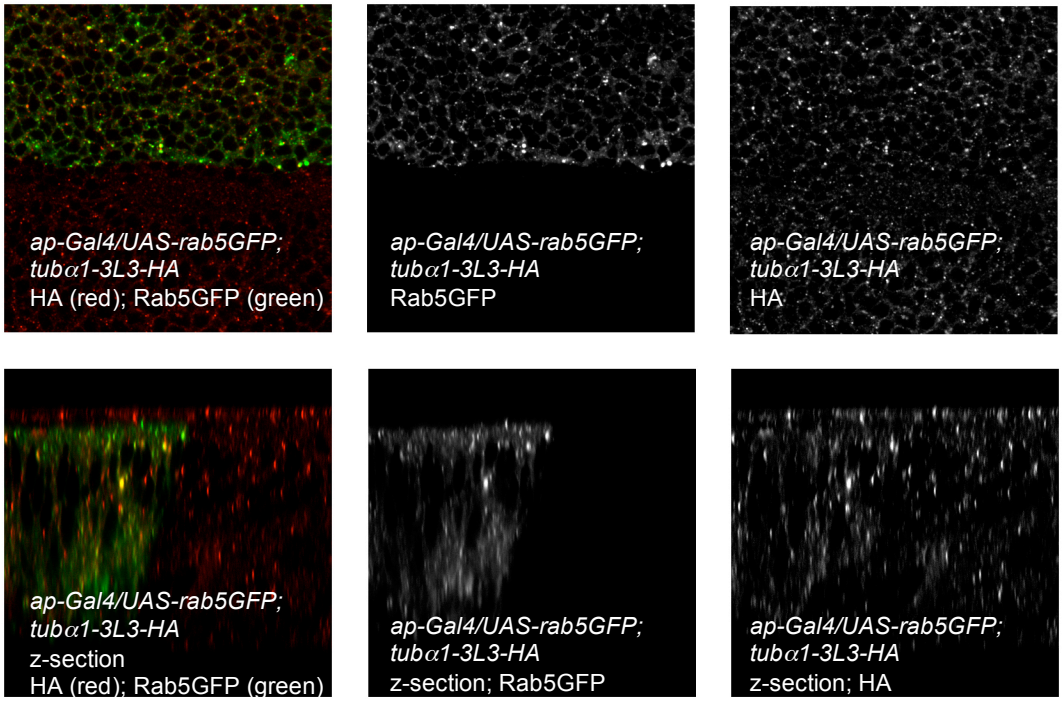

Figure 60 - Horizontal section (upper row) and vertical section (lower row) of an imaginal wing disc of a larva, which carries the transgenes *tubα1-3L3-HA, ap-Gal4* and *UAS-rab5GFP*. Rab5 is shown in green, whereas 3L3 in red (through the GFP fluorescence). The pictures in the middle column show Rab5GFP and the ones in the right column show 3L3 alone.

We also looked at Rab5GFP together with Wg staining and could notice that some dots of Wg in the *wg*- and non-*wg*-expressing cells co-localized with Rab5GFP staining. This means that Wg is probably recycled in both cell types, as already shown for the embryonic epidermis (van den Heuvel et al., 1989; Gonzales et al., 1991).

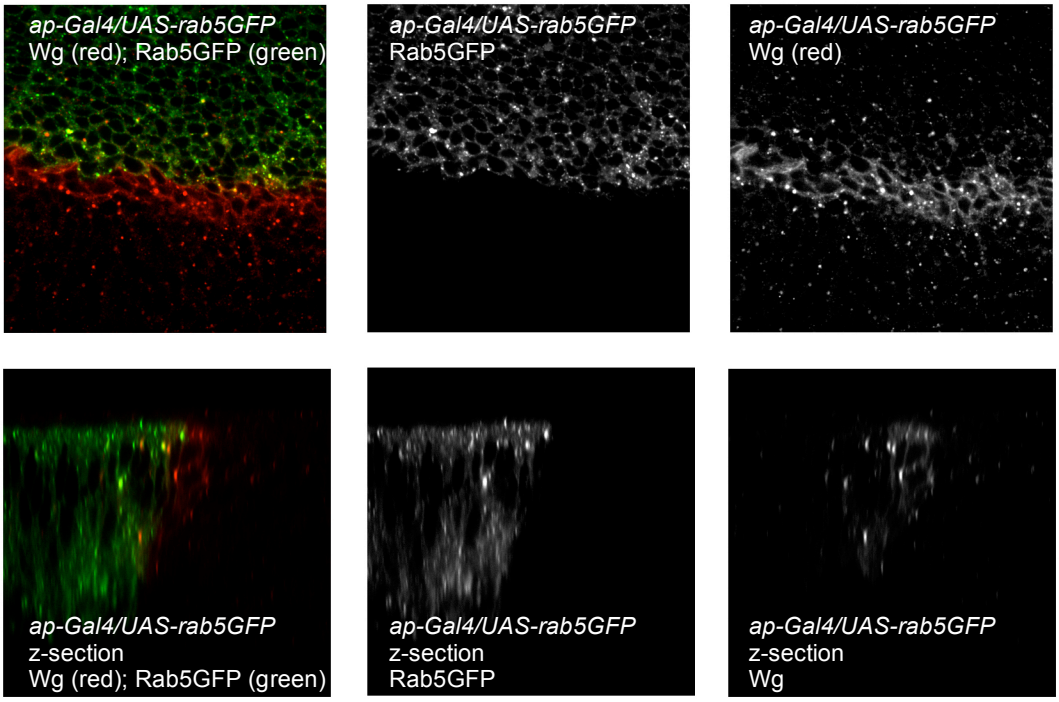

Figure 61 - Imaginal wing disc of a larva stained for Wg (in red) and Rab5 (in green). The upper row shows a horizontal section, whereas the lower row shows a vertical section of the same imaginal wing disc. The pictures in the middle column show Rab5 and the ones in the right column show Wg alone.

Rab11 is an important molecule for the targeting of vesicles to the recycling compartment. Also in this case the transgene *UAS-Rab11GFP* was available and we drove its expression under the control of *ap-Gal4. tubα1-3L3* was also present.

When we looked at the vesicles stained for Rab11, we noticed that only few of them were also positive for 3L3.

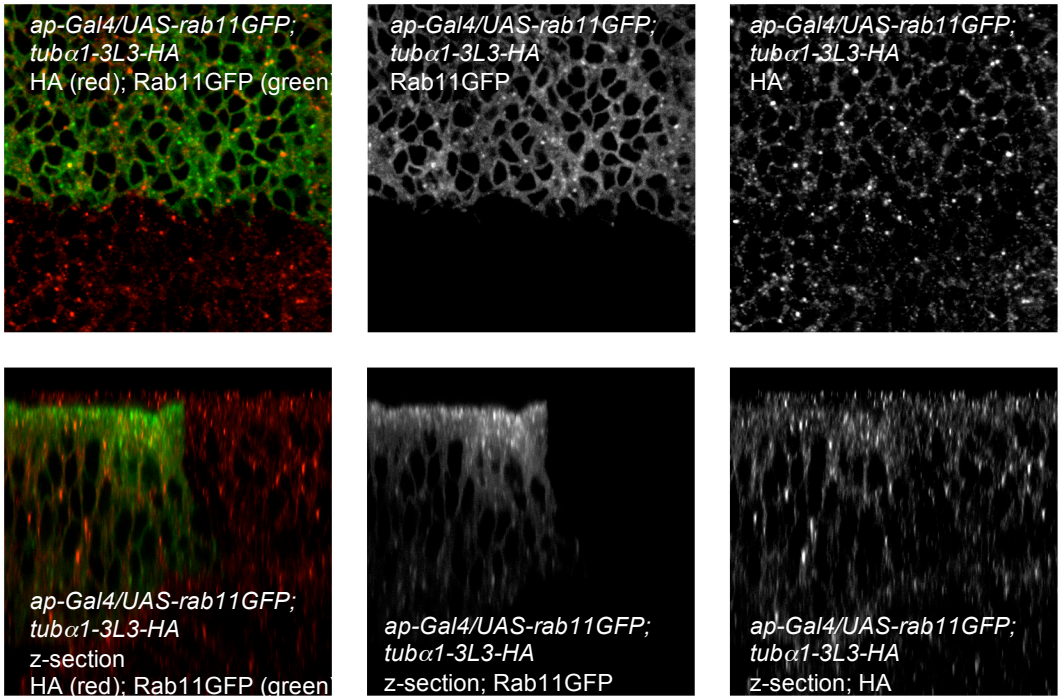

Figure 62 - Imaginal wing disc of a larva, which carries the transgenes *tubα1-3L3-HA, ap-Gal4* and *UAS-rab11GFP*. Rab11 is shown in green, whereas 3L3 in red. The upper row displays a horizontal section, whereas the lower row displays a vertical section of the same imaginal wing disc. The pictures in the middle column show Rab11 and the ones in the right column show 3L3 alone.

The last marker we utilized in order to study the localization of 3L3 was Rab7, which mediates lysosomal targeting and localizes in the late endosomes. When we looked at dots positive for Rab7 (visualized by the *Rab7GFP* construct), we noticed that most big dots positive for 3L3 were also positive for Rab7, and that most Rab7 dots were positive for 3L3 too. This result suggests that 3L3 might also play a role in the degradation of Wg.

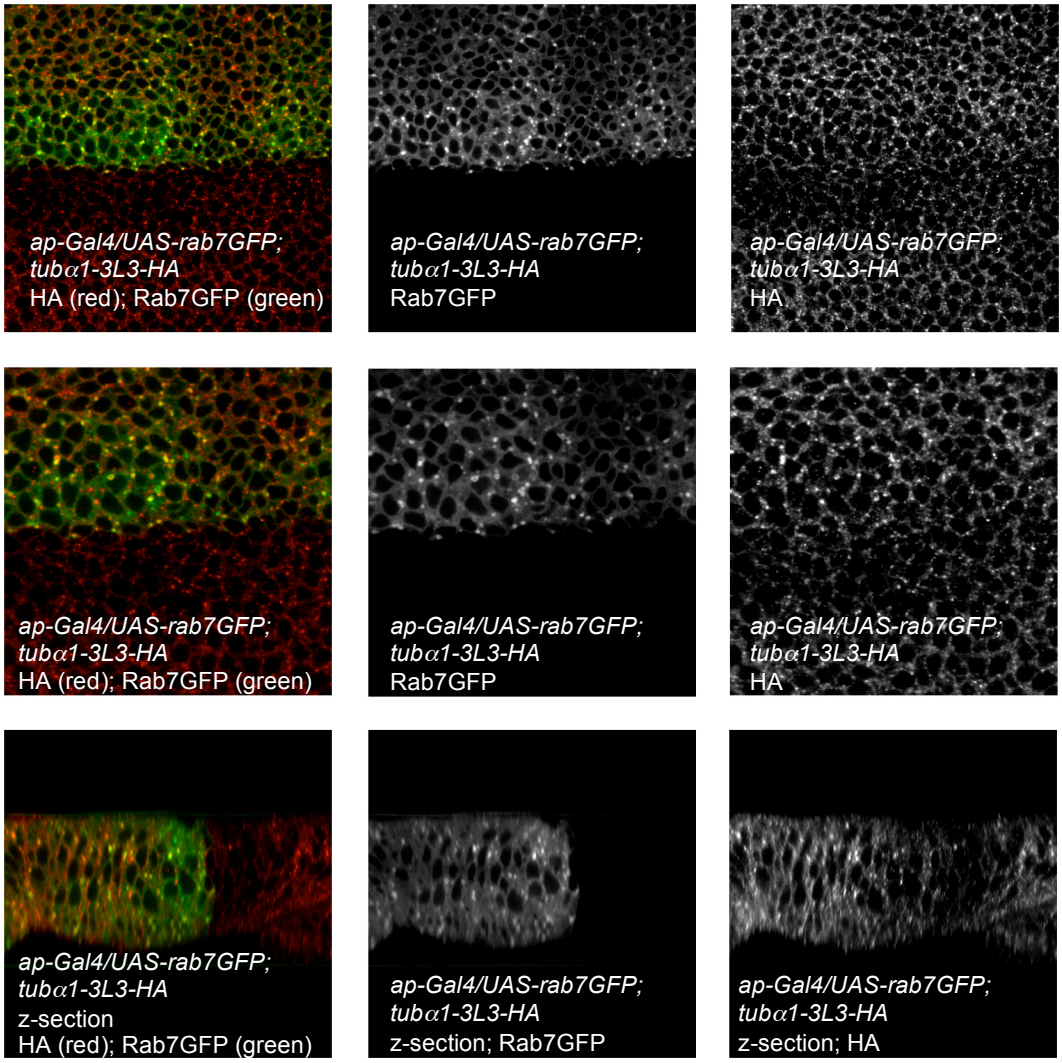

Figure 63 - Imaginal wing disc of a transgenic larva, which carries the transgenes *tubα1-3L3-HA, ap-Gal4/UAS-rab7GFP.* Rab7 is shown in green, whereas 3L3 in red. Two upper rows: horizontal sections at different magnifications of a wing disc. Lowest row: vertical section of the same imaginal wing disc. The pictures in the middle column show Rab7 and the ones in the right column show 3L3 alone.

When we looked at Rab7 and Wg, we noticed that big dots of Wg co-localized with the ones of Rab7, and this probably represents Wg, which is going to be degraded. This result agrees with previous data found in the literature (van den Heuvel et al., 1989; Gonzales et al., 1991).

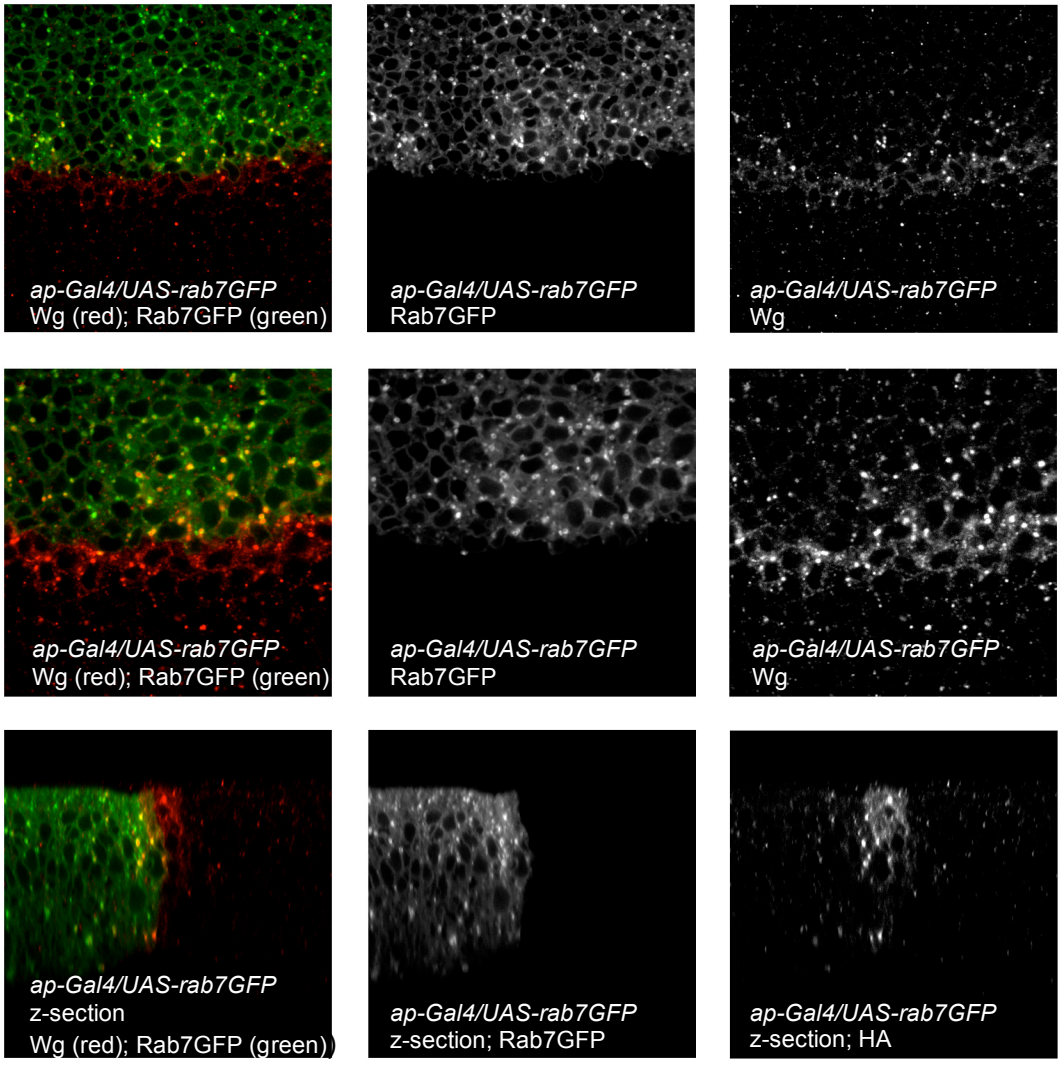

Figure 64 - Horizontal section (upper row) and vertical section (lower row) of an imaginal wing disc of a larva, which carries the transgenes *tubα1-3L3-HA, ap-Gal4* and *UAS-rab7GFP.* Rab7 is shown in green, whereas 3L3 in red. The pictures in the middle column show Rab7 and the ones in the right column show Wg alone.

3.13 *CG6210* and the *dynamin* homologue *shibire*

As mentioned in the introduction, *shibire* encodes the *Drosophila* homologue of the GTP-ase Dynamin, and thus it has been implicated in the internalization of clathrin-coated endocytic vesicles and in the internalization of caveolae (Strigini and Cohen, 2000; and references therein).

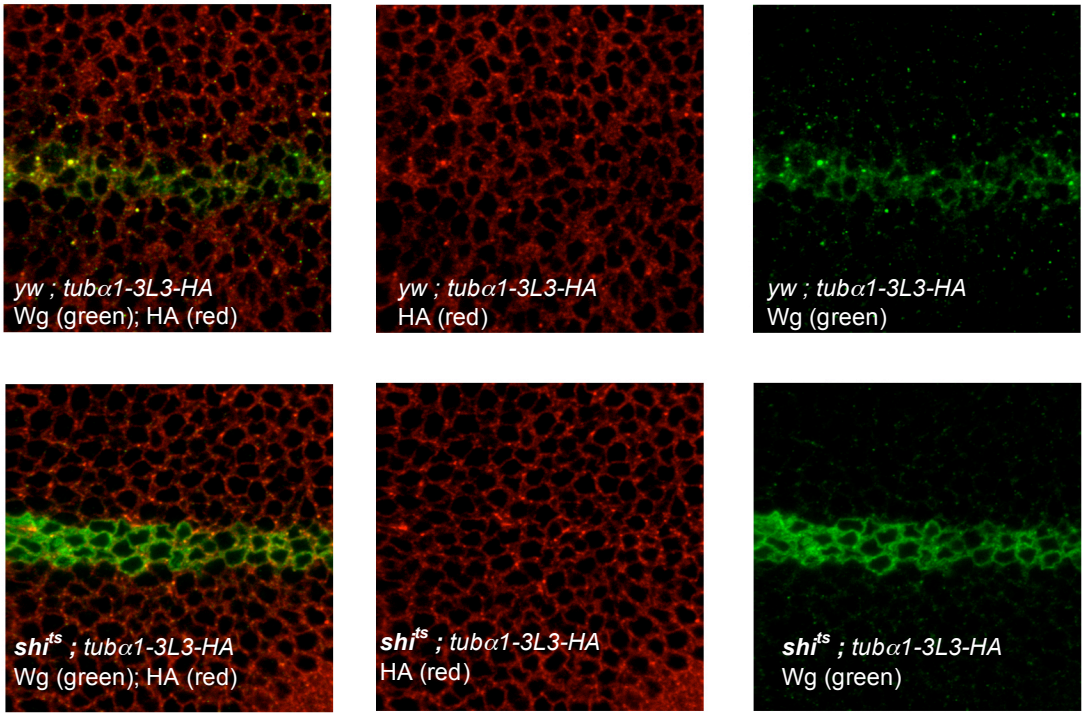

Figure 65 –Wild-type (upper row) and hemizygous *shi*^{ts} (lower row) wing discs, which express *HA-3L3* under the control of the *tubulin*α*1* promoter. Wg is stained in green and HA3L3 in red.

Male larvae hemizygous mutant for *shi*^{ts} and carrying the *tub*α*1-HA-3L3* construct were dissected at restrictive temperature. Immediately thereafter wing discs were taken, fixed and stained for Wg and HA (i.e. for 3L3). The restrictive temperature was used in order to inactivate *shi* and such a condition had been shown to block the uptake as well as the secretion of Wg (Strigini and Cohen, 2000). As shown in the upper panel, wild-type wing discs showed normal Wg staining at the D/V boundary and normal gradient with dots of Wg.

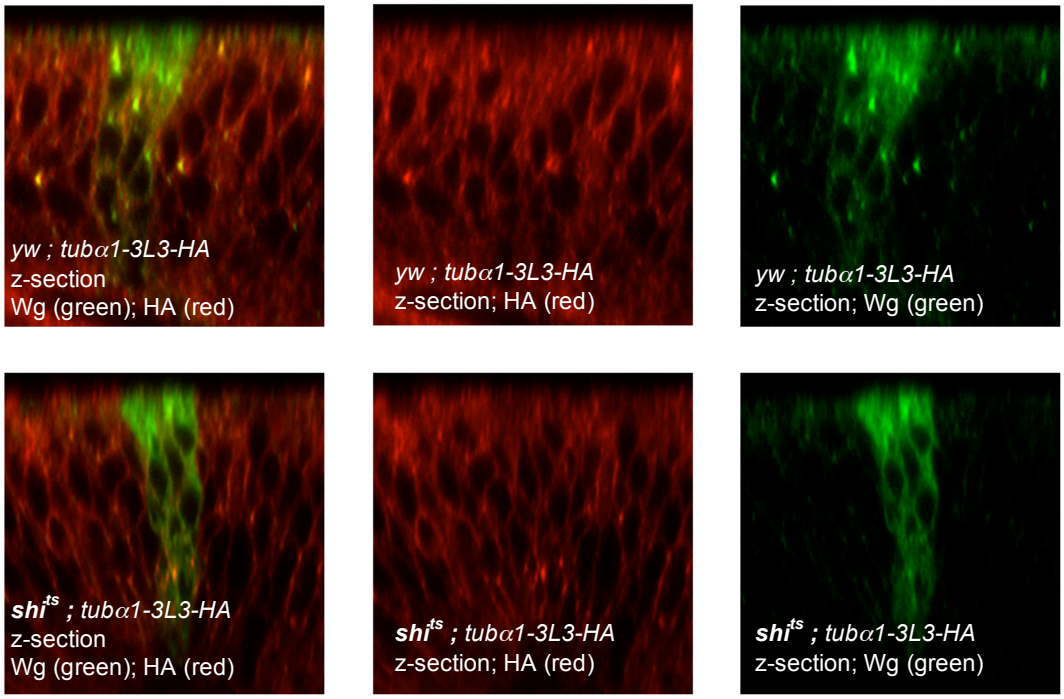

Figure 66 – Vertical sections through a wild-type (upper row) and a hemizygous *shi*^{ts} (lower row) wing disc, both of which express *HA-3L3* driven by the *tubulinα1* promoter. Wg is stained in green and HA-3L3 in red.

As expected and previously described, in the *shi* mutant situation Wg accumulates inside the producing cells at the D/V boundary and no dots of Wg are present. Importantly, dots of 3L3 are still formed and this means that localization clustering of 3L3 is independent of the function of Shi.

3.14 *CG6210* and Wingless^{CE7}, a truncated version of Wingless

wg^{CE7} is a *wg* null allele, which encodes an identical product to *wg*^{S84} (Bejsovec and Wieschaus, 1995). In the *wg*^{CE7} allele a nucleotide substitution at the 3' end of the fourth intron changes the splice acceptor site for exon 5 from AG to AA, and this results in the failure to splice out the fourth intron. The first three nucleotides of the intron code for a stop codon, and this leads to a truncation of the protein at the end of the fourth exon. This short form of the Wg protein is normally secreted, but is nonfunctional. To test whether *3L3* may also influence the release of Wg^{CE7} we made use of transgenic flies,

which carry the construct *sev-wg*^{CE7}. The promoter of this construct is the same as the one we used for the experiments with *sev-wg,* and thus contains a *heat-shock* (*hsp70*) promoter. We drove *wg* expression ubiquitously by a heat-shock, after generating Minute$^{+/+}$ clones mutant for *3L3* (using the allele *su20.53*) in a Minute$^{+/-}$ background.

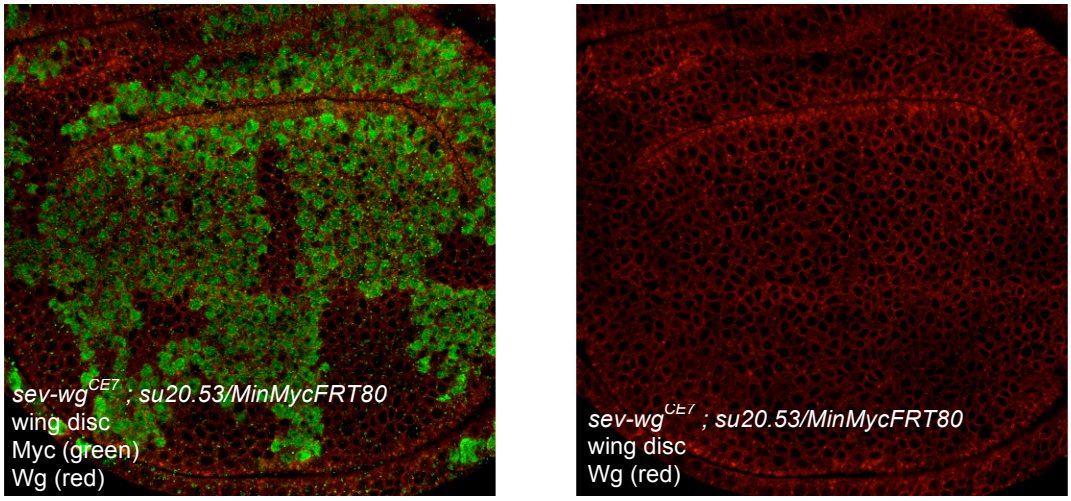

Figure 67 - Wing disc stained for Wg and Wg^{CE7} (in red) does not show any change in the staining in Minute$^{+/+}$ clones mutant for *CG6210* (these are marked by the absence of the green labeling).

The staining for Wg and Wg^{CE7}, made with the usual anti-Wg antibody, revealed a difference only in the behaviour of Wg in the *wg*-expressing cells, when we compared wild-type and *3L3* mutant tissue. In the remainder of the wing disc, where only Wg^{CE7} is synthesized, no enhanced staining was observed, suggesting that *3L3* does not play a role in the production and release of Wg^{CE7}. Most probably, 3L3 interacts very specifically with full-length wild-type Wg.

4 Discussion

4.1 *CG6210* is a positive component of the Wingless pathway

One of the three complementation groups found in the screen for recessive suppressors of the Wg dependent “rough-eye phenotype” was called *3L3* and its two alleles carry mutations in the gene *CG6210*.

Enhancers of the eye phenotype caused by the *sev-wg* construct can represent loss-of-function mutations in a negative component of the Wg signaling pathway, a gain-of-function mutation in a positive component or, more probably, a mutation in a gene responsible for the eye development. For this reason enhancers of the rough-eye phenotype are less interesting than its suppressors.
In fact, suppressors of the eye phenotype represent most likely loss-of-function mutations in a positive component of the Wg signaling cascade. An unrelated mutation, which recovers the phenotype, is much less likey. Taken together, these considerations suggest that the gene *CG6210* is probably a positive component in the Wg signaling pathway and that the mutations found in the alleles of its complementation group are loss-of-function mutations.

Many developmental processes in *Drosophila melanogaster* are dependent on the Wg signaling pathway and this fact can be used to study the role of the gene of interest.

Germline clones are necessary to get rid of the maternal component of a gene and to study its role in the segmentation process of the embryo. When we performed this experiment eliminating the function of the gene *CG6210*, we noticed a so-called “lawn-of-denticle phenotype”. This phenotype can be due to a reduction in signaling of either the Hh or the Wg pathway or both. This result confirms a possible role of *CG6210* in the Wg signaling pathway, but does not rule out a function in the Hh signaling pathway.

Apart from the segmentation process of the exoskeleton in embryos, Wg signaling is also required for the proper formation of appendages like antennae, legs and wings. Homozygous mutant animals for *CG6210* die as pharate adults, and we searched for possible phenotypes in the appendages at this developmental stage. Interestingly, we

noticed that antennae and legs were dysmorphic. Most surprisingly, 5% of pharate adults showed a so-called “wing-to-notum transformation”, which is a historical description and gave the name to the ligand of the signaling pathway. This phenotype is pathognomonic for a reduction in the signaling of the Wg pathway, and this definitively leads us to conclude that *CG6210* is a positive component of the pathway.

When we carefully looked at the legs of the *3L3* homozygous mutant pharate adults, we noticed that there was a reduction of the ventral structures, which are specified by Wg signaling. This again points to the role of *CG6210* in the pathway.
In the leg imaginal discs, *wg* partially represses *dpp* ventrally and *dpp* represses *wg* dorsally; in the homozygous mutant situation we found an increase in the *dpp-LacZ* expression and Wg was almost absent, i.e. the phenotype is amplified via the cross-regulatory interactions between Wg and Dpp pathways.

These data suggest that *CG6210* may play a role in the uptake of Wg or in the signal transduction in the Wg-receiving cells or that Wg transport is impaired in the mutant situation. Alternatively, *wg*-expressing cells synthesize a less functional protein or the secretion in these cells is decreased.

Finally, loss of bristles and the presence of notches found in big clones mutant for *CG6210* in adult wings confirmed again its importance as a positive component in the Wg signaling cascade.

4.2 Effects of *CG6210* mutation on Wingless target genes

Since we know that *CG6210* is a positive component of the Wg signaling pathway, its function could be carried out in the *wg*-expressing cells (for the synthesis of an active molecule or for its proper secretion), in the Wg receiving cells (for the up-take of the ligand, and for the signal transduction) or in the transport of Wg.
In all cases, if we mutate *CG6210* we should find a reduction in the expression of the Wg target genes. These target genes are the best tool to detect the level of activation of the pathway and can conveniently be studied in the wing imaginal discs.
We chose *Dll* as long-range target gene and *sens* as short-range target gene.

In the case of *Dll-LacZ* we noticed a reduction in the signaling pathway only when the mutant clone was big and comprising the *wg*-expressing cells.

In the case of *sens*, the size of the mutant tissue was less important, but again some *wg*-expressing cells had to be mutant to detect any reduction in the pathway. If the *sens*-expressing cells were mutant, but the nearby *wg*-expressing cells were wild-type, we could not see any decrease in *sens* expression and hence in Wg signaling.
This means that *CG6210* is not necessary in non-*wg*-expressing cells for signal transduction and expression of Wg target genes and it is not necessary for the up-take of the Wg ligand.

CG6210 seems thus to be important for the synthesis of Wg, for its secretion, transport or movement.

4.3 Effects of *CG6210* mutations on Wingless protein

The experiments discussed above suggest a role of *CG6210* in the *wg*-expressing cells or in the transport of Wg.
If *CG6210* is involved in the secretion or transport of Wg, we can imagine that it should be possible to detect a different behaviour in the staining of the ligand Wg in the mutant versus wild-type cells. If instead *CG6210* is necessary for the synthesis of a functional Wg protein in the *wg*-expressing cells, a staining for Wg could be unable to detect any difference between mutant and wild-type tissue.

When mutant clones for *CG6210* were induced in wing imaginal discs, we noticed that an increase of Wg staining was present in mutant *wg*-expressing cells, compared to wild-type cells. The effect was independent of the size of the clones.
Wg expression in the wing imaginal discs is regulated through a negative feed-back by Wg itself. In order to exclude that any regulatory effect is the cause of the observed accumulation, several experiments were performed with different constructs, which drove *wg* expression at a constant level. Again an increase in Wg staining was detected in tissue mutant for *CG6210.* The confirmation that all differences observed between the mutant and the wild-type tissue were due to a post-transcriptional effect made us conclude that the increase in the staining for Wg in the mutant tissue is due to a retention in the *wg*-expressing cells. This retention could be due to a change in the physiological synthesis process of the Wg protein or to an impaired secretion. The transport of Wg seems to be unaffected since no change in the staining of Wg was noticed on the non-*wg*-expressing cells (e.g. no shadow or increase in the staining).

4.4 *CG6210* is essential only in the *wingless*-expressing cells

If the function carried out by *CG6210* is necessary only in the *wg*-expressing cells, a rescue experiment performed with the combination of the two transgenes *wg-Gal4* (three different lines were tested) and *UAS-3L3* should lead to a wild-type looking fly. The phenotype of many flies was completely rescued. We interpreted this result as a suggestion that the function of *CG6210* is necessary only in the *wg*-expressing cells and the partial rescue observed in some flies was due to a weaken expression of *CG6210* by the *Gal4* line. Alternatively, one could think that *CG6210* accomplishes a secondary function also in non-*wg*-expressing cells.

4.5 *CG6210* is specific for the Wingless pathway

An important question about the function of *CG6210* is its dedication to the Wg signaling pathway.

In order to study this issue, we performed some experiments described above (4.2), but we looked for effects on another signaling pathway, namely the Hh signaling pathway. This choice was based on the fact that the ligand of the pathway has some common characteristics with Wg (e.g. both are morphogens and undergo hydrophobic modifications), and that the segment polarity phenotype observed (3.3) could be due to a function of *CG6210* in the Hh pathway.
No effect of *CG6210* mutant tissue was detected either on the ligand Hh or on the Hh target genes *ptc* and *dpp*. These data suggest that *CG6210* is not involved in the Hh signaling pathway.

We also studied the effect of *CG6210* mutant tissue on the behaviour of CD2, which is a membrane tethered protein and undergoes N-linked glycosylation. Also in this case we were not able to observe any difference in wild-type versus mutant tissue.

So far we can conclude that *CG6210* appears not to be necessary for general secretion or synthesis of palmitoylated proteins, and does not alter the behaviour of proteins, which are N-linked glycosylated.

Some other considerations further support the idea that *CG6210* is dedicated to the Wg pathway. The fact that flies can be rescued only by driving the expression of *3L3* either ubiquitously or in the *wg*-expressing cells suggests that its function is coupled with the one of Wg. Moreover, *CG6210* mutant tissue does not have any influence on the staining of the shorter allele Wg^{CE7}, and this could suggest a very specific interaction between Wg and CG6210. A weaker, but interesting remark comes from BLAST and database searches, which reveal that homologues of the gene *CG6210* are found in all metazoans. Since the same is true for the Wg signaling, we can speculate that *CG6210* evolved together with the pathway.

4.6 Distribution of the morphogen Wingless in *3L3* mutant tissue

Wg has been shown to pass through the Endoplasmic Reticulum (ER) and Golgi apparatus of *wg*-expressing cells; moreover it has been detected in intracellular vesicles and in multivesicular bodies in those cells and in adjacent non-*wg*-expressing cells. In wing discs, spots of Wg in cells away from the source appear to reflect vesicles of internalized Wg protein, and in these cells Wg was also observed to co-stain with the endosome marker Hrs.

When we studied the behaviour of Wg in the wing imaginal discs, we noticed the well-known gradient, which starts at the D/V boundary.
wg-expressing cells show Wg close to the cell membrane and in the form of dots inside the cells. In contrast, non-*wg*-expressing cells show only the presence of Wg dots, which altogether form the gradient.

In *CG6210* homozygous mutant wing discs, a stronger staining for Wg is observed and dots are detected neither in *wg*-expressing nor in non-*wg*-expressing cells.
When the dorsal compartment of the wing disc is rescued by the combination of *ap-Gal4/UAS-3L3*, the accumulation of Wg in the rescued *wg*-expressing cell disappears and the presence of the dots in the rescued *wg*-expressing cell and non-*wg*-expressing cells is restored. It is important to notice that in the ventral compartment (where cells are not rescued), few dots of Wg in the non-*wg*-expressing cells are present. If we consider the distance from the boundary between the two compartments, we can say that the

amount of dots is very similar. This suggests that *CG6210* is not necessary in the non-*wg*-expressing cells for the formation of the gradient and dots.

This hypothesis is further supported by two other experiments.
First, when homozygous mutant clones for *CG6210* are formed in non-*wg*-expressing cells of the wing disc, dots of Wg are still observed. This means that the formation of the Wg gradient is not independent on the presence of *CG6210* in the non-*wg*-expressing cells. Secondly, when only the *wg*-expressing cells are rescued by the combination *ND382-Gal4/UAS-3L3*, an almost complete rescue of the Wg gradient (i.e. the presence of the Wg dots) in the *wg*-expressing cells and in the non-*wg*-expressing cells is achieved.

We can conclude that *CG6210* is necessary in the *wg*-expressing cells for the proper secretion of Wg and for the proper formation of a gradient; it can play a role in the synthesis (modifications included) or simply in the release of a normally synthesized Wg protein.

Strigini and Cohen (Strigini and Cohen, 2000) developed a method to stain only extracellular proteins. When this procedure is applied to wing discs for detecting Wg, a gradient, but no obvious dots (which are intracellular organelles and represent up-taken Wg) is observed.
Again rescue experiments were performed. When the posterior compartment was rescued and the anterior compartment was homozygous mutant for *CG6210*, the posterior compartment showed a normal gradient; when the dorsal compartment was rescued, the gradient in the ventral and in the dorsal compartment were rescued. When compared to the dorsal compartment, the ventral compartment shows a slightly narrower gradient, and again this could be due to the different distance from the rescued *wg*-expressing cells. Importantly, when only the *wg*-expressing cells are wild-type (we used the *ND382-Gal4* line) the gradient is restored too.
These last data support the idea that *CG6210* is necessary for the proper release of Wg, either for its secretion alone or for its proper synthesis, which could be necessary for a proper folding and hence secretion.

4.7 Possible localization of CG6210

The data regarding the localization of CG6210 seem to be more difficult to interpret.
An important observation is the very good co-localization of CG6210 and Wg.
From the experiments performed with the different Rab markers, it appears that CG6210 is well present in the early endosomes and in the common endosomes, while few recycling endosomes are positive for CG6210.
Moreover, big dots positive for CG6210 are also positive for Wg and for Rab7, meaning that all these proteins are present in the late endosomes.
Before drawing any conclusions from these data, we have to consider the fact that when the function of Shibire is blocked, we cannot detect dots of Wg, whereas dots of CG6210 are still present.

4.8 Possible role of *CG6210* in the Wingless signaling pathway

The function of *CG6210* is necessary only in the *wg*-expressing cells, since all phenotypes, Wg gradients, and Wg dots are rescued when these cells express *CG6210*. Moreover, Wg target gene expression does not depend on *CG6210* in the non-*wg*-expressing cells, but only in the *wg*-expressing cells.

Wg cannot leave the *wg*-expressing cells when these are mutant for *CG6210*, and this can be explained by a function of *CG6210* in the synthesis of a proper Wg protein or only in its release.
About the possible role of *CG6210* in the synthesis of Wg, we can say that in the tissue mutant for *CG6210*, Wg can still be recognized by the anti-Wg antibody (i.e. the synthesis of the amino acid chain still takes place) and that *CG6210* is probably not involved in the glycosylation for the clear missing co-localization of CG6210 and Golgi marker. *CG6210* could still be involved in the palmytoylation of Wg in the ER, since *por* mutant *wg*-expressing cells show a similar accumulation of Wg.
Regarding the possible function of *CG6210* in the release of Wg, we can speculate that *CG6210* is necessary for the proper folding of Wg; alternatively, *CG6210* could associate with Wg in order to guide it to the right organelles for its release.

From the localization experiments we can suppose that CG6210 is located in the early endosomes and in the common endosomes. Wg would come from the trans-Golgi, then associate with CG6210 and be released to the cell membrane for secretion.
Wg and CG6210 would also be recycled together: in fact, they co-localize in the early endosomes and in the common endosomes.
Wg and CG6210 would also be degraded together: they would leave the common endosomes and reach the late endosomes for degradation. In fact, they co-localize in the late endosomes.

We can now try to explain the results of the experiments performed with *shibire* mutant larvae. When the function of Shibire is blocked, we cannot detect dots of Wg, whereas dots of CG6210 are still present. First, we have to consider that Shibire is implicated in the internalization of clathrin-coated endocytic vesicles and in the internalization of caveolae. Moreover, Shibire may have a role in the formation of transport vesicles at the trans-Golgi network.
If Wg has to pass through the trans-Golgi to reach the common endosome and to be released, and if Wg is also uptaken in early endosome to be recycled or degraded, then *shibire* mutant tissue would show an accumulation of Wg only inside the *wg*-expressing cells (in the ER and Golgi) and no dots in other compartments would be found. In fact, Wg could not be taken up, but only degraded and secreted and in a few hours Wg inside the cells would be found only in the ER and Golgi compartments.

CG6210 could reside in the common endosomes and then either travel to the cell membrane (and then be taken up in early endosomes) or to the late endosomes. Apart from the uptake in the early endosomes, the localization of CG6210 would be unaffected by the function of Shibire.

Conclusion: CG6210 is located in the early endosomes, in the common endosomes, and in the late endosomes. Wg travels from the trans-Golgi to the common endosome, then associates with CG6210 and is released to the cell membrane for secretion.
Wg and CG6210 are also recycled together through the early endosomes and the common endosomes.
Wg and CG6210 are degraded together: they leave the common endosomes and reach the late endosomes for degradation.

5 Appendix

5.1 Other results related to the main project of *CG6210*

5.1.1 CG6210, Wingless alleles and Porcupine

As discussed in the Introduction a defect in the secretion of has been observed in some mutants of Wg/Wnt and in the absence of the putative palmitoyl-transferase Por.
In order to study a possible role of *CG6210* in the process of palmitoylation, we first performed experiments using two different fly strains heterozygous mutant for *wg*. In one case, larvae were heterozygous for the allele wg^{IL11}, which is a temperature sensitive allele (at 16-18 degrees it behaves as a wild-type allele, whereas at 25-29 degrees it behaves as a null allele) and carries a C to S mutation at the amino acid 104.
In the second case, larvae were heterozygous for the temperature sensitive allele wg^{S21}, which carries a C to Y mutation at the palmitoylation site (the amino acid 93), and thus cannot be palmitoylated.
When compared to the staining in wild-type larvae, we observed a clear accumulation of Wg in wing discs of larvae heterozygous for either of the two *wg* alleles (data not shown).
This result supports a possible role of cysteines in the secretion of Wg, possibly related to the formation of intramolecular disulphide bridges needed for proper folding of Wg.
It is important to note that the accumulation observed in the imaginal discs of larvae heterozygous for the allele Wg^{S21} cannot be explained by the proposed interference caused by a free sulhydryl group, which is present when Wg is not palmitoylated. We can only speculate that during the synthesis and folding of Wg the number and location free sulhydryl groups are important and highly regulated.

In order to test whether the accumulation of the Wg allele Wg^{S21} can further increase in the absence of *por*, we expressed the *UAS-*wg^{S21} transgene ubiquitously in the wing disc and induced the formation of *por* mutant clones.

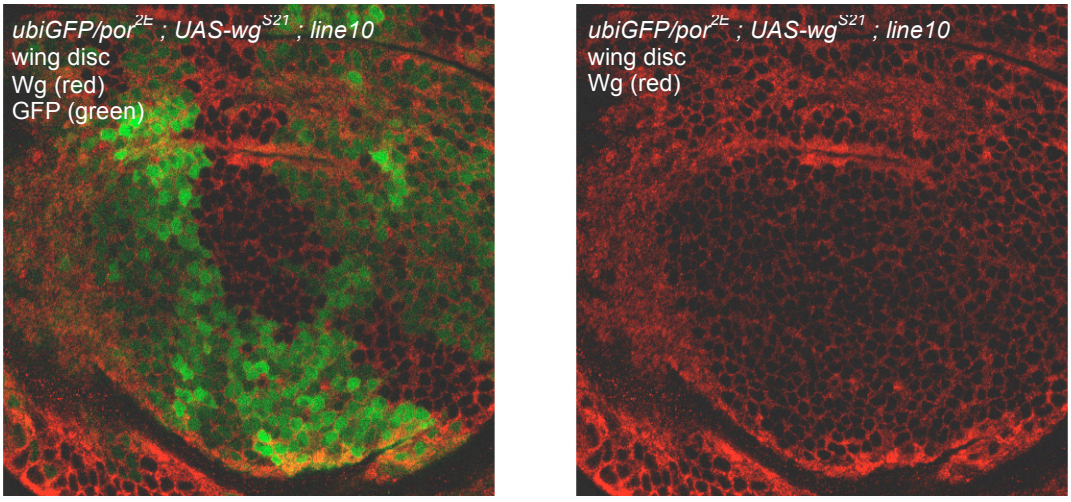

Figure 68 – Wing disc expressing *wg*^{S21} (in red) with clones homozygous mutant for *por*. On the left: mutant clones, marked by the absence of GFP, show no change in the staining for Wg^{S21}. On the right: Wg^{S21} staining alone.

We did not detect any difference in the expression/distribution of Wg^{S21} between wild-type versus *por* mutant tissue. This suggests that *por* is not necessary for the proper distribution of the *wg*^{S21} allele, since this cannot be palmitoylated. Alternatively, the expression of the transgene might be too strong and therefore does not allow the detection of any possible difference.

We then tried to rescue the accumulation of the Wg alleles Wg^{S21} and Wg^{IL114} through the over-expression of the *UAS-3L3* transgene. We could not observe any reduction of the staining for Wg in homozygous or heterozygous tissue when *CG6210* was over-expressed. This is compatible with previous results, in which over-expression of *CG6210* showed no visible phenotype.

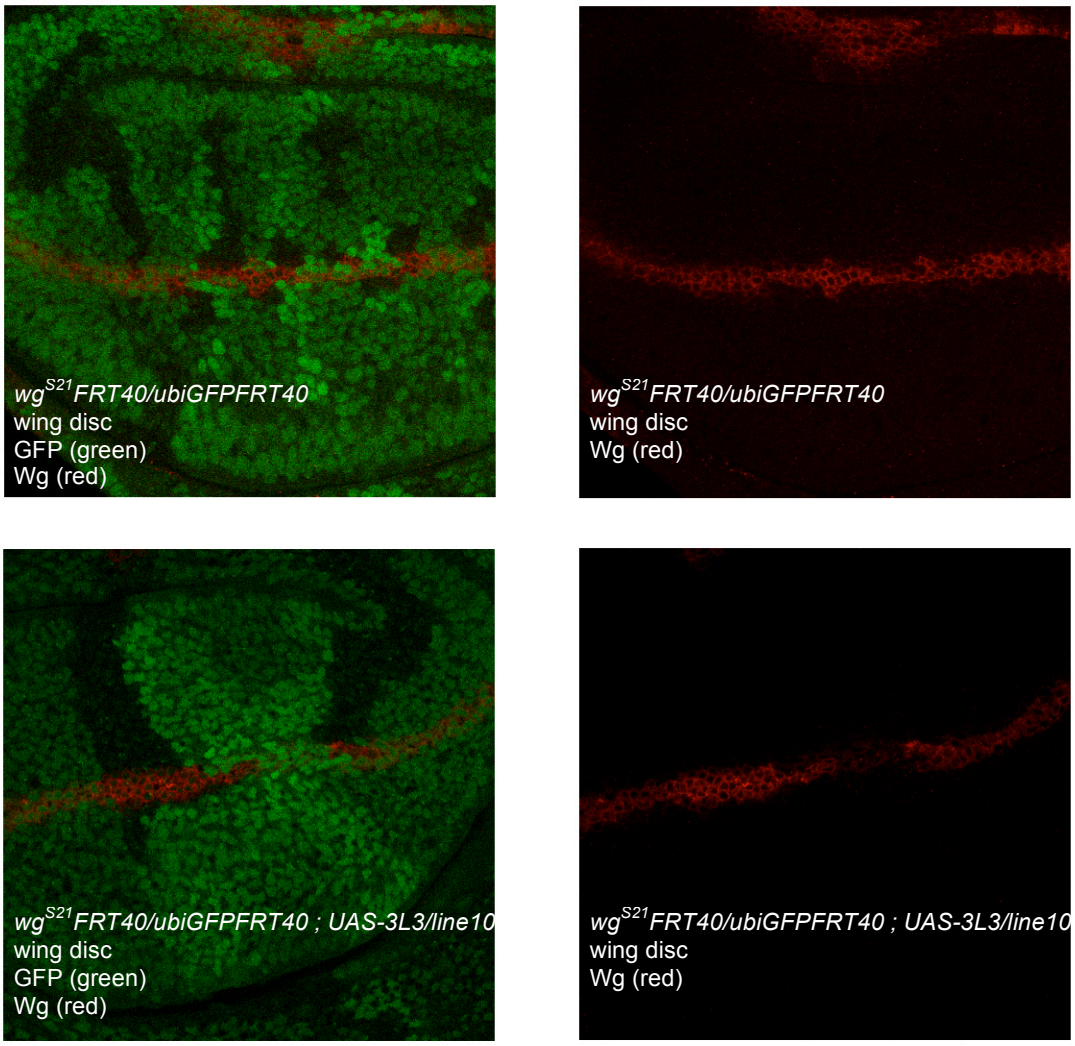

Figure 69 - Wing discs heterozygous for the allele *wg*^{S21}. They show clones, which are homozygous for the allele *wg*^{S21} and are marked by the absence of GFP, and twin spots, which are homozygous for wild-type *wg* and are marked by a stronger staining for GFP. Wg and Wg^{S21} are shown in red, whereas GFP is shown in green. The upper panel shows a wing disc wild-type for the expression of *CG6210*; the lower panel shows a wing disc, which over-expresses *CG6210*.

In another experiment we tried instead to rescue the accumulation of Wg observed in the wing discs of larvae homozygous mutant for *CG6210* by the over-expressing of the *por* transgene. *por* was over-expressed in the posterior compartment generating an internal control for staining in the anterior compartment. Unfortunately, over-expression of *por* led to lethality at a very early stage and therefore we could not draw any conclusion.

Next, we investigated whether the accumulation of Wg observed in *CG6210* mutant tissue is enhanced when the palmitoylation of Wg is impaired.

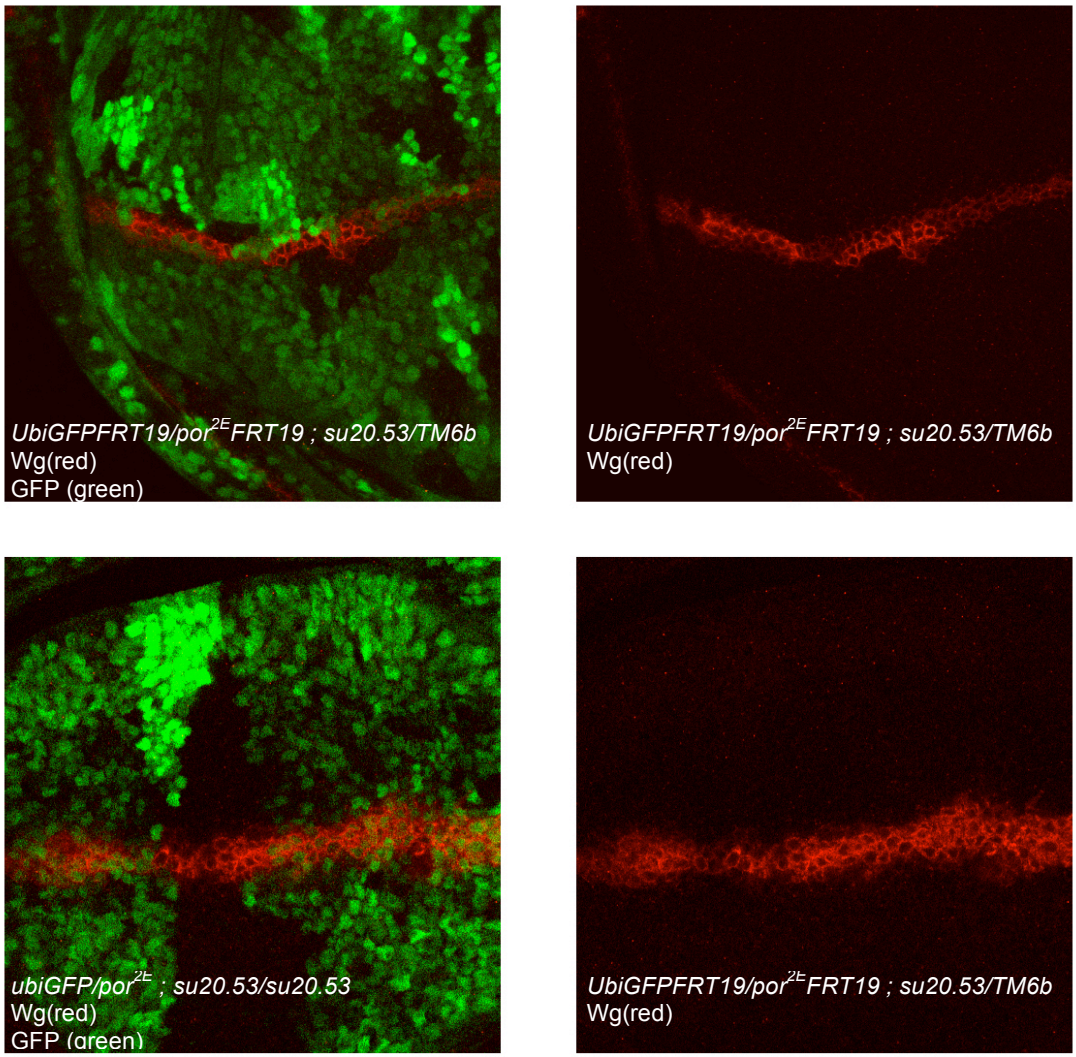

Figure 70 - Wing discs stained for Wg (in red) carry clones, which are homozygous mutant for *por* and are marked by the absence of GFP. The upper panel shows a wing disc, which is heterozygous for *CG6210* and shows the usual accumulation of Wg in clones homozygous mutant for *por*; the lower panel shows a wing disc, which is homozygous mutant for *CG6210* and does not show any increase in the accumulation of Wg in clones homozygous mutant for *por*.

We induced, in wing discs of larvae homozygous mutant for *CG6210*, the formation of clones homozygous for *wg* alleles (wg^{S21} or wg^{IL114}) or homozygous mutant for *por*.
In the situation with clones homozygous for wg alleles, no second instar larvae were found due to a strong genetic interaction between these *wg* alleles and *CG6210*. In

second situation with *por* mutant clones we could not detect any enhanced accumulation of Wg in a *CG6210* homozygous mutant background.

5.1.2 CG6210 and Nrt-Wingless

We were interested to know whether the function of the protein CG6210 is also needed when Wg is tethered to the membrane by a nonlipid anchor.

To address this question, we used the fusion protein Nrt-HA-wg, in which the N terminus of Wg is fused to the C terminus of *Drosophila* Neurotactin (Nrt), a type-II transmembrane protein. This derivative of Wg has previously been shown to be effectively tethered to the expressing cells and to retain biological activity even in absence of endogenous Wg (Zecca et al., 1996). We expressed *HA-wg* (line D214/T236), and the control *Nrt-HA-wg* (line D215/T237) under the control of different *Gal4* drivers in *CG6210* mutant versus wild-type tissue. We observed a larval lethal phenotype with the embryonically active drivers *ptc-Gal4, en-Gal4, arm-Gal4, tubα1-Gal4, actin5c-Gal4*, whereas under the control of *vg-Gal4* and *ap-Gal4* (at 25 as well as at 18 degrees) we noticed a very strong expression of the transgenes. This very strong expression was probably the reason why no difference was detected between wild-type versus *CG6210* homozygous mutant tissue.

We observed a very strong and patchy expression at 25 and 18 degrees with the use of the wing disc specific driver called *line10*.

Last, we used two temperature sensitive drivers like *sev-Gal4* (which contains the *hsp70* promoter) and *hs70-Gal4*. The first driver gave a larval lethal phenotype (at 18 as well as 25 degrees), whereas the second driver resulted, at 25 degrees, in a larval lethal phenotype and, at 18 degrees, in an expression pattern, which was very similar to the one observed with the driver *line10*.

5.1.3 In situ hybridization

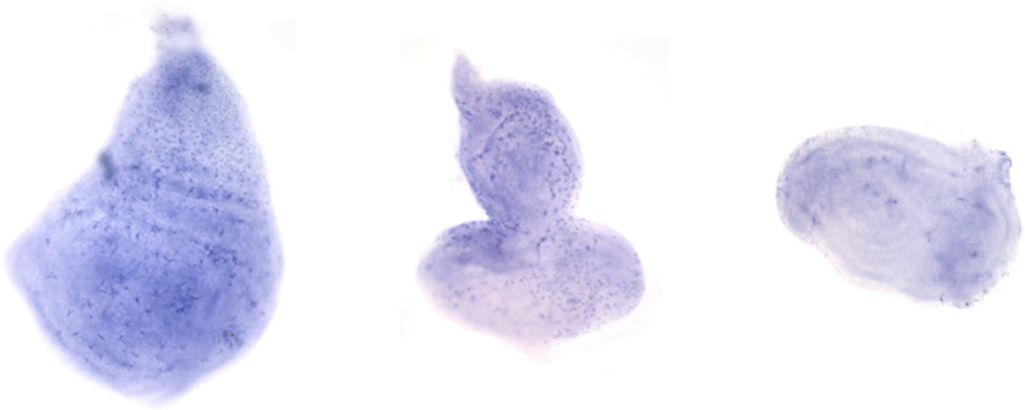

Figure 71 – In situ hybridization of wing, eye, and leg disc for the gene *CG6210*.

The expression of the mRNA of *CG6210* appears to be ubiquitous in the wing, eye, and leg discs.

5.1.4 *CG6210* and S2 cells

In order to confirm the role of *CG6210* in the Wg signaling pathway, we performed some preliminary experiments in S2 cells stably transfected with a Wg responsive luciferase reporter construct. In the reporter cells, the expression of *luciferase* is downstream of multimerised LEF binding sites and is expressed when the Wg signaling pathway is activated. The levels of Luciferase can be detected and are proportional to the level of activation of the pathway (Schweizer and Varmus, 2003).

We tried to induce the Wg signaling cascade by the addition to the reporter cells of LiCl, dsRNA against *shaggy*, dsRNA against *axin*, or by the addition of heat-shocked *hs-wg* S2 cells. We found that only the last two approaches gave reliable induction.

When we tried to block the signaling cascade by the addition of different dsRNA (against *gfp*, *lgs* or *CG6219*) in the reporter cells, we found that only with dsRNA against *lgs* was a significant down-regulation achieved. We had no effect with 4 different forms of dsRNA against *CG6210*.

We then tested if dsRNA given to the *hs-wg* S2 before the induction could lead to an effect on Wg signaling. Surprisingly, we found that dsRNA against *lgs* resulted in a

significant down-regulation of the activation of the reporter system, in contrast to dsRNA against *gfp*, *por,* and four different parts of *CG6210*, which had no effect.

5.1.5 Additional observations

The transgenes *UAS-wg*^{A} and *UAS-wg*^{S} carry a C to A and C to S mutation at the palmitoylation site (the amino acid 93), and thus cannot be palmitoylated. Wg^{A} and Wg^{S} are completely inactive since their expression in the eyes driven by the *sev-Gal4* driver and their expression driven by an embryonically active driver like *en-Gal4* caused no phenotype.

A strong genetic interaction was observed between *CG6210* and the *wg* allele *wg*$^{SB21.2B}$: Flies carrying *su20.53* and *wg*$^{SB21.2B}$ were weak, and *3L3* transheterozygous animals carrying this *wg* mutation died at the 3rd instar-larval stage.

We tried to rescue the lethality phenotype of *3L3* homozygous mutant animals by the over-expression of *wg* in the *wg*-expressing cells. Unfortunaltely, the combination of transgene *UAS-wg* with the *wg-Gal4* driver was lethal. As a consequence, we could not test whether an increase production of Wg would rescue a possible reduced secretion of Wg in the *3L3* mutant tissue.

5.2 Test of the recessive suppressors of the “rough-eye phenotype”

Apart from the 3 complementation groups on the 3rd chromosome arm, many single hits were found in the EMS mutagenesis screen for so-called recessive components of the Wnt/Wg signaling pathway.

In order to test the possible role in the Wg pathway of these suppressors of the “rough-eye phenotype”, we performed germline clones experiments and studied the adult wing phenotype of Minute$^{+/+}$ mutant clones in a Minute$^{+/-}$ background for some of the suppressors.

The embryonic segmentation phenotype was studied using germline clones experiments in the two following series of putative recessive suppressors: C81, C82, C83, C84, C85, C85, C86, which are located on the left arm of the 2nd chromosome, and C61, C63, C67,

C69, C71, C72, which are located on the left arm of the 3rd chromosome. We found no abnormal cuticle phenotype in any of them.
For the same group of putative suppressors no adult wing phenotype of Minute$^{+/+}$ mutant clones in a Minute$^{+/-}$ background, i.e. no notches, was observed.
We concluded that the single hits we tested probably do not represent mutations in positive components of the Wg pathway.

5.3 Results related to the group of dominant suppressors of the "rough-eye-phenotype"

In the "loss-of-function" screen performed by our group (Brunner et al., 1997), several dominant suppressors of the "rough-eye phenotype" were found and many of them turned out to be important positive components of the Wg/Wnt signaling pathway.
The role of some candidates found in the screen remain unstudied, and the following experiments deal with the attempt to characterize the 3rd chromosomal mutants of the screen, i.e. *M2, EB89, EB112, EB128, EB129, EB131, EB132, EB133, EB136, EB137,* and *EB139.*

We first re-tested their suppressive activities regarding the "rough-eye phenotype". For this purpose we crossed each mutant with flies carrying the *sev-wg* construct, and gave each eye phenotype average values ranging from –1 (i.e. enhancement of the phenotype) to 5 (i.e. complete suppression of the phenotype):

M2/sev-wg	4-3
EB89/sev-wg	0
EB112/sev-wg	3
EB128/sev-wg	2-3
EB129/sev-wg	2
EB131/sev-wg	4-5
EB132/sev-wg	4
EB133/sev-wg	-1
EB136/sev-wg	2
EB137/sev-wg	4-3
Controls:	
$EB130^{pygo}$*/sev-wg*	4
yw/sev-wg	0
yw flies	5

We then performed a complementation analysis and found two complementation groups consisting of two, respectively three different alleles.
Mutants *M2* and *EB112* were found in the first complementation group and they most probably represented the same allele (mutant *M2* arose as a misinterpretation of writing of *EB112*). The second complementation group was composed by the mutants *EB128, EB131,* and *EB137*.

Induction mitotic recombination is a very useful genetic tool to characterize the loss of function phenotype of the gene of interest in different situations. For this purpose we recombined each 3rd chromosomal suppressor with FRT80 and FRT82 sequences.
It is also important to consider that the suppressive activity of a mutant on the “rough-eye phenotype” is probably due to a mutation of a single gene. Hence, if the suppressive activity is still present in most recombinants for the FRT on one chromosome arm, the activity will be probably lost in the recombinants for the FRT on the other chromosome arm. Indirectly this experiment should allow a first row mapping of the suppressive activity.

5.3.1 *Belle* is mutated the second complementation group of dominant suppressors

The alleles *EB128*, *EB131*, and *EB137* were crossed with different deficiencies and mutants in order to find out which gene was mutated in this group. All three alleles were found not to complement the mutant *l(3)85Acb3*. This is a presumed null allele of the gene called *belle* (*bel*), since it presents a 500 bp deletion of the first exon (ATG included) and is homozygous lethal. We called it *EB109*.

The gene *bel* maps at the cytological position 85A5-85A7, has four exons, its CDS has a length of 2397 nucleotides, and encodes a protein of 798 amino acids.
Based on the sequence, *bel* appears to be an RNA-helicase; helicases are known to be enzymes that unwind duplex DNA or RNA in reactions coupled to nucleoside 5' triphosphate binding and hydrolysis, and that play central role in processes affecting nucleic acids (Lohman and Bjorson, 1996). On the basis of amino acid sequence homology, helicases have been classified into five super-families (Gorbalenya and Koonin, 1993). Although the overall sequence homology is low, conserved regions or "helicase" motifs within each family have been identified (Gorbalenya et al., 1989).

In order to better characterize the second complementation group, which appeared to be mutant for the gene *bel*, we used some other alleles and deficiencies, which cover the region of the gene.

Bel^{6} (also called *l(3)85Acprl34* or *BL4024*) is recessive lethal at larval stage.

bel^{neo30} (also called *BL10063*) is a hypomorphic allele with a P-element insertions, is homozygous lethal, and shows male and female sterility.

bel$^{cap\text{-}1}$ (also called *ms(3)00940* or *BL11778*) carries a P-element insertion at the base 225/5044 (1st exon) and is recessive male sterile.

P222 (also called *l(3)L4740*^{L4740} or *BL10222*) carries a P-element insertion at base 1847/5044 (1st intron) and is homozygous viable.

EP(3)3692 (also called *bel*^{EP3692} or *BL101871*) is recessive lethal, and has an EP-element insertion at base 1131/5044 (1st intron).

Df(3R)CA3 (also called *BL1516*) is a deficiency, which covers the region 84F2; 85A6-7.

Df(3R)Dhod15 (also called *BL1891*) is a deficiency, which covers the region 85A5; 85A5-85A6.

Df(3R)G1 (also called *BL1892*) is a deficiency, which covers the region 85A5; 85A6-11.

Df(3R)CA1 (also called *BL3053*) is a deficiency, which covers the region 84E12-13; 85A6-11.

As already said, the alleles *EB128*, *EB131*, and *EB137* formed a complementation group with *EB109*, which is a null allele of the gene *bel*. This suggested that all four contain a mutation in the same gene.

We then performed a complementation analysis with the alleles bel^{EP3692}, bel^{6}, $bel^{cap\text{-}1}$, *P222, EB109,* bel^{neo30}. *EB109,* bel^{EP3692}, and bel^{6} did not complement each other; *EB109* did not complement the allele *P222*.
So, we could build the following allelic series:
EB109 > bel^{6} and bel^{EP3692} > *P222* > bel^{neo30}.

We then tested the deficiencies listed above by crossing them with the alleles bel^{EP3692}, $bel^{cap\text{-}1}$, *EB109* and we could confirm that they were lacking the region, which contains the gene *bel*. In fact, the crosses using bel^{EP3692} and *EB109* were lethal and the crosses with allele $bel^{cap\text{-}1}$ resulted in a male sterility phenotype. The deficiency *Df(3R)Dhod15* was also crossed with the alleles *EB131* and *EB137* and both crosses gave a lethality phenotype, which suggested again that both are mutant for *bel*.

We then sequenced the alleles found in the second complementation group.
The allele *EB131* carries a C to T mutation at position 1481; this leads to a missense mutation of the amino acid serine to leucine at position 494. This mutation locates to the conserved domain called SAT.

The allele *EB128* carries a G to A mutation at position 392; this leads to a missense mutation of the amino acid glycine to aspartate at position 131. In addition, a C to T mutation was found at position 1861, which leads to an arginine to cysteine substitution at position 621. This second mutation is also located in a conserved domain.

In order to confirm that the alleles of the second complementary groups were mutant for the gene *bel*, we performed a rescue experiment with the following constructs:

pTK203 *ptub-Flag-bel*

pTK209 *ptub-bel-Flag*

We tried to rescue the homozygous situation of the alleles *EB128, EB131, EB137*, and *Bel*^{6}. We found a rescue only for the allele EB137 crossed with the *pTK203* construct, which drives the expression of the N-terminal tagged form of *bel*. The reason why the other alleles could not be rescued was probably due to the presence of second hits on the same chromosome. We then tried to rescue the alleles *EB109, EB128, EB131, EB137*, and *Bel*^{6} crossing them with the deficiency *Df(3R)Dhod15*. In this situation, all the alleles could be rescued, but only with the N-terminal tagged version of *bel* (insertions *pTK203.4*). These results again suggested that *EB109, EB128, EB131, EB137* are *bel* alleles.

We had another transgenic line carrying the *sev-wg* construct on the X chromosome; these flies showed a stronger “rough-eye phenotype” than flies used for the screen, which carried the *sev-wg* construct on the third chromosome. When we crossed the allele *EB131* with this other line, we noticed a clear suppression of the phenotype, and this suppression was even stronger than the one observed with the *pygo* allele *EB130*^{pygo}.

We then investigated whether the “rough-eye phenotype” was sensitive to the amount of Bel. For this purpose, we first crossed flies carrying the *sev-wg* construct with the allele *EB131*: as expected the eyes looked almost normal. When the *tubulinα1-Flag-belle* construct (*pTK203.4*) was crossed into an *EB131 sev-wg* background, the phenotype once again resembled the original “rough-eye phenotype”. Moreover, if only the *sev-wg* construct and the *tubulinα1-Flag-bel* construct were present, the phenotype was stronger than the usual “rough-eye phenotype”. This suggested that the phenotype caused by the construct *sev-wg* was dependent on the amount of Bel protein available.

We then wanted to be sure that the effects observed so far were not just due to an interaction of the protein Bel with the construct *sev-wg*, since the transcript of the *sev-wg* construct forms secondary structures in its 5’UTR and *bel* is an RNA-helicase. In fact,

Bel could be needed for the translation initiation of the construct and thus for the synthesis of Wg. In the absence of Bel there could be a reduced translation initiation of the Wg protein, a reduced Wg signaling, and thus a reduction of the eye phenotype. In order to rule out such a possibility, we tried to express Wg through combinations of the lines *sev-Gal4* or *GMR-Gal4* with the line *UAS-wg*. With this setup no secondary structures were present.

We first looked for a suitable eye phenotype, crossing 6 different *Gal4* lines (one *sev-Gal4* on the second chromosome from the stock K24; one *sev-GAL4* on the third chromosome from the stock K25; the line *sE-sP-Gal4* from the stock kk12/2, which carried a *sevenless* enhancer and a *sevenless* promoter driving the *Gal4* on the second chromosome; the line *sE-sP-Gal4* from the stock kk12/3, which carried a *sevenless* enhancer and a *sevenless* promoter driving the *Gal4* on the third chromosome; the line *2xsE-sP-Gal4* from the stock kk13/3, on the third chromosome; one *GMR-Gal4* line on the second chromosome) with 2 different *UAS-wg* lines (one on the third chromosome from the stock D87.2 and one with an *HA-tag* on the second chromosome from the stock D214/T236). All combinations with the *sev-Gal4* and the *sE-sP-Gal4* lines from the stock kk12/2 led to lethality, whereas the other combinations led to a “rough-eye phenotype”, which in some cases was very strong. The line *sE-sP-Gal4* from the stock kk12/3 combined with the *UAS-wg* line from the stock D214/T236 gave a strong phenotype, which was suppressed by the allele *EB131* and by a *legless* allele (lgs^{17E}) in heterozygous state.
We could conclude that the suppressive activity of the “rough-eye phenotype” observed with the *bel* alleles was not simply due to an unspecific interaction with the *sev-wg* construct.

We performed another experiment to further exclude the possibility that the suppression of the “rough-eye phenotype” was related to the secondary structures present in the *sev-wg* construct, and thus to a reduced translation initiation of the Wg protein. We crossed flies carrying the *sev-wg* construct with wild-type flies or flies carrying the *EB131* allele and performed an antibody staining for Wg in the eye discs. We couldn’t detect any difference in the staining for Wg in the eye discs, meaning that the synthesis of the Wg protein is note impaired in *bel* heterozygous mutant flies. This suggested that the suppression of the “rough-eye phenotype” was due to a down-regulation of the Wg pathway downstream of the Wg production.

We then tested the specificity of *bel* for the Wg signaling pathway and looked whether *bel* mutants showed any effects in other signaling pathways. To test this hypothesis, we crossed the allele *EB131*, which showed the strongest suppression of the "rough-eye phenotype", with fly stocks carrying different combinations of transgenes. These flies had different phenotypes, and represented a sensitized background, which allowed to study the effect of *EB131* on different signaling pathways. So, we crossed *EB131* with:

yw ; UAS-lgs^{17E}/UAS-lgs^{17E} ; Sal-Gal4/TM2 (wing notches; Wg pathway is reduced)

yw ; GMR-Gal4/GMR-Gal4 ; UAS-Drac/UAS-Drac (rough eye phenotype; the constitutively active form of *ras* is expressed)

yw ; GMR-Gal4 UAS-InR/Cyo (big eye phenotype; the Insulin pathway is constitutively active)

yw ; sev-Gal4,Tsev11.5/TM3 (rough eye phenotype; mutation in the gene *sev*)

yw ; GMR-Gal4,UAS-TNF/Cyo (very small eye; TNF pathway is activated)

yw ; Sal-Gal4,UAS-ptc/Cyo (small wings and vein pattern defect; over-expression of the Hh receptor Ptc, thus reducing the Hh signaling)

We could detect only a very mild reduction of the phenotypes of the stocks *yw ; UAS-lgs^{17E}/UAS-lgs^{17E} ; Sal-Gal4/TM2* and *yw ; GMR-Gal4/GMR-Gal4 ; UAS-Drac/UAS-Drac*. As control, we crossed the *pygo* allele *EB130^{pygo}* with the same fly stocks and never observed any kind of suppression. We thus supposed that the effect seen with *bel* mutants regarding the "rough-eye phenotype" was probably specific.

Several developmental processes are altered if the Wg signaling pathway is hyper-activated. To test whether an over-expression of *bel* could lead to an increase in the signaling of the Wg pathway, we drove the expression of the N- and C-terminal tagged version of *bel* (*pTK202.4* and *pTK208.3*, both are *UAS-bel* constructs) with different *Gal4* lines and looked at possible phenotypes in the adult flies.
bel driven by *sal-Gal4* (expression between the 2nd and the 5th vein of the wing), *dpp-Gal4*, *en-Gal4*, and two ubiquitous *Gal4* lines (*actin5c-Gal4* from the stock bK390, and *69B-Gal4* from the stock bK373) did not give rise to any significant phenotype.
We then tried to drive *bel* expression with eye specific *Gal4* lines. With the *sev-Gal4* line

we could not detect any alteration in the eye structure, and with the line *GMR-Gal4* we only saw a slight reduction of the phenotype, which is normally observed with the *Gal4* line alone.
We concluded that over-expression of the gene *bel* did not induce an increase in the Wg signaling pathway.

In order to better characterize the role of *bel* in the Wg signaling pathway, we performed the following epistatic analysis. We recombined the *GMR-Gal4* line with the *UAS-arm*^{s10} transgene to constitutively activate the Wg pathway downstream of *arm* in the eye discs. As controls, we crossed these recombinants with the *pygo* allele *EB130*^{pygo} or with two *pangolin* mutants (*dTCF*^{2} and *dTCF*^{3}) and detected a good suppression of the phenotype at 25 degrees and a weaker one at 18 degrees (not performed for the two *pangolin* mutants). Similar crosses made with the allele *EB131* did not show any rescue of the phenotype (at both temperature). We could conclude that the putative role of *bel* in the Wg signaling pathway is upstream of *arm*.

5.3.1.1 Summary of experiments performed with the suppressor *EB131*

The allele *EB131* was sequenced and shown to carry a mutation in the CDS of the gene *bel*. Moreover, it did not complement the allele *EB109*, which is a known null allele of *bel*.
Interestingly, *EB131* and all the alleles of the first complementation group coming from the screen for recessive suppressors (*3L1*) did not complement each other. Note that *bel* maps at position 85A5, and the suppressive activity of first complementation group of recessive suppressors maps at position 74.

We then tried to map the suppressive activity of *EB131*, and looked at the recombination frequency between its suppressive activity and a marker (a P-element carrying a *y*+) located at position 73C-74D. We screened 553 flies and found 32 recombinants. We could conclude that the suppressive activity of *EB131* is lying at 5,79 cM from the *y*+ marked P-element, i.e. at position 69-70 or 84-87. This last position would be very close to the one of the gene *bel*.
It is important to notice that there were two groups of recombinants: one group carrying the suppressive activity and the marker, the other carrying none of them. The proportion we found between the two groups was of 23:9, whereas the expected proportion should

be 1:1.This last observation, the interaction with the first complementation group of recessive suppressors, and the impossibility to rescue *EB131* homozygously led to the hypothesis that the third chromosome of *EB131* could carry a second hit. Alternatively, there could be a strong genetic interaction between the mutation in the gene *bel* and the locus 74.

To rule out a lethal hit at the cytological position 73C-74D on the chromosome of *EB131*, we recombined its suppressive activity with an *y+* marked EP-line located at the cytological position 74D (*EP43-0006*). y+ recombinants, which still suppressed the "rough-eye phenotype", were crossed with two alleles of the first complementation group of recessive suppressors (*C64* and *C68*). Interestingly they complemented each other, suggesting that the allele *EB131* carried a lethal mutation at a position close to 74D.

Once again we tried to map the suppressive activity of the "rough-eye phenotype" of *EB131.* We measured the recombination frequency between the mutation responsible for the suppressive activity and a marker located at the cytological position 85B (we used two y+ insertions of the *polyketoid* gene, *CG8351*). Importantly, none of the two markers suppressed the "rough-eye phenotype". If the mutation in the *bel* gene was responsible for the suppressive activity, we should find a very low recombination rate. We found a recombination rate of 0-4/351 for the first marker (*43-222*), and a recombination rate of 0-3/637 for the second one (*44-0500*). A control made with the allele bel^{EP3692} gave one recombination frequency of 0/1005 and one of 0-3/1385. We concluded that the suppressive activity of the "rough-eye phenotype" of *EB131* was located very close to the cytological position 85B, and was very probably due to the mutation in the gene *bel*.

We were also able to exclude a possible strong genetic interaction between the locus of *bel* and the one of the first complementation group of recessive suppressors. In fact, we couldn't rescue the combination of with the *EB131* and the allele *C64* or *C68* (recessive suppressors of the first complementation group) with the transgene *tubulinα1-Flag-bel* (*pTK203.4*).

5.3.1.2 Summary of experiments performed with the suppressor *EB109*

The null allele *EB109* carries a deletion of 500 bp in *bel* gene, which includes the start codon. Interestingly, this allele did not complement all the allele (recessive and

dominant) of the second complementation group of recessive suppressors of the “rough-eye phenotype”. The suppressive activity of this second complementation group was mapped cytogenetically to position 78. We should notice that the deficiency *Df(3R)Dhod15*, allele *EB128, EB131,* and *EB137* did complement the alleles of this second group (*C40* and *C70*).

We made following hypotheses to explain the results observed:
1. *EB109* also carries also a mutation at position *78*.
2. the alleles of the second recessive complementation group carry also a mutation at the *bel* locus (position *85*).
3. there is a strong genetic interaction between the two loci.

To rule out the first hypothesis, we should cross a deficiency of *bel* with an allele of the second recessive complementation group and observe a lethality phenotype. We could rule out the second hypothesis since all alleles of the second recessive complementation group were created by independent mutations.

It could also be possible to get rid of the eventual lethal hit at position *78* on the *EB109* allele by making recombinants with a marker (e.g. the y+ marked EP line as *EP10.144*) located at *78A* and the suppressive activity of *EB109*. If the cause of the lethality were due to this eventual second hit, we should observe complementation between the recombinants and the recessive suppressors of the second complementation group.

If there were a genetic interaction between EB109 and the second recessive complementation group, the allele *EB131* would not be a null allele.

We tried many times to induce a recombination between the sequences FRT80 or FRT82 and the *bel* locus of *EB109*, but it was not possible; this could be due to the presence of an inversion on the chromosome and this should be verified observing the polythene chromosomes of the salivary glands (“squashing”).

5.3.1.3 Chip experiment

We performed the following chip experiment with two goals. On the one hand, we were interested in genes, which are influenced by the up- or down-regulation of the Wg

signaling pathway. On the other hand, we wanted to compare the effect of *bel* and *lgs* to get information about the function of this helicase.

We induced the Wg pathway by adding to S2 cells dsRNA against the negative component *axin*. In one case, we added *lgs* dsRNA to block the pathway removing one specific positive component down-stream of *axin*, whereas in a second case, we added *bel* dsRNA. The negative control was performed with *gfp* dsRNA.
dsRNAs against *legs*, *belle*, *gfp* was also used in the absence of *axin* dsRNA, i.e. without induction of the Wg pathway.
Importantly, all the conditions were made in triplicate to get more reliable results.

We first looked at the genes, which were down-regulated (up-regulated) when *belle* was knocked down, and compared them with the same group of genes in the case of the dsRNA against *lgs.* The reference was in both cases the condition with dsRNA against *gfp*. Surprisingly, loss of Lgs did not lead to any significant change in any genes, whereas Belle knock down led to an up-regulation of 143 genes and to a down-regulation of 34 genes.

We then performed the same comparison when the Wg pathway was stimulated through the down-regulation of the negative component *axin*.
First, we would like to notice that the down-regulation of Axin and GFP (*gfp* dsRNA was added to always compare double treated cells) led to an up-regulation of 63 genes and to a down-regulation of 17 genes.
Between the up-regulated ones, we found known targets of the Wg pathway as the receptor *dfz3* and *wingful*.
If Lgs and Axin were knocked down, the expression of 24 up-regulated genes out of the 63 returned to their normal levels, whereas the one of 39 remained up-regulated. 41 genes were newly up-regulated.
In addition, we observed that the expression of 10 down-regulated genes returned to their normal transcriptional levels and the one of 7 remained down-regulated; 18 genes were newly down-regulated.
When we knocked down of Belle and Axin, the expression of 10 up-regulated genes out of the 63 returned to their normal levels, whereas the one of 53 remained up-regulated. 99 genes were newly up-regulated.

In addition, we observed that the expression of only one down-regulated genes returned to their normal transcriptional levels and the one of 16 remained down-regulated; 106 genes were newly down-regulated.
These data suggested that *lgs* has a more specific effect in the Wg pathway compared to *bel*, since *lgs* knock down can restore the normal expression level of many genes, which are activated by the treatment with dsRNA against the negative component *axin*. Importantly, the target genes *dfz3* and *wingful* are down-regulated when dsRNA against *lgs* is added, but are still up-regulated in the case of dsRNA against *bel*.

To further study the specificity of *bel* and *lgs* on the activated Wg pathway, we compared genes, which were up-regulated by *axin* dsRNA, with genes, which are down-regulated when *lgs* dsRNA is added in the activated state. Out of the 63 genes, which were up-regulated by the *axin* dsRNA, 30 were down-regulated when *lgs* was knocked down.
When *bel* dsRNA was used instead of *lgs* dsRNA, only 3 genes out of 63 up-regulated genes got down-regulated. This suggested that Lgs is necessary for the activation of many genes, which are activated by the Wg pathway, whereas the effect of Belle is much less specific.

Another comparison between *lgs* and *bel* was made. We compared the genes, which were down-regulated (up-regulated) if *bel* dsRNA is added in the activated state (i.e. when *axin* dsRNA is also present) with genes, which are down-regulated (up-regulated) if *lgs* dsRNA is also added in the activated state.
From this comparison we can say that the specificity of the genes *belle* and *lgs* are quite different.

When Wg signaling is not activated (i.e. in the absence of *axin* dsRNA), *lgs* dsRNA had no influence on the transcription of any gene, whereas the down-regulation of *bel* led to the transcriptional activation of 143 genes and to a transcriptional reduction of other 34 genes.
To study whether the effect of *bel* were constant in all the situations, we compared genes, which were up- (down-) regulated when only *bel* dsRNA is added, with genes that were up- (down-) regulated when *bel* dsRNA was added in the activated state.
We observed that there was no clear overlap; therefore the effect of a reduction of Belle depends on the activation of the Wg signaling pathway.

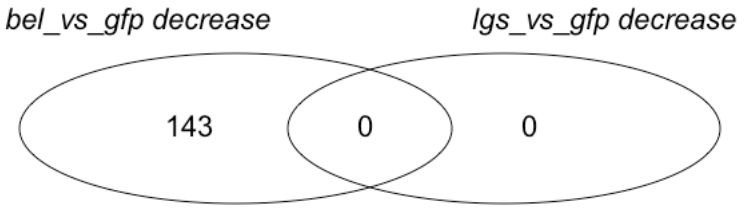

Gene down-regulated only in cells treated with *bel* dsDNA versus *gfp* dsDNA	Gene down-regulated in cells treated with *bel* dsDNA versus *gfp* dsDNA and in cells treated with *lgs* dsDNA versus *gfp* dsDNA	Gene down-regulated only in cells treated with *lgs* dsDNA versus *gfp* dsDNA
142480_at 142709_s_at 146024_at 146244_at 146946_s_at 149213_at 149514_at 149615_at 152003_at 153355_at 154880_at 155069_at 141232_at 141670_at AFFX-DapX-3_at 142157_at 142196_at 142211_at 142238_at 142245_at 142349_at 142357_at 142390_at 142433_at 142479_at 142538_at 142643_at 142673_at 142737_at 143093_at 143299_at 143438_at 143588_at 143665_at 143682_at 143853_at 143858_at 143879_at 143949_at 144160_i_at 144161_r_at 144586_at 144728_at 144882_at 145183_at 145330_at 145612_at 145685_at 145803_at 145804_at 145970_at 145975_at 146025_at		

146056_at 146084_at 146133_at 146138_at 147277_at 147353_at 147354_at 147379_at 147497_at 147919_at 147974_at 148260_at 148295_at 148854_at 149016_at 149583_at 149759_at 149940_at 149974_at 150222_at 150696_at 150697_at 150902_at 151378_at 151479_at 151509_at 151541_s_at 151598_at 151845_at 151875_at 151918_s_at 152119_at 152148_at 152151_at 152162_at 152259_at 152276_at 152366_at 152374_at 152519_at 152584_at 152608_at 152689_at 152701_at 152711_at 152758_at 152791_at 152899_at 152941_at 152970_at 153109_at 153117_at 153172_at 153220_at 153323_at 153367_at 153381_at 153490_at 153560_at 153566_at 153575_at 153657_at 153725_at 153730_at 153739_at 153765_at 153828_at 153916_at 153927_at 153983_at		

153992_at 154078_at 154086_at 154088_at 154129_at 154200_at 154208_at 154218_at 154567_at 154653_at 154703_at 154924_at 155091_at 141226_at 141512_at 141556_at 141621_at 141691_at 141712_at 141793_at		

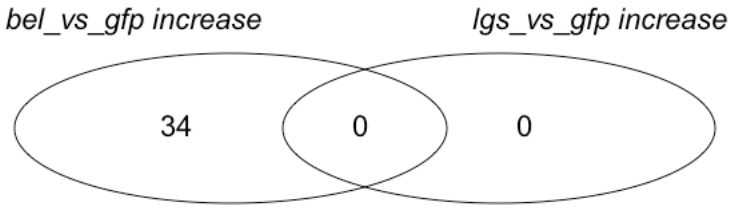

Gene up-regulated only in cells treated with *bel* dsDNA versus *gfp* dsDNA	Gene up-regulated in cells treated with *bel* dsDNA versus *gfp* dsDNA and in cells treated with *lgs* dsDNA versus *gfp* dsDNA	Gene up-regulated only in cells treated with *lgs* dsDNA versus *gfp* dsDNA
Gene Name Description 142696_at 145131_at 146882_at 149319_at 151662_s_at 151816_at 152058_at 152174_at 153648_at 153752_at 153997_at 154035_at 154259_at 154307_at 154748_at 155161_at 141595_at 141667_at 141753_at 142661_at 143391_i_at 143757_at 143848_at 145020_at 145384_at 147882_at 148090_at 149279_at 151238_at		

151799_at 154368_at 141285_at 141318_at 141737_at		

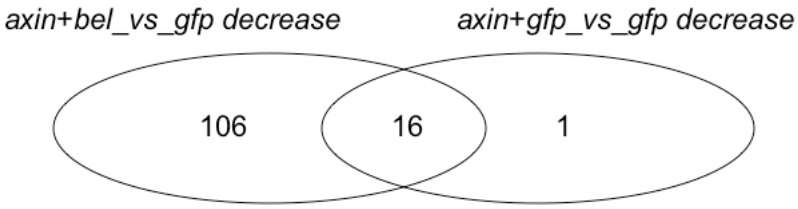

Gene down-regulated only in cells treated with *bel* and *axin* dsDNA versus *gfp* dsDNA	Gene down-regulated in cells treated with *bel* and *axin* dsDNA versus *gfp* dsDNA and in cells treated with *lgs* and *axin* dsDNA versus *gfp* dsDNA	Gene down-regulated only in cells treated with *lgs* and *axin* dsDNA versus *gfp* dsDNA
142479_at 142778_at 143120_at 143139_at 143201_at 143262_at 143276_at 143438_at 143537_at 143563_at 143702_at 143794_at 143808_at 143867_at 144017_at 144061_at 144153_at 144160_i_at 144273_at 144998_at 145005_at 145327_s_at 145594_at 145620_at 145685_at 145803_at 145804_at 145988_at 146024_at 146056_at 146151_at 146372_at 146374_at 146946_s_at 147277_at 147882_at 147919_at 148089_at 148223_at 148295_at 148469_at 149305_at 149514_at 149528_at 149615_at 149782_at 149869_at 149938_at 149968_at 150039_s_at 150113_at 150580_at 150710_at 150902_at	142480_at 142673_at 143130_at 143665_at 143682_at 145941_at 146100_at 146244_at 147353_at 147974_at 150696_at 151669_at 152148_at 152880_at 153165_at 154838_at	154545_at

151723_at 151764_at 151826_at 151918_s_at 152015_at 152162_at 152204_at 152283_at 152424_at 152608_at 152701_at 152723_at 152814_at 153117_at 153185_at 153220_at 153232_at 153296_at 153307_at 153323_at 153392_at 153432_at 153490_at 153624_at 153776_at 153792_at 153842_at 153882_at 153927_at 154007_at 154058_at 154129_at 154218_at 154660_at 154703_at 154814_at 154880_at 155069_at 141212_at 141240_at 141412_at 141512_at 141568_at 141578_at 141633_at 141652_at 141664_at 141666_at 141731_at 141749_at 141780_at 141793_at		

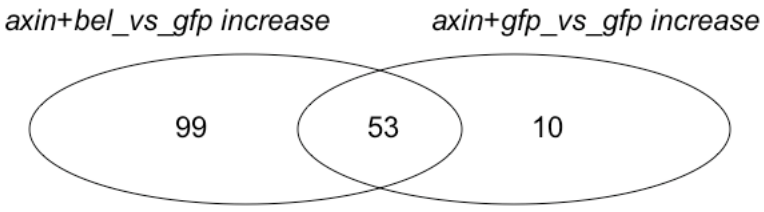

Gene up-regulated only in cells treated with *bel* and *axin* dsDNA	Gene up-regulated in cells treated with *bel* and *axin* dsDNA versus *gfp*	Gene up-regulated only in cells treated with *lgs* and *axin* dsDNA

versus *gfp* dsDNA	dsDNA and in cells treated with *lgs* and *axin* dsDNA versus *gfp* dsDNA	versus *gfp* dsDNA
142345_at	142387_at	142196_at
142582_at	142534_at	142671_at
142661_at	143046_at	142709_s_at
142696_at	143664_at	144882_at
142876_at	143868_at	145970_at
142919_s_at	144005_at	146426_at
142927_at	144177_at	149477_at
142988_at	144283_at	151694_at
143021_at	144724_at	152003_at
143072_at	145273_at	152151_at
143221_at	145582_at	
143391_i_at	145583_at	
143392_r_at	146119_at	
143565_at	146165_at	
143773_at	148048_at	
143968_at	148109_at	
144665_at	148450_at	
144712_at	148834_at	
144806_at	148840_at	
144814_at	148841_at	
145131_at	148973_at	
145384_at	149470_at	
145466_at	149867_at	
145534_at	150831_at	
145584_at	151038_at	
146732_at	151237_at	
146757_at	151360_at	
146882_at	151551_i_at	
146898_at	151681_at	
147472_at	151726_at	
148967_at	151760_at	
149027_at	151989_at	
149279_at	152114_at	
149319_at	152119_at	
149675_at	152306_at	
149768_s_at	152312_at	
149866_at	152436_at	
149967_at	152476_at	
149982_at	152675_at	
151222_at	153074_at	
151340_at	153218_at	
151475_at	153366_at	
151662_s_at	153378_at	
151706_s_at	153381_at	
151736_at	153779_at	
151816_at	154480_at	
151923_at	154571_at	
152020_at	154723_at	
152050_at	155072_at	
152058_at	141264_at	
152174_at	141472_at	
152205_at	141657_at	
152375_at	141762_at	
152425_at		
152430_at		
152453_at		
152624_at		
152715_at		
152767_at		
152873_at		
152899_at		
152933_at		
153031_at		
153082_at		
153374_at		
153648_at		

153761_at 153997_at 154035_at 154107_at 154259_at 154286_at 154287_at 154307_at 154336_at 154424_at 154443_at 154552_at 154605_at 154652_at 154697_at 154731_at 154744_at 154748_at 155006_at 155150_at 155152_at 155161_at 141332_at 141381_at 141382_at 141595_at 141622_at 141641_at 141667_at 141701_at 141748_at 141753_at 141776_at		

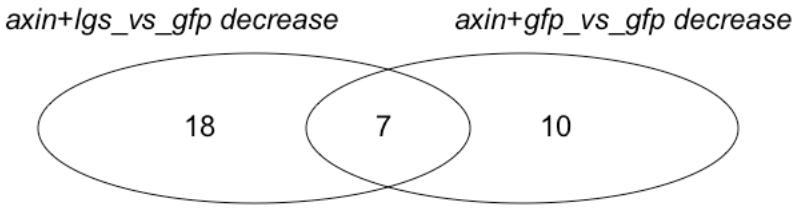

Gene down-regulated only in cells treated with *lgs* and *axin* dsDNA versus *gfp* dsDNA	Gene down-regulated in cells treated with *lgs* and *axin* dsDNA versus *gfp* dsDNA and in cells treated with *gfp* and *axin* dsDNA versus *gfp* dsDNA	Gene down-regulated only in cells treated with *gfp* and *axin* dsDNA versus *gfp* dsDNA
AFFX-Dros-ACTIN_3_at AFFX-Dros-ACTIN_M_r_at AFFX-Dros-ACTIN_5_at 143201_at 146024_at 146285_at 147106_at 147882_at 149782_at 150465_at 151287_at 151441_at 151620_at 153296_at 153350_at 153425_at 153455_at 153858_at	142480_at 143130_at 143682_at 146100_at 147353_at 151669_at 154838_at	142673_at 143665_at 145941_at 146244_at 147974_at 150696_at 152148_at 152880_at 153165_at 154545_at

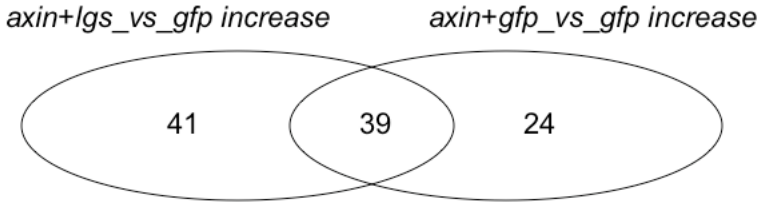

Gene up-regulated only in cells treated with *lgs* and *axin* dsDNA versus *gfp* dsDNA	Gene up-regulated in cells treated with *lgs* and *axin* dsDNA versus *gfp* dsDNA and in cells treated with *gfp* and *axin* dsDNA versus *gfp* dsDNA	Gene up-regulated only in cells treated with *gfp* and *axin* dsDNA versus *gfp* dsDNA
142390_at 142413_at 142453_at 143093_at 143565_at 143577_at 143773_at 145584_at 146882_at 147472_at 149732_at 149733_at 149759_at 149866_at 151340_at	142387_at 143046_at 143664_at 144005_at 144882_at 145582_at 145583_at 145970_at 148109_at 148450_at 148834_at 148973_at 149470_at 150831_at 151038_at	142196_at 142534_at 142671_at 142709_s_at 143868_at 144177_at 144283_at 144724_at 145273_at 146119_at 146165_at 146426_at 148048_at 148840_at 148841_at

151554_at	151360_at	149477_at
151587_at	151681_at	149867_at
151612_at	151726_at	151237_at
151876_at	151760_at	151551_i_at
152020_at	151989_at	151694_at
152050_at	152003_at	153378_at
152205_at	152114_at	153779_at
152425_at	152119_at	154571_at
152519_at	152151_at	141472_at
152715_at	152306_at	
152758_at	152312_at	
153028_at	152436_at	
153172_at	152476_at	
153355_at	152675_at	
153566_at	153074_at	
153828_at	153218_at	
153835_at	153366_at	
153892_at	153381_at	
153987_at	154480_at	
153991_at	154723_at	
154424_at	155072_at	
154605_at	141264_at	
141382_at	141657_at	
141852_at	141762_at	
141933_at		
142008_at		

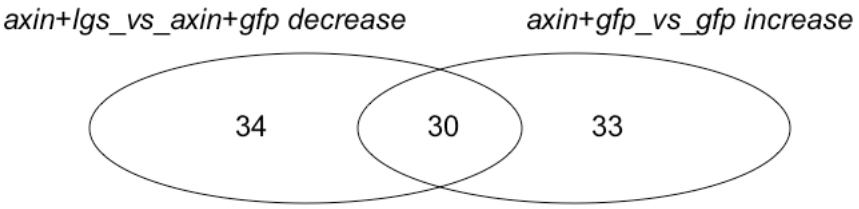

Gene down-regulated only in cells treated with *lgs* and *axin* dsDNA versus *gfp* and *axin* dsDNA	Gene down-regulated in cells treated with *lgs* and *axin* dsDNA versus *gfp* and *axin* dsDNA and up-regulated in cells treated with *gfp* and *axin* dsDNA versus *gfp* dsDNA	Gene up-regulated only in cells treated with *gfp* and *axin* dsDNA versus *gfp* dsDNA
AFFX-Dros-18S_rRNA_M_at AFFX-Dros-18S_rRNA_3_at 142216_at 142393_at 142439_at 143004_at 143689_at 143778_at 144716_at 145143_at 149019_at 149027_at 149559_at 149866_at 150661_at 151022_at 151468_s_at 151498_at 151583_s_at 152532_at 152727_at 152743_at 153116_at 153313_at 153455_at 153767_at 153822_at 154253_at 154368_at 154421_at 154777_at 154862_at 141289_at 141463_at	142387_at 142534_at 143664_at 144005_at 144177_at 146165_at 148048_at 148450_at 148834_at 148840_at 148841_at 148973_at 149470_at 150831_at 151237_at 151360_at 151551_i_at 151694_at 152114_at 152119_at 152151_at 152436_at 153074_at 153779_at 154571_at 154723_at 155072_at 141264_at 141657_at 141762_at	142196_at 142671_at 142709_s_at 143046_at 143868_at 144283_at 144724_at 144882_at 145273_at 145582_at 145583_at 145970_at 146119_at 146426_at 148109_at 149477_at 149867_at 151038_at 151681_at 151726_at 151760_at 151989_at 152003_at 152306_at 152312_at 152476_at 152675_at 153218_at 153366_at 153378_at 153381_at 154480_at 141472_at

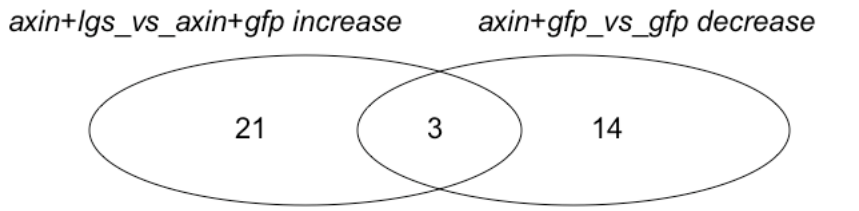

Gene up-regulated only in cells treated with *lgs* and *axin* dsDNA versus *gfp* and *axin* dsDNA	Gene up-regulated in cells treated with *lgs* and *axin* dsDNA versus *gfp* and *axin* dsDNA and down-regulated in cells treated with *gfp* and *axin*	Gene down-regulated only in cells treated with *gfp* and *axin* dsDNA versus *gfp* dsDNA

	dsDNA versus *gfp* dsDNA	
143223_at 143240_at 143566_i_at 144094_at 151127_f_at 151276_f_at 151479_at 151511_r_at 151656_at 151683_at 151723_at 151758_at 152405_at 152507_at 153509_at 153835_at 153983_at 154079_at 154761_at 141508_at 141574_at	143130_at 143665_at 152880_at	142480_at 142673_at 143682_at 145941_at 146100_at 146244_at 147353_at 147974_at 150696_at 151669_at 152148_at 153165_at 154545_at 154838_at

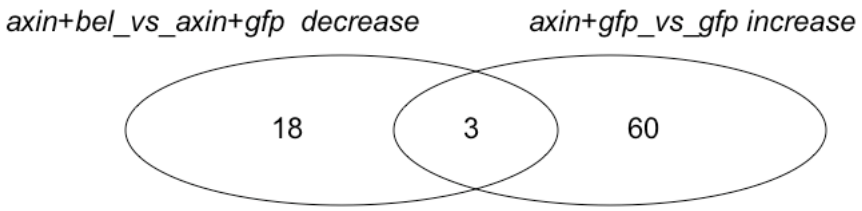

Gene down-regulated only in cells treated with *bel* and *axin* dsDNA versus *gfp* and *axin* dsDNA	Gene down-regulated in cells treated with *bel* and *axin* dsDNA versus *gfp* and *axin* dsDNA and up-regulated in cells treated with *gfp* and *axin* dsDNA versus *gfp* dsDNA	Gene up-regulated only in cells treated with *gfp* and *axin* dsDNA versus *gfp* dsDNA
142480_at 146024_at 146244_at 146946_s_at 147220_s_at 149213_at 149514_at 149615_at 149782_at 152204_at 152723_at 153355_at 154229_at 154880_at 155069_at 141232_at 141568_at 141670_at	142709_s_at 150831_at 152003_at	142196_at 142387_at 142534_at 142671_at 143046_at 143664_at 143868_at 144005_at 144177_at 144283_at 144724_at 144882_at 145273_at 145582_at 145583_at 145970_at 146119_at 146165_at 146426_at 148048_at 148109_at 148450_at 148834_at 148840_at 148841_at 148973_at 149470_at 149477_at 149867_at 151038_at 151237_at 151360_at 151551_i_at 151681_at 151694_at 151726_at 151760_at 151989_at 152114_at 152119_at 152151_at 152306_at 152312_at 152436_at 152476_at 152675_at 153074_at 153218_at 153366_at 153378_at 153381_at 153779_at 154480_at

		154571_at 154723_at 155072_at 141264_at 141472_at 141657_at 141762_at

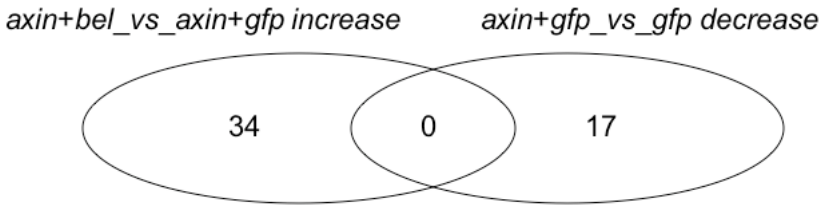

Gene up-regulated only in cells treated with *bel* and *axin* dsDNA versus *gfp* and *axin* dsDNA	Gene up-regulated in cells treated with *bel* and *axin* dsDNA versus *gfp* and *axin* dsDNA and down-regulated in cells treated with *gfp* and *axin* dsDNA versus *gfp* dsDNA	Gene down-regulated only in cells treated with *gfp* and *axin* dsDNA versus *gfp* dsDNA
142696_at 142876_at 143773_at 144005_at 145131_at 146882_at 148450_at 149319_at 149470_at 151222_at 151237_at 151662_s_at 151816_at 151923_at 152058_at 152174_at 153648_at 153752_at 153902_at 153997_at 154035_at 154107_at 154259_at 154287_at 154307_at 154571_at 154652_at 154697_at 154748_at 155152_at 155161_at 141595_at 141667_at 141753_at		142480_at 142673_at 143130_at 143665_at 143682_at 145941_at 146100_at 146244_at 147353_at 147974_at 150696_at 151669_at 152148_at 152880_at 153165_at 154545_at 154838_at

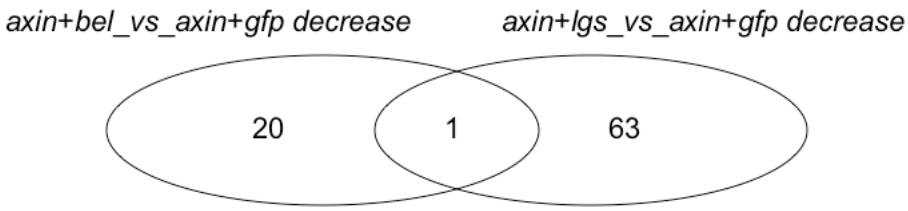

Gene down-regulated only in cells treated with *bel* and *axin* dsDNA versus *gfp* and *axin* dsDNA	Gene down-regulated in cells treated with *bel* and *axin* dsDNA versus *gfp* and *axin* dsDNA and down-regulated in cells treated with *lgs* and *axin* dsDNA versus *gfp* and *axin* dsDNA	Gene down-regulated only in cells treated with *lgs* and *axin* dsDNA versus *gfp* and *axin* dsDNA
142480_at 142709_s_at 146024_at 146244_at 146946_s_at 147220_s_at 149213_at 149514_at 149615_at 149782_at 152003_at 152204_at 152723_at 153355_at 154229_at 154880_at 155069_at 141232_at 141568_at 141670_at	150831_at	AFFX-Dros-18S_rRNA_M_at AFFX-Dros-18S_rRNA_3_at 142216_at 142387_at 142393_at 142439_at 142534_at 143004_at 143664_at 143689_at 143778_at 144005_at 144177_at 144716_at 145143_at 146165_at 148048_at 148450_at 148834_at 148840_at 148841_at 148973_at 149019_at 149027_at 149470_at 149559_at 149866_at 150661_at 151022_at 151237_at 151360_at 151468_s_at 151498_at 151551_i_at 151583_s_at 151694_at 152114_at 152119_at 152151_at 152436_at 152532_at 152727_at 152743_at 153074_at 153116_at 153313_at 153455_at 153767_at 153779_at 153822_at 154253_at 154368_at 154421_at

		154571_at 154723_at 154777_at 154862_at 155072_at 141264_at 141289_at 141463_at 141657_at 141762_at

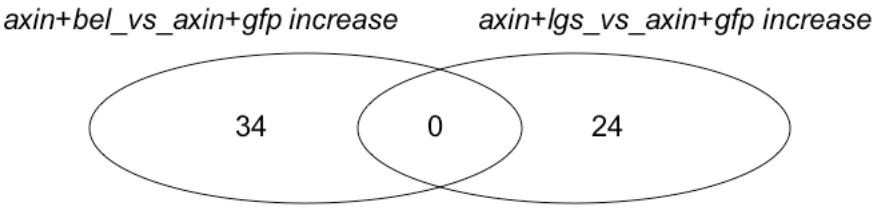

Gene up-regulated only in cells treated with *bel* and *axin* dsDNA versus *gfp* and *axin* dsDNA	Gene up-regulated in cells treated with *bel* and *axin* dsDNA versus *gfp* and *axin* dsDNA and up-regulated in cells treated with *lgs* and *axin* dsDNA versus *gfp* and *axin* dsDNA	Gene up-regulated only in cells treated with *lgs* and *axin* dsDNA versus *gfp* and *axin* dsDNA
142696_at 142876_at 143773_at 144005_at 145131_at 146882_at 148450_at 149319_at 149470_at 151222_at 151237_at 151662_s_at 151816_at 151923_at 152058_at 152174_at 153648_at 153752_at 153902_at 153997_at 154035_at 154107_at 154259_at 154287_at 154307_at 154571_at 154652_at 154697_at 154748_at 155152_at 155161_at 141595_at 141667_at 141753_at		143130_at 143223_at 143240_at 143566_i_at 143665_at 144094_at 151127_f_at 151276_f_at 151479_at 151511_r_at 151656_at 151683_at 151723_at 151758_at 152405_at 152507_at 152880_at 153509_at 153835_at 153983_at 154079_at 154761_at 141508_at 141574_at

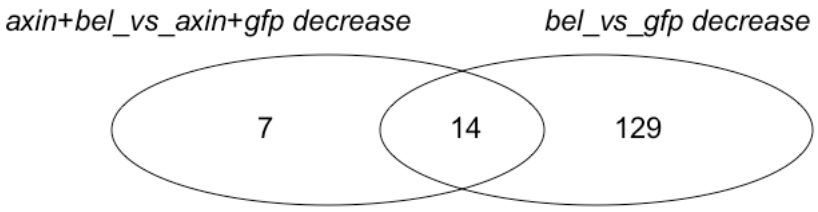

Gene down-regulated only in cells treated with *bel* and *axin* dsDNA versus *gfp* and *axin* dsDNA	Gene down-regulated in cells treated with *bel* and *axin* dsDNA versus *gfp* and *axin* dsDNA and down-regulated in cells treated with *bel* dsDNA versus *gfp* dsDNA	Gene down-regulated only in cells treated with *bel* dsDNA versus *gfp* dsDNA
147220_s_at 149782_at 150831_at 152204_at 152723_at 154229_at 141568_at	142480_at 142709_s_at 146024_at 146244_at 146946_s_at 149213_at 149514_at 149615_at 152003_at 153355_at 154880_at 155069_at 141232_at 141670_at	AFFX-DapX-3_at 142157_at 142196_at 142211_at 142238_at 142245_at 142349_at 142357_at 142390_at 142433_at 142479_at 142538_at 142643_at 142673_at 142737_at 143093_at 143299_at 143438_at 143588_at 143665_at 143682_at 143853_at 143858_at 143879_at 143949_at 144160_i_at 144161_r_at 144586_at 144728_at 144882_at 145183_at 145330_at 145612_at 145685_at 145803_at 145804_at 145970_at 145975_at 146025_at 146056_at 146084_at 146133_at 146138_at 147277_at 147353_at 147354_at 147379_at 147497_at 147919_at 147974_at 148260_at 148295_at 148854_at

		149016_at 149583_at 149759_at 149940_at 149974_at 150222_at 150696_at 150697_at 150902_at 151378_at 151479_at 151509_at 151541_s_at 151598_at 151845_at 151875_at 151918_s_at 152119_at 152148_at 152151_at 152162_at 152259_at 152276_at 152366_at 152374_at 152519_at 152584_at 152608_at 152689_at 152701_at 152711_at 152758_at 152791_at 152899_at 152941_at 152970_at 153109_at 153117_at 153172_at 153220_at 153323_at 153367_at 153381_at 153490_at 153560_at 153566_at 153575_at 153657_at 153725_at 153730_at 153739_at 153765_at 153828_at 153916_at 153927_at 153983_at 153992_at 154078_at 154086_at 154088_at 154129_at 154200_at 154208_at 154218_at 154567_at 154653_at 154703_at 154924_at 155091_at 141226_at

		141512_at 141556_at 141621_at 141691_at 141712_at 141793_at

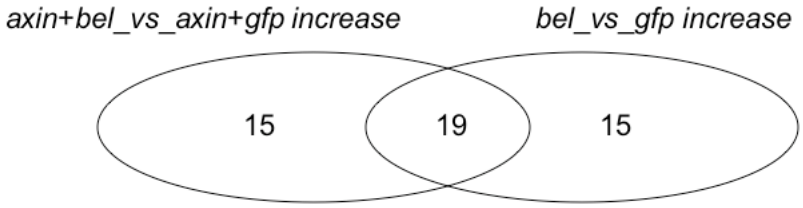

Gene up-regulated only in cells treated with *bel* and *axin* dsDNA versus *gfp* and *axin* dsDNA	Gene up-regulated in cells treated with *bel* and *axin* dsDNA versus *gfp* and *axin* dsDNA and up-regulated in cells treated with *bel* dsDNA versus *gfp* dsDNA	Gene up-regulated only in cells treated with *bel* dsDNA versus *gfp* dsDNA
142876_at 143773_at 144005_at 148450_at 149470_at 151222_at 151237_at 151923_at 153902_at 154107_at 154287_at 154571_at 154652_at 154697_at 155152_at	142696_at 145131_at 146882_at 149319_at 151662_s_at 151816_at 152058_at 152174_at 153648_at 153752_at 153997_at 154035_at 154259_at 154307_at 154748_at 155161_at 141595_at 141667_at 141753_at	142661_at 143391_i_at 143757_at 143848_at 145020_at 145384_at 147882_at 148090_at 149279_at 151238_at 151799_at 154368_at 141285_at 141318_at 141737_at

6 Methods and Materials

6.1 Plasmid constructs

All constructs of general interest made in the course of this thesis are listed. The construct numbers are followed by a short description of the plasmid.

pDS1

pOP-118-HA_bel, pTK193 x Asp718, NotI ligated into pOP-118 x Asp718, NotI

pDS2

pDA469-HA_bel, pTK193 x Asp718, NotI ligated into pDA469 x Asp718, NotI

pMZ55-HA_DDX3

pMZ55-HA_DDX3, PCR (CSODG004YH17) DDX3_5'_Nhe1, DDX3_3'_EcoR1 x NheI, EcoRI ligated into pMZ55 x NheI, EcoRI

pMZ55-HA_DBY

pMZ55-HA_DBY, PCR (DKFZp434M209) DBY_m209_5'_Nhe1, DBY_209_3_EcoR1 x NheI, EcoRI ligated into pMZ55 x NheI, EcoRI

pDS_A1/4

pKB609-HA_wg_C_to_A(93), PCR Wg_As_Nar_alanin5, Wg_XbaI_3'_primer x NarI, BglII ligated into pKB609 x NarI, BglII

pDS_S1/3

pKB609-HA_wg_C_to_S(93), PCR Wg_Asp_Nar_serin5, Wg_XbaI_3'_primer x NarI, BglII ligated into pKB609 x NarI, BglII

pDS_UAS_wg_A

pUAST-HA_wg_C_to_A(93), pDS_A1/4 x Asp718, XbaI ligated into pUAST x Asp718, XbaI

pDS_UAS_wg_S

pUAST-HA_wg_C_to_S(93), pDS_S1/3 x Asp718, XbaI ligated into pUAST x Asp718, XbaI

pDS_MZ99_Nrt_wg_A

pMZ99-HA_Nrt_wg_C_to_A(93), pDS_UAS_wg_A x BSSHII, XbaI ligated into pMZ99 x BSSHII, XbaI; notice that the Nrt sequence is not complete

pDS_MZ99_Nrt_wg_S

pMZ99-HA_Nrt_wg_C_to_S(93), pDS_UAS_wg_S x BSSHII, XbaI ligated into pMZ99 x BSSHII, XbaI; notice that the Nrt sequence is not complete

pDS_UAS_Nrt_wg_A

pUAST-Nrt_HA_wg_C_to_A(93), pDS_MZ99_Nrt_wg_A x Asp718, XbaI ligated into pUAST x Asp718, XbaI; notice that the Nrt sequence is not complete

pDS_UAS_Nrt_wg_S

pUAST-Nrt_HA_wg_C_to_S(93), pDS_MZ99_Nrt_wg_S x Asp718, XbaI ligated into pUAST x Asp718, XbaI; notice that the Nrt sequence is not complete

pDS_UAS>CDy+>Nrt_wg_A

pUAST>CDy+>Nrt_HA_wg_A(93), pDS_MZ99_Nrt_wg_A x KspI ligated into pMZ111 x Ksp; notice that the Nrt sequence is complete

pDS_UAS>CDy+>Nrt_wg_S

pUAS>CDy+>Nrt_HA_wg_S(93), pDS_MZ99_Nrt_wg_S x KspI ligated into pMZ111 x Ksp; notice that the Nrt sequence is complete

6.2 Plasmid gifts and provided vectors

pBluescript II SK (-)

cloning vector (Stratagene)

pKB609

3 HA tags, *WINGLESS* cDNA, tubulin 3' UTR (KpnI – XbaI) in pBluescript SK (Konrad Basler)

pMZ55

3 HA tags, tubulin 3’ UTR in pBluescript SK (Myriam Zecca)

pMZ99

part of the *Nrt* sequence, 3 HA tags, tubulin 3’ UTR in pBluescript SK (Myriam Zecca)

pOP118

pCasper-tub, tubulin promoter in pCasper4 (EcoRI - Asp718) (Oliver Peter)

pUAS-T

minimal *hsp70* promoter, 5 UAS binding sites, polylinker, SV40 3' UTR (Konrad Basler)

pDA469

pUAS-T with modified polylinker (with *KpnI, BglII, NotI*, but without *EI, XhoI, XbaI*) (Denise Nellen)

6.3 Oligonucleotides

6.3.1 Oligonucleotides used for sequencing

Bel1_ex1
CGAGAACGCAGTAGCTTGTG

Bel2_ex1
CACCAGATCGCTTACTCCTGG

Bel3_ex
GCGTTGCTAAGAGGAAGAGC

Bel4_ex2
CTGCTCGTTGAGGTTGCTACC

Bel5_ex3
GGTACTATTGGCTAACAGGTG

Bel6_ex3
GCTGTTCGACGATGCGACG

Bel7_ex3
GGTTGCCATCTGATTGTGG

Bel8_ex3
TGCGTTCGAAGAGTGCGAGG

Bel9_ex4
GTGGAGGAGTATGTCCACC

Bel10_ex4
CGATGCGACTGCTGATGCTG

Bel 3’
TAGGAAACCACATTTGATGC

Bel 8’

AATCCACTGTTAAGTTTCTGC

bel2'seq
GCCACCGCATACACATGCG

bel_seq3'
GCAAGACTTCCACTAACTCG

bel_seq4'
GGTGACTGGAATCGCAGC

bel_seq5'
TGCAGAAGCACGCCATTCC

bel_seq6'
CCTAGAGGACATGATCACAC

bel_seq7'
GGATCTGCTCTCGTCTATCC

bel_seq8'
TCGTTTCGATCAGCAGCTC

bel_seq9'
GTACATCTGGTTGAGAATCGG

DBY_HUMAN_5'_596
CTCGTCCTACTCCAGTGC

DBY_HUMAN_5'_828
GGCTGTACAGATCTATGAGG

DBY_HUMAN_5'_1104
GCCACCAAAGGGCGTTCGTC

DBY_HUMAN_5'_1443
CCTTCACCAGTTTCGCTCAGG

DBY_HUMAN_5'_1811

GTGGTTCCAGCAGTTCTGGC

DDX3_HUMAN_5'_498
TCCAGTTGAGGCAACAGGCA

DDX3_HUMAN_5'_817
GCACCAACGAGAGAGTTGGC

DDX3_HUMAN_5'_1109
TGCCTCCAAAGGGTGTCCG

DDX3_HUMAN_5'_1413
CCATGGAGACCGTTCTCAGAG

DDX3_HUMAN_5'_1742
AGGGTAGCAGTCGTGGAACGT

Nrt_5'_580
AAGCAGCTGGTCAACGGGTGAC

Nrt_3'_610
TTGCTTCAGCTGTGGCTTCAG

Wg_5'_1360
CGAGGTGAAGTGCAAGCTG

Wg_3'_1360
ACAGCTTGCACTTCACCTCG

Nrt_5'_180
GCAAGAAATCCTCACCAGTGG

Nrt_5'_1980
ATCCTTCCGATACCTGGAAAGC

Nrt_3'_1980
CTTCCAGGTATCGGAAGGATG

Nrt_3'_2500

TGCTGATCCAGTAGTTGCAGG

Nrt_5'_1000
CCTGCTATTTGTGCTCCTGTTG

Nrt_3'_1000
CAACAGGAGCACAAATAGCAGG

6.3.2 Oligonucleotides used for cloning

DBY_m209_5'_Nhe1
AAAGCTAGCAGTCATGTGGTGGTGAAAAATGAC

DBY_209_3_EcoR1
AAAGAATTCTCAGTTGCCCCACCAGTCAACCC

DDX3_5'_Nhe1
AAAGCTAGCAGTCATGTGGCAGTGGAAAATGCG

DDX3_3'_EcoR1
AAAGAATTCTCAGTTACCCCACCAGTCAACCC

Wg_XbaI_3'_primer
CTAGTCTAGAGAACCCGAATCCGATGTTGTCG

Wg_Asp_Nar_serin5
CGGGGTACCGGCGCCAACTTGGCCATTAGCGAGAGCCAACACCAGTTCAGAAATC GCCG

Wg_As_Nar_alanin5
CGGGGTACCGGCGCCAACTTGGCCATTAGCGAGGCCCAACACCAGTTCAGAAATC GCCG

6.3.3 Oligonucleotides used for in situ experiments

T7-3L3-5'-430
GTAATACGACTCACTATAGGAGGTGGAGCAGGATTCAACAA

T3-3L3-3'-1490
AATTAACCCTCACTAAAGGCCTTCATAATGGAGTCGTCGA

T7-3L3-5'-2080
GTAATACGACTCACTATAGGCTTGTATGTGCAGCTCTGACC

T3-3L3-3'-2900
AATTAACCCTCACTAAAGGAATCTGTCGACAATTTGGCAC

6.3.4 Oligonucleotides used for dsRNA experiments in S2 cells

bel T7 fw 1
TAATACGACTCACTATAGGGTACATCTGGTTGAGAATCGG

bel T7 fw 2/3
TAATACGACTCACTATAGGTCGTTTCGATCAGCAGCTC

bel T7 rev 1
TAATACGACTCACTATAGGGGTGACTGGAATCGCAGC

bel T7 rev 2
TAATACGACTCACTATAGGGGTTGCCATCTGATTGTGG

bel T7 rev 3
TAATACGACTCACTATAGGCCTAGAGGACATGATCACAC

porc_1_5'
TAATACGACTCACTATAGGTTGCCTACCTGGGCTACATC

porc_2_3'
TAATACGACTCACTATAGGGTGAATGCCAGATTAGTGAGC

porc_3_5'
TAATACGACTCACTATAGGGTGACTTCTTCGGGGATAGC

porc_4_3'
TAATACGACTCACTATAGGGCGAAGGCTCCAGATAGACA

shaggy_5’
TAATACGACTCACTATAGGATCAACTTGGTGTCCCTGCT

shaggy_3’
TAATACGACTCACTATAGGTATAGCGCCAGTTGCTGTTG

3L3_5’_2700_1A
TAATACGACTCACTATAGGGAGCATCGCTACCTGGATTGTG

3L3_5’_2850_1B
TAATACGACTCACTATAGGGCCAAATGAACCTGCAGTTCG

3L3_5’_2200_3
TAATACGACTCACTATAGGTTCGAGCAACCAAGATGTCG

3L3_5’_4220_5
TAATACGACTCACTATAGGTATCTTCGCCCTGCTCATCCTG

3L3_3’_3400_2
TAATACGACTCACTATAGGGGAAATAAATGGCTGCCGAAACTC

3L3_3’_3010_4
TAATACGACTCACTATAGGCCCACTACGAATGGAAACAG

3L3_3’_4750_6
TAATACGACTCACTATAGGCCACCCTTGAACGTTATTACAC

6.4 *Drosophila* strains

A fraction of fly strains used for the experiments described in this thesis are listed. For more complete information refer to the fly database.

6.4.1 Balancer strains

y w hsp-flp ; Sp/Cyo ; MKRS/TM6b (bK8)

y w hsp-flp ; Sp/Cyo ; MKRS/TM6by+ (bK174)

y w hsp-flp ; Sp/Cyoy+ ; MKRS/TM6b (bK20)

y w hsp-flp ; Sp/Cyo ubiGFP ; TM6b/TM2

6.4.2 Strains used for clone induction

y w hsp-flp ; ubiGFP FRT40/Cyo ; su20.53/TM6by+

y w hsp-flp ; ubiGFP FRT40/Cyo ; line10/TM6by+

y w hsp-flp ; ubiGFP FRT40/ubiGFP FRT40

y w hsp-flp ; ubiGFP FRT40/Cyo ; MKRS/TM6by+

y w; FRT40 y+

y w; FRT42 ubiGFP/FRT42 ubiGFP

y w hsp-flp ; FRT42 ubiGFP/Cyo ; su20.53/TM6b

f hsp-flp ; P[f+] Minute FRT80/TM2 (bK 58)

y w hsp-flp ; πMyc [w+] Minute P[y+] FRT80/TM6b (former bK 50)

y w hsp-flp ; ubiGFP [w+] FRT80/TM6b

y w hsp-flp ; Sp/Cyo ; ubiGFP [w+] FRT80/TM6b

y w hsp-flp ; ovo^{D} [w+] FRT80/TM6b

y w ; hs CD2y+ FRT80/TM2

y w hsp-flp ; Sp/Cyo; hs-CD2y+ FRT80/TM6b

y w hsp-flp ; ubiGFP FRT80/TM6b

y w hsp-flp ; Sp/Cyo ; ubiGFP FRT80/TM6by+

eyflp ; Min w+ FRT80/TM6by+

y w hsp-flp ; πMyc [w+] Minute P[y+] FRT80/TM6b

FRT82GFP/TM6b

y w hsp-flp ; Sp/Cyo ; FRT82 ubiGFP/TM6by+

y w hsp-flp ; FRT82 ubiGFP/TM6b

y w hsp-flp ; Sp /Cyo ; FRT82 disp (377) (w+)/TM6b (bK85)

y w hsp-flp ; Sp/Cyo ; FRT82 pygo/TM6by+

6.4.3 Strains containing *wingless* alleles

wg^{IL114} (K493)

y w hsp-flp ; wg^{IL114}FRT40/Cyo

$Wg^{SB21.2A}$/Cyo (Adh^{UF3} $wg^{SB21.2A}$ pr, ch/Cyo)

$Wg^{SB21.2B}$/Cyo (Adh^{UF3} $wg^{SB21.2B}$ pr, ch/Cyo)

y w hsp-flp ; $wg^{SB21.2B}$ FRT40/Cyo

y w hsp-flp ; wg^{IL114}FRT40/Cyo ; MKRS/TM6by+

y w hsp-flp ; $wg^{SB21.2B}$ FRT40/Cyo ; MKRS/TM6b

y w hsp-flp ; wg^{IL114}FRT40/Cyo ; UAS-3L3 (1-2)/TM6by+

y w hsp-flp ; $wg^{SB21.2B}$ FRT40/Cyo ; UAS-3L3 (1-2)/TM6b

y w hsp-flp ; wg^{IL114}FRT40/Cyo ; su20.53/TM6by+

y w hsp-flp ; $wg^{SB21.2B}$ FRT40/Cyo ; su20.53/TM6b

6.4.4 Strains carrying *wingless-Gal4* or related drivers

S476 (wg-Gal4)

ND382/Cyo (wg-Gal4)

S180/Cyo (wg-Gal4)

S239/S239 (wg-like expression pattern) (2^{nd} chromosome)

S393/S393 (wg-like expression pattern) (3^{rd} chromosome)

S450 (wg-like expression pattern) (2^{nd} chromosome)

ND270/270 (wg-like expression pattern) (3^{rd} chromosome)

MD618/Cyo

y w hsp-flp ; S180/Cyo; su20.53/TM6by+

y w hsp-flp ; MD618/Cyo ; su20.53/TM6b

y w hsp-flp ; ND382/Cyo ; su20.53/TM6b

6.4.5 Strains carrying other *Gal4* drivers

y w hsp-flp; actin5c-Gal4/Cyo ; su20.53/TM6by+

yw ; actin5c-Gal4/Cyo ; MKRS/TM6by+ (BK389)

y w hsp-flp ; Sp /Cyo ; act>CD2>Gal4/TM6b

y w hsp-flp ; su20.53 act>CD2>Gal4/TM6b

y w hsp-flp ; ap-Gal4/Cyo; MKRS/TM6by+

y w hsp-flp ; ap-Gal4/Cyo^{ubiGFP} ; su20.53/TM6b

y w hsp-flp ; ap-Gal4/Cyoy+ ; su20.53/TM6b

y w hsp-flp ; ap-Gal4/Cyo ; su20.53/TM6by+

y w hsp-flp ; ap-Gal4/Cyo ; ubiGFP FRT80/TM6by+

y w hsp-flp ; ap-Gal4/Cyo+ ; ubiGFP FRT80/TM6b

arm-Gal4 (II)

y w hsp-flp ; arm-Gal4/Cyo; MKRS/TM6b

Sp/Cyo ; dpp-Gal4/TM6b (K54)

ombz; dpp-Gal4 UAS-GFP/TM6b

y w ; en-Gal4 UAS-GFP/ enGAL4 UAS-GFP

y w hsp-flp ; en-Gal4 UAS-GFP/Cyo; MKRS/TM6by+

y w ; en-Gal4/Cyo

y w ; en-Gal4/Cyo ; MKRS/TM6b

y w hsp-flp ; en-Gal4/Cyo ; su20.53/TM6b

y w hsp-flp ; en-Gal4 UAS-GFP/Cyo ; su20.53/TM6by+

y w hsp-flp ; en-Gal4/Cyo ; ubiGFP FRT80/TM6b

hs-GAL4 (BL2077: P{GAL4-Hsp70.PB})

y w hsp-flp; hs-Gal4/Cyo ; ubiGFPFRT80/TM6b

ptc-Gal4 (II) (K228)

ptc-Gal4 UAS-GFP/Cyo (K534)

y w hsp-flp ; ptc-Gal4 UAS-GFP/Cyo ; ubiGFP FRT80/TM6b

y w hsp-flp ; ptc-Gal4 UAS-GFP/Cyo ; su20.54/TM6b

y w hsp-flp ; Sp/Cyo ; Sal-Gal4/TM6b

yw ; UAS-lgs^{17E}/Cyo ; Sal-Gal4/TM6b

y w hsp-flp ; sev-Gal4/Cyo ; MKRS/TM6by+ (K24)

ry^{506} ; sev-Gal4/Cyo (II) (K24)

ry^{506} ; sev-Gal4/sev-Gal4 (III) (K25)

y w hsp-flp ; sev-Gal4 (K24)/Cyo ; su20.53/TM6b

y w hsp-flp ; sev-Gal4 (K24)/Cyo ; ubiGFPFRT80/TM6b

yw ; tubα1-Gal4^{w+}/TM3 (BL5138)

yw ; tub>CD2>Gal4/SM5 (bK107)

y w hsp-flp ; tub>CD2>Gal4/Cyo ; MKRS/TM6by+

y w; vg-Gal4/Cyo ; TM2/TM6b

y w; wg-Gal4/Cyo ; MKRS/TM2

line 10/TM3

y w hsp-flp ; Sp/Cyo ; line 10/TM6by+

yw ; UAS-lgs^{17E}/Cyo ; line 10/TM6b

6.4.6 Strains carrying a *UAS-wingless* transgene

y w hsp-flp; D208.1/T230/Cyo ; MKRS/TM6by+

y w hsp-flp; D214/T236/Cyo ; MKRS/TM6by+

y w hsp-flp; D215/T237/Cyo ; MKRS/TM6by+

y w hsp-flp; D208.1/T230/Cyo ; su20.53/TM6by+

y w hsp-flp; D211/T233/Cyo ; su20.53/TM6by+

y w hsp-flp; D214/T236/Cyo ; su20.53/TM6by+

y w hsp-flp; D214/T236/Cyoy+ ; su20.53/TM6b

y w hsp-flp; D215/T237/Cyo ; su20.53/TM6by+

y w hsp-flp; D215/T237/Cyoy+ ; su20.53/TM6b

y w hsp-flp; D214/T236/Cyoy+ ; ubiGFPFRT80/TM6b

y w hsp-flp; D215/T237/Cyoy+ ; ubiGFPFRT80/TM6b

y w hsp-flp; D215/T237/Cyo ; ubiGFPFRT80/TM6b

y w hsp-flp; D214/T236/Cyo ; hsCD2y+FRT80/TM6by+

y w hsp-flp; D215/T237/Cyo ; hsCD2y+FRT80/TM6by+

y w hsp-flp D214/Cyo; K13/3/TM6b

y w hsp-flp D214/Cyo; K12/3/TM6by+

6.4.7 Strains carrying a *UAS-wingless* transgene with a point mutation at C93

y w hsp-flp ; Sp/Cyo ; UAS-wg^{S1}/TM6b

y w hsp-flp ; UAS-wg^{S2}/Cyo ; MKRS/TM6b

y w hsp-flp ; UAS-wg^{S3}/Cyo

y w hsp-flp ; UAS-wg^{S4}/Cyo ; MKRS/TM6by+

y w hsp-flp ; UAS-wg^{S5}/Cyo ; MKRS/TM6b

y w hsp-flp ; Sp/Cyo ; UAS-wg^{S6}/TM6by+

y w hsp-flp UAS-wg^{A1}/Cyo ; MKRS/TM6b

y w hsp-flp ; Sp/Cyo ; UAS-wg^{A2}/TM6b

y w hsp-flp ; Sp/Cyo ; UAS-wg^{A3}/TM6b

y w hsp-flp ; UAS-wg^{S2}/Cyo^{y+} ; ubiGFPFRT80/TM6b

y w hsp-flp ; UAS-wg^{A1}/Cyo^{y+} ; ubiGFPFRT80/TM6b

y w hsp-flp ; UAS-wg^{S2}/Cyo ; su20.53/TM6by+

y w hsp-flp ; UAS-wg^{A1}/Cyo ; su20.53/TM6b

y w hsp-flp ; UAS-wg^{A1}/Cyo^{y+} ; MKRS/TM6b

y w hsp-flp ; UAS-wg^{S2}/Cyo^{y+} ; MKRS/TM6b

sev-Gal4/Cyo ; UAS-wg^{S1}/TM6b

6.4.8 Strains carrying other *UAS* transgenes

y w hsp-flp ; UAS-GFP/Cyo ; MKRS/TM6b

y w hsp-flp ; Sp/Cyo ; UAS-GFP^{nls}/ UAS-GFP^{nls}

y w ; UAS-Dfz2/TM3

y w hsp-flp ; UAS-arm^{S10} UAS-GFP/Cyo ; MKRS/TM6by+

y w hsp-flp ; UAS-arm^{S10} UAS-GFP/Cyo ; su20.53/TM6by+

y w hsp-flp ; UAS-arm^{S10}/Cyo ; MKRS/TM6by+

y w hsp-flp ; UAS-GFP/Cyo ; su20.53/TM6b

6.4.9 Strains carrying a *Lac-Z* transgene

y w hsp-flp ; Dll-LacZ /Cyo ; su20.53/TM6by+

y w hsp-flp ; Dll-LacZ /Cyo ; ubiGFPF80/TM6b +

y w hsp-flp ; dpp-LacZ /Cyo ; su20.53/TM6b

y w hsp-flp ; dpp-LacZ /Cyo ; ubiGFPF80/TM6b

y w hsp-flp ; en-LacZ /Cyo ; ubiGFPF80/TM6b

y w hsp-flp ; ptc-LacZ/Cyo ; MKRS/TM6b

y w hsp-flp ; ptc-LacZ /Cyo ; ubiGFPF80/TM6b

y w hsp-flp ; ptc-LacZ/Cyo; ; F82ubiGFP/TM6b

y w hsp-flp ; Sp/Cyo$^{Sal\text{-}LacZ}$; F82ubiGFP/TM6b

y w hsp-flp ; wg-LacZ (K37)/Cyo ; MKRS/TM6by+

y w hsp-flp ; wg-LacZ (K39)/Cyo ; MKRS/TM6b

y w hsp-flp ; wg-LacZ (K37)/Cyo ; su20.53/TM6b

y w hsp-flp ; wg-LacZ (K39)/Cyo ; su20.53/TM6b

6.4.10 Strains used for localization studies

w ; UAS-Rab4RFP (2nd chr) (BL8505)

y w hsp-flp ; UAS-Rab4mRFP/Cyo; su20.53/TM6b

w ; UAS-Rab5GFP/TM3

w ; UAS-Rab7GFP/Cyo

w ; UAS-Rab11GFP (2nd chr) (BL8506)

y w hsp-flp ; UAS-Rab11GFP/Cyo ; su20.53/TM6b

w ; UAS-Grasp65 GFP (2nd chr) (BL8507)

y w hsp-flp ; UAS-Grasp 65 GFP/Cyo ; su20.53/TM6b

w ; sqh-EYFP-Golgi (BL7193)

w ; sqh-EYFP-Mito (BL7194)

w ; sqh-EYFP-ER/TM6b (BL7195)

6.4.11 Strains used for the experiments related to *CG6210*

y w hsp-flp ; su20.53/TM6by+

y w hsp-flp ; su20.54/TM6by+

y w hsp-flp ; Sp/Cyo ; su20.53/TM6by+

y w ; Sp/Cyo ; tubα1-3L3$^{4-61}$/TM6b

y w ; Sp/Cyo ; tubα1-3L3-HA$^{2-22}$/TM6b

yw ; Sp/Cyo ; tubα1-3L3$^{4-61}$/TM6b

yw ; tubα1-3L3-HA(2-32)/Cyo ; TM6b/TM2

y w hsp-flp ; UAS-3L3-HA/Cyo ; su20.53/TM6b

UAS-3L3-HA (2nd chrom) (3-23)

UAS-3L3-HA (3rd chrom) (3-31)

y w hsp-flp ; ap-Gal4/Cyo ; UAS-3L3 (1-2)/TM6b

y w hsp-flp ; en-Gal4/Cyo ; UAS-3L3 (1-2)/TM6b

y w hsp-flp ; UAS-3L3(1-9)/Cyo ; su20.53/TM6b

y w hsp-flp ; UAS-3L3-HA(3-23)/Cyo ; su20.53/TM6b

mwh jv[70b] (K277)

mwh su20.54 FRT80/TM6b (3)

mwh su20.54 FRT80/TM6by+ (2nd chromosome)

y w sev wg/FM7

sev-wg/TM6b

sev-hs70-wg^{CE7} (K462)

y w ; sev-hs70-wg/TM6b (K147)

shi^{1} (ts allele of shibire) (BL1328)

w shi^{1}/FM6 (BL7068)

shi^{ts}FRT18A (w+)

hs-HA-GFP-HA FRT 19 ; linie10/TM6b

hs-HA-GFP-HA FRT19 ; D215/T237/Cyo

hs-HA-GFP-HA FRT19 ; su20.54/TM6b

ubiGFP FRT19 ; su20.54/TM6b

FM7i, P{w[+mC]=ActGFP}JMR3/C(1)DX, y[1] f[1] (green balancer FM7) (BL4559)

yw P[y+, hsp-HA-GFP-HA] hsp-flp FRT19 (bK190)

w por^{2E}/FM7

w por^{PB16}/FM7a (BL4768)

w por^{PB16}/FM7(act-GFP) (w por^{PB16} from former BL4768*)*

y w ; UAS-por^{A} (A/ II)

y w hsp-flp ; UAS-por^{A}/Cyo ; MKRS/TM6by+

y w hsp-flp ; UAS-por^{A}/Cyo ; ubiGFPFRT80/TM6by+

y w ; UAS-por^{B} (III / B)

y w hsp-flp ; Sp/Cyo ; UAS-por^{A} /TM6by+

6.4.12 Strains used for the experiments related to *belle*

EB M2, EB 89, EB 109, EB 112, EB 128, EB 129, EB 131, EB 132, EB 133, EB 136, EB 137, EB 139

BL10222

BL11778 (bel^{cap-1})

y w hsp-flp ; Sp/Cyo ; BL4024 (bel^{6})/TM6b

y w hsp-flp ; Sp/Cyo ; BL10063 (bel^{neo30})/TM6b

BL1891 (Df(3R)Dhod15)

y w hsp-flp ; Sp/Cyo ; BL1891 (Df(3R)Dhod15)/TM6b

y w hsp-flp ; Sp/Cyo ; BL1892 (Df(3R)G1)/TM6b

EP(3)3692/TM3

y w hsp-flp ; Sp/Cyo ; FRT82 EP(3)3692/TM6by+

y w hsp-flp ; EB131 sev wg/TM6b (I)

y w hsp-flp ; TK202.4/202.4

TK203.4/Cyo ; MKRS/TM6b

y w hsp-flp ; TK208.3

TK209

GMR-Gal4(2)/Cyo ; MKRS/Tm6b (weak)

Sp/Cyo ; UAS-arm^{S10}/ UAS-arm^{S10} (weak)

GMR-Gal4 UAS-arm^{S10}/Cyo A (weak)

GMR-Gal4 UAS-arm^{S10} TM6by+ (weak)

y w hsp-flp ; GMR-Gal4 UAS-arm^{S10}/Cyo (recombinant 1 and 2)

y w hsp-flp ; DS2.2/3 / Cyo; MKRS/TM6b

y w hsp-flp ; DS2.2/5 / Cyo; MKRS/TM6b

y w hsp-flp ; DS2.2/8 / Cyo; MKRS/TM6by+

6.4.12.1 *EB* alleles recombined with FRT80

y w hsp-flp ; EBM2/12/TM6by+

y w hsp-flp ; EB128/12/TM6by+ (A1, C4, D1)

y w hsp-flp ; EB129/12/TM6by+ (A1, B3)

y w hsp-flp ; EB131/12/TM6by+ (C1)

EB132/12/TM6by+ (B1, B2, B3)

EB133/12/TM6by+ (B1, B2)

EB136/12/TM6by+ (A2, B2, C1)

EB139/12/TM6by+ (B1, D1, C)

6.4.12.2 *EB* alleles recombined with FRT82

y w hsp-flp ; EBM2/15/TM6by+ (A1, B3, C1)

y w hsp-flp ; EB89/15/TM6by+ (A2, B2)

y w hsp-flp ; EB112/15/TM6by+ (D1, E3)

y w hsp-flp ; EB128/15/TM6by+ (A1, C2)

y w hsp-flp ; EB129/15/TM6by+ (A2, B1, B3)

y w hsp-flp ; EB132/15/TM6by+ (A1)

y w hsp-flp ; EB136/15/TM6by+ (B2)

y w hsp-flp ; EB137/15/TM6by+ (A1, B2)

y w hsp-flp ; EB139/15/TM6by+ (A1, A2)

y w hsp-flp ; 4024/15/TM6by+ (A1, C1, E1)

6.5 Experimental Methods

6.5.1 Molecular Cloning

Standard molecular biology techniques are described in Sambrook J. and Russell D.W. *Molecular Cloning—A Laboratory Manual*. (2001) Cold Spring Harbor, NY: Cold Spring Harbor Laboratory Press.

6.5.2 *Drosophila* Biology

6.5.2.1 Preparation of legs and wings of adult flies and pupae

Adult flies and pupae were transferred into a solution of ethanol and glycerol (at a volume proportion of 1:3). After at least one day, appendages were removed and put into ethanol 70% and then washed in pure ethanol. Finally, they were mounted in Euparal®.

6.5.2.2 Rescue experiment

ND382 and *S180* transgenes were derived from the P-element based enhancer trap screen, which was carried out in the lab by Offer Gerlitz (Gerlitz et al., 2002).

6.5.2.3 Induction of homozygous clones in the *Drosophila* larva through mitotic recombination

In order to induce homozygous clones in the imaginal discs of *Drosophila* larvae, we made use of flies carrying the yeast-specific recombinase *flippase* (*flp)*, driven by the *heat-shock promoter* (*hs-flp*), which recognizes and induces mitotic recombination between two FRT sites. When these FRT sites are located at the same cytological position on homologue chromosomes Flp-mediated recombination results in a somatic sector that is homozygous for all genes distal to the FRT-bearing P element (Xu and Rubin 1993). Such sectors can be identified by absence of a cell-autonomous marker present on one of the two chromosome arms carrying the FRT site. This method allows analysis of the function of genes that are otherwise homozygous lethal.

In order to get big clones in imaginal discs, we generated Minute$^{+/+}$ clones mutant for *3L3* in a Minute$^{+/-}$ background. Minute mutations (Morata et al., 1975) are dominant mutations, defective in the production of ribosomal proteins (Lambertsson, 1998). In such a situation the environment of the *3L3* homozygous mutant clones is heterozygous for a Minute mutation, and this gives a growth advantage to the clone. Moreover the twin spot, which arises during the mitotic recombination, is a homozygous Minute$^{-/-}$ clone and its cells will disappear.

Notes for conditions used for clone induction and protein expression in the imaginal discs:
Unless specified, mitotic recombination was induced 24-72 hours AEL (After Egg Lay) with a heat-shock performed for 1 hour at 37 degrees.
In the wing and eye discs of flies carrying the *sev-wg* construct, the ubiquitous expression of Wg was achieved by a heat-shock of 1.5 hours at 37 degrees, 0.5 hours before the dissection of the larvae.
In the wing discs of flies carrying the *sevwgCE7* construct, the ubiquitous expression of Wg was achieved by a heat-shock of 1 hour at 37 degrees, 1 hour before the dissection of the larvae.

6.5.2.4 Germline clones experiments for the suppressors of the “rough-eye phenotype”

FRT recombinants carrying a mutation with suppressive activity were crossed with flies carrying the same FRT sequences and the *ovo^{D}* mutation. 3rd instar larvae from this cross were heat-shocked for 1.5 hours at 38 degrees. Since, the *ovo^{D}* mutation gives a dominant sterile phenotype, only ovarial tissue without the *ovo^{D}* mutation will produce fertilizable eggs. These eggs will be homozygous mutant for the mutation with suppressive activity. Hatched virgins were crossed with males carrying the same suppressive mutation and FRT sequence, and which were balanced with a y+ marked chromosome. This cross was allowed to lay eggs for one night on agar plate. On the following morning embryos were collected, bleached for 3 minutes, washed with tap water, and finally put into a plate containing water for 24 hrs. In order to remove the vitellum, embryos were shaken in a biphasic solution containing an equal amount of methanol and heptane. Embryos were subsequently washed 4 times with methanol, 4 times with Triton-X100 0.1%, and then incubated for at least 6 hrs at room temperature.

After mounting them on a slide with Hoyer-Lactate and after an incubation of at least 12 hours at 60^0C for the digestion of proteins, cuticles were examined under the light microscope. y^- cuticles were derived from homozygous mutant embryos, whereas y+ cuticles were derived from heterozygous mutant embryo.

6.5.2.5 Antibody staining for the imaginal discs

Larvae were dissected on ice in Ringer solution and then fixed at room temperature in 200 µl tubes with PEM (200 µl)+ 5% formaldehyde (10,7 µl) + 0.05% Triton X-100 (1 µl) for 20 minutes. After washing (4 times, plus 1 hour, plus 2-3 times with PBT + Na-Azid), they were incubated over night with the primary antibodies (diluted in PBT + Na-Azid) at 4 degrees. The next day, larvae were washed (5 times plus 30 minutes with PBT + Na-Azid + 1% HINGS) and incubated with the secondary antibodies diluted in PBT + Na-Azid for 2 hours, at room temperature. Larvae were washed (again 5 times plus 2 hours; if longer, they were kept at 4 degrees) with PBT + Na-Azid and imaginal discs were mounted in PPDA®. Imaginal discs were finally observed at the confocal microscope.

Antibody staining for extacellular proteins in imaginal discs (modified from Strigini and Cohen, 2000):
Larvae were dissected in ice-cold Ringer solution and incubated for 30-60 minutes on ice (in the 4-degree room) with primary antibodies diluted in PBS. Larvae were rinsed 5 times with ice-cold PBS and fixed for 20 minutes in ice-cold PBS containing 4% formaldehyde for 20 minutes, in the 4-degree room. Larvae were again fixed for 20 minutes at room temperature in PBS containing 4% formaldehyde. The following steps were the same as in the conventional antibody labeling protocol.

Notes:
In order to reduce the background of the staining, diluted secondary antibodies were centrifuged at maximal speed for at least 5 minutes at 4 degrees.
When GFP was expressed the washing steps were reduced. This was necessary to maintain a detectable level of GFP.

The following antibodies were used for the staining in the wing discs.

Primary antibodies	**Dilution**	**Company**
monoclonal mouse α-CD2	1:400	Serotec®

monoclonal mouse α-Dll	1:500	gift from I.Duncan
polyclonal rabbit α-Dfz2	1:400	gift form S. Cumberledge
monoclonal mouse α-β-Galactosidase	1:2000	Promega®
polyclonal rabbit α-β-Galactosidase	1:2000	Cappel®
polyclonal chicken α-β-Galactosidase	1:1000	ICL®
monoclonal mouse α-Golgi, Drosophila	1:500	Calbiochem®
polyclonal rabbit α-HA	1:500	ICL®
polyclonal rabbit α-lgs	1:5000	homemade (Kramps, et al.)
polyclonal rabbit α-c-Myc	1:300	Santa Cruz®
polyclonal guinea pig α-Sens (GP55)	1:800	gift from H. Bellen
monoclonal mouse α-Wg (4D4)	1:1000	DSHB
polyclonal rabbit α-Wnt4	1:100	gift from Jacques Pradel and Betsy Wilder
polyclonal guinea pig α-Hrs (GP59)	1:1000	gift from H. Bellen

Secondary antibodies	**Dilution**	**Company**
Alexa Fluor 594 goat α-chicken	1:200	Molecular Probes®
Alexa Fluor 488 goat α-mouse	1:200	Molecular Probes®
Alexa Fluor 594 goat α-mouse	1:200	Molecular Probes®
Alexa Fluor 488 goat α-rabbit	1:200	Molecular Probes®
Alexa Fluor 594 goat α-rabbit	1:200	Molecular Probes®
Cy5 goat α-rabbit	1:200	Jackson Lab®
Alexa Fluor 568 goat α-guinea pig	1:200	Molecular Probes®

6.5.2.6 Shibire inactivation in the imaginal discs

Shibire was inactivated by keeping *shi*^{ts} larvae at 32 degrees for 3 hours; larvae were then dissected in Ringer solution at the same temperature, and thereafter immediately fixed. Such conditions were shown to block the uptake as well as the secretion of Wg (Strigini and Cohen, 2000).

6.5.2.7 Experiment with the recessive marker *mwh* for homozygous mutant clones in adult wings

In order to mark *3L3* homozygous mutant clones in adult wings, the recessive wing marker *mwh* located at the cytological position 70 was used. The marker was recombined with one mutant allele of *CG6210* (at the cytological position 68A9), and these recombinant flies were crossed with the stock *y w hsp-flp ; πMyc [w+] Minute P[y+] FRT80 / TM6b.* Heat-shock was applied 24-72 hours AEF (After Egg Laying) at 37.5 degrees for 30 minutes and mutant clones were recognized by the abnormal hair pattern.

6.5.2.8 Recombination between the dominant suppressive mutations of the "rough-eye phenotype" and the FRT sequences

To characterize the 3rd chromosomal dominat suppressors of the "rough-eye phenotype", recombination between each putative mutation responsible for the suppressive activity and FTR80 and FRT82 sequences were induced. First, male dominant suppressors were crossed with females of the stock *yw eyflp; w+FRT80/w+FRT80* (respectively *yw eyflp; FRT82w+/FRT82w+*). Virgins with the genotype *yw eyflp/+; Mut/w+FRT80* (respectively *yw eyflp/+; mut/FRT82w+*) were re-crossed again with the stock *yw eyflp; w+FRT80/w+FRT80* (respectively *yw eyflp; FRT82w+/FRT82w+*). As a consequence of the *flippase* expression driven by the *eyless* promoter, recombination between the FRT sequence and the w+ marker leads to progenitors with mosaic eyes. These flies with mosaic eyes will have most of the chromosome arm carrying the FRT sequences recombined, since the w+ markers map close to the FRT sequences. Each recombinant was then tested for the suppression of the "rough-eye phenotype".
It is also important to consider that the suppressive activity of the mutants is probably due to a single mutation; hence, the suppressive activity will be unequally distributed between the two groups of recombinants. Inderectly, this allows a first mapping of the mutation.

6.5.2.9 Neomycin selection for the FRT80 sequence

200 µl of a solution containing the neomycin analogue Geneticin were poured into a tube containing food. Flies fed on it die unless they synthesize a neomycin resistence

transgene. Since this is present next to the FRT sequences, only flies carrying these recombinogen sequences survive. Flies were changed everyday to avoid overcrowding of the larvae, and possible escapers.
Geneticin was available with the commercial name of G418 (GIBCO^{TM}), diluted at a concentration of 10 mg per ml H_2O, and then stored at –20 degree at dark.

6.5.3 Cell culture

6.5.3.1 Experiment with dsRNA treatment in the reporter S2 cells

RNAi was performed essentially as described in Clemens et al. (2000) or in Schweizer et al. (2000). Briefly, 50 μl of reporter S2 cells were diluted in SFM at a concentration of 1x10^6/μl. 5 μl of dsRNA (against *gfp*, *lgs* or *cg6219*) at a concentration of 1 μg/μl was then added. After one hour, we added 50 μl of fetal calf serum 20%, and again we waited 24 hours. We then induced the pathway by LiCl (5 μl at 5M), by dsRNA (at a concentration of 1 μg/μl) against *shaggy* or *axin*, or by the addition of heat-shocked *hs-wg* S2 cells. For this last way of induction, 50 μl of *hs-wg* S2 cells (at a concentration of 2x10^6/ml) were added 30' after a heat-shock of 30' at 37 degrees. The analysis of amount of Luciferase present in the different conditions was performed 48 hours after the induction.

6.5.3.2 Experiment with dsRNA treatment in the *hs-wg* S2 cells

50 μl of *hs-wg* S2 cells were diluted in SFM at a concentration of 1x10^6/μl. 5 μl of dsRNA (against *gfp*, *lgs*, *por*, or *cg6219*) at a concentration of 1 μg/μl was then added. After one hour, we added 50 μl of fetal calf serum 20%, and again we waited 24 hours. We then induced *wg* expression by a heat-shock of 1 hour at 37 degrees, and let the cells recover at room temperature for 1 hour. Finally we added 50 μl of reporter S2 cells at a concentration of 0.5x10^6/μl, and we waited 48 hours before analysis.

6.5.3.3 Chip experiment

The experiment was performed with mRNA extracted from S2 cells on chips provided by Affimetrix®. S2 cells were previously treated with dsRNA of 600 to 800 bp, which was synthesized using the MEGAscript® (Ambion®) kit. The final concentration of the dsRNA

was 3 μg/μl (the dsRNA concentration in μg/μl was calculated multiplying the OD measurement by the dilution and then by 0.045).

$2x10^6$ S2 cells were washed twice with PBS, diluted in 2ml of serum-free media, put in a well of a 6-well plate, and then different dsRNAs (15μg/$1x10^6$ cells for each dsRNA) were added; after 60 minutes, serum was added to reach a final serum concentration of 10%. After 72 hours 1.10^7 S2 cells out of the $1.5\text{-}2.10^7$ S2 cells then normally present (the duplication time of S2 cells is around 24hrs) were finally lysed with β-Mercaptoethanol and Buffer RLT, and homogenized with the QIAshredder spin columns. For the RNA extraction the RNeasy Mini kit of Qiagen® was used. DNase digestion was also performed, and finally the RNA was eluted twice in a final volume of 75μl of Rnase-free water.

To detect any eventual RNA degradation, the quality of the RNA was tested with the Bioanalyzer®.

In parallel, small aliquots of the dsRNAs were tested with S2 cells, which carried the reporter system of the luciferase assay for Wg signaling.

Chip data allowed the comparison of two different conditions at the time, and different parameters were set to establish when the difference in the expression of a gene was considered to be significant. The most important parameter was represented by the number of significant changes in the different comparisons. Since every experimental condition was made in triplicate, 9 comparisons were possible (two groups of 3 data). The cut-off was set at 7; i.e. 7 out of 9 comparisons had to show a different level of the mRNA of interest. All genes with 7 or more comparisons with significant changes in their mRNA levels were then taken into consideration and ordered by the average fold change (on a logarithmic scale).

The analysis of the data was made in collaboration with the University of Geneva.

7 References

Alexandre, C., Jacinto, A., and Ingham, P.W. (1996). Transcriptional activation of *hedgehog* target genes in *Drosophila* is mediated directly by the Cubitus interruptus protein, a member of the GLI family of zinc finger DNA-binding protein. *Genes Dev*. **10**, 2003-2013.

Amit S., Hatzubai A., Birman Y., Andersen J.S., Ben-Shushan E., Mann M., Ben-Neriah Y., and Alkalay I. (2002) Axin-mediated CKI phosphorylation of beta-catenin at Ser 45: a molecular switch for the Wnt pathway. *Genes Dev.* **16**, 1066-76.

Baeg, G.H., Lin, X., Khare, N., Baumgartner, S., and Perrimon, N. (2001). Heparan sulfate proteoglycans are critical for the organization of the extracellular distribution of Wingless. *Development* **128**, 87–94.

Baker, N.E. (1988). Transcription of the segment polarity gene *wingless* in the imaginal discs of *Drosophila*, and the phenotype of a pupal-lethal *wg* mutation. *Development* **102**, 489-497.

Basler, K., and Struhl, G. (1994). Compartment boundaries and the control of *Drosophila* limb pattern by Hedgehog protein. *Nature* **368**, 208-214.

Behrens, J., von Kries, J. P., Kuhl, M., Bruhn, L., Wedlich, D., Grosschedl, R., and Birchmeier, W. (1996). Functional interaction of beta-catenin with the transcriptionfactor LEF-1. Nature 382, 638-642.

Bejsovec, A., and Martinez Arias, A. (1991). Roles of wingless in patterning the larval epidermis of Drosophila. *Development* **113(2)**, 471-85.

Bejsovec, A., and Wieschaus, E. (1995). Signalling activities of the *Drosophila wingless* gene are separably mutable and appear to be transduced at the cell surface. *Genetics* **139**, 309–320.

Belenkaya, T.Y., Han, C., Yan, D., Opoka, R.J., Khodoun, M., Liu, H., and Lin, X. (2004). Drosophila Dpp morphogen movement is independent of dynamin-mediated endocytosis but regulated by the glypican members of heparan sulfate proteoglycans. *Cell* **119(2)**, 231-44.

Bernfield, M., Gotte, M., Park, P. W., Reizes, O., Fitzgerald, M. L., Lincecum, J., and Zako, M. (1999). Functions of cell surface heparan sulfate proteoglycans. *Annu. Rev. Biochem.* **68**, 729 –777.

Bhanot, P., Fish, M., Jemison, J.A., Nusse, R., Nathans, J., and Cadigan, K.M. (1999). Frizzled and Dfrizzled-2 function as redundant receptors for Wingless during Drosophila embryonic development. *Development* **126(18)**, 4175-86.

Binari, R. C., Staveley, B. E., Johnson, W. A., Godavarti, R., Sasisekharan, R., and Manoukian, A. S. (1997). Genetic evidence that heparin-like glycosaminoglycans are involved in wingless signaling. *Development* **124**, 2623 -2632

Blair, S.S., Brower, D.L., Thomas, J.B., and Zavortink, M. (1994). The role of apterous in the control of dorsoventral compartmentalization and PS integrin gene expression in the developing wing of Drosophila. *Development* **120(7)**, 1805-15.

Boulianne, G.L., de la Concha, A., Campos-Ortega, J.A., Jan, L.Y., and Jan, Y.N. (1991). The *Drosophila* neurogenic gene *neuralized* encodes a novel protein and is expressed in precursors of larval and adult neurons. *Embo J.* **10**, 2975-2983.

Bornemann, D. J., Duncan, J. E., Staatz, W., Selleck, S., and Warrior, R. (2004). Abrogation of heparan sulfate synthesis in Drosophila disrupts the Wingless, Hedgehog and Decapentaplegic signaling pathways. *Development* **131**, 1927 -1938

Bradley, R.S., and Brown, A.M. (1990). The proto-oncogene int-1 encodes a secreted protein associated with the extracellular matrix. *EMBO J.* **9**, 1569–1575.

Brook, W.J., and Cohen,S.M. (1996). Antagonistic interactions between Wingless and Decapentaplegic responsible for dorsal-ventral pattern in the *Drosophila* leg. *Science* **273**, 1373-1377.

Brook, W. J., Diaz-Benjumea, F. J., and Cohen, S. M. (1996). Organizing spatial pattern in limb development. *Annu. Rev. Cell. Dev. Biol.* **12**, 161-80. Review.

Brunner, E., Peter, O., Schweizer, L., and Basler, K. (1997). pangolin encodes a Lef-1 homologue that acts downstream of Armadillo to transduce the Wingless signal in *Drosophila*. *Nature* 385, 829-833.

Bryant, P.J. (1970). Cell lineage relationship in the imaginal wing disc of *Drosophila melanogaster*. *Dev*. *Biol*. **22**, 389-411.

Burke, R., Nellen, D., Bellotto, M., Hafen, E., Senti, K.A., Dickson, B.J., and Basler, K. (1999). Dispatched, a novel sterol-sensing domain protein dedicated to the release of cholesterol-modified hedgehog from signaling cells. *Cell* **99(7)**, 803-15.

Cadigan, K. M., and Nusse, R. (1997). Wnt signaling: a common theme in animal development. *Genes Dev.* **11**, 3286-3305.

Cadigan, K. M., Fish, M. P., Rulifson, E. J., and Nusse, R. (1998). Wingless repression of Drosophila frizzled 2 expression shapes the Wingless morphogen gradient in the wing. *Cell* **93**, 767 –777.

Caricasole, A., Ferraro, T., Rimland, J.M., and Terstappen, G.C. (2002). Molecular cloning and initial characterization of the MG61/PORC gene, the human homologue of the Drosophila segment polarity gene Porcupine. *Gene* **288(1-2)**, 147-57.

Carroll S.B., Gates, J., Keys, D.N., Paddock, S.W., Panganiban, G.E.F., Selegue, J.E., and Williams, J.A. (1994). Pattern formation and eyespot determination in butterfly wings. *Science* **265**, 109-114.

Caspary, T., Garcia-Garcia, M. J., Huangfu, D., Eggenschwiler, J. T., Wyler, M. R., Rakeman, A. S., Alcorn, H. L., and Anderson, K. V. (2002). Mouse Dispatched homolog1 is required for long-range, but not juxtacrine, Hh signaling. *Curr. Biol.* **12**,1628 -1632

Chamoun, Z., Mann, R.K., Nellen, D., von Kessler, D.P., Bellotto, M,. Beachy, P.A., and Basler, .K. (2001). Skinny hedgehog, an acyltransferase required for palmitoylation and activity of the hedgehog signal. *Science* **293**, 2080-2084.

Chen, C.M., and Struhl, G. (1999). Wingless transduction by the Frizzled and Frizzled2 proteins of Drosophila. *Development* **126(23)**, 5441-52.

Chen, M.S., Obar, R.A ,Schroeder, C.C., Austin, T.W., Poodry, C.A., Wadsworth, S.C., and Vallee, R.B. (1991). Multiple forms of dynamin are encoded by *shibire*, a *Drosophila* gene involved in endocytosis. *Nature* **351**, 583–586.

Cho, K.O., Chern J., Izaddoost, S., and Choi, K.W. (2000) Novel signaling from the

peripodial membrane is essential for eye disc patterning in *Drosophila*. *Cell* **103**, 331–342.

Clemens, J.C., Worby, C.A., Simonson-Leff, N., Muda, M., Maehama, T., Hemmings B.A., and Dixon, J.E. (2000). Use of double-stranded RNA interference in Drosophila cell lines to dissect signal transduction pathways. *Proc. Natl. Acad. Sci. USA*. **97(12)**, 6499-503.

Cohen, S.M., Brönner, G., Küttner, F., Jürgens, G., and Jäckle, H. (1989). *Distal-less* encodes a homeodomain protein required for limb development in *Drosophila*. *Nature* **338**, 432-434.

Couso, J.P, Bishop, S.A., and Martinez Arias, A. (1994). The Wingless signaling pathway and the patterning of the wing margin in *Drosophila*. *Development* **120**, 621-636.

Couso, J. P., and Arias, A. M. (1994). Notch is required for wingless signaling in the epidermis of Drosophila. *Cell* **79**, 259 –272.

Cox, R. T., Pai, L. M., Kirkpatrick, C., Stein, J., and Peifer, M. (1999). Roles of the C terminus of Armadillo in Wingless signaling in Drosophila. *Genetics* **153**, 319-332.

Damke, H., Baba, T., Warnock, D.E., and Schmid, S.L. (1994). Induction of mutant dynamin specifically blocks endocytic vesicle formation. *J. Cell. Biol.* **127**, 915–934.

Datta, S. (1995). Control of proliferation activation in quiescent neuroblasts of the Drosophila central nervous system. *Development* **121**, 1173 -1182.

Desplan, C., Theis, J., and O'Farrell, P.H. (1985). The *Drosophila* development gene, *engrailed*, encodes a sequence-specific DNA binding activity. *Nature* **318**, 630-635.

De Wit , H., Lichtenstein, Y., Kelly, R.B., Geuze, H.J., Klumperman, J., and van der Sluijs, P. (2001). Rab4 regulates formation of synaptic-like microvesicles from early endosomes in PC12 cells. *Mol.Biol.Cell* **12**, 3703-3715.

Diaz-Benjumea, F.J., and Cohen, S.M. (1993). Interaction between dorsal and ventral cells in the imaginal disc directs wing development in Drosophila. *Cell* **75(4)**, 741-52.

Diaz-Benjumea, F.J., and Cohen, S.M. (1995). Serrate signals through Notch to establish a Wingless-dependent organizer at the dorsal/ventral compartment boundary of the *Drosophila* wing. *Development* **121**, 4215-4225.

DiNardo, S., Sher, E., Heemskerk-Jongens, J., Kassis, J.A., and O'Farrell, P.H. (1988). Two-tiered regulation of spatially patterned engrailed gene expression during *Drosophila* embryogenesis. *Nature* **332**, 604–609.

Domìnguez, M., Brunner, M., Hafen, E., and Basler, K. (1996). Sending and receiving the Hedgehog signal: control by the *Drosophila* Gli protein Cubitus interruptus. *Science* **272**, 1621-1625.

Dubois, L., Lecourtois, M., Alexandre, C., Hirst, E., and Vincent, J.-P. (2001). Regulated endocytic routing modulates wingless signaling in *Drosophila* embryos. *Cell* **105**, 613–624.

Dunphy, J.T., and Linder, M.E. (1998). Signalling functions of protein palmitoylation. *Biochim. Biophys. Acta* **1436(1-2)**, 245-61.

Entchev, E.V., Schwabedissen, A., and Gonzalez-Gaitan, M. (2000). Gradient formation of the TGF-b homolog Dpp. *Cell,* **103**, 981-991.

Esko, J. D., and Selleck, S. B. (2002). Order out of chaos: assembly of ligand binding sites in heparan sulfate. *Annu. Rev. Biochem.* **71**, 435 –471.

Gallet, A., Rodriguez, R., Ruel, L., and Therond, P.P. (2003). Cholesterol modification of hedgehog is required for trafficking and movement, revealing an asymmetric cellular response to hedgehog. *Dev. Cell* **4,** 191-204.

Garcia-Bellido, A., Ripoll, P., and Morata, G. (1973). Developmental compartmentalization of the wing disk of *Drosophila*. *Nature New Biol*. **245**, 251-253.

Gerlitz, O., Nellen, D., Ottiger, M., and Basler, K. (2002). A screen for genes expressed in Drosophila imaginal discs. *Int. J. Dev. Biol.* **46(1)**, 173

Gerlitz, O., and Basler, K**.** (2002). Wingful, an extracellular feedback inhibitor of Wingless. *Genes Dev.* **16**, 1055 –1059.

Gibson, M.C., and Schubiger, G. (2000) Peripodial cells regulate proliferation and patterning of *Drosophila* imaginal discs. *Cell* **103**, 343–350.

Giraldez, A. J., Copley, R. R., and Cohen, S. M. (2002). HSPG modification by the secreted enzyme Notum shapes the Wingless morphogen gradient. *Dev. Cell* **2**, 667-676.

Golic, K. (1991). Site-specific recombination between homologous chromosomes in *Drosophila*. *Science* **252**, 958-961.

Gonzalez, F., Swales, L., Bejsovec, A., Skaer, H., and Martinez Arias, A (1991) Secretion and movement of wingless protein in the epidermis of the *Drosophila* embryo. *Mech. Dev.* **35(1)**, 43-54.

Gorbalenya, A.E., and Koonin, E.V. (1993). Helicases: Amino acid sequence comparisons and structure-function relationships. *Curr. Opin. Struct. Biol.* **3**, 419-429.

Gorbalenya, A.E., Koonin, E.V., Donchenko, A.P., and Blinov, V.M. (1989). Two related superfamilies of putative helicases involved in replication, recombination, repair, and expression of DNA and RNA genomes. *Nucleic Acids Res.* **17**, 4713-4730.

Greco, V., Hannus, M., and Eaton, S. (2001). Argosomes: a potential vehicle for the spread of morphogens through epithelia. *Cell* **106**, 633–645.

Hacker, U., Lin, X., and Perrimon, N. (1997). The Drosophila sugarless gene modulates Wingless signaling and encodes an enzyme involved in polysaccharide biosynthesis. *Development* **124**,3565 –3573.

Hall, T. M., Porter, J. A., Young, K. E., Koonin, E. V., Beachy, P. A., and Leahy, D. J. (1997). Crystal structure of a Hedgehog autoprocessing domain: homology between Hedgehog and self-splicing proteins. *Cell* **91**, 85 –97.

Haerry, T. E., Heslip, T. R., Marsh, J. L., and O'Connor, M**. B.** (1997). Defects in glucuronate biosynthesis disrupt Wingless signaling in Drosophila. *Development* **124**, 3055 –3064.

Han, C., Belenkaya, T. Y., Khodoun, M., Tauchi, M., and Lin, X. (2004). Distinct and collaborative roles of Drosophila EXT family proteins in morphogen signalling and gradient formation. *Development* **131**, 1563 –1575.

Han, C., Yan, D., Belenkaya, T. Y., and Lin, X. (2005). Drosophila glypicans Dally and Dally-like shape the extracellular Wingless morphogen gradient in the wing disc. *Development* **132(4)**, 667-79.

He, X., Semenov, M., Tamai, K., and Zeng, X. (2004). LDL receptor-related proteins 5 and 6 in Wnt/beta-catenin signaling: arrows point the way. *Development* **131**, 1663 – 1677.

Held, L.I, Jr., Heup, M.A., Sappington, J.M., and Peters,S.D (1994). Interactions of *decapentaplegic*, *wingless*, and *Distalless* in the Drosophila leg. *Roux's Arch. Dev. Biol.* **203**, 310-319.

Henley, J.R., Krueger, E.W.A., Oswald, B.J., and McNiven, M.A. (1998). Dynamin-mediated internalization of caveolae. *J. Cell Biol.* **141**, 85–99.

Hidalgo, A., and Ingham, P. (1990). Cell patterning in the *Drosophila* segment: spatial regulation of the segment polarity gene patched. *Development* **110**, 291–301.

Hoekstra, D., Tyteca, D., and van Ijzendoorn, S.C. (2004). The subapical compartment: a traffic center in membrane polarity development. *J. Cell. Sci.* **117(11)**, 2183-92. Review.

Hofmann, K. (2000) A superfamily of membrane-bound O-acyltransferases with implications for wnt signaling. *Trends Biochem. Sci.* **25(3)**, 111-2.

Ikonen, E., and Simons, K. (1998). Protein and lipid sorting from the trans-Golgi network to the plasma membrane in polarized cells. *Semin. Cell Dev. Biol.* **9(5)**, 503-9.

Ingham, P.W., and Martinez Arias, A. (1992). Boundaries and fields in early embryos. *Cell* **68**, 221–235.

Jiang, J., and Struhl, G. (1996). Complementary and mutually exclusive activities of Decapentaplegic and Wingless organize axial patterning during *Drosophila* leg development. *Cell* **86**, 401-409.

Johnson, K. G., Ghose, A., Epstein, E., Lincecum, J., O'Connor, M. B., and van Vactor, D. (2004). Axonal heparan sulfate proteoglycans regulate the distribution and efficiency of the repellent slit during midline axon guidance. *Curr. Biol.* **14**, 499 –504.

Jones, S.M., Howell, K.E., Henley, J.R., Cao H., and McNiven, M.A. (1998). Role of dynamin in the formation of transport vesicles from the trans-golgi network. *Science* **279**, 573–577.

Kadowaki, T., Wilder, E., Klingensmith, J., Zachary, K., and Perrimon, N. (1996). The segment polarity gene *porcupine* encodes a putative multitransmembrane protein involved in wingless processing. *Genes Dev.* **10**, 3116–3128.

Kawakami, T., Kawcak, T., Li, Y. J., Zhang, W., Hu, Y., and Chuang, P. T. (2002). Mouse dispatched mutants fail to distribute hedgehog proteins and are defective in hedgehog signaling. *Development* **129**, 5753 –5765.

Khare, N., and Baumgartner, S. (2000). Dally-like protein, a new Drosophila glypican with expression overlapping with wingless. *Mech. Dev.* **99**, 199 –202.

Kim, J., Irvine, K.D., and Carroll, S. (1995). Cell recognition, signal induction, and asymmetrical gene activation at the dorsal-ventral boundary of the developing *Drosophila* wing. *Cell* **82**, 795-802.

Kramps, T., Peter, O., Brunner, E., Nellen, D., Froesch, B., Chatterjee, S., Murone, M., Zullig, S., and Basler, K. (2002). Wnt/wingless signaling requires BCL9/legless-mediated recruitment of pygopus to the nuclear beta-catenin-TCF complex. *Cell* **109**, 47-60.

Kerszberg, M., and Wolpert, L., (1998). Mechanisms for positional signalling by morphogen transport: a theoretical study. *J. Theor. Biol.* **191**, 103–114.

Lambertsson, A. (1998). The *Minute* genes in *Drosophila* and their molecular functions. *Adv. Genet.* **38**, 69-134.

Lander, A.D., Nie, Q., and Wan, F.Y., (2002). Do morphogen gradients arise by diffusion?. *Dev. Cell* **2**, 785–796.

Lawrence, P.A., Sanson, B., and Vincent, J.P. (1996). Compartments, wingless and engrailed: patterning the ventral epidermis of *Drosophila* embryos. *Development* **122(12)**, 4095-103.

Lawrence, P.A., and Struhl, G. (1996). Morphogens, compartments, and pattern: lessons from *Drosophila*? *Cell* **85**, 951-961.

Lecuit, T., Brook, W.J., Ng, M., Calleja, M., Sun, H., and Cohen, S.M., (1996). Two distinct mechanisms for long-range patterning by Decapentaplegic in the *Drosophila* wing. *Nature* **381**, 387–393.

Lee, J.J., Ekker, S.C., von Kessler, D.P., Porter, J.A. Sun, B.I., and Beachy, P.A. (1994). Autoproteolysis in hedgehog protein biogenesis. *Science* **266**, 1528–1537.

Lewis, I.H., Jr. (2002). Imaginal Discs. The genetic and cellular logic of pattern formation. Cambridge. University Press.

Lin, X., and Perrimon, N. (1999). Dally cooperates with Drosophila Frizzled 2 to transduce Wingless signalling. *Nature* **400**, 281 –284.

Lin, X., and Perrimon, N., (2000). Role of heparan sulfate proteoglycans in cell-cell signaling in Drosophila. *Matrix Biol.* **19**, 303–307.

Lin, X. (2004). Functions of heparan sulfate proteoglycans in cell signaling during development. *Development* **131**, 6009-6021.

Linder, M.E., and Deschenes, R.J. (2003). New Insights into the Mechanisms of Protein Palmitoylation. *Biochemistry **42*(15)**, 4311 – 4320.

Liu, C., Li, Y., Semenov, M, Han, C., Baeg, G.H., Tan, Y., Zhang, Z., Lin, X., and He, X. (2002). Control of beta-catenin phosphorylation/degradation by a dual-kinase mechanism. *Cell* **108**, 837-847.

Lloyd, T.E., Atkinson, R., Wu, M.N., Zhou, Y., Pennetta, G., and Bellen, H.J. (2002). Hrs regulates endosome membrane invagination and tyrosine kinase receptor signaling in Drosophila. *Cell* **108(2)**, 261-9.

Lohman, T.M., and Bjornson K.P. (1996). Mechanisms of helicase-catalyzed DNA un-

winding. *Annu. Rev. Biochem.* **65**, 169-214.

Martinez Arias, A., Baker, N.E., and Ingham, P.W. (1988) Role of segment polarity genes in the definition and maintenance of cell states in the *Drosophila* embryo. *Development* **103**, 157–170.

Martinez Arias, A. (1993). Development and patterning of the larval epidermis of *Drosophila*. In Bate, M. and Martinez Arias, A. (eds), *The Development of Drosophila Melanogaster*. Cold Spring Harbor Laboratory Press, Cold Spring Harbor, NY, pp. 517–608.

Moline, M.M., Southern, C., and Bejsovec, A. (1999). Directionality of wingless protein transport influences epidermal patterning in the *Drosophila* embryo. *Development* **126**, 4375–4384.

Morata, G., and Ripoll, P. (1975). *Minutes*: mutants of *Drosophila* autonomously affecting cell division rate. *Dev. Biol.* **42**, 211-221.

Nakato, H., Futch, T. A., and Selleck, S. B. (1995). The division abnormally delayed (dally) gene: a putative integral membrane proteoglycan required for cell division patterning during postembryonic development of the nervous system in Drosophila. *Development* **121**, 3687 –3702.

Nellen, D., Burke, R., Struhl, G., and Basler, K., 1996. Direct and long-range action of a DPP morphogen gradient. *Cell* **85**, 357–368.

Neumann, C.J., and Cohen, S.M. (1997). Long-range action of Wingless organizes the dorsal-ventral axis of the *Drosophila* wing. *Development* **124**, 871-880.

Ng, M., Diaz-Benjumea, F.J., Vincent, J.P., Wu, J., and Cohen, S.M. (1996). Specification of the wing by localized expression of wingless protein. *Nature* **381**, 316-8.

Nolo, R.., Abbott, L.A., and Bellen, H.J. (2000). Senseless, a Zn finger transcription factor, is necessary and sufficient for sensory organ development in *Drosophila*. *Cell* **102**, 349-362.

Noordermeer, J., Johnston, P., Rijsewijk, F., Nusse, R., and Lawrence, P.A. (1992). The consequences of ubiquitous expression of the wingless gene in the Drosophila embryo.

Development **116(3)**, 711-9.

Nusse, R., and Varmus, H.E. (1982). Many tumors induced by the mouse mammary tumor virus contain a provirus integrated in the same region of the host genome. *Cell* **31**, 99–109.

Nusse R., Brown A., Papkoff J., Scambler P., Shackleford G., McMahon A., Moon R., and Varmus H. (1991). A new nomenclature for int-1 and related genes: the Wnt gene family. *Cell* ***64***, 231.

Nusse, R. (2003). Wnts and Hedgehogs: lipid-modified proteins and similarities in signaling mechanisms at the cell surface. *Development* **130**, 5297 –5305.

Nüsslein-Volhard, C., and Wieschaus, E. (1980). Mutations affecting segment number and polarity in *Drosophila*. *Nature* **287**, 795–801.

Nybakken, K., and Perrimon, N. (2002). Heparan sulfate proteoglycan modulation of developmental signaling in Drosophila. *Biochim. Biophys. Acta* **1573**, 280 –291.

Oh, P., McIntosh, D.P., and Schnitzer, J.E. (1998). Dynamin at the neck of caveolae mediates their budding to form transport vesicles by GTP-driven fission from the plasma membrane of endothelium. *J. Cell Biol.* **141**, 101–114.

Panakova, D., Sprong, H., Marois, E., Thiele, C., and Eaton, S. (2005) Lipoprotein particles are required for Hedgehog and Wingless signalling. *Nature* **435(7038)**, 58-65.

Pandur, P., Maurus, D., and Kuhl, M. (2002). Increasingly complex: new playersenter the Wnt signaling network. *Bioessays* **24**, 881-884.

Payre, F., Vincent, A., and Carreno, S. (1999). ovo/svb integrates Wingless and DER pathways to control epidermis differentiation. *Nature* **400**, 271–275.

Peifer, M., and Polakis, P. (2000). Wnt signaling in oncogenesis and embryogenesis--a look outside the nucleus.. *Science* **287(5458)**, 1606-9.

Pepinsky, R. B., Zeng, C., Wen, D., Rayhorn, P., Baker, D. P., Williams, K. P., Bixler, S. A., Ambrose, C. M., Garber, E. A., and Miatkowski, K. et al. (1998). Identification of a palmitic acid-modified form of human Sonic hedgehog. *J. Biol. Chem.* **273**, 14037 –

14045.

Perrimon, N., Hacker, U., Sanson, B., and Tabata, T. (2004). Wingless, hedgehog and heparan sulfate proteoglycans. *Development* **131**, 2509 -2513.

Peters, C., Baars, T.L., Buhler, S., and Mayer, A. (2004). Mutual control of membrane fission and fusion proteins. *Cell*, **119(5)**, 667-78.

Pfeiffer, S., Ricardo, S., Manneville, J.-B., Alexandre, C., and Vincent, J.-P. (2002). Producing cells retain and recycle Wingless in *Drosophila* embryos. *Curr. Biol.* **12**, 957–962.

Phillips, R.G., and Whittle, J.R.S. (1993). *wingless* expression mediates determination of peripheral nervous system elements in late stages of *Drosophila* wing disc development. *Development* **118**, 427-438.

Polakis, P. (2001). More than one way to skin a catenin. *Cell* **105**, 563-566.

Porter, J.A, Young, K.E., and Beachy, P.A. (1996). Cholesterol modification of hedgehog signaling proteins in animal development. *Science* **274**, 255–259.

Ramirez-Weber, F.A., and Kornberg, T.B. (1999) Cytonemes: cellular processes that project to the principal signaling center in *Drosophila* imaginal discs. *Cell* **97**, 599–607.

Reichsman, F., Smith, L., and Cumberledge, S. (1996). Glycosaminoglycans can modulate extracellular localization of the wingless protein and promote signal transduction. *J. Cell Biol.* **135**, 819–827.

Resh, M.D. (1999). Fatty acylation of proteins: new insights into membrane targeting of myristoylated and palmitoylated proteins. *Biochim. Biophys. Acta* **1451**, 1–16.

Rocheleau, C. E., Downs, W. D., Lin, R., Wittmann, C., Bei, Y., Cha, Y. H., Ali, M., Priess, J. R., and Mello, C. C. (1997). Wnt signaling and an APC-related gene specify endoderm in early C. elegans embryos. *Cell* **90**, 707 –716.

Rulifson, E.J., and Blair, S.S. (1995). Notch regulates wingless expression and is not required for reception of the paracrine wingless signal during wing margin neurogenesis in Drosophila. *Development* **121(9)**, 2813-24.

Rulifson, E.J., Micchelli, C.A., Axelrod, J.D., Perrimon, N., and Blair, S.S. (1996). *wingless* refines its own domain on the *Drosophila* wing margin. *Nature* **384**, 72-74.

Sanson, B. (2001). Generating patterns from fields of cells. Examples from *Drosophila* segmentation. *EMBO Reports* **2(12)**, 1083-8.

Schweizer, L., and Varmus, H. (2003). Wnt/Wingless signaling through beta-catenin requires the function of both LRP/Arrow and frizzled classes of receptors. *BMC Cell Biol.* **4**, 4.

Seto, E.S., and Bellen, H.J. (2004). The ins and outs of Wingless signaling. *Trends Cell Biol.* **14(1)**, 45-53. Review.

Seugnet, L., Simpson, P., and Haenlin, M. (1997), Requirement for dynamin during Notch signaling in *Drosophila* neurogenesis. *Dev. Biol.* **192**, 585–598.

Sharma, R.P., and Chopra, V.L. (1976). Effect of the Wingless (wg1) mutation on wing and haltere development in Drosophila melanogaster. *Dev. Biol.* ***48***, 461-5.

Simons, K., and Ikonen, E., (1997). Functional rafts in cell membranes. *Nature* **387**, 569–572.

Spring, J., Paine-Saunders, S. E., Hynes, R. O., and Bernfield, M. (1994). Drosophila syndecan: conservation of a cell-surface heparan sulfate proteoglycan. *Proc. Natl. Acad. Sci. USA* **91**, 3334 –3338.

Steigemann, P., Molitor, A., Fellert, S., Jackle, H., and Vorbruggen, G. (2004). Heparan sulfate proteoglycan syndecan promotes axonal and myotube guidance by slit/robo signaling. *Curr. Biol.* **14**, 225 –230.

St Johnston, D., and Nüsslein-Volhard, C. (1992). The origin of pattern and polarity in the *Drosophila* embryo. *Cell* **68**, 201–219.

Strigini, M., and. Cohen, S..M. (2000). Wingless gradient formation in the *Drosophila* wing. *Curr. Biol.* **10**, 293–300.

Struhl, G., and Basler, K. (1993). Organizing activity of wingless protein in Drosophila. *Cell* **72**, 527-40.

Srivastava, A., and Bell, J.B. (2003). Further developmental role of the Vestigial/Scalloped transcription complex during wing development in *Drosophila melanogaster*. *Mechanisms of Development* **120**, 587-596.

Tabata, T., and Takei, Y. (2004). Morphogens, their identification and regulation. *Development* **131**, 703-712.

Takei, Y., Ozawa, Y., Sato, M., Watanabe, A., and Tabata, T. (2004). Three Drosophila EXT genes shape morphogen gradients through synthesis of heparan sulfate proteoglycans. *Development* **131**, 73–82.

Tanaka, K., Kitagawa, Y., and Kadowaki, T. (2002). Drosophila segment polarity gene product porcupine stimulates the posttranslational N-glycosylation of wingless in the endoplasmic reticulum. *J. Biol. Chem.* **277(15)**, 12816-23.

Tanaka, K., Okabayashi, K., Asashima, M., Perrimon, N., and Kadowaki, T. (2000). The evolutionarily conserved porcupine gene family is involved in the processing of the Wnt family. *Eur. J. Biochem..* **267(13)**, 4300-11.

Teleman, A.A., and Cohen, S.M., (2000). Dpp gradient formation in the *Drosophila* wing imaginal disc. *Cell* **103**, 971–980.

Teleman, A.A., Strigini, M., and Cohen, S.M. (2001). Shaping morphogen garadients. *Cell* **105**, 559-562.

Thorpe, C.J., Schlesinger, A., Carter, J.C., and Bowerman, B. (1997). Wnt signaling polarizes an early C. elegans blastomere to distinguish endoderm from mesoderm. *Cell* **90(4)**, 695-705.

Tolwinski, N. S., Wehrli, M., Rives, A., Erdeniz, N., DiNardo, S., and Wieschaus, E. (2003). Wg/Wnt signal can be transmitted through arrow/LRP5,6 and Axin independently of Zw3/Gsk3beta activity. *Dev. Cell* **4**, 407 -418.

Toyoda, H., Kinoshita-Toyoda, A., Fox, B., and Selleck, S. B. (2000a). Structural analysis of glycosaminoglycans in animals bearing mutations in sugarless, sulfateless, and tout-velu. Drosophila homologues of vertebrate genes encoding glycosaminoglycan biosynthetic enzymes. *J. Biol. Chem.* **275**, 21856 -21861.

Toyoda, H., Kinoshita-Toyoda, A., and Selleck, S. B. (2000b). Structural analysis of glycosaminoglycans in Drosophila and Caenorhabditis elegans and demonstration that tout-velu, a Drosophila gene related to EXT tumor suppressors, affects heparan sulfate in vivo. *J. Biol. Chem.* **275**, 2269 –2275.

van den Heuvel, M., Harryman-Samos, C., Klingensmith, J., Perrimon, N., and Nusse, R. (1993). Mutations in the segment polarity genes *wingless* and *porcupine* impair secretion of the wingless protein. *EMBO J.* **12**, 5293–5302.

van den Heuvel, M., Nusse, R., Johnston, P., and Lawrence, P.A. (1989). Distribution of the wingless gene product in *Drosophila* embryos: a protein involved in cell-cell communication. *Cell* **59(4)**, 739-49.

van der Bliek, A.M., and Meyerowitz, E.M. (1991). Dynamin-like protein encoded by the *Drosophila shibire* gene associated with vesicular traffic. *Nature* **351**, 411–414.

van der Bliek, A.M. (1999). Functional diversity in the dynamin family. *Trends Cell Biol.* **9**, 96–102.

van de Wetering, M., Cavallo, R., Dooijes, D., van Beest, M., van Es, J., Loureiro, J.,Ypma, A., Hursh, D., Jones, T., Bejsovec, A., et al. (1997). Armadillo coactivates transcription driven by the product of the Drosophila segment polarity gene dTCF. *Cell* **88**, 789-799.

Vincent, J.P., and O'Farrell, P.H. (1992). The state of engrailed expression is not clonally transmitted during early Drosophila development. *Cell* **68(5)**, 923-31.

Vincent, J.P., and Dubois, L. (2002). Morphogen transport alog epithelia, and integrated trafficking problem. *Developmental Cell* **3**, 615-623.

Voigt, A., Pflanz, R., Schafer, U., and Jackle, H. (2002). Perlecan participates in proliferation activation of quiescent Drosophila neuroblasts. *Dev. Dyn.* **224**, 403–412.

Wehrli, M., Dougan, S. T., Caldwell, K., O'Keefe, L., Schwartz, S., Vaizel-Ohayon, D., Schejter, E., Tomlinson, A., and DiNardo, S. (2000). arrow encodes an LDL-receptor-related protein essential for Wingless signalling. *Nature* **407**, 527–530.

Willert, K., and Nusse, R. (1998). Beta-catenin: a key mediator of Wnt signaling. *Current Opinion in Genetics & Development* **8**, 95-102.

Willert, K., Brown, J.D., Danenberg, E., Duncan, A.W., Weissman, I.L., Reya, T., Yates, III J.R., and Nusse R. (2003). Wnt proteins are lipid-modified and can act as stem cell growth factors. *Nature* **423**, 448–452.

Williams, J.A., Bell, J.B., and Carroll, S.B. (1991). Control of *Drosophila* wing and haltere development by the nuclear *vestigial* gene product. *Genes Dev*. **5**, 2481-2495.

Wodarz, A., and Nusse, R. (1998). Mechanisms of Wnt signaling in development. *Annual Review of Cell & Developmental Biology* **14**, 59-88.

Wolpert, L. (1998). Principles of Develpoment. Oxford University Press, New York.

Yanagawa, S., Matsuda, Y., Lee, J.S., Matsubayashi, H., Sese, S., Kadowaki, T., and Ishimoto, A. (2002). Casein kinase I phosphorylates the Armadillo protein and induces its degradation in Drosophila. *EMBO J.* **21**, 1733-42.

Zecca, M., Basler, K., and Struhl, G. (1996). Direct and long-range action of a Wingless morphogen gradient. *Cell* **87**, 833-844.

Zerial, M., and McBride, H. (2001). Rab proteins as membrane organizers. *Nat. Rev. Mol. Cell Biol.* **2(2)**, 107-17. Review. Erratum in: *Nat. Rev. Mol. Cell Biol.* (2001) **2(3)**, 216.

Zhai, L., Chaturvedi, D., and Cumberledge, S. (2004). Drosophila wnt-1 undergoes a hydrophobic modification and is targeted to lipid rafts, a process that requires porcupine. *J. Biol. Chem*. **279(32)**, 33220-7.

8 Acknowledgements

This study was carried out under the supervision of Konrad Basler. During our Wednesday discussions he taught me the scientific way of thinking and he transmitted me his enthusiasm. I thank him for listening to me and for understanding my thoughts and my feelings.

I would like to thank Carla Bänziger for the very nice collaboration, for the interesting discussions, and for her invitation to the opera,

Denise Nellen for introducing me into the world of flies and of molecular biology,

Zeina Chamoun for the scientific help (even from Geneva), for her moral support during the difficult moments and for our long evening discussions while dissecting larvae, thank you,

George Hausmann for his endless patience and kindness, for pushing me to do some sport, and for the nice moments spent in Zurich, Ticino and Italy,

Eduardo Moreno for the very interesting discussions in the fly room, for showing me what passion for research means, and for believing in my qualities,

Thomas Kramps and Bruno Müller for their help when I first arrived to the lab,

Tamara Elmore for her technical help, for our “educated” talks, and for her presents,

Sandipan Chatterjee for his philosophy of “not postponing joy” and the time we spent at the Festival of Locarno,

Rebecca Buob for our daily discussion about the weather in Ticino, for preparing excellent cakes, and for picking up my phone calls,

Chloé Spichiger-Hausermann for her kindness, for not complaining about my terrible bench, and for her help with the writing,

Gerlinde Reim and Johannes Bischof for accepting me in their offices, for eating sandwiches and Bircher-müesli in record times in the cafeteria, and for the nice dinner on my birthday,

Rajesh Narasimamurthy for his technical help, for heat-shocking my larvae during the week-end, and for being always in a good mood,

Reto Städeli for his help in cloning, and for the trip to Verona to see the “Rigoletto”,

Peder Zipperlen for helping me during the microarray experiments in Geneva, and for his “C. elegans contribution” to the project,

Christian Mosimann for discussion and for helping me in the choice of the lab,

Raymond, Peter, and Michi for the soccer matches played with all kind of weather,

Gerald Schwank for watching Asian movies with me.

Many thanks to Ernst Hafen and Peter Gallant and to the people of their labs for discussion, suggestions and for always being ready to help me.

Hugo Bellen for providing antibodies, Marcos Gonzàlez-Gaitàn and Tatsuhiko Kadowaki for flies,

Christina Eugster for her kind technical help and for sending me material in record time.

I still would like to thank Alessandra Fontecedro for her sympathy, for the lunchtime in the cafeteria, and for the funny holiday in Rome,

Maria and Cristina for being my “second mothers” in Zurich and making me feel less homesick,

Chrigi and Esther for their kind help,

My flat-mate Mario for not complaining about my late dinners,

My friends Alex, Dario, Matthias, Mattia, Zeljko, Fiorenza, Claudia, Rosy, Raluca, and Romina for their support and the nice moments spent together during this period,

Michela Bianchi for her immense support,

My relatives from Ticino, and specially my aunt “Zi Lu” for her phone calls in the lab,

Jorge for his help during the Spanish period,

My father Pietro, my mother Ivana, and my special sister Claudia for supporting me in all my decisions and in all the difficult moments.

9 Curriculum Vitae

Name	Soldini
Vorname	Davide
Geboren	am 05. Februar 1976 in Locarno, Schweiz
Heimatort	Coldrerio, Schweiz
Nationalität	Schweizer
Sprachen	Italienisch, Französisch, Deutsch, Englisch, Spanisch

Schulbildung

1995	Liceo Cantonale di Mendrisio
1995-2001	Medizinstudium an der Universität Bern
2001	Medizinische Doktorarbeit am Institut für Pathologie der Universität Bern unter Leitung von Prof. Dr. Luca Mazzucchelli
2002	Klinische Forschung in Ospedale Regionale Bellinzona e Valli unter Leitung von Prof. Dr. Claudio Marone
2002-2005	Aufnahme in das MD-PhD Programm an der Universität Zürich und tätig als Doktorand am Institut für Molekularbiologie der Universität Zürich unter der Leitung von Prof. Dr. Konrad Basler.

Publikationen

Soldini, D., Gugger, M., Burckhardt, E., Kappeler, A., Laissue, J.A., and Mazzucchelli, L. (2003). Progressive genomic alterations in intraductal papillary mucinous tumours of the pancreas and morphologically similar lesions of the pancreatic ducts. *J. of Pathol.* **199(4)**, 453-61.

Soldini, D., Zwahlen, H., Gabutti, L., Marzo, A., and Marone, C. (2005). Pharmacokinetics of N-acetylcysteine following repeated intravenous infusion in haemodialysed patients. *Eur J Clin Pharmacol*. **60(12)**, 859-64.